

DRAFT

Future Research Activities at LNF
Working Group Report

A. Antonelli, D. Babusci, G. Bencivenni, M. Benfatto, M.E. Biagini,
S. Bianco, C. Biscari, C. Bloise, F. Bossi, R. Cimino, G. Cinque,
S. Dabagov, S. Dell'Agnello, A. Fantoni, G. Felici, M. Ferrario,
M.A. Franceschi, A. Gallo, A. Ghigo, P. Gianotti, S. Guiducci,
G. Isidori, A. Marcelli, C. Milardi, M. Mirazita, S. Miscetti,
V. Muccifora, F. Murtas, E. Pace, L. Pancheri, C. Petrascu,
P. Raimondi, M. Ricci, C. Sanelli, F. Terranova

30/10/2005

Editorial Board:

M. Benfatto, M. Biagini, C. Bloise, A. Fantoni,
G. Isidori, E. Pace, F. Terranova

Contents

1	Introduction	7
2	The INFN Frascati Laboratory	9
2.1	Technical services in the Accelerator Department	10
2.1.1	Electronics and diagnostic	10
2.1.2	Magnet engineering	10
2.1.3	Mechanical engineering	10
2.1.4	Cryogenics	10
2.1.5	Radio-Frequency	11
2.1.6	Vacuum	11
2.2	DAΦNE	11
2.2.1	DAΦNE Beam Test Facility	13
2.3	SPARC	14
2.4	CNAO	15
2.5	International Projects	16
2.5.1	CTF3	16
2.5.2	TESLA/TTF	17
2.5.3	Other International Projects	17
2.6	Computing and Dataweb	18
2.6.1	Computing service	18
2.6.2	Dataweb	19
2.6.3	KLOE computing center	19
2.7	Technical services for experimental setup	21
2.7.1	Detector development	21
2.7.2	Engineering Support for experimental apparata	22
2.7.3	Electronic workshop	22
2.8	Particle Physics at Accelerators	23
2.8.1	KLOE	24
2.8.2	BABAR	25
2.8.3	Experiments at Fermilab	25
2.8.4	Experiments at the LHC	26
2.9	Neutrino and Astroparticle Physics	27
2.9.1	OPERA	28
2.9.2	The satellite mission PAMELA	28
2.9.3	The LAZIO-SiRad project	29
2.9.4	Experimental Detection of Gravitational Waves	30
2.10	Hadronic and Nuclear Physics	30
2.10.1	DEAR/SIDDHARTA	30

2.10.2	FINUDA	31
2.10.3	HERMES	32
2.10.4	AIACE	32
2.11	The Synchrotron Radiation Facility	33
2.11.1	Infrared activities	33
2.11.2	Soft X-Ray activities	34
2.11.3	GILDA activities	35
2.12	Theoretical Physics	35
3	Plans in the World	39
3.1	Open problems and main directions in high-energy physics	39
3.1.1	The Standard Model	39
3.1.2	Model building and the high-energy frontier	40
3.1.3	Precision tests and the high-intensity frontier	41
3.1.4	Understanding QCD	41
3.2	Particle-physics experiments at accelerators	42
3.2.1	Tests of the Standard Model	42
3.2.2	The quest for the Higgs boson, including SUSY	44
3.2.3	Quarks flavor, and the CP-violation enigma	46
3.3	Hadronic and nuclear physics	49
3.3.1	Hadron spectroscopy	50
3.3.2	Chiral symmetry breaking by means of exotic-atom studies	50
3.3.3	Spin structure of the nucleon: status and perspectives	51
3.3.4	Understanding the nucleon structure by the Generalized Parton Distributions	52
3.3.5	Elastic Form Factors	53
3.3.6	The search of the Quark Gluon Plasma	54
3.4	Astroparticle physics	54
3.4.1	Ultra High Energy Cosmic Rays	55
3.4.2	Gamma Rays	55
3.4.3	High Energy Neutrinos	56
3.4.4	Dark Matter	56
3.4.5	Matter-Antimatter asymmetry in the Universe	57
3.5	Neutrino physics	57
3.6	Experimental detection of gravitational waves	59
3.7	Electron-positron storage rings	62
3.7.1	ϕ -factories	62
3.7.2	Light-quark factories	63
3.7.3	τ -charm factories	63
3.7.4	B-factories	63
3.7.5	Next generation factories	64
3.8	Free Electron Laser	64
3.9	Linear Collider	68
4	Future Activities at the LNF	75
4.1	R&D on Free Electron Laser	75
4.1.1	SPARC Phase II	75
4.1.2	SPARXINO	76
4.1.3	PVFEL	77
4.2	Studies on new accelerators	78
4.2.1	DAΦNE luminosity optimization	79

4.2.2	DAΦNE energy upgrade	79
4.2.3	Higher Luminosity ϕ -Factory	80
4.2.4	τ -charm-Factory	81
4.3	Kaon physics	81
4.3.1	K_S decays	82
4.3.2	Neutral Kaon Interferometry	84
4.3.3	Charged Kaons	84
4.4	Light Quark Spectroscopy	84
4.5	Charm physics	85
4.6	The τ lepton	86
4.7	High-resolution spectroscopy of hypernuclei	87
4.7.1	Hyperon-nucleon interaction	88
4.7.2	Impurity nuclear physics	89
4.7.3	Medium effect	89
4.7.4	High resolution hypernuclear γ spectroscopy with FINUDA	89
4.8	Kaonic-atom physics	90
4.8.1	Precision measurements of kaonic hydrogen and deuterium	90
4.8.2	Kaonic-helium measurement	91
4.8.3	Measurement of other kaonic atoms	92
4.8.4	Sigmonic-atom physics	92
4.8.5	Precision measurement of the charged kaon mass	92
4.9	Time-like nucleon form factors	93
4.9.1	Moduli of Form Factors: cross section measurement	95
4.9.2	Phase of proton Form Factors: polarization measurement	96
4.10	Use of the LINAC/SPARXINO beam as a neutron source	97
4.11	Testing T invariance in electromagnetic interactions	98
4.12	Measurement of 2γ contributions in elastic scattering	99
4.13	Experiments with Synchrotron Radiation	99
4.13.1	Infrared	100
4.13.2	Soft X-Ray	101
4.13.3	VUV Beam Lines	102
4.14	Resonant detectors for gravitational waves	103
5	Participation to Offsite Activities	109
5.1	Accelerators	109
5.1.1	Linear Collider	109
5.1.2	EUROFEL	111
5.2	High Energy Physics	111
5.2.1	Physics at Tevatron	112
5.2.2	B physics at PEP-II	112
5.2.3	The LHC program	112
5.2.4	Kaon physics at hadron machines	113
5.2.5	Plans for the International Linear Collider	114
5.3	Hadronic and Nuclear Physics	114
5.3.1	Experimental measurements for accessing Generalised Parton Distributions	115
5.3.2	Transversity measurements	115
5.3.3	Exotic hadrons of multiquark states	116
5.3.4	Antiproton Physics at GSI with PANDA Spectrometer	117
5.3.5	Spin Physics at GSI: PAX project	118
5.3.6	The Quark Gluon Plasma at LHC: the ALICE experiment	119

5.4	Astroparticle physics	119
5.5	Neutrino physics	120
5.6	Interferometric detectors of gravitational waves	122
5.6.1	Long-term future of the GW experiments	123
5.7	Synchrotron Radiation experiments at ESRF	124
6	Plans in High-Technology Areas	129
6.1	Detectors for High Energy Physics	129
6.1.1	Gas Detectors: wire chambers	130
6.1.2	Gas Detectors: Micro-pattern	131
6.1.3	KLOE upgrades	132
6.1.4	Detector studies for next Linear Collider	134
6.2	Detectors for neutrino experiments and space physics	136
6.2.1	Detectors for neutrino physics	136
6.2.2	Detectors for space physics	136
6.3	Detectors for nuclear experiments	138
6.3.1	A Large Area Silicon Drift Detectors for SIDDHARTA	138
6.3.2	The central tracker for PANDA	138
6.3.3	Time Projection Chambers	139
6.4	Synchrotron radiation	139
6.5	Capillary Optics	140
7	Conclusions	143
8	Acknowledgments	147

Chapter 1

Introduction

The Frascati National Laboratory (LNF) is the largest structure of INFN (Istituto Nazionale di Fisica Nucleare), with 325 permanent positions (see Table 1.1), 50 temporary contracts, and 140 employees of Universities and other Research Institutions involved in the LNF projects. The Laboratory nowadays is for various, important aspects the product of the efforts devoted to the DAΦNE project, started in the 90s.

	Working in Administration	Technicians	Technologists	Researchers	Total
Directorate	2	-	-	1	3
LNF Administration	22	19	4	-	45
Accelerator Division	2	60	22	5	89
Research Division	12	76	18	82	188

Table 1.1: *LNF Permanent Positions in year 2004*

DAΦNE experience has to be considered extremely positive. Not only it has revived a long standing expertise in the field of building and running e^+e^- colliders, but it has also attracted a wide community of high-energy and nuclear physicists.

Three detectors have been built and have taken data at DAΦNE: a general purpose detector for particle physics, KLOE, a hypernuclear physics detector, FINUDA, and a detector for the investigation of low energy kaon-nucleon interaction, DEAR.

The ϕ -factory is a source of monochromatic, correlated kaon pairs and the KLOE experiment was optimized for the study of neutral kaons. Besides the measurement of neutral and charged kaon decays, the versatility of the DAΦNE project allows for a rich physics program, including measurements of kaonic atoms, hadronic cross sections, radiative ϕ decays, and hypernuclei spectroscopy, among other topics. Many of the interesting processes have cross sections of $\mathcal{O}(10^2)$ pb or smaller. For such precision measurements the collider has been designed to achieve a luminosity exceeding 10^{32} $\text{cm}^{-2}\text{s}^{-1}$ and the detectors to provide thousands of well measured events per second. The enterprise, challenging from the point of view of the collider and the experiments as well, gave the opportunity to learn and exercise different kind of professional skills, from the design and the construction of the collider components, to the construction of large particle detectors and the associated electronics, to the operation of huge computer farms, to the software development for data acquisition, data processing and simulation. Many students from Italian and foreign universities had the opportunity in the LNF to experience the wide spectra of physics issues related to the accelerator, to the experiments at DAΦNE and to the Synchrotron Radiation Facility.

The human resources and the structures allow relevant issues¹⁾ of the programs carried out in other Laboratories, like CERN, DESY, Fermilab, JLab, LNGS and SLAC to be pursued as well. The balance between the activities related to DAΦNE and the participation to the other projects has been demonstrated in these years to be really fruitful for the scientific impact and the international reputation of the LNF.

This document is centered on the physics cases that can suggest further developments of the collider and on the question of which kind of facilities can be envisaged for the mid-term future in the Lab.

The document is made up of other seven chapters. The next is devoted to a brief status report on the current activities. More details can be found in the Annual Report¹⁾ published yearly. The main on-going projects in the world of interest for the LNF are summarized in Chapter 3. The short, mid, and, in some cases, long-term plans are discussed in Chapters 4 and 5 separately for the accelerators and the experiments at Frascati and for the participation to accelerator projects and research activities in other Labs. The field of high-technologies such as particle detectors and electronics is presented in Chapter 6. Chapter 7 gives a summary and some conclusions.

References

1. INFN-LNF 2004 Annual Report - LNF-05/05 (IR) - available on <http://www.lnf.infn.it/rapatt>

Chapter 2

The INFN Frascati Laboratory

This chapter is intended as a status report of the wide range of research activities of interest for the LNF, supporting the opinion of a lively, well experienced scientific community.

The first part is devoted to the Accelerator Activities, starting with the technical services (Sec. 2.1) and discussing all the ongoing projects (Sec. 2.2, 2.3, 2.4, 2.5).

The second part is a status report of the Research Activities, including a brief description of the Computing Center in Sec. 2.6 and of the other Technical Services, reported in Sec. 2.7. The following sections are devoted to the experiments in High Energy Physics (Sec. 2.8), in Astroparticle and Neutrino Physics (Sec. 2.9), and in Nuclear Physics (Sec. 2.10). The Synchrotron Radiation activities are described in Sec. 2.11, while the topics of interest for the Theoretical Physics group are presented in Sec. 2.12.

Accelerator Activities

The Accelerator Division (AD) involves 42 physicists and engineers, and 62 technicians. The Division is organized into several technical services in charge for the design, the construction and the maintenance of the accelerator components and for the machine operation. Technical services in the AD include the electronic and diagnostics, the magnet engineering, the mechanical engineering, the cryogenics, the radiofrequency and the vacuum. All of them are briefly presented in Sec. 2.1.

Beginning from 1991, the AD efforts have been focused on the design, construction and commissioning of the ϕ -factory, DAΦNE, entirely conceived and realized at the LNF (Sec. 2.2).

In 2002 another machine project, the SPARC photo-injector for SASE-FEL experiments was proposed and funded. The SPARC design has been finalized and the project is entering the construction phase (Sec. 2.3).

Besides DAΦNE and SPARC, the AD is involved in other accelerator projects, as the Italian facility for hadron therapy CNAO (Sec. 2.4), and international projects (Sec. 2.5), such as the CTF3 and the TESLA-TTF programs, and collaborates to the R&D activities for the Free Electron Laser and the future Linear Collider, i.e. EUROFEL, CARE, EUROTEV.

Moreover, the AD participates to the design of the PEP-II B-factory upgrade, at SLAC, and to the study of new components for the Large Hadron Collider (LHC), at CERN.

2.1 Technical services in the Accelerator Department

2.1.1 Electronics and diagnostic

The group deals with the design, realization and maintenance of the electronics of the LNF accelerators, including the power pulsers of the injection kickers, the beam diagnostics, the controls, the feedback and timing systems. Specialized topics are covered by the “electronic” laboratory with advanced instrumentation (including Radio Frequency) and CAD; the “power” laboratory for development and maintenance of high-voltage/high-current power pulsers; the “diagnostic bench” for the characterization of transfer and coupling impedance of the diagnostic devices and the vacuum chamber components; the workshop for the production of limited series of custom electronic boards. The group is involved in the measurement and interpretation of beam characteristics, in the experimental aspects of beam dynamics and in the handling of beam instabilities, using also feedback systems.

2.1.2 Magnet engineering

The group has designed, realized and measured the ~ 350 magnets and 550 power supplies of the DAΦNE complex.

The group has the expertise to design conventional and superconducting magnets using the most recent simulation codes like Poisson (2D) and OPERA (3D). The last one has been recently updated also by TEMPO, the Vector Field code to simulate the thermal characteristics of the magnets. Once the magnet is built, it can be magnetically and electrically tested in the Magnet Measurement Hall, where different test-systems are available. An Hall-Plate-based measurement system allows the scanning of a volume as large as $2.5 \times 1.0 \times 0.4 \text{ m}^3$ with positioning precision of the order of $5 \text{ }\mu\text{m}$ and a magnetic field measurement precision of 0.05 Gauss. A second system is devoted to multipole magnets (like quadrupoles, sextupoles and so on) and allows the harmonic analysis of the magnetic field using the method of the rotating coil. Many different, high precision, power supplies are available in the hall to power magnets under measurement.

The group can also design the special power supplies for storage rings and synchrotrons, simulating their performance and defining their characteristics and main components.

2.1.3 Mechanical engineering

The mechanical engineering group is able to design any machine component (conventional or peculiar) using both, numerical codes to evaluate stresses or strains, and CAD solid modeling; to perform the alignment of the accelerator components, realizing the necessary reference networks and using advanced measurement techniques; to manage all the installation phases of complex components; to perform any specific mechanical measurement.

2.1.4 Cryogenics

The group is in charge of mechanical and cryogenic designs; of the operation of the superconducting and the cryogenic systems for the KLOE magnet and for the two DAΦNE compensating solenoids. Software tools widely used include Hepak for TS He diagram on excel platform; Ansys for the

structural and thermal finite-element analysis; Sinda/fluint for the thermofluidodynamics and the radiative calculation by finite-difference analysis; Autocad; Inventor. The group is responsible for the operation of the vacuum pumps (2 turbo, 1 big rotative); 1 small rotative with vapour pumping option, 1 scroll); 1 leak detector; 1 LN2 evaporator; 4 cryogenic adsorbers; 2 He purity detector; 1 He purity detector with pyrolizer (oil detection); 2 LN2 dewars; the cryogenics plant constituted by a Lind TCF 50 Refrigerator.

2.1.5 Radio-Frequency

The Radio Frequency (RF) group is in charge for the design, construction, operation and maintenance of the RF complex of the LNF storage rings. The complex includes the power plants, the RF cavities and structures, the low-level electronics and the computer controls. The design activity of the RF structures is based on the use of the best simulation codes presently available on the market, such as the High Frequency Structure Simulator (HFSS) by Ansoft, and the MAXwell Finite Integration Algorithm (MAFIA) by CST. The RF team has gained expertise in designing reliable and efficient systems, with special care for all the aspects related to beam dynamics. This approach, together with the implementation of dedicated feedback systems, is essential to store huge beam currents, as demanded by modern colliders. The RF group is also involved in the design and construction of the low-level and synchronization electronics of high pulsed power RF systems for Linear Accelerators, which is a crucial piece of hardware to minimize the beam emittance. The group is well-experienced as well in the design and construction of special devices for diagnostics and beam manipulation, such as beam deflectors, kickers, stripline monitors, RF shields.

2.1.6 Vacuum

Challenging aspects of the group activity include ultra-high vacuum system and related mechanics design for particle accelerators; vacuum brazing; realization of general and high vacuum systems.

Software packages widely used are Ansys for the structural and thermal finite-element analysis and CAD (Autocad, Inventor, Solid Edge). The group deals with the oil free vacuum oven; 3 oil free leak detectors; 1 standard leak detector; the cleaning facility for vacuum components (5 ultrasonic baths, up to 2m long, 2000 l distilled water tank, 2 drying ovens); 1 vacuum system for vacuum gauge calibration; 1 vacuum system for residual gas analyzer calibration; 5 residual gas analyzers; several vacuum gauges; several fore vacuum karts; sputter ion pumps; non-evaporable getter pumps; turbo pumps; 2 laminar-flow work benches; 1 metallurgical microscope; 1 low-energy electron gun; 1 ion gun; 1 pyrometer.

2.2 DAΦNE

DAΦNE¹⁾ is an e^+e^- collider at the center of mass energy of the ϕ resonance, 1.02 GeV. The beams circulate in two independent 97-m-long rings merging in two straight sections, the Interaction Regions (IR1 and IR2) and colliding with a horizontal crossing angle. A maximum of 120 bunches can be stored in the two rings; however a gap of 10 to 20 bunches is needed to get rid of the ions produced by the electron beam. The injection system includes the Linac, the intermediate damping ring and the 180-m-long transfer lines. The KLOE detector is permanently installed in IR1, while the DEAR and the FINUDA detectors share IR2. Two synchrotron-light beam lines for Infrared and X-rays are also operational. The history of DAΦNE can be summarized through its achievements in terms of peak luminosity, reported in Fig. 2.1.

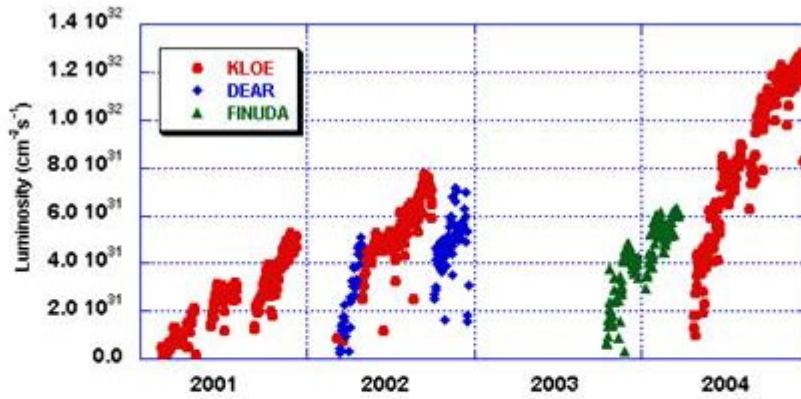


Figure 2.1: DAΦNE peak luminosity in 2001-2004.

At present, typical DAΦNE currents in collision are ~ 1.2 A for positrons and ~ 1.7 A for electrons, in 105 bunches. With these values a peak luminosity of $1.4 \times 10^{32} \text{ cm}^{-2} \text{ s}^{-1}$ has been achieved.

This performance has been obtained thanks to the continuous work aimed at increasing beam currents while keeping low background rates.

Simulations and machine measurements, an always progressing field, have been crucial to understand beam dynamics and beam-beam interactions, among other issues affecting luminosity. For the increase in beam currents a fundamental role is played by the longitudinal bunch-by-bunch and transverse feedbacks. Both, optimization of beam parameters (e.g. orbit, linear and nonlinear dynamics), and hardware modifications (e.g. scrapers and IR masks) are responsible for background reduction. The colliding currents, in spite of the intrinsic sensitivity of beam dynamics at low energy, are comparable to those obtained at the B-factories.

Coupling correction, tuning of the working point, lower IR beta functions and nonlinear dynamics studies have all contributed to the DAΦNE performance.

DAΦNE is the only high-luminosity factory to operate at such a low energy and to allow data taking for three experiments in two IRs, which has met thanks to the commissioning time devoted to machine optimization in the three rather different configurations.

A brief history of the collider performance is reported hereafter.

DAΦNE became operational in summer 2000 when KLOE started data taking at a peak luminosity of $10^{31} \text{ cm}^{-2} \text{ s}^{-1}$. KLOE is the most demanding experiment at DAΦNE in terms of integrated luminosity and background level on the detector as well. Through an optimization of the collider optics and the beam currents, a peak luminosity of $0.5 \times 10^{32} \text{ cm}^{-2} \text{ s}^{-1}$ was reached in autumn 2001 with 50 bunches.

Optics in IR2 were modified in 2002 in order to optimize the data taking of the DEAR experiment. The new configuration provided 30% reduction in the horizontal beam size at the first parasitic crossing and 20% increase in the horizontal crossing angle. This allowed DAΦNE to collide with 100 bunches, i. e. all RF (Radio-Frequency) buckets full except for the 20% ion gap, with currents up to 1.3 A for positrons and 0.8 A for electrons routinely used in collision. DAΦNE is the collider working with the shortest inter-bunch distance (2.7 ns or 80 cm) in the world. In four months an integrated luminosity of 68 pb^{-1} has been delivered to DEAR, sufficient for the experimental program, i.e. the observation of kaonic Nitrogen ²⁾ followed by the measurement of the kaonic Hydrogen ³⁾.

KLOE resumed operation in May 2002, running up to September 2002. The improvement in the collider performance, reaching the peak luminosity of $0.75 \times 10^{32} \text{ cm}^{-2} \text{ s}^{-1}$, was achieved

Experiment	L_{peak} [cm^2s^{-1}]	L_{int}/day [pb^{-1}]	L_{int} [pb^{-1}]	N. bunches
KLOE 2002	0.75×10^{32}	4.8	300	49
DEAR 2002	0.7×10^{32}	2.2	68	100
FINUDA 2003-2004	0.6×10^{32}	4.	256	100
KLOE 2004	1.26×10^{32}	7.6	780	105
KLOE Feb-Oct 2005	1.4×10^{32}	9.0	1000	109

Table 2.1: DAΦNE luminosities in the last 2 years

through continuous machine optimization.

During the shutdown in year 2003 FINUDA was installed in IR2, and in the meantime the collider structure was upgraded. Relying on the experience gathered during the runs for the DEAR experiment, the magnetic layout of IR1 was modified and all the quadrupoles were equipped with independently rotating supports in order to improve the coupling correction efficiency and the ring flexibility, making possible to work with arbitrary values of the KLOE solenoidal field, in particular with the KLOE magnet switched off during FINUDA data taking. For wider operation flexibility the new mechanical structure allowing for quadrupole rotation was installed in IR2 as well. The upgrade of the eight wiggler magnets was also important: each pole profile was modified adding longitudinally and horizontally reshaped plates on the poles to improve field quality. With these modifications the wigglers showed a significant reduction of the 2nd and 3rd order terms in the field around wiggling trajectories, thus improving dynamic aperture and consequently the integrated luminosity. A peak luminosity of $0.6 \times 10^{32} \text{ cm}^{-2} \text{ s}^{-1}$ and a total integrated luminosity of $\sim 260 \text{ pb}^{-1}$, with low background rates, was delivered to FINUDA, which has fulfilled the first part of the physics program, that will be completed in 2006.

In spring 2004 FINUDA detector was rolled out and DAΦNE restarted operation for the KLOE experiment, which will continue data taking until the end of 2005. Continuous tuning of machine parameters has allowed colliding currents, number of bunches and lifetimes to be increased, and background rates to be kept lower than the level measured in 2002.

A summary of the delivered luminosities in the last two years is in Table 2.2, while Fig. 2.2 shows the time sharing between KLOE, DEAR and FINUDA.

2.2.1 DAΦNE Beam Test Facility

DAΦNE Beam Test Facility (BTF) ⁴⁾, operational since November 2002, is a beam transfer line optimized for the production of pre-determined numbers of electrons or positrons in a wide intensity range, from single particle to 10^{10} particles per pulse, and energy from few tens of MeV up to 750 MeV. The pulse width can also be changed, either 1 or 10 ns, at a maximum repetition rate of 50 Hz. The facility in single electron mode is particularly suitable for testing particle detectors, allowing energy calibration and efficiency measurements to be performed, while beam diagnostics devices can be studied at high intensities. Operation is shared with the data taking of the experiments at DAΦNE thanks to the beam attenuation and energy selection system which allows for sharing the accumulator ring transfer line. The facility showed a very good performance, both from the point of view of operation reliability and flexibility in order to fulfill the experimental requirements. In the last two years many experiments, like AGILE, AIRFLY, APACHE, BTeV, CaPiRe, CRYSTAL, FLAG, LCCal, LHCb, MCAL, MEG, NANO, RAP, SIDDHARTA, carried out successfully the study of detector prototypes at the test-beam with very different beam conditions in terms of intensity and energy.

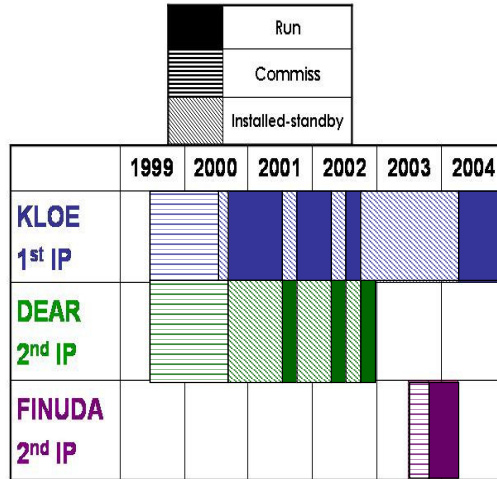


Figure 2.2: Time sharing of the experiments at DAΦNE .

2.3 SPARC

SPARC ⁵⁾ project is an R&D activity proposed by ENEA, INFN, CNR, Roma Tor Vergata University and INFN-ST; it has been funded in June 2003 by the Italian Government with 11 MEuro (70% from the Government and 30% from INFN) and a 3 years time schedule.

Main goal of this project is to build an advanced photo-injector for the generation of a high brightness electron beam at 150 MeV, able to drive a self-amplified spontaneous free-electron laser (SASE FEL) experiment in the green visible light (500 nm) and higher harmonics generation. This activity aims at acquiring expertise in the construction, commissioning and characterisation of an advanced photo-injector system and at performing experimental investigations on two theoretical predictions recently conceived, namely the new working point ⁶⁾ for high brightness RF photo-injectors and the velocity bunching technique to achieve RF bunch compression through the photo-injector with emittance preservation ⁷⁾.

The injector is presently being built inside an available bunker of the LNF: the general layout of the system is shown in Fig. 2.3. The system consists of a 1.6 cell RF gun operated at S-band and high peak field on the cathode (120-140 MeV/m) with an incorporated metallic photo-cathode, generating a 6 MeV beam to be properly focused and matched into 3 accelerating sections of SLAC type (S-band, travelling wave).

The first planned experiment will be the test of the beam emittance compensation method by means of the measurement of the emittance oscillation in the drift after the gun, where a double-minima behavior is expected. For this purpose a dedicated movable emittance measurement station has been designed ⁸⁾. The characterization of the longitudinal and transverse phase space of the

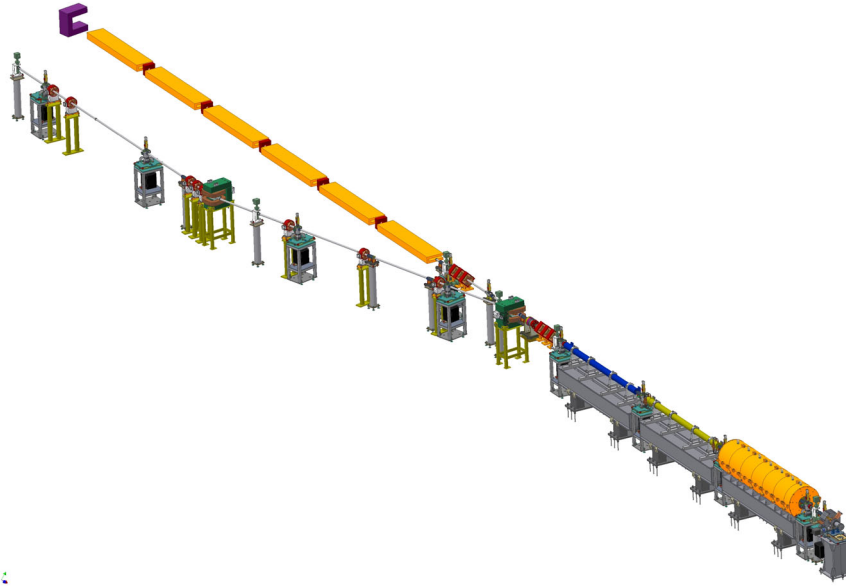


Figure 2.3: Layout of SPARC R&D project.

beam is another crucial point to establish the photo-injector performance.

The ultra-brilliant beam photo-injector will be used as a SASE FEL-based source. The FEL SASE experiment will be conducted using a 15-m-long permanent magnet undulator built by ENEA.

2.4 CNAO

High-energy ionising radiation has proved to be effective in the treatment of cancerous tumours by causing double-strand breaks in the cell DNA. In particular, hadrons, i.e. protons and light ions, have the useful property of penetrating the body at a depth which depends on their initial energy. The primary aim of the CNAO (Centro Nazionale di Adroterapia Oncologica) project is to design and build a machine for the proton and carbon ion cancer therapy with a high precision active scanning, a technique that uses a pencil beam to localize the tumour with sub-millimetric accuracy. Longer times with smoother beam spills are required for this treatment to facilitate the on-line dosimetry and the accelerator has to produce a well focused beam with a high spatial precision and well defined energy. A dedicated foundation has been instituted to build the CNAO centre in Pavia (Italy)⁹. A collaboration agreement signed in November 2003 made the INFN co-responsible in CNAO for the construction of the accelerator complex. The collaboration will cover the period 2004-2007, when the CNAO Centre will deliver the first dose to the first patient. INFN funded the project for ~ 4 MEuro out of a total cost of ~ 70 MEuro. The sketch of the accelerator complex is shown in Fig. 2.4.

The LNF AD is in charge for the design, construction and test of the conventional magnets and their power supplies; for the magnetic measurements; for the design, construction and test of the vacuum system; for the design, construction and commissioning of the electric and fluid plants; for the installation and alignment of the accelerator components; for the design of the radioprotection system.

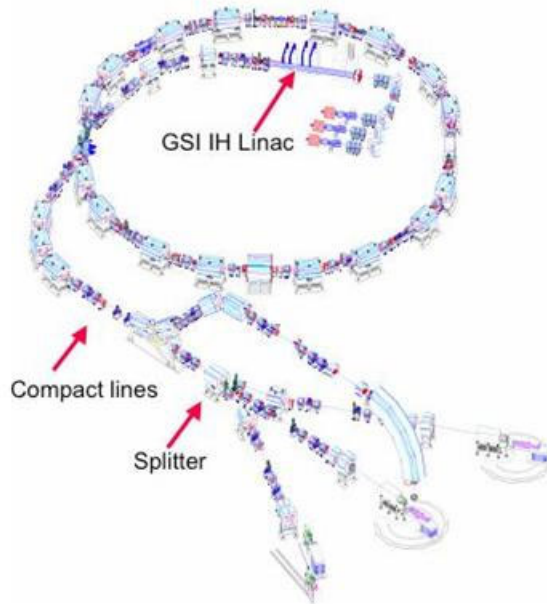


Figure 2.4: The CNAO accelerator complex.

2.5 International Projects

2.5.1 CTF3

The Compact Linear Collider (CLIC) is the international project for a multi-TeV e^+e^- collider based on a new two-beam acceleration concept: a high-intensity drive beam powers the main beam of a high-frequency (30 GHz) linear accelerator with a gradient of 150 MV/m by means of transfer structure sections¹⁰. The aim of the CLIC Test Facility 3 (CTF3) is to make exhaustive tests of the main CLIC parameters. INFN-LNF contributes to the realization of the recombination system, consisting of two rings that multiply the bunch frequency and pulse current by a factor of ten. CTF3 is being realized as an intermediate step to demonstrate the technical feasibility of producing 30 GHz RF power at the required intensity and pulse length, so that all 30 GHz components for CLIC can be tested at nominal parameters. The facility is in the realization phase in the existing infrastructure of the LPI (LEP Pre-Injector) as a collaboration between CERN, INFN-LNF, LAL (France), SLAC (USA) and Uppsala University (Sweden).

LNF budget for years 2003-2006 is 2 MEuro. The AD is in charge for the design and the realization of the transfer lines from the Linac and the first of the two rings of the compressor system called Delay Loop (DL). At the exit of this ring the frequency of the bunches coming from the Linac (1.5 GHz) will be doubled with an increase of the average current by a factor of two. Two RF deflectors to be used in CTF3 combiner rings have been built and tested at LNF¹¹. The first part of the CTF3 transfer line has already been installed: it includes a chicane in which, because of the very flexible lattice and large aperture vacuum chamber, it is possible to change the bunch length in a wide range by tuning the R_{56} element of the transfer matrix. The magnetic layout of the Delay Loop has been completed using existing dipole and quadrupole magnets of the EPA (Electron-Positron Accumulator) complex at CERN, together with the injection/extraction septum magnets. Vacuum chamber components and new magnets have been studied, designed and built.

Prototype construction was completed in 2002, transfer line and chicane were installed and commissioned in 2004, Delay Loop installation and commissioning are planned for 2005.

2.5.2 TESLA/TTF

TESLA (TeV Energy Superconducting Linear Accelerator) is an international collaboration for R&D on a superconducting e^+e^- collider in the TeV energy range. In March 2001 TESLA has published the Technical Design Report (TDR) ¹²⁾ for a Linear Collider with integrated Free Electron Laser for X-ray production. The accelerator consists of two 33-Km-long Superconducting Linacs, an Electron Gun, a Positron Source, two 17-Km-long Damping Rings (DR) with dog-bone shape, and a Beam Delivery System to drive beams in the Final Focus where the beam sizes are squeezed. For the TDR the LNF AD has chaired the realization by Ansaldo Ricerca of the technical design and the cost estimate of the DR ¹³⁾. The DR are a critical part of the injector complex responsible for producing the tiny vertical emittances needed to obtain high luminosities. These rings require state-of-the-art designs for most systems. The 1 ms injected linac bunch train corresponds to about 350 Km and ~ 3000 bunches with bunch distance of ≈ 400 ns. The length of the DR is determined by the capability of the injection system to reduce the bunch distance. With a DR 17 Km long, the bunches has to be compressed by a factor 20, leading the bunch distance at 20 ns. The inverse process of bunch decompression is necessary at the extraction point, before the injection in the linac. An injection/extraction scheme for TESLA based on RF deflectors, opening the possibility of obtaining a much shorter bunch distance and shorter ring circumference, has been suggested by the LNF group and a solution for the present DR design has been worked out ¹⁴⁾. TESLA collaboration also operates a test facility at DESY (TTF), aimed to demonstrate the feasibility of a SC Linac and SASE FEL. After the successful operation of TTF-I, which has produced coherent radiation at 80 nm, a second generation test facility which will be used as VUV FEL is now operational. The AD collaborates with TTF-II on the diagnostic, emittance measurements, image elaboration and transfer, and on beam dynamics studies.

2.5.3 Other International Projects

SLAC and KEK Laboratories have studied upgrades to their B-factories with the aim to reach, in a ten year span, peak luminosities of the order of 10^{35} to 10^{36} $\text{cm}^{-2} \text{s}^{-1}$. At PEP-II the possibility to reach a 3×10^{34} $\text{cm}^{-2} \text{s}^{-1}$ peak luminosity with minor modifications of the present machine layout is currently under study. The upgrade, having a small impact on the accelerator, could be operational already in 2006-2007. In this framework LNF AD and PEP-II AD collaborate to the design of a modified Interaction Region, with lower β_y^* and possibly a crossing angle (similar to the DAΦNE and the KEK-B design) to increase the number of colliding bunches while keeping small parasitic crossing tune-shifts, and therefore increasing the luminosity ¹⁵⁾. The design of a new longitudinal feedback kicker for high beam currents, originally developed at LNF, has also been applied to the PEP-II Low Energy Ring (LER) ¹⁶⁾, and the kicker has been installed in September 2004. RF issues at high currents and assessment of longitudinal feedback and low-level RF, able to cope with a higher number of bunches (1700) and higher currents are also under study at LNF.

A collaboration with CERN for the LHC project has been established to study vacuum chamber components and to make impedance calculation and optimization, in particular for Beam Position Monitors, Collimators, Recombination Chambers and the so-called “coldex” section of the Super Proton Synchrotron SPS ¹⁷⁾.

Finally, the AD is also involved in R&D activities refereed by the INFN Scientific Committee V, such as: *e-Cloud*, an R&D activity for the study of instabilities in proton and positron rings (e.g. LHC and DAΦNE) due to the formation of the so-called e-cloud, with beam measurements and the analysis of the vacuum pipe materials (started in 2004); *CORA*, for the study of a RF compressor for the SPARC accelerator (completed in 2004); *SAFTA2*, for the simulation of the impedance in the LHC beam pipe (through 2005); *SALAF*, for the design of 11 GHz accelerating

structures (new proposal for 2005).

Research Activities

The Research Division, besides people directly involved in the experiments, is constituted by several technical services providing the necessary support for the whole department and, as in the case of the Computing Service, is in charge also for special projects of general interest for the INFN.

2.6 Computing and Dataweb

In this section a status report of the initiatives in the field of computing and related issues, is given. The report includes the LNF Computing Center, the Dataweb project, and the KLOE Computing Center; the last being presented because is currently one of the largest in the INFN.

2.6.1 Computing service

The Computing Service is in charge for the management of the central computing resources and for the configuration and operation of the network of both, the Laboratory, and the INFN Central Administration.

It provides also technical support in order to install and operate the Informatic System of the INFN, used by central and local administrations. The INFN Informatic System is installed on a computer cluster running the SUN-Solaris operative system, which has been configured as the Oracle Database Server for the relational storage of any information concerning personnel, finance, research activities, legislation, etc. Two additional computer clusters running, respectively, the SUN Solaris, and the Windows operative system, have been configured as Application and Presentation Server for the Oracle DataBase to interfacing the administrative procedures. The second cluster is devoted to the handling of documents and, in particular, to the automatic assignment of the reference labels to administrative papers. The system includes the SAN (Storage Area Network) for data storage on disk.

The local network is constituted by a complex structure based on optical fibers connecting the buildings one each other, and on copper cables within each building; by the routing and switching devices ensuring Ethernet connectivity at 10/100/1000 Mb/s; by the wireless network devices; by essential services like DHCP, DNS, etc., and by the devices devoted to the Informatic Security like Firewall, VPN Concentrator, etc.

At present, the central computing resources include:

- computers and other devices to operate the local storage system, mainly based on SAN (Storage Area Network) with Fiber Channel connection. An integrated system of servers is used in order to manage the distributed File Systems (AFS, NAS, etc.) together with the automated magnetic-tape library for backup/restore and archive/retrieve operations;
- computers devoted to the management of the essential services like Mail relay, IMAP, Antivirus, Antispam, Web, Proxy, Authentication, Monitoring, Database, etc.;
- a computing farm for the users;
- a computing farm integrated in the European GRID;
- X-Terminals, printers and other distributed peripherals.

Finally, the Computing Service provides support to the users for central computers, distributed peripherals, and also for the workstations and the PC's used by the INFN personnel, the students, and the employees of Universities and other Research Institutions involved in the LNF activities.

2.6.2 Dataweb

A system of Web Servers and Database MySQL has been realized during the last two years and installed on computers belonging to the LNF Computing Center. The project is finalized to improve the sharing of scientific and administrative information within the INFN. It recently became an INFN Service named Servizio Coordinamento Banche Dati Ricerca (Dataweb).

The people working on the Dataweb project is divided in two groups, those devoted to the System Administration, belonging to the Computing Center, and those devoted to the database and web-application development.

Main activity of the Service is the support to the Scientific National Committees covering the three phases of the cost estimate, the finance allocation, and the Scientific final report on the funded experiments.

All the information collected along the year on the three phases can be shared and used to realize both, the INFN annual previewed budget, and the report on the scientific activity which is provided in two forms, a detailed report for internal use, and a summary for general public.

The Dataweb System is the main tool for the collection of the documents needed in order to write the annual evaluation report and the INFN Products selection, requested by the Italian Research Department.

Moreover, the Dataweb has realized the web site devoted to internal job training and the web site to start the procedure for obtaining the permit to be associated to the INFN scientific activities, which is annually used by about 3000 researchers from the main Italian Universities.

The Dataweb project, summarized in the Tab.2.2 includes also the archiving in a relational Database of the collection of multimedia documents constituted of images and historical video realized in the INFN structures that will be available on INFN web site.

The entire software system has been realized with the open source standard LAMP (Linux-Apache-MySQL-Perl-PHP), that allow the cost reduction on the side of the software licences (all these packages are in fact free of charge) and shows a good flexibility for the development of web applications.

Main hardware is constituted of few servers:

- 5 cpu units for the web servers ;
- 2 cpu units for the database servers ;
- 1 cpu unit for the server streaming;
- 2 servers for software development.

Work is in progress to interface the Dataweb with a new system realized by the Oracle-Bull Company that will provide a more efficient connection between administrative and scientific information.

2.6.3 KLOE computing center

The KLOE computing center is currently one of the largest of the INFN, dimensioned to process up to 8 pb^{-1} of integrated luminosity at DAΦNE per day (i.e. of the order of 5×10^7 completely reconstructed events per day), to reach a substained throughput of the order of 100 Mb/s, and a total storage capacity in the PetaByte range.

General	Outreach	Administrative
Home Pages : INFN, LNF Conferences LNF Seminars INFN Preprint Associations to INFN activities Finance Estimates and Final Reports Master and PHD Thesis INFN Evaluation and Product Selection Thesis at LNF	Image database : INFN, LNF INFN Brochure INFN News Press Office INFN Home Page Press Review	Home Page : INFN CA Legal Papers Insurance FAI Founds Selections & Fellowships Job Training Finance Allocation

Table 2.2: Topics covered by the Dataweb project.

The offline farm consists of 24 IBM 7026-B80 SMPs running AIX, each with four 375-MHz Power3 CPUs, and 10 IBM p630 servers, each with four 1.45-GHz Power4+ processors, providing a total processing power equivalent to about 60 000 SPECint2000.

At present, 80% of the processing power is used for production-related tasks; the remainder is allocated to physics analyses. Additional machines can be opened to user batch and interactive sessions as the need arises.

From the point of view of both hardware and software, the operation of the offline system is seen to be smooth and reliable.

As part of an offline-system upgrade for the year 2005, 24 new 1.9-GHz Power5 processors will be acquired. This increases the total CPU power to about 110 000 SPECint2000.

When new data are acquired, the online servers write the raw files to the online-disk pool. These files are then asynchronously archived to the tape library over an NFS mount by the archiver daemon. The archiving processes are tailored to minimize the number of tape mounts while guaranteeing enough space on the disk pool.

Normally, reconstruction is performed while the raw files are still resident on disk. For input to the reconstruction processes from the online disk, events are either read across an NFS mount or served by the data-handling system using a custom TCP/IP protocol, which is provided by the KLOE Integrated Dataflow package. Reconstruction output is written via NFS to the offline-disk pool, from which it is asynchronously archived to tape. DSTs for each run are produced from the reconstruction output files, usually immediately after the run has been completely reconstructed. When files already archived and deleted from the online- or offline-disk pools must be processed on the offline farm, the data-recalling daemon restores the files from tape to the disk cache, from where they are served to the offline processes using a custom package, KID. The spacekeeper daemon ensures the availability of disk space in the staging areas by deleting files that have been archived.

The same model for data access used for reconstruction applies to user analysis jobs running on the offline farm.

A central database based on DB2 is used to keep track of the locations of the several million files comprising the data set.

Data are permanently stored in two IBM 3494 tape libraries. The first library has 12 Magstar 3590 tape drives which can read and write at 14 MBs, dual active accessors, and space for about 5400 60-GB cartridges, for a maximum capacity of 324 TB. The second library has 6 Magstar tape drives, dual active accessors, and space for 4000 300-GB cartridges for a maximum capacity of 1200 TB. The libraries are maintained using IBM's Tivoli Storage Manager. The experiment will reach a total data storage of about 800 TB when data acquisition, data reconstruction

and Monte Carlo production for the entire data set of about 2.4 fb^{-1} will be completed, during the second quarter of year 2006.

A 6.3-TB offline-disk pool is used for data transfers to and from the library. The disk pool consists of Fibre Channel (FC) and SSA disks. Two IBM servers mount the offline-disk pool and tape libraries. With the two file servers working in concert, aggregate I/O rates of over 100 MB/s have been obtained.

Analysis jobs usually use DSTs (Data Summary Tapes) as input. About 5.5 TB of the offline disk pool is used to cache files recalled from the tape library by the data-handling system; copies of the bulk of the DSTs reside in this cache for prompt access. The total disk space needed for the efficient handling of the final data set will be of about 50 TB.

The output from analysis jobs is written to user and working-group areas on the KLOE AFS cell. The AFS cell, of total capacity of 2.2 TB, is served by two IBM 7026-H70 SMPs. Users can access the AFS cell from PCs running Linux on their desktops to perform the final stages of the analyses.

2.7 Technical services for experimental setup

2.7.1 Detector development

Research Division includes the Technical Services for R&D on particle detectors and for the construction of experimental setup, namely the “Servizio Sviluppo e Costruzione Rivelatori” or SSCR.

It includes three departments devoted, respectively, to Design, Construction, and Metrology. They are in charge

- for mechanical design of the experimental setup and detectors, exploiting also the performance of the CAD/CAE software design systems;
- for detector-prototype construction; realization of large detector systems; design and construction of precise mechanical structures. A wide set of mechanical tools are routinely used, including the numerical control machines of which the most recent acquisition has been a lathe capable of auto-learning for high-precision works;
- for dimension and operation tests; alignment of mechanical structures and experimental setup; material characterization. The instrumentation includes a computerized metrology center, a machine for material characterization, a computerized teodolite, and, recently, a machine for traction and compression tests of the materials;
- to contact the companies and to commission the realization of large mechanical structures.

The SSCR has been recently involved in a series of activities related to the experiments currently running at the LNF and in preparation for taking data outside. The SSCR has provided technical support for the opening and the closure operations of the KLOE experimental setup; has designed and realized the Automatic Wiring Machine for mass production of the ATLAS MDT's, the components for the assembly and the handling of these chambers, and the containers for their warehousing and transport, participating also to the preparation of the procedures for final installation at CERN and performing precise measurements on mechanical items for the assembly; has designed the mechanical structure for the OPERA detectors and participated to the final assembly at LNGS studying the procedures for installation and performing the alignments. OPERA has realized an automated machine to assembly the emulsion bricks, and the SSCR has contributed to the design and to the drafting of the technical document needed to carry out the bid for choosing the constructor company. Further work on this topic has been done to design a packing procedure for the emulsion bricks. The design and the realization of some mechanical items of the support structure of the muon-detector system for the LHCb experiment has been recently finalized after completion of the studies on prototypes. Moreover, the SSCR performed dimension tests of

the frames for the MWPC's and the maintenance of the moulds for their production together with the realization of some tools and mechanical items for the chamber assembly. Other contributions have been given to the design of the support structure for the straw-tubes of the BTeV experiment; to the construction of the frame of the Main Electronic Box for Lazio-SiRad; to the setting up of the BTF, and to the detectors of NEMO, CAPIRE, BABAR, FINUDA, HERMES, TIBET, among other experiments that have required support to the workshop and to the metrology department, using a total of about 30% of the available manpower.

2.7.2 Engineering Support for experimental apparata

The “Servizio Progettazione Apparati Sperimentali” or SPAS is in charge for the study and the design of parts of the large experimental setup required by the LNF research programs.

ATLAS, FINUDA, MAGIA and OPERA are among the experiments recently supported.

The SPAS involves one engineer and four mechanical designers which routinely use CATIA as 2D/3D modelling CAD system, CALCING for structural calculations, and ANSYS for finite-element analyses.

In particular, the service takes care of the technical reports needed in order to carry out the bids for choosing the constructor companies of different kinds of components of the experimental setup; these are often very peculiar items based on custom designs fulfilling experimental requirements that are unique. The SPAS is in charge also for the supervision of the installation procedures and for the performance tests on the operational setup.

2.7.3 Electronic workshop

The electronic workshop provides support for particle detector instrumentation. Workshop expertise has grown up according to the experimental requirements, ranging from design of the DC power supplies, to low S/N processing of high-frequency signals, to the design of high-density FPGA.

In the following, some examples of the design activity recently carried out for KLOE, OPERA, HERMES and LHCb are given.

Low S/N processing of high-frequency signals. KLOE drift chamber, 3.3 m long and 4 m in diameter, is one of the largest drift chamber used in HEP experiments. The drift chamber has 12582 sense wires and is flushed with an He-based gas mixture. Besides the detector dimension, the challenging aspect of the project was the requirement for the readout electronics to be sensitive to the first ionization cluster, with 1.6 electrons on average. The overall design (front-end and detector grounding) allows chamber operation at a threshold as low as 3 fC.

Fast signal processing. The second detector of the KLOE experiment is a Pb-scintillating fiber electromagnetic calorimeter. It is equipped with about 5000 fast photomultipliers producing high bandwidth level signals. Since precise timing information is crucial for data analysis, special techniques have been used for the readout signal chain (i.e. high bandwidth preamplifiers and low time-walk discriminators) to maintain the overall timing resolution within 50 ps.

LV power supply systems. One of the sources of timing jitter when dealing with very high timing resolution systems, is the power supply residual ripple. To reduce as much as possible the ripple of the generators used to supply the e.m. calorimeter timing system, the workshop has developed a special 600 W power supply powered by three-phase AC line.

HV measurement system. The OPERA experiment uses RPCs to instrument the detector spectrometer. To minimize the number of HV power supplies, many RPCs are supplied with the same HV channel missing information about single RPC dragged currents (i.e. one of the most important parameters to control the RPC status). To overcome the problem a high-voltage, high-range measurement system have been developed. The instrument can measure currents ranging

from nA to μA at a maximum voltage of 5 kV. Each system is made of 24 channels and is managed by a CAEN interface.

High frequency data transmission through optical links. One of the components of the front-end electronics of the LHCb muon spectrometer is the Off-Detector Electronics system. The system is made of about 150 boards. Each board is capable of processing up to 192 LVDS input signals at a frequency of about 40 MHz and of sending them to the trigger and DAQ by means of 13 optical fibers with a sustained throughput of 1.6 Gbits/sec and a BER less than 10^{-16} .

High frequency signal transmission. A low-noise, high-frequency analog signal transmission system has been designed for the HERMES experiment. The system, based on custom transmitter and receiver crates, with dedicated low-noise power supplies, uses twisted-pair copper links to manage DC coupled signals with bandwidth up to 300 MHz.

High density digital devices. The FPGA complexity has increased enormously in the last years. At present, state-of-art FPGA consists of nine hundred BGA pin devices, incorporating a 3.2 Gbits/sec serializer/de-serializer and an embedded power-pc. To manage such complex device, the old schematic design procedure has been replaced by a language-based (VHDL, Verilog) design. The LNF workshop uses since a few years the language-based design procedure and organize annually teaching courses on the subject.

DAQ boards Besides systems and boards already mentioned, the workshop has developed several VME boards for data acquisition. Some examples of these boards are :

- the 32-channels-continuous-sampling ADC for dE/dx measurements with the KLOE drift chamber;
- the 64-channels scaler for rate measurements used in the quality-control procedure for the construction of the LHCb MWPC's;
- the 8-channels-3.2 Gbits/s-optical-link-transmitter/receiver board for the front-end readout of the ATLAS MDT's.

Embedded processors. Embedded processors are widely used both, to manage system configurations, and to readout data by means of standard communication protocols. The LNF workshop has developed systems based on embedded processors supporting RS232, CAN and LAN communication protocols.

2.8 Particle Physics at Accelerators

The LNF personnel involved in the activities of interest for the INFN Scientific Committee I (CSN1) ¹⁸⁾ is composed by 68 physicists, 33% of which are in the KLOE Collaboration, 33% in the CERN Experiments (ATLAS and LHCb), and the others in the USA Experiments, at Fermilab (CDF-II, E831-FOCUS and BTeV) and at SLAC (BABAR).

People with permanent positions are 41, 4 are under temporary contracts, 8 are Doc and Post-Doc Students and 15 are employees of other Institutions involved in the CSN1 projects carried out at the LNF.

A total man power of ~ 25 technicians represents the available support for the experiments, in the particle detector design, construction, test and maintenance. A quarter of the technicians are mostly devoted to the detector read out electronics, and the others to the mechanics and the operation of the devices. The construction phase itself has been often carried out by private firms on designs finalized by the LNF personnel or has been realized in the Lab involving people coming under temporary contracts.

The experiments are undergoing different phases of their life, from design to construction and installation, to data taking and data analysis. More than 50% of the physicists will get involved into new projects within 3-4 years, so that it is of particular interest to discuss now about different

open perspectives for the Lab.

2.8.1 KLOE

The KLOE experiment ¹⁹⁾ has been designed primarily for the measurement of all the relevant CP and CPT violation parameters in neutral kaon decays. The large amount of neutral kaon pairs ($\sim 10^{10}$) produced by DAΦNE with 10 fb^{-1} of integrated luminosity, would allow the measurement of $\text{Re}(\epsilon'/\epsilon)$ with a statistical accuracy ($\sim 10^{-4}$) comparable to the fixed target experiments but with completely different systematic effects.

Kaon pairs are produced at DAΦNE in a state with well defined quantum numbers (those of the photon) and are emitted almost back to back. These unique features allow for the determination of the nature of each produced kaon by looking at the decay of its companion in the opposite direction (*tagging*), as well as to perform quantum interferometry measurements.

The research program of the experiment includes measurements of numerous decays of charged and neutral kaons, radiative ϕ decays, and measurement of the hadronic cross section, among other topics.

The most interesting channels have a branching ratio of $\mathcal{O}(10^{-3})$ or smaller. For precision measurements of these decays, the KLOE detector, i.e. the drift chamber and the calorimeter, has been designed to provide thousands of well measured events per second.

KLOE is by far the largest and most complex detector built in the Laboratory. The drift chamber, 2 m radius, 4.2 m length, for a gran total of 52140 wires is the largest drift chamber ever built. The performance specifications for its use are very demanding to guarantee good momentum resolution for low energy particles and low absorption for photons. The requirement of high transparency poses severe constraints in the choice of materials and thickness of the chamber walls, in Carbon fibers. Many innovative techniques have been devised for the construction of the mechanical stucture and the stringing of the wires ²⁰⁾. The use of low density, high ionization potential gas is highly demanding for the front-end electronics.

The lead-scintillating fibers electro-magnetic calorimeter was designed to detect with very high efficiency photons with energy as low as 20 MeV, and to accurately measure their energy and time of flight. Particularly relevant is the performance in terms of time resolution, which scales as $57 \text{ ps}/\sqrt{E(\text{GeV})}$. The modules of the end-cap calorimeter are C-shaped to minimize dead zones, a solution which was never tried before ²¹⁾.

The ϕ production cross section is about $3 \mu\text{b}$ so that the event rate from ϕ decays at the reference luminosity of $5 \cdot 10^{32} \text{ cm}^{-2} \text{ s}^{-1}$ is 1.5 kHz, to which a similar yield of Bhabha events plus machine background and cosmic rays must be added. With an average event size of 2.7 kB, KLOE needs a data acquisition ²²⁾ capable to handle with high efficiency a throughput of 10 Mbytes per second, a data processing environment with file servers providing a bandwidth of order of 100 MBytes/s, and a data storage in the Petabyte range.

The high sensitivity $\mathcal{O}(10^{-3})$ needed to study CP violation effects and the quantum interference patterns in the neutral kaon system, requires a careful control of the systematics so that billions of well simulated events, including the most realistic description of the beam background, must be generated ²³⁾.

All these numbers put the KLOE experiment on the side of the challenging projects, dimensioned like the major HEP experiments running nowadays.

Although the integrated luminosity is not sufficient yet to complete the ambitious program of the experiment, KLOE has demonstrated to fulfill the experimental requirements producing several important physics results with the $\sim 450 \text{ pb}^{-1}$ collected in years 2001-2002. These span from rare or medium-rare K_S and K_L decays ²⁴⁾, to charged kaon decays ²⁵⁾, and to the study of the nature

of scalar and pseudoscalar mesons through radiative ϕ decays²⁶⁾. In particular, the measurements of the semileptonic decays of charged and neutral kaons, together with a novel determination of the f_K form factors and with the improvement in precision of the K_L and K^\pm lifetimes will provide a more strict test of the unitarity of the first row of the CKM matrix. Preliminary results on this topic have been presented at ICHEP04²⁷⁾. Another important, recently published result is the measurement at the percent level of the $e^+e^- \rightarrow \pi^+\pi^-\gamma$ cross-section below 1 GeV, which has relevant implications in the theoretical interpretation of the muon magnetic anomaly²⁸⁾.

2.8.2 BABAR

BABAR is an experiment running at the SLAC asymmetric B-factory PEP-II; the physics program is centered on, but not limited to, the study of the CP violation effects in the decay of neutral B mesons. The B system is the best suited to study CP violation because the expected effects are large, should appear in many final states and, most importantly, can be directly related to the Standard Model parameters. The large data sample now being collected has already allowed significant advances in a large number of topics in B^{29, 30, 31)}, charm³²⁾ and top quark physics.

PEP-II (see also 3.7.4) is a two-ring e^+e^- storage ring, colliding 9 GeV electrons with 3.1 GeV positrons, energies chosen to maximize the production of B mesons. The c.m. energy corresponds to the mass of the $\Upsilon(4S)$ resonance which decays 50% in B^+B^- , 50% in $B^0\bar{B}^0$. The energy asymmetry is necessary to boost the B mesons momentum, so that the decay length can be measured with the accuracy needed to prove the CP violation effects.

During the year 2004 PEP-II has successfully committed a new operation mode in which both beams in the high- and low-energy ring are continuously refilled, resulting in quite remarkable improvements on the machine stability of operations, and consequently on an average luminosity greater than 700 fb^{-1} , routinely achieved in one day.

The BABAR detector³³⁾ has been designed primarily for CP studies, but it is also serving well for the other physics objectives of the experiment. The asymmetry of the beam energies is reflected in the detector design: the apparatus is centered 37 cm ahead of the collision point, along the direction of the high-energy beam, to increase forward acceptance and all services are placed on the opposite side of the detector, in order to minimize multiple scattering in the forward direction.

The momentum of the charged tracks is obtained from the curvature in a solenoidal field of 1.5 T and is measured in a low mass Drift Chamber. Different species of hadrons are identified in the DIRC, a dedicated device of a novel kind, based on the detection of Čerenkov light. Excellent photon detection and electron identification are provided by a CsI crystals electromagnetic calorimeter.

Muons and neutral hadrons are identified in the iron magnet's yoke, made of a 6-sided barrel and 2 endcaps with a total thickness of 65 cm of Fe plates, segmented in 18 slabs of graded thickness (from 2 to 10 cm) and instrumented with Resistive Plate Counters (RPC's).

The LNF group involved in BABAR has designed, built and installed the RPC's, contributed to many aspects of the software environment, and is currently participating to analyses, including the measurement of branching fractions of D^* mesons, of CP-violation angles, and of spectroscopic processes accessible via Initial State Radiation (ISR).

2.8.3 Experiments at Fermilab

The LNF participates to the CDF, FOCUS and BTeV Collaborations at the Fermilab TeVatron collider.

During the data taking period currently in progress (RUN-II), the Tevatron is being upgraded to reach the luminosity of $2 \times 10^{32} \text{ cm}^{-2} \text{ s}^{-1}$ by shortening time interval between bunch crossings to 132 ns. Consequently, the CDF-II detector underwent substantial upgrades. The LNF group constructed the iron-scintillator calorimeters and is currently responsible for hardware maintenance and calibration. Additional responsibilities in RUN-II are the control of the high-voltage system for central and end-wall calorimeters, the realization of discriminator boards for the calorimeter timing and the development of the Central Analysis Farm. There are short-term plans to contribute also to an upgrade of the HV system of the central tracking chamber.

The Tevatron performance has improved substantially over the last two years reaching a peak luminosity of $8.2 \times 10^{31} \text{ cm}^{-2} \text{ s}^{-1}$ and delivering more than 500 pb^{-1} to CDF and D0.

The Tevatron is officially scheduled ³⁴⁾ to run until 2009 and is expected to collect ³⁵⁾ up to ~ 4 (8) fb^{-1} according to the base (design) plan. In any case, the search for the SM Higgs boson ³⁶⁾ will probably not result in a discovery while an exclusion region at 90% C.L. can be set for masses up to $130 \text{ GeV}/c^2$. Given for granted an increase by a factor of more than 40 in the number of collected top-quark events, an ultimate precision of $\sim 2 \text{ GeV}/c^2$ on M_T is expected at the end of Tevatron operation. Large improvements on the $t\bar{t}$ production cross-section measurement and on the study of the top properties are also expected. Apart from high- P_T physics, CDF/D0 are nowadays the only sources of B_s mesons; at the end of RUN-II a sensitivity of 9 ps on ΔM will be achieved.

FOCUS (E831 at Fermilab) ³⁷⁾ took data in 1996, collecting more than one million of completely reconstructed charm decays, photoproduced at high energy, at the wideband photon beam of the Fermilab Tevatron. LNF responsibility has been the design, construction, commissioning and operation of the Outer EM calorimeter (1300 channels of Pb-plastic scintillator strips), successfully used for π^0 reconstruction and electron identification. The group is wrapping up data analysis, which has been focused on excited charmed meson and light quark spectroscopy.

BTeV ³⁸⁾ at the Tevatron was the Fermilab experiment devoted to B-physics. In February 2005, DOE funding for the BTeV engineering design in 2006 has been cancelled apparently without any advanced warning. The detector was composed of pixel vertex devices (used at first level trigger), forward magnetic spectrometer, RICH particle ID, high-resolution crystal electromagnetic calorimetry, and muon detectors. The BTeV forward tracker employed straw tubes, and silicon microstrips in the small angle region. The LNF group was responsible for the integration of straws and microstrips via the small angle straw modules, realized with a novel design in which straws was not mechanically tensioned but rather glued in a rohacell frame, for a total of about 4000 straws ³⁹⁾. LNF was also responsible for position monitoring of pixel, strips and straws via Fiber Bragg Grating sensors.

2.8.4 Experiments at the LHC

LNF participates to the ATLAS and the LHCb experiments.

ATLAS is a general purpose detector ⁴⁰⁾ designed to perform high p_T physics at the LHC. The experiment has been optimized for exploiting the full physics potential of the LHC described in Sec. 3.2.2. The LNF group is active in ATLAS since the start of the ECFA (European Committee for Future Accelerators) study groups on the experimentation at the LHC, in year 1990. The group has given a very relevant contribution on the design and construction of the high precision system for the muon tracking. The muon spectrometer ⁴¹⁾ is characterized by a very good momentum resolution and is based on a system of three very large superconducting air-core toroid magnets.

To obtain the required performance, very precise tracking chambers have been designed. The selected technology is the MDT ⁴²⁾ (Monitored Drift Tube) where each chamber is composed by an assembly of drift tubes operated at high pressure (3 bars) to reduce diffusion and improve space resolution. The fundamental characteristic of the MDT is its stringent mechanical precision. The assembly technique has been developed by the LNF group. The responsibility of the group was the construction of all the muon precision tracking chambers of the middle stations in between the coils of the air toroidal magnet. The construction of 94 chambers of the middle station has been completed in 2004.

The LNF group contributes also to the software and the computing for the experiment, being involved in the Data Challenge-1 (DC1) event production and validation, in the studies of physics channels with simulated events, and in the DAQ software development, contributing to the DataFlow system for event monitoring after Event Building.

In 2004, the installation of a TIER-2 of the LHC-Grid ⁴³⁾ for the first phase of the ATLAS DataChallenge-2 has started in close collaboration with the LNF computing center. LNF is also involved in the analysis of the test beam data and participates to the working group devoted to the Higgs search.

The LHC situation is evolving quickly and the ATLAS detector is being installed in the experimental hall at CERN. In particular, MDT Chambers are being assembled together with RPC's and related electronics. A new phase will start soon, with the commissioning of a slice of the detector and the following cosmic data taking in the pit. In 2007 it is planned to have single beams to study beam-gas and halo and exercise detector and data-acquisition, while waiting for colliding beams by the end of the year.

The LHCb experiment is dedicated to B-physics, and in particular to precise measurements of CKM parameters and to search for new physics via CP violating phenomena and rare decays ⁴⁴⁾. B mesons of any flavor are copiously produced at 14 TeV, $\sigma_{b\bar{b}} \sim 500 \mu\text{b}$, corresponding to $\sim 10^{12}$ $b\bar{b}$ produced per year at a luminosity of $2 \times 10^{32} \text{ cm}^{-2} \text{ s}^{-1}$.

The LNF group contributes to the realization of the muon detector system, to the related readout electronics, and to the support mechanics.

The apparatus is a single-arm forward spectrometer, composed of the silicon vertex locator, the trigger tracker, the dipole magnet, two Ring Imaging Cherenkov detectors (RICHs) for particle identification, three tracking stations, the electromagnetic and the hadronic calorimeters, and the muon system. Due to the large inelastic cross section, $\sigma_{b\bar{b}}/\sigma_{inelastic} \sim 0.6\%$, the experiment requires excellent triggering capabilities to reduce the minimum-bias background.

The performance of the muon detector system is crucial for the experiment since the level-0 trigger reconstructs the highest E_T hadron, electron and photon cluster in the calorimeter and the two highest p_T muons in the muon chambers. The chambers are required to provide stand-alone muon reconstruction with 20% p_T resolution, combining strip and pad data from five muon stations, and must achieve a detection efficiency of 99% per station ^{45, 46)}.

LNF is responsible for the construction of $\sim 1/4$ of the multiwire proportional chambers (292 WPC) and half of the gas electron multiplier devices (GEMs) that are being built in Frascati. The group is also responsible for the front-end boards of the Level-0 trigger that have to process muon chamber information. Detector production, started at the end of 2003, will be completed in 2006.

2.9 Neutrino and Astroparticle Physics

The LNF personnel involved in Astroparticle Physics research programs (within the activities of the INFN Scientific Committee II) is composed by 30 physicists and engineers, and 10 technicians.

The major experiments cover different fields, like neutrino physics at the Gran Sasso Laboratory (ICARUS, OPERA) and underwater (NEMO), gravitational waves (ROG, VIRGO) and space experiments (WIZARD/PAMELA, LARES). Apart from ROG, with its local NAUTILUS resonant gravitational antenna (Sec. 2.9.4) which is operating since 1995, the other experiments are in different phases of preparation and installation. Hence, in the forthcoming years significant efforts will be required at LNF for the subsequent phase of data analysis.

2.9.1 OPERA

Along the last two decades LNF has contributed significantly to the scientific program of the INFN Gran Sasso Lab. Presently, LNF plays a leading role in the construction of the OPERA experiment. The aim of OPERA ⁴⁷⁾ is the observation of $\nu_\mu \rightarrow \nu_\tau$ oscillations in the parameter region indicated by Super-Kamiokande as the explanation of the zenith dependence of the atmospheric neutrino deficit. OPERA is a long baseline experiment located at the Gran Sasso Laboratory (LNGS) in the CNGS neutrino beam from the CERN SPS. The discovery potential of OPERA originates from the observation of a ν_τ signal with exceptionally low background level. The direct observation of $\nu_\mu \rightarrow \nu_\tau$ appearance will constitute a milestone in the study of neutrino oscillations. Moreover, OPERA has some sensitivity to the sub-dominant $\nu_\mu \leftrightarrow \nu_e$ oscillations in the region indicated by the atmospheric neutrino experiments ⁴⁸⁾ and will improve significantly current limits from reactors.

The detector design is based on a massive lead/nuclear emulsion target complemented by solid scintillators and two magnetized iron spectrometers, whose active detectors consist of chambers of drift tubes and bakelite RPC's. The lead/emulsion target is made up of emulsion sheets interleaved with 1mm lead plates and packed into removable "bricks" (56 plates per brick). The bricks are located in vertical support structures ("walls" of about $7 \times 7 \text{m}^2$). Nuclear emulsions are used as high resolution tracking devices for the direct observation of the decay of the τ leptons produced in ν_τ charged current interactions. Plastic scintillators positioned after each wall locate the events in the emulsions. The two magnetised iron spectrometers measure charge and momentum of the muons. Moreover, planes of RPCs are inserted between the magnet iron plates. They allow a coarse tracking inside the magnet to identify muons and ease track matching between the precision trackers. They also provide a measurement of the tail of the hadronic energy leaking from the target and of the range of muons which stop in the iron.

The OPERA magnet ⁴⁹⁾, the wall support structure housing the lead/emulsion bricks and the overall support structure have been designed at LNF. Frascati is also involved in the construction and installation of the RPC planes and the corresponding readout electronics. The mass production of the detectors started in Jan 2003 and the RPC for the first spectrometer have already been installed at LNGS after development of a dedicated test station at surface ⁵⁰⁾. The second spectrometer is nearly completed and is being commissioned. Presently, Technical Coordination of the experiment falls under the LNF responsibility. Moreover, the group contributes to software development and, since 2002, it has been involved in the construction of the Brick Assembly Machine ⁵¹⁾.

2.9.2 The satellite mission PAMELA

The LNF WIZARD group is presently involved in the PAMELA satellite experiment. PAMELA (Payload for Antimatter Matter Exploration and Light-nuclei Astrophysics) is a cosmic ray space experiment that will be installed on board a Russian satellite (Resurs-DK1) whose launch is foreseen in September 2005 from the cosmodrome of Baikonur, Kazakhstan, by a Soyuz TM2 rocket. The

satellite will fly for at least 3 years in a low altitude, elliptic orbit (300-600 km) with an inclination of 70.4° . The PAMELA apparatus consists of a permanent magnetic spectrometer equipped with a double-sided silicon microstrip tracking system surrounded by a scintillator anticoincidence system. A Si-W imaging calorimeter, complemented by a scintillator shower tail catcher and a Transition Radiation Detector perform particle identification. Fast scintillators are used for Time-Of-Flight measurements and provide the primary trigger. Finally, a neutron detector, placed at the bottom of the instrument, allows the extension of the energy range for particle measurements up to the TeV region (52, 53). The observational objectives of the PAMELA experiment are the measurement of antiprotons, positrons and nuclei spectra in a wide energy range to search for antimatter and for indirect signatures of dark matter and for the study of the cosmic ray fluxes over a portion of the solar cycle. In addition, as a consequence of the long experiment lifetime and of the orbit characteristics, it will be possible to monitor the long and short term modulation of cosmic rays in the heliosphere, to detect particles from the sun and to study the fluxes of high-energy particles up to 10 TeV.

The LNF group is responsible for the Mechanical Ground Support Equipment (MGSE) and for the assembly and the integration of the entire apparatus. LNF has also been responsible for the organization and the coordination of beam-tests at CERN PS and SPS. The group contributes to the preparation and test of the Mass Dimensional and Thermal Model at TsSKBProgress plant (Samara, Russia) where the Soyuz satellite is assembled, to the preparation and assembly of the Technological (Engineering) Model and to the assembly and final integration and test of the Flight Model.

2.9.3 The LAZIO-SiRad project

An R&D experiment called LAZIO-SiRad (Low Altitude Zone Ionization Observatory) has been recently launched (spring 2005) from the Baikonur cosmodrome (54) as part of the Italian Soyuz Mission 2 (ISM2). The Soyuz crew of this flight will include an Italian ESA astronaut, R. Vittori. The spacecraft will be docked with the International Space Station (ISS) for a period of about 10 days. The experiment is being built by a collaboration of several universities and labs, led by INFN within the Scientific Committee V. The LNF group has built two structural mechanical parts: the LAZIO-SiRad Main Electronics Box (MEB), which is the overall mechanical enclosure (both the qualification model, QM, and the flight model, FM), and the EGGLE MB box, which is external to the LAZIO-SiRad MEB. LAZIO is equipped with the high precision low frequency magnetometer EGGLE (Esperiaos Geomagnetometer for a Low frequency wave Experiment). Magnetic field signals detected by the EGGLE magnetic head probe are amplified, filtered and acquired by the EGGLE acquisition and data handling board located into the EGGLE MB box. Although LAZIO-SiRad is not a large project, it is a very integrated space mission, since it involves several space agencies and has to be launched with a tight time schedule (in practice less than 6 months). The goal of LAZIO-SiRad is the monitoring of real-time variations of the radiation environment in the ISS and the measurement of the activity of the Van Allen belts in Low Earth Orbit (LEO). Scintillators are used to trigger on the passage of charged particles and silicon detectors will measure their charge up to $Z=25$ (Iron nuclei) in the range ~ 10 to ~ 100 MeV, with a large geometric aperture ($GF \sim 60 \text{ cm}^2\text{sr}$). Together, they will record particle arrival times, their line of arrival (pitch angle) and their direction of arrival. EGGLE will measure the magnetic environment inside the ISS concurrently to the measurement of charged particle fluxes and will examine potential pre- and post-seismic effects. LAZIO-SiRad integration has been done in Rome Tor Vergata, where a first acceptance test has been performed by ESA in December 2004. Afterwards, space qualification (SQ) tests will be conducted at the INFN-Perugia SERMS SQ facility. Another acceptance test for outgassing will take place at the ESA ESTEC site (Holland) and the final ones before launch

either in Moscow or at Baikonur.

2.9.4 Experimental Detection of Gravitational Waves

The ROG group is currently operating two cryogenic gravitational wave bar detectors: EXPLORER (at CERN) and NAUTILUS (at LNF). The main goal of this search is the direct detection of the gravitational waves that could be emitted by astrophysical sources (Supernovae, Coalescing Binaries, etc.). The relevance of the experiments for general relativity and astrophysics is discussed in Sec. 3.6. The ultra-cryogenic detector NAUTILUS is operating at LNF since December 1995. It consists of an Al5056 cylindrical bar, 2300 kg in weight and 3 m in length, cooled to a temperature of 0.1 K by means of a dilution refrigerator, and equipped with a resonant capacitive transducer and a dc SQUID amplifier. The two characteristic resonance frequencies, due to the coupling of the antenna and the transducer are about 926 and 941 Hz. NAUTILUS is equipped with a cosmic ray detector. It has taken data until February 2002, when it was warmed up for improvements⁵¹⁾. The bar was replaced by a new bar tuned at 935 Hz, the frequency where a pulsar, remnant of the SN1987A is expected to emit gravitational waves. A new readout chain (the same used for EXPLORER), plus a new suspension cable, to provide a more stable position setting, were mounted. The new run started in May 2003. The EXPLORER antenna is located at CERN and is very similar to NAUTILUS, but is cooled to 2.6 K. In 2001 EXPLORER and NAUTILUS were the only two detectors running. Their sensitivity was the best ever reached by gravitational wave detectors. A coincidence excess⁵⁵⁾ was found from sidereal hour 3 to 5. The seven coincidences between NAUTILUS and EXPLORER in these two sidereal hours, when the antenna is optimally oriented with respect to the Galactic Disk, besides to be time-correlated are also strongly energy-correlated. On the contrary, no significant coincidence excess between the two experiments shows up at any solar hour.

2.10 Hadronic and Nuclear Physics

The LNF personnel involved in the activities of interest of the INFN Scientific Committee III is composed by 36 physicists, 41% involved in internal activities, specifically in the FINUDA and in the SIDDHARTA Collaborations, while 59% are involved in external activities, mainly in the HERMES experiment at DESY and in the AIACE experiment at the Jefferson Laboratory.

People with permanent positions are 16, 12 are under temporary contracts, 7 are Doc and Post-Doc Students. A total manpower of 6.5 technicians represents the available support for the experiments, in the particle detector design, test and maintenance.

2.10.1 DEAR/SIDDHARTA

The SIDDHARTA (Silicon Drift Detector for Hadronic Atom Research) experiment is continuing the successful research line initiated by the DEAR (DAΦNE Exotic Atom Research) experiment in the field of kaonic atoms. DEAR has performed the first measurement of the yields of a pattern of gaseous kaonic nitrogen transitions²⁾, showing the way to perform in the future the measurements of the charged kaon mass at keV level. Moreover, DEAR has done the most precise measurement of kaonic hydrogen X-ray transitions to the 1s level (the K-complex), disentangling for the first time the various individual transitions ($K\alpha$, $K\beta$, etc)³⁾. This measurement allowed the extraction of the shift and the width of the 1s level with respect to the purely electromagnetic calculated values generated by strong interaction between negative kaons and protons. DEAR ended in 2002 and was limited in performing an even more precise measurement by the signal/background

ratio, consequence of the use of slow, non-triggerable detectors, namely Charge-Coupled Device (CCD) for the X-rays. SIDDHARTA's aim is to push the precision on the measurement of the kaonic hydrogen to the eV level, and to perform the first measurement on kaonic deuterium, from which it is possible to extract the antikaon-nucleon isospin dependent scattering lengths, important quantities for the understanding of chiral symmetry breaking in systems containing the strange quark. To do this, SIDDHARTA will make use of the newly developed large area Silicon Drift Detectors (SDD), with an energy resolution of ~ 140 eV at 6 keV and with a trigger possibility at the level of 1 μ s. The trigger is given by the back-to-back topology of the kaons produced at DAΦNE; the use of the trigger will allow the signal/background ratio to be improved by about 2 orders of magnitude respect to DEAR. Presently, SDD detectors are under construction and testing, the electronics under development and the setup under design. The scientific program of SIDDHARTA envisages the measurement of kaonic helium as well, and a feasibility study for other types of exotic atoms.

2.10.2 FINUDA

FINUDA (Fisica Nucleare a DAΦNE) is the first hypernuclear physics experiment carried out at an e^+e^- collider. At the DAΦNE collider, the Λ -hypernuclei are produced by means of the reaction $K_{stop}^- + {}^A Z \rightarrow {}^A_\Lambda Z + \pi^-$ stopping the low energy negative kaons from the ϕ decay into a thin (200 \div 300 mg/cm²) nuclear target. The positive kaons emitted on the other side are extremely useful to tag the reaction (56).

At present, after the end of the activities at KEK and BNL, the only running hypernuclear factories are DAΦNE at LNF and CEBAF at JLab.

FINUDA is a non-focusing magnetic spectrometer designed to achieve a resolution $\Delta p/p$ of 0.35% (*FWHM*) for the π^- emitted in hypernucleus formation. This translates into an energy resolution of 830 keV for the levels of the hypernucleus. Furthermore, it detects the charged particles and the neutrons emitted after the Λ decay, performing at the same time hypernuclear spectroscopy and studies on hypernuclear decay modes. FINUDA is a high acceptance, high resolution cylindrical spectrometer consisting of a superconducting solenoid instrumented with two concentric sets of MWPC, and of six layers of straw tubes used to reconstruct the trajectories of the charged particles. Two arrays of bi-dimensional Si-microstrips are placed before and after the target station for precise measurements of the stopping points of K^- and K^+ and the exit point of π^- . The 2424 straw tubes of the tracking detector have been designed and built by the LNF group. They are in operation since 1997 with good performance and reliability.

The first round of the FINUDA data taking has been performed from October 2003 to March 2004. An integrated luminosity of about 50 pb⁻¹ has been collected both, for machine, and detector calibration purposes; further 200 pb⁻¹ are being used for scientific analyses. With the two ${}^6\text{Li}$ targets FINUDA can access light hypernuclear systems; ${}^6_\Lambda\text{Li}$ is unstable for proton emission that makes it decaying into ${}^5_\Lambda\text{He} + p$ or transforming into ${}^4_\Lambda\text{He} + p + n$ or into ${}^4_\Lambda\text{H} + p + p$ via a Coulomb-assisted mechanism. Furthermore, ${}^6\text{Li}$ data are used to look for neutron-rich hypernuclei. The ${}^7\text{Li}$ target has been chosen since ${}^7_\Lambda\text{Li}$ is the most extensively studied hypernucleus with γ -ray spectroscopy with the aim to provide the first data on its decay modes. Another aspect that can be addressed through the light target data is the existence of deeply-bound kaonic systems (57). ${}^{12}_\Lambda\text{C}$ is the best known hypernuclear system, therefore the three targets of this material are used for the calibration procedure of the apparatus and will provide enough statistics to perform non-mesonic decay studies. Finally, ${}^{27}\text{Al}$ and ${}^{51}\text{V}$ are medium-heavy nuclei not well known. For ${}^{27}_\Lambda\text{Al}$ there are old data taken using K^- in flight and very coarse energy resolution (6 MeV *FWHM*). The excitation spectrum of ${}^{51}_\Lambda\text{V}$ has been measured at KEK (58) with an energy resolution of 1.65 MeV (*FWHM*). The peaks corresponding to p and d orbits show possible splitting that can be better

resolved with the higher resolution FINUDA spectrometer.

2.10.3 HERMES

HERMES (HERa MEasurement of Spin) ⁵⁹⁾ is one of the four experiments at HERA electron proton collider at DESY. It uses the high current, longitudinally polarised electron beam, with energy of ~ 27.5 GeV, together with polarised and unpolarised gas targets internal to the storage ring. Scattered electrons and particles produced in the deep-inelastic electron-nucleon interaction are detected and identified by an open-geometry forward spectrometer with large momentum and solid angle acceptance ⁶⁰⁾. Main scientific goal of HERMES is the detailed investigation of nucleon spin structure. Physics reach of the experiment extends beyond this topic of hadronic physics and the experiment can be considered as a facility to explore many details of the hadron structure, hadron production and hadronic interactions with electromagnetic probes at $\sqrt{s} \sim 7$ GeV.

HERMES was approved in 1993 and commissioned in 1995. Up to year 2000 HERMES collected data with a longitudinally polarised H, D and ³He internal gas targets: from these runs the most accurate and complete data set for the polarised structure function g_1 has been provided and direct flavor decomposition of the nucleon spin has been achieved ⁶¹⁾. Data on several unpolarised nuclear gas targets have been also collected, to allow a detailed study of the hadronization process and the modification of the quark fragmentation function in the cold nuclear matter. The second phase of data taking started in 2002. It was dedicated to the measurements with a transversely polarised hydrogen target for the first determination of the so-called *transversity* distribution ⁶²⁾ and the measurements with the high density unpolarised hydrogen for detailed studies of exclusive processes.

The LNF group plays a major role in the experiment. Both, the deputy spokesman, and the analysis coordinator are LNF physicists. The group designed and constructed the electromagnetic calorimeter, and contributed also to the project and to the construction of the RICH detector, for the identification of π , K , p , μ in the full kinematic range. It is currently involved in the project of a new recoil detector which will be installed at the end of 2005 for improving the separation between exclusive processes by detecting all final state particles.

2.10.4 AIACE

The Continuous Electron Beam Accelerator Facility (CEBAF) at the Thomas Jefferson Laboratory (JLab) is devoted to the investigation of the electromagnetic structure of mesons, nucleons and nuclei using high power electron and photon beams with energies up to 6 GeV and 100% duty cycle. The primary electron beam of the accelerator can be sent simultaneously to the 3 experimental Halls A, B and C, which are instrumented with complementary equipments. The accelerator routinely delivers luminosities of the order of 10^{38} cm⁻² s⁻¹, allowing statistical sensitivity comparable to hadronic reactions to be obtained.

Since the start of the JLab activity in the Hall B in 1992, the LNF group participates to the AIACE (Attività Italiana A Cebaf) Collaboration, which includes also physicists of the Genova INFN and University.

Hall B ⁶³⁾ is equipped with the Cebaf Large Angle Spectrometer (CLAS). This detector is particularly well suited for the study of exclusive reactions, since it can fully detect multi-particle final states with high resolution. The goals of the CLAS Collaboration include the study of the elementary and nuclear excitation of N^* resonances, the spin structure of the nucleon, the inclusive electron scattering on nucleons and nuclei, the production and decay of hyperons, the structure of few-body systems and the modification of the nucleon properties in nuclear matter. In the last year, major efforts have been devoted to the search for exotic pentaquark baryons.

LNF group provided the Large Angle Calorimeter (LAC) of the CLAS detector ⁶⁴, which has been installed in 1996. In 2004, in the framework of the new experiments devoted to the pentaquark searches, the group has contributed to the construction and installation of the new Start Counter detector, which allowed the efficiency of the CLAS detector to be improved for photon runs by a factor of 3.

The LNF group is fully involved in the search for exotic pentaquark baryons, among other topics of the broad physics program, In 2004, two experiments have taken new photoproduction data on proton and deuteron. Pentaquarks will be searched for in several exclusive reaction channels and in all possible decays. New results are expected in 2005. Two more runs, mainly devoted to the study of higher mass pentaquark states are planned in 2005 and 2006.

2.11 The Synchrotron Radiation Facility

In the last twenty years Synchrotron Radiation (SR) has proven to be an invaluable tool for scientific research in many fields, from Biology to Earth and Environmental Sciences, and nowadays more than forty dedicated machines are available in the world for the production of SR light. INFN and, in particular LNF, has a long-standing tradition in using synchrotron radiation for interdisciplinary studies, started in 1975 with the creation of the PULS project for using ADONE as a second-generation SR source. This machine has been the focal point of the Italian researches in the field until the closing of the activities due to the start of the construction of the new DAΦNE storage ring in the 1993. At the same time, two new projects started in Italy: ELETTRA, the third-generation machine at Trieste for studies in the soft X-ray energy range, and the participation to the European Synchrotron Radiation facility (ESRF) at Grenoble. With ADONE the LNF has been almost for two decades a reference laboratory, not only for the synchrotron radiation Italian community. Its extensive use as a SR source stimulated the growth of a qualified scientific community, both internal and external to INFN, which uses the present SR source in fully parasitic regime and is willing to use DAΦNE at least as a partially dedicated photon source. Almost ten years ago, INFN decided to support the construction of two beam lines at DAΦNE and one at ESRF. DAΦNE is a low energy machine, a storage ring of 510 MeV, with very high currents (up to 2.0 A). These characteristics, with the value of the emittance suitable for the high-energy physics experiments, make DAΦNE a photon source with a very high photon flux but moderate brilliance. All those allow researches ranging from the infrared to the VUV and up to the soft X-ray energy domain, and allow performing a number of specific spectroscopy experiments which require high flux but not an extreme energy resolution and brilliance. On the other side, the energy of the beam at ESRF makes possible researches in the hard X-ray energy region, and the Italian beam line GILDA covers the X-ray range up to 90 keV. Nowadays, all the SR activities at DAΦNE have been performed in parasitic mode with few exceptions for very peculiar experiments. In the following some details are given.

2.11.1 Infrared activities

The infrared region of the electromagnetic spectrum is a very wide region that covers three orders of magnitude from 10 up to 10000 cm^{-1} . In this wide energy domain, infrared (IR) spectroscopy probes low-energy phenomena of basic importance for condensed matter physics, chemistry, biophysics, and material science. The development of the techniques, of the sources and of the instrumentation allowed IR spectroscopy to become one of the most applied characterization techniques in industry and in many technological processes. The main characteristics of the synchrotron sources, e.g. the high brilliance and the stability, make the modern low energy storage rings, like

DAΦNE, nearly perfect sources for IR spectroscopy up to the far-IR domain. The use of the Fourier transform interferometer technique makes possible to gain even three orders of magnitude in sensitivity in the IR spectroscopy with respect to the conventional sources when is applied to the investigations of very small samples (hundreds of μm). A growing area of applications of IR synchrotron radiation is micro-spectroscopy, a technique that combines microscopy and spectroscopy for microanalysis purposes. Spatial resolution within a microscopic field of view, is the goal of the modern infrared micro-spectroscopy applied to condensed matter physics, materials science, biophysics and now, also to medicine. IR-microscopy is a micro-analytical and imaging technique, which achieves contrast via the intra-molecular vibrational modes that appear at different positions with different relative intensities. Each spectral difference reflects possible structural differences in the system. Therefore, vibrational spectroscopy allows defining sets of IR marker absorption bands. The method is the same used in X-ray microscopy where contrast is achieved by recording spectra before and after the absorption edges of an element contained in the specimen. The use of infrared microscopes coupled to synchrotron radiation sources has started recently, and has rapidly met with outstanding success. Indeed, the high brilliance of this source allows one to reduce the instrument apertures to define geometrical areas of a few μm in the mid-IR region, e.g., at the diffraction limit, with good S/N. Synchrotron infrared microscopy is the only practical way to obtain high quality spectra of individual cells from tissue and cell samples in an acceptably short measuring time. The first few published reports of synchrotron infrared microspectroscopy studies of cells and tissues have already appeared, and these researches confirmed the capability of synchrotron infrared microscopy to obtain clinically relevant spectral information from tissues and cell cultures at the level of single cells. The beam line at DAΦNE and the available instrumentations already allow spectroscopic research in this field both in transmission and reflection mode. Nowadays, in Europe only 5 synchrotron infrared beam lines are operational: Berlin, Daresbury, Frascati, Karlsruhe and Lund. This compared very un-favourably with the situation in the USA where many more IR beam lines are operative. Although five further beam lines are under construction or are planned in the next years the situation will remain critical due to the increasing demand of users in this area from several fields.

2.11.2 Soft X-Ray activities

It has long been realized that interesting science and challenging experiments can be done with soft X-rays between 1 and 5 keV. The considerable advantages in using a low-energy storage ring below 1 GeV, as DAΦNE, reside in a negligible heat load on the optics and in the absence of contamination by higher order SR harmonics, thus providing high quality monochromatic soft X-ray beams. This energy range covers the K absorption edges of Mg, Al, Si, P, S and Ca, the L edges of transition metals, and the M and N edges of rare-earth atoms: many of these elements are important in a large number of condensed matter studies as well as in biophysics. Since the high circulating current in DAΦNE, generally exceeding 1 A, the wiggler SR beam line in operation at the LNF delivers a high-flux of soft X-rays and accesses a niche of energies covered at few worldwide facilities. Among the spectroscopic techniques, X-ray Absorption Spectroscopy (XAS) is routinely applied to probe both local structures and electronic states around an absorbing site in a wide class of materials, going from biological samples to minerals. The present DAΦNE beam line allows XAS spectroscopy in the 1–4 keV energy range by a double crystal fixed exit monochromator using different crystal equipments to cover the whole energy range.

2.11.3 GILDA activities

The Italian Collaborating Research Group GILDA at ESRF is a general-purpose beam line using a bending magnet as X-ray source. It is funded by INFN, CNR and INFN. Since 1994, GILDA is delivering light to Italian and international scientific community. This beam line rises as a collaboration between the LNF and several Italian Universities and provides an X-ray beam in the energy range 4–90 keV, with an energy resolution $\Delta E/E \approx 10^{-5}$ – 10^{-4} , a spot size of about 2×2 mm² and a flux up to 10^{10} – 10^{11} ph/s at the sample position. The main purpose of the GILDA beam line is to perform structural investigations in several systems, from biological to solid-state sample, by using X-ray Absorption Spectroscopy (XAS) and X-ray Diffraction (XRD) techniques. For this purpose, dedicated instrumentations are available for users in the three hutches dedicated to the experimental systems.

2.12 Theoretical Physics

The LNF Theory Group (personnel belonging to the INFN Scientific Committee IV) is composed by 9 staff members and a similar number (fluctuating in time) of graduate students, post-docs and INFN associates of other institutions. The research activities of this group can be divided into two main areas: theory and phenomenology of high-energy physics ($\approx 60\%$); theory and phenomenology of condensed matter and many-body systems ($\approx 40\%$).

The research activities and the expertise of the high-energy group cover several areas, which can be roughly divided into four main categories: i) Flavour Physics, ii) QCD Studies, iii) Model-building and Astroparticle Physics, iv) String Theory and other extensions of the Standard Model.

The research in the field of *Flavour Physics* concerns the phenomenology of weak decays (within and beyond the Standard Model–SM); theoretical studies of effective field theories relevant to *K* and *B* physics; light-meson spectroscopy and, more in general, the study of the low-energy limit of the SM. This field of research has been particularly active since the approval of the DAΦNE project: the Frascati Theory Group has been the leading team in three successful European Research Network activities focused on this field of research. Among the most significant results recently achieved in this area, it is worth to recall the precision study of rare *K* decays, which provides the theoretical basis for several analyses carried out by various existing experiments in this field, and also the basis for future experimental projects in kaon physics.

The area of *QCD Studies* includes non-perturbative numerical studies of Quantum Chromodynamics by means of lattice simulations, aimed to determine the structure of possible phase transitions in QCD at finite temperature and finite chemical potential. It also includes phenomenological studies of hadronic cross sections and form factors in the non-perturbative regime (asymptotic behaviors; soft-gluon resummations). The main expertise in *Model-building and Astroparticle Physics* concerns the study of possible supersymmetric extensions of the Standard Model and of grand-unified theories; studies of the stability of the Higgs potential, about neutrino physics and about the impact of astrophysical constraints on model building. The Theory Group also includes a prolific activity in the field of *String Theory* and other extensions of the SM.

The theoretical activity of the condensed matter group is mainly linked to synchrotron radiation (SR) activities to provide a suitable theoretical framework for the interpretation of the experimental data coming from the different spectroscopies. This activity has been focused both on the general aspect of the theory to shed light on the “real” information that can be derived from the data and phenomenological applications to different systems, from crystal to biological materials. Both structural and the electronic aspects of the problem have been considered in detail. In particular, a new method for performing a complete fit of the low energy part of the absorbing spectrum from core level (XANES energy region) in terms of selected structural parameters has

been proposed. This method is based on the full multiple scattering theory for the calculation of the photoabsorption cross-section and the use of a phenomenological approach to the calculations of the inelastic losses of the photoelectron. In this way a complete fit of the first two hundred eV of the spectrum can be done and several applications, from crystals to proteins, have been investigated. At the same time, the problem of the electronic correlations and their influence in the experimental data of different spectroscopies have been analysed in detail. In particular, the analysis of synchrotron radiation experiments (resonant X-ray scattering, absorption and dichroism) in strongly correlated electron systems, like the prototypical Mott-Hubbard material V2O3, the multi-layered manganite and the geometrically frustrated pyrochlore materials have been performed with a detailed tensor analysis of the circular and linear dichroism in photoemission, photoabsorption and anomalous diffraction data. Moreover a detailed investigation of the electronic ground state of magnetic oxides has been performed with the aim to correlate the degree of degeneracy of the ground state with the different phases present in these materials.

References

1. G. Vignola and DAΦNE Project Team: “DAΦNE, The First Φ-Factory”, 5th European Particle Accelerator Conference, Sitges (Spain), June 1996, p.22, LNF-96/033 (P).
2. T. Ishiwatari *et al.*, Phys. Lett. B **593** (2004) 48.
3. DEAR Collaboration, Phys. Rev. Lett. (2005) , in print.
4. G. Mazzitelli and P. Valente, Nucl. Instr. Meth. A **515** (2003) 516.
5. SPARC Project Team, “Sparc Injector TDR”, <http://www.lnf.infn.it/acceleratori/sparc>
6. M. Ferrario *et al.*, “Homdyn Study for the LCLS RF Photoinjector” , in The Physics of High Brightness Beams, J. Rosenzweig and L. Serafini ed., World Sci., ISBN 981-02-4422-3, June 2000.
7. L. Serafini and M. Ferrario, “Velocity Bunching in PhotoInjectors”, AIP CP 581, 2001, pag.87.
8. A. Cianchi *et al.*, “Design Study of a Movable Emittance Meter Device for the SPARC Photoinjector”, presented at EPAC 2004, July 2004.
9. <http://www.cnao.it>
10. G. Guignard (ed.) *et al.*, “A 3 TeV e^+e^- linear collider based on CLIC technology”, CERN 2000-008.
11. D. Alesini *et al.*, “RF beam deflectors for CTF3 combiner ring”, Proceedings of EPAC 2002, Paris, France.
12. TESLA Technical Design Report, DESY-2001-011.
13. C. Sanelli *et al.*, “Technical Layout of the TESLA Damping Ring”, LNF-01-003 (NT), 2001.
14. “TESLA DR Injection extraction scheme with RF Deflectors”, TESLA Reports 2003-26.
15. M. Sullivan *et al.*, “IR upgrade plans for the PEP-II B-Factory”, proc. of EPAC 2004, Lucerne, Switzerland, July 2004.

16. F. Marcellini *et al.*, “An over-damped cavity longitudinal kicker for the PEP-II LER”, Proc. of PAC 2003, Portland, Oregon (US), May 2003.
17. D. Brandt *et al.*, Nucl. Instr. Meth. A **517** (2004) 19.
18. <http://www.presid.infn.it/csn.htm>
19. KLOE Collaboration - KLOE : A general purpose Detector for DAΦNE - LNF-92/019 (IR)
20. M. Adinolfi *et al.*, Nucl. Instr. Meth. A **488** (2002) 51.
21. M. Adinolfi *et al.*, Nucl. Instr. Meth. A **482** (2002) 364.
22. M. Adinolfi *et al.*, Nucl. Instr. Meth. A **492** (2002) 134; M. Aloisio *et al.*, Nucl. Instr. Meth. A **516** (2004) 288.
23. F. Ambrosino *et al.*, Nucl. Instr. Meth. A **534** (2004) 403.
24. KLOE Collaboration, Phys. Lett. B **535** (2002) 37, Phys. Lett. B **538** (2002) 21, Phys. Lett. B **566** (2003) 61.
25. KLOE Collaboration, Phys. Lett. B **597** (2004) 139.
26. KLOE Collaboration, Phys. Lett. B **536** (2002) 209, Phys. Lett. B **537** (2002) 21, Phys. Lett. B **541** (2002) 45, Phys. Lett. B **591** (2004) 49, hep-ex/0411030.
27. KLOE Collaboration, ICHEP’04 Conference Papers **8-0811** and **8-0813**.
28. KLOE Collaboration, Phys. Lett. B **606** (2005) 12.
29. BABAR Collaboration Phys. Rev. Lett. **86** (2001) 2515, Phys. Rev. Lett. **87** (2001) 091801, Phys. Rev. D **66** (2002) 032003, Phys. Rev. Lett. **89** (2002) 201802, Phys. Rev. Lett. **89** (2002) 281802, Phys. Rev. Lett. **91** (2003) 161801, Phys. Rev. Lett. **92** (2004) 201802, Phys. Rev. D **70** (2004) 012007, Phys. Rev. Lett. **93** (2004) 071801, Phys. Rev. Lett. **93** (2004) 081801, Phys. Rev. Lett. **93** (2004) 181805, Phys. Rev. Lett. **93** (2004) 201801, Phys. Rev. Lett. **93** (2004) 231804.
30. BABAR Collaboration, Phys. Rev. Lett. **93** (2004) 131801.
31. BABAR Collaboration, Phys. Rev. Lett. **90** (2003) 242001, Phys. Rev. D **69** (2004) 031101.
32. BABAR Collaboration, Phys. Rev. Lett. **91** (2003) 121801, Phys. Rev. Lett. **91** (2003) 171801, Phys. Rev. D **70** (2004) 091102.
33. BABAR Collaboration, Nucl. Instr. Meth. A **479** (2002) 1.
34. http://www.fnal.gov/directorate/program_planning/schedule/index.html
35. P.H. Garbincius, hep-ex/0406013.
36. Higgs Working Group Collaboration, hep-ex/0010338.
37. <http://www-focus.fnal.gov/>
38. <http://www-btev.fnal.gov/>
39. E. Basile *et al.* LNF-04-25-P, Dec 2004 and hep-ph/0412100

40. <http://atlas.web.cern.ch/Atlas/TP/tp.html>
41. <http://atlas.web.cern.ch/GROUPS/MUON/TDR/Web/TDR.htm>
42. <http://atlas.web.cern.ch/Atlas/project/MDT/www/mdt.html>
43. <http://atlas.web.cern.ch/Atlas/GROUPS/SOFTWARE/OO/Grid/>
44. LHCb Collaboration, CERN-LHCC-98-004 and also <http://lhcb-tp.web.cern.ch/lhcb-tp/>
45. LHCb Collaboration, CERN-LHCC-2003-031 and also <http://lhcb.web.cern.ch/lhcb/TDR/trigtldr.pdf>
46. LHCb Collaboration, CERN-LHCC-2001-010, CERN-LHCC-2003-002 also on <http://lhcb-muon.web.cern.ch/lhcb-muon/results/tdr.pdf>, <http://lhcb-muon.web.cern.ch/lhcb-muon/TDR/addendum.pdf>
47. M. Guler *et al.*, OPERA proposal, CERN/SPSC 2000-028, SPSC/P318, LNGS P25/2000.
48. M. Komatsu, P. Migliozi and F. Terranova, *J. Phys. G* **29** (2003) 443.
49. M. Ambrosio *et al.*, *IEEE Trans. Nucl. Sci.* **51** (2004) 975.
50. R. Brugnera *et al.*, *Nucl. Instr. Meth. A* **533** (2004) 221; G. Barichello *et al.*, *Nucl. Instr. Meth. A* **533** (2004) 42.
51. INFN-LNF 2004 Annual Report - LNF-05/05 (IR) - available on <http://www.lnf.infn.it/rapatt>
52. M. Simon for the PAMELA collaboration: "Status of the PAMELA experiment", Proceedings 28th International Cosmic Ray Conference (Tsukuba, Japan, 2003) OG 1.5 p.2117.
53. O. Adriani *et al.*, *Nucl. Instr. Meth. A* **478** (2002) 114.
54. D. Babusci *et al.*, "Select Experimental Trends in Astro-Particle Physics in Space", LNF-04/26(IR).
55. P. Astone *et al.*, *Class. Quantum Grav.* **19** (2002) 5449.
56. C. Milardi *et al.*, Proceeding of the 9th EPAC, July 2004, Lucerne.
57. H. Outa for the FINUDA collaboration, Proceedings of the DAΦNE 04 Conference, Frascati Physics Series.
58. T. Nagae *et al.*, *Nucl. Phys. A* **691** (2001) 76c.
59. <http://www-hermes.desy.de/>
60. HERMES Collaboration, *Nucl. Instr. Meth. A* **417** (1998) 230.
61. HERMES Collaboration, *Phys. Rev. D* **71** (2005) 012003.
62. HERMES Collaboration, *Phys. Rev. Lett.* **94** (2005) 012002.
63. <http://www.jlab.org/Hall-B/>
64. CLAS Collaboration, *Nucl. Instr. Meth. A* **A503** (2003) 513.

Chapter 3

Plans in the World

This chapter is intended as a reference to evaluate in a more general context the LNF programs discussed through in the document. The most relevant research activities in progress or under discussion in the major nuclear and particle-physics laboratories worldwide are reported.

The chapter is organized as follows: a brief theoretical discussion about open problems in high-energy physics is presented in Sec. 3.1. Main particle-physics programs at the e^+e^- facilities, as well as at the LHC and the other hadronic colliders, are presented in Sec. 3.2. Future experiments in nuclear physics are reported in Sec. 3.3. The experimental developments in neutrino and astroparticle physics are discussed in Sec. 3.4 and 3.5, respectively. Sec. 3.6 contains a brief excursus on the gravitational-wave detection. Finally, the present and planned e^+e^- facilities are reviewed in Sec. 3.7, 3.8, 3.9.

3.1 Open problems and main directions in high-energy physics

3.1.1 The Standard Model

The Standard Model (SM) has been the backbone of particle physics theory for more than a quarter of a century. This model successfully describes particle interactions over a wide (and unprecedented) range of energies/distances: from the atomic scale down to 10^{-3} fm. It is also a relatively simple and economical model, whose main building blocks can be summarized as follows:

1. it is a four-dimensional Lorentz-invariant quantum field theory (QFT);
2. it is a chiral gauge QFT, based on the symmetry group $SU(3)_C \times SU(2)_L \times U(1)_Y$, which incorporates strong, weak and electromagnetic interactions, and which is spontaneously broken into $SU(3)_C \times U(1)_{em}$;
3. the matter content is provided by three replica (identical from the point of view of gauge interaction) of a basic chiral family of quarks and leptons (Q_L, u_R, d_R, L_L, e_R);
4. the spontaneous breaking of the gauge group, the non-vanishing fermion masses and the breaking of the flavour symmetry, are all induced by the non-vanishing vacuum expectation value (v.e.v.) of a single fundamental scalar field (the Higgs doublet), with a renormalizable potential and appropriate Yukawa couplings.

Despite the great success of the SM in laboratory-based experiments, there are several arguments which indicate that this model can only be the low-energy limit of a more fundamental theory, with new degrees of freedom (and possibly new symmetries) showing up above the electroweak scale (i.e. energies above 100 GeV or distances below 10^{-3} fm). Mentioning only some of these arguments:

Theoretical problems The SM is not able to incorporate gravity in a consistent way. If the model is extended well above the electroweak scale, quantum corrections destabilize the Higgs sector which suffers of a serious fine-tuning problem [hierarchy problem]. The SM does not provide a natural explanation for the flavour structure [flavour problem], for the smallness of neutrino masses and for the quantization of the electric charge [signs of a grand-unified theory?].

Cosmological problems The SM badly fails when confronted with the cosmological model emerging by astrophysical observations: the SM does not provide a dark-matter candidate nor a natural explanation for the cosmological constant; it does not have enough amount of CP violation to explain the matter-antimatter asymmetry; there is no mechanism which could generate an inflationary epoch.

On general grounds, one can say that the search for the theory that will extend/complement the SM at high energies (hopefully solving some of these problems) is presently the main effort of particle physics, both on the experimental and on the theoretical side.

3.1.2 Model building and the high-energy frontier

The extensions of the SM which have been proposed could be roughly classify according to which of the four building blocks listed in Sec. 3.1.1 is put under doubt, or to which of the main open problems is solved. The weakest point of the SM is definitely the Higgs sector (point n. 4), mainly because of its theoretical problems, but also because the physical Higgs boson has not been directly observed yet. It is then not surprising that all SM extensions have a different Higgs or better a different gauge-symmetry-breaking sector. All the realistic attempts proposed so far to improve this sector solving the hierarchy problem (supersymmetric models, models with composite Higgs fields, etc. . .) predict the existence of new degrees of freedoms around the TeV scale, which should be accessible at the LHC ¹). The theoretical progress in this direction is therefore intimately related to the experimental progress at the high-energy frontier.

While the solution of the hierarchy problem is naturally linked to the Higgs sector and, possibly, to the existence of new degrees of freedom just above the electroweak scale, the situation is much less clear for the other problems. The ambitious attempts to find a coherent solution of the problems connected with gravity and cosmology, naturally point toward more drastic modifications of the theory, which go beyond QFT and beyond four dimensions (string theory, models with extra spatial dimensions, etc. . .). Despite the high intrinsic theoretical interest, these theories suffer of a poor predictive power: so far, all the attempts to extract from these ambitious models a clear connection with the SM (which must be the low-energy limit of any realistic model) have been quite unsuccessful.

Altogether, it is fair to say that best compromise between predictivity and improvements of the theory is achieved by the (low-energy) supersymmetric extensions of the SM ²). Within this framework, the model remains a QFT based on the SM gauge group up to very high energy scales (i.e. the first two main hypothesis of the SM remain valid well above the e.w. scale). The supersymmetrization of the model requires a doubling of matter and gauge-field content (with scalar and fermion partners for each SM fermion or gauge-boson field) and at least two Higgs doublets (with corresponding fermion partners). These new degrees of freedoms (which should

appear – at least in part – close to the TeV scale) and the extra symmetry allow a consistent and predictive description of particle physics up $M_{\text{GUT}} \sim 10^{15}$ GeV, where the SM gauge group is naturally embedded in a grand-unified theory (GUT). Problems such as the flavour structure and the inclusion of gravity can be consistently postponed at the grand-unification scale or above.

3.1.3 Precision tests and the high-intensity frontier

The search for new degrees of freedom beyond the SM is not performed only at the high-energy frontier, but it proceeds also via the high-intensity frontier, namely via high-precision low-energy experiments.³⁾ Also in this case progress can be made only with a strong link between theory and experiments. On the theory side, it is necessary to identify observables particularly sensitive to non-standard contributions, evaluate their expectations in different new-physics models, and be sure that the SM cannot generate such effects (even at high orders in the perturbative expansion).

The most powerful probes in this type of searches are processes that are completely forbidden within the SM, such as proton decay or neutrinoless double-beta transitions. The evidence of such processes, which in several scenarios is predicted to be close to the present experimental limits, would be a clear evidence of physics beyond the SM and also a key information about its symmetry properties. A unique and fundamental information can also be achieved by high-statistics studies of lepton-flavour violating processes (such as $\mu \rightarrow e\gamma$ and $\tau \rightarrow \mu\gamma$)⁴⁾; electric dipole moments of both quarks and leptons⁵⁾; short-distance dominated flavour-changing neutral-current transitions in rare B and K decays⁶⁾.

Searches for violations of even more basic conservation laws, such as Lorentz invariance or CPT, are less likely to yield positive results, but the implications of a discovery would be so important that is certainly useful to improve existing bounds.

It is worth to stress that there is full complementarity between the high-energy and the high-intensity frontiers: one would benefit from the progress of the other. In particular, high-precision low-energy experiments usually provide a much deeper probe of certain symmetries of the new degrees of freedom (such as the flavour structure, both in the quark and in the lepton sector) than high-energy experiments.

Last but not least, high-statistics low-energy experiments (correlated with high-precision theoretical analyses) are also the only way to determine fundamental SM parameters, such as CKM angles, quark masses and gauge couplings. Also this program has some complementarity with the new physics searches performed at high-energies: several parameters of the SM Lagrangian (particularly in the Yukawa sector) are likely to be determined (in terms of fewer couplings) by some unknown high-energy dynamics. Their precise knowledge, which can be obtained only at low energies, could help to shed slight on physics beyond the SM.

3.1.4 Understanding QCD

Despite the continuous theoretical and experimental progress, the present understanding of the low-energy world is still quite limited. In particular, the non-perturbative behavior of QCD at low energies still prevent us to compute several low-energy hadronic observables starting from the fundamental couplings of the SM Lagrangian. The efforts toward a deeper understanding QCD are very welcome both *per se* (since they would imply a deeper understanding of quantum field theories in the non-perturbative regime) and also to improve the knowledge of the fundamental SM couplings (which, as discussed above, has important implications in shedding slight on physics beyond the SM).

Here it is possible to identify two main directions of research: numerical studies of QCD by

means of lattice simulations and analytical studies by means of effective theories, such as chiral perturbation theory (CHPT or χ PT) ⁷⁾, the heavy-quark effective theory (HQET) ⁸⁾, and other approaches. The QCD studies on the Lattice have made a substantial progress in the last few years, and there is no doubt that Lattice-QCD is the master tool to compute hadronic quantities from first principles. Nonetheless, not all observable quantities can be directly accessed by realistic Lattice simulations. Similarly, realistic lattice simulations cannot be performed with too light or too heavy quark masses. Effective field theories turn out to be very useful tools to address these two problems, extending the validity of any realistic lattice simulation.

Progress in this field is mainly determined by the developments on the theoretical side (including the improvements in computing power and algorithms efficiency, as far as Lattice QCD is concerned). Nonetheless, also in this case a close collaboration between theory and experiments is very useful. In particular, on the experimental side it would be important to improve the determination of all the low-energy quantities which can provide a benchmark for Lattice calculations. The best examples of these observables are the weak decay constants and the $H_1 \rightarrow H_2$ weak and electromagnetic form factors of long-lived hadrons (several of these observables are still known with poor accuracy). Similarly, it would be useful to improve the knowledge of observables that can provide a benchmark for low-energy effective field theories (such as π - π and π - N scattering lengths at thresholds, etc. ⁹⁾) Last but not least, it is important to recall that several open experimental issues still exist also in meson and baryon spectroscopy, which constitutes the most natural playground to test any approach to non-perturbative QCD.

3.2 Particle-physics experiments at accelerators

3.2.1 Tests of the Standard Model

SM represents today the reference framework for the experimental results achieved by the High Energy Physics (HEP) research programs at the accelerators. Starting from years 80's, stringent tests of the Electroweak Theory have been obtained by the experiments at LEP (CERN), by NuTeV, by the Fermilab Collaborations, CDF and D0 and by SLD at SLAC. The conclusion is that the SM is able to describe all the measurements rather well or, in other words, the experiments and the comparison of their results do not present any compelling evidence for phenomena beyond those described by the SM.

With the experimental accuracy being sensitive to the loop induced effects, the electroweak measurements, exploiting the precise SM calculations, are able to predict the top, W and Higgs masses and the strong coupling constant α_s . Top and W masses are in agreement with the direct measurements carried out at Fermilab, demonstrating the consistency of the theory in this area.

The availability of both, highly accurate measurements, and theoretical predictions, often at the per mil level precision, is a powerful system to probe the unknown sector of the Higgs coupling and to access alternative scenarios of the theories beyond the SM.

The present world average value of the W mass M_W is (80.425 ± 0.034) GeV. Within the SM this mass is:

$$M_W = \sqrt{\frac{\pi\alpha}{G_f\sqrt{2}}} \frac{1}{\sin\theta_W\sqrt{1-\Delta R}}, \quad (3.1)$$

where α is the fine structure constant, G_f the Fermi constant and θ_W the Weinberg angle. Radiative corrections ΔR receive contributions from M_{top}^2 and $\log(M_{Higgs})$.

Short-term Fermilab program (RUN-II) ¹⁰⁾ includes the improvement of the measurement of the W mass M_W at the 15 MeV level, and of the top mass M_{top} at the level of 2 GeV, constraining SM Higgs mass M_{Higgs} with 30% precision.

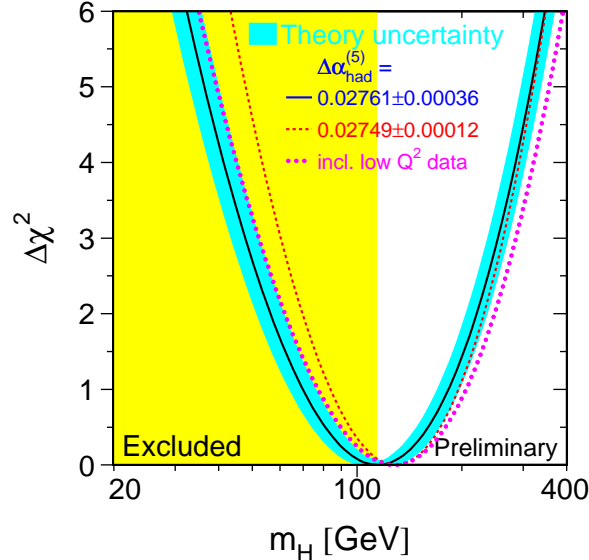


Figure 3.1: $\Delta\chi^2$ curve derived from EW measurements performed at LEP and by SLD, CDF and D0 as a function of the SM Higgs Boson mass. The preferred Higgs mass corresponds to the minimum of the curve, at 114 GeV with experimental uncertainty of +69 and -45 GeV, at 68% C.L. ¹²⁾.

In this context the improvement of existing measurements of the top quark is really relevant, as the latest re-analysis ¹¹⁾ of M_{top} done by D0 collaboration on Run-I Tevatron data has demonstrated. The new world average value used in Fig.3.1 ($M_{top} = 178.0 \pm 4.3 \text{ GeV}/c^2$) shifts the best-fit value of M_{Higgs} from 96 to 114 GeV/ c^2 .

Running experiments at Tevatron Run-II and especially future experiments at CERN, thanks to the huge statistics of $t\bar{t}$ pairs produced at the pp collider at $\sqrt{s} = 14 \text{ TeV}$, will improve substantially the knowledge of the top quark properties (mass, production cross-section, decay channels).

The direct search for the Higgs boson, the only experimentally missing entry of the SM, constitutes one of the major tasks for the completion of the tests of the theory.

The Higgs boson has been also directly searched for at LEP, leading to the conclusion that the SM Higgs must be heavier than 114.4 GeV at 95% confidence level. Thus the mass of the SM Higgs boson is now constrained to a small range of values. It will become a precision test of this sector with the expected improvement in M_{top} , M_W and the direct measurement of the mass at the LHC.

To verify the SM is also relevant to measure the self-interaction of the gauge fields of the electroweak lagrangian. This leads to triple gauge couplings (TGCs) of the form $WW\gamma$, WWZ and quartic gauge couplings (QGCs) $WWWW$, $WWZZ$, and so on. The SM TGCs have been confirmed at LEP but new physics can determine anomalous TGCs (ATGC). The LHC has a large potential ¹³⁾ to study TGCs because the sensitivity to anomalous contributions is enhanced at high energies. The cleanest final states are those where all W's and Z's decay leptonically, $W\gamma \rightarrow l\nu\gamma$ and $WZ \rightarrow l\nu ll$. These measurements are limited by statistics : a few thousands events are expected each 100 pb^{-1} of integrated luminosity.

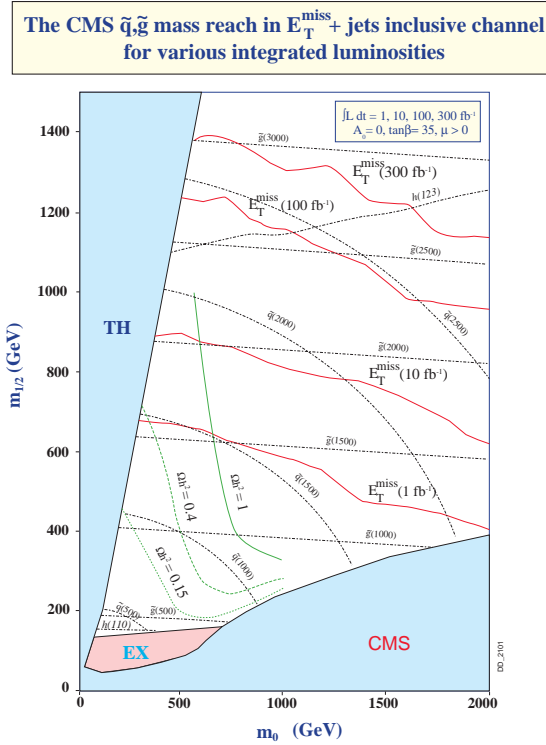


Figure 3.2: Squark and gluinos mass reach for various integrated luminosities at the LHC ¹⁴⁾. m_0 and $m_{1/2}$ are parameters of the supersymmetric model, namely the universal scalar and gaugino masses at GUT scales.

3.2.2 The quest for the Higgs boson, including SUSY

CERN is building the Large Hadron Collider (LHC), a p-p collider at $\sqrt{s} = 7 + 7$ TeV and the experiments ATLAS, CMS, LHCb and ALICE. This is the first enterprise to explore directly the TeV scale, particularly interesting for the discovery of the Higgs boson and the search for new physics.

The LHC initial luminosity will be $10^{33} \text{ cm}^{-2} \text{ s}^{-1}$, the target luminosity being $10^{34} \text{ cm}^{-2} \text{ s}^{-1}$. CERN plans to complete the LHC in the last quarter of 2006, with first beams injected during 2007 and first collisions by the end of the year.

The direct search for Higgs bosons at the LHC will be possible in the mass region from 110 GeV up to 1 TeV. Experimentally accessible decay channels are $H \rightarrow \gamma\gamma, WH, ttH (H \rightarrow \gamma\gamma), t\bar{t}H \rightarrow t\bar{t}b\bar{b}$, for the low-mass region and $H \rightarrow ZZ^{(*)} \rightarrow 4l, H \rightarrow WW^{(*)} \rightarrow l\nu l\nu, qqH \rightarrow qqWW^{(*)}, qqH \rightarrow qq\tau^+\tau^-, H \rightarrow ZZ \rightarrow ll\nu\nu, H \rightarrow WW \rightarrow lvjj$, for the intermediate and high-mass regions.

At the initial luminosity one expects to produce (in 10^7 s): $10^8 W \rightarrow e\nu, 10^7 Z \rightarrow e^+e^-, 10^7 t\bar{t}, 10^{12} b\bar{b}, 10^5 H^0 (m = 130 \text{ GeV}), 10^4 \tilde{g}\tilde{g} (m = 1 \text{ TeV}), 10^3 BH (m > 3 \text{ TeV}), \sigma(pp \rightarrow BH) \sim 100 \text{ fb}$.

After ten years of data taking at nominal luminosity (corresponding to $\int L = 300 \text{ fb}^{-1}$) one expects to measure the Higgs boson mass with 10^{-3} precision if it lays in the low-mass range, and one percent precision if in the high-mass range.

As discussed in Sec. 3.1.2, quantum corrections destabilize the Higgs sector (the so called hierarchy problem) and several solutions have been proposed, supersymmetry being the most popular.

If world is populated by supersymmetric particles then the Higgs mass is determined by the scale of SUSY breaking. Minimal SUSY Models (MSSM) are compatible with LEP and Tevatron results and a neutral lightest SUSY particle is in this case a favorite candidate for cold dark matter. MSSM contains five Higgs bosons and SUSY partners to all known particles. SUSY decays are to neutral particles, giving rise to events with missing energy. In particular, if SUSY particles are connected with the hierarchy problem, i.e. can stabilize the electroweak scale, their mass should be less than 1 TeV and some of them should be discovered at the LHC.

The production of supersymmetric particles at the LHC will be dominated by coloured particles, i.e. gluinos and squarks. The uncoloured particles, that in many SUSY models are lighter than the coloured ones, could be detected from cascade decays of heavy gluinos and squarks, leading to complicated final states.

The LHC discovery potential for squarks and gluinos, that are searched for in the events with many high- p_T jets and large missing transverse energy, is summarized in Fig. 3.2, showing that the mass reach extends up to ~ 2.5 TeV.

A feasibility study for upgrading the LHC has been launched at CERN ¹⁵⁾, which develops scenarios for increasing both, the luminosity by a factor of 10 and the energy by a factor of two.

The increased physics potential ranges from precise measurements within the SM, related in particular to the rare decay modes of the Higgs boson and to the multiple gauge boson production to improve the knowledge of triple and quartic gauge couplings, to the discover reach for several New Physics processes, like new gauge bosons and Extra-dimensions. The detector performance at high luminosity has an impact on the measurement of the particle cascades while is less crucial for the detection of extremely heavy particles. Careful studies are needed to understand the conditions under which the event pile-up, the reduced efficiencies and the increased backgrounds do not spoil the advantage to run at higher luminosity.

There are world based studies for new accelerator complexes ^{16, 17, 18)} such as a linear collider in the TeV or multi-TeV region.

Let one concentrate on the impact of an e^+e^- linear collider (LC) starting at 500 GeV with the possibility to be upgraded to 1 TeV.

Physics at the LHC and at a future Linear Collider (LC) will be complementary, similarly to the situation with previous generations of hadrons and lepton colliders. The LHC has a large mass reach for direct discoveries, while measurements suffer from the presence of that part of the event related to the interaction of the spectator partons, so that kinematic reconstructions are normally restricted to the transverse direction. QCD cross sections at the LHC are huge, giving backgrounds many orders of magnitude larger than the signal which is mostly of electroweak nature. An LC in the energy range of 0.5-1 TeV provides a much more clear environment being well suited for precision physics. The better knowledge of the momenta of the interacting particles allows for more stringent kinematic constraints to reconstruct final states. Direct discoveries of new particles at LC are limited by the available energy, while the indirect sensitivity to effects of new physics is significantly larger than at the LHC. There is a worldwide working group investigating the interplay between the LHC and the LC ¹⁹⁾ in searches for new physics and for other topics including symmetry breaking and electroweak precision tests.

In the most optimistic scenario the LC will see its birth somewhere after 2016, in the long-term future. This would guarantee a substantial period of overlapping running with the LHC, since the LHC (including upgrades) is expected to deliver data for twenty years. During the simultaneous running the analyses on each machine could be adapted to benefit for the results obtained at the other collider, and the LC results could give essential input for choosing suitable upgrade options for the LHC.

The scientific case for the LC is in changing the focus from the LHC goal of discovering the Higgs boson to measuring its properties. For instance, the precise determination (relative accuracy

at the percent level) of the BR to all possible final states ²⁰⁾ $\gamma\gamma$, bb , cc , WW can be employed to identify the SM or MSSM nature of the light neutral Higgs boson, and the mass, spin, parity can be determined.

The LC has good prospects for the production of light, uncoloured SUSY particles and the possibility to adjust the collider energy to the production threshold could allow a precise determination of the mass and the spin of the new particles. In particular, the precise measurement of the Lightest Supersymmetric Particle (LSP) at the LC could be crucial to understand the details of the decay chains of the more massive, coloured SUSY particles detected at the LHC.

For the study of the Higgs sector, if the Higgs boson will be discovered by the LHC in the $H \rightarrow \gamma\gamma$ decay and the mass measured within ± 200 MeV, the LC measurement of the top mass at the 100 MeV precision level will be mandatory to match the experimental results with the theoretical predictions.

Although the LC provides an exceptionally clean experimental environment, the detectors will present a technical challenge due to the goals of precision required. As an example, the calorimetry should be able to reconstruct with high resolution the $H \rightarrow b\bar{b}$, $W, Z \rightarrow jj$ and $t \rightarrow Wb \rightarrow jjb$ decays. Typical requirements for LC calorimetry are $35 - 40\% / \sqrt{E/GeV}$ in the jet energy resolution. In order to do so the developing technique of energy-flow ²¹⁾ requires state-of-art calorimeters with very high granularity (Si/W or hybrid proposals) or new detectors ²²⁾ where a high hadronic resolution is obtained by Dual Readout methods. Outstanding precisions are also required for vertexing detectors and tracking chambers.

The international project for the LC is now in the phase to find an agreement on the mechanisms for funding the LC and on its final location.

The LHC and the project for the LC just presented will unravel the TeV scale at some extent; however some aspects of the physics are expected to need higher energy colliders. For example, if there is a light Higgs boson its self-coupling can be studied in the multi-TeV energy region, or if the SUSY particles are discovered, the multi-TeV region is quite likely needed to complete the observation of the s-particle spectrum. CERN and collaborating Institutes have already discussed the feasibility of the multi-TeV e^+e^- collider, CLIC ¹⁷⁾, while other accelerators for reaching multi-TeV energies, such as a $\mu^+\mu^-$ collider ¹⁸⁾ or a very large hadron collider ²³⁾, seem to be more distant projects.

Summarizing,

- the LHC at CERN will explore the TeV region discovering, if it exists, the SM Higgs boson;
- the sub-TeV LC, especially suited for precision studies of the properties of a light Higgs boson and also useful to disentangle SM from MSSM physics, is in a well advanced phase of the project definition;
- accelerator R&D on multi-TeV energy regime is needed to prepare the era for studying SUSY or to discover alternative scenarios.

3.2.3 Quarks flavor, and the CP-violation enigma

Flavor physics constitutes a vast subject of the research program in HEP, addressing also the questions about relationships between the three families of elementary particles. In the SM the quark masses are produced via the Higgs mechanism through Yukawa couplings corresponding to 10 independent physics quantities: 6 quark masses and 4 quark mixing parameters, the elements of the CKM mixing matrix. These parameters are not predicted by the SM, but are fundamental constants that must be extracted from experimental data. Many theoretical approaches have been pursued to gain a deeper understanding of the flavor phenomenology and part of the research

programs on this subject is devoted to the discovery of processes signalling the nature of this new physics.

An additional feature of the SM explored by the flavor physics is CP violation, originally discovered in the neutral kaon decays ²⁴⁾.

CP violation causes particles and antiparticles to behave differently. There are two main reasons to study CP violation. The first reason is that many theories beyond the SM predict effects in this realm. The second reason is that CP violation phenomena in lepton and hadron interactions are expected to be related to the matter/anti-matter asymmetry in the early formation of the Universe determining the present composition.

The study of K meson decays has always been one of the most powerful source of experimental information for the foundation of the Standard Model (SM). Kaons have provided evidence of P, CP violation, as well as for the mechanism of flavor mixing in hadronic weak decays.

In the last decade the main attention in the field was devoted to the issue of understanding the nature of CP violation in $K \rightarrow 2\pi$ decays. The two results from the NA48 experiment at CERN ²⁵⁾ and KTeV at FNAL ²⁶⁾ firmly established the existence of a direct CP violating mechanism, as predicted by the Standard Model, therefore ruling out more exotic interpretation of the phenomenon, as the Superweak Model. The average of the two experimental results for the parameter $\text{Re}(\epsilon'/\epsilon)$ is $(16.6 \pm 1.6) \times 10^{-4}$.

It must be noted that the two measurements are only marginally compatible. Actually, NA48 measures $\text{Re}(\epsilon'/\epsilon) = (14.7 \pm 2.2) \times 10^{-4}$, while KTeV measures $\text{Re}(\epsilon'/\epsilon) = (20.7 \pm 2.8) \times 10^{-4}$.

It is however important to underline that the interpretation of the measurement in terms of fundamental SM quantities is now limited by theoretical uncertainties in the calculation of the operators which describe $K \rightarrow \pi$ transitions. Therefore, a new measurement of $\text{Re}(\epsilon'/\epsilon)$, although important to assess the experimental controversy, is not likely to help improving our theoretical description of the phenomenon.

At present, the interest of the kaon-physics community is focused on the issue of observing $K \rightarrow \pi l \bar{l}$ decays. These are GIM-suppressed decays in which diagrams with loops containing heavy quarks dominate. For this reason, in the SM these decays are sensitive to the product of the couplings $V_{ts}^* V_{td}$. In terms of the unitarity triangle (UT), constructed from the unitarity relation between CKM elements $V_{ud} V_{ub}^* + V_{cd} V_{cb}^* + V_{td} V_{tb}^* = 0$, the height is proportional to $\sqrt{BR(K_L^0 \rightarrow \pi^0 \nu \bar{\nu})}$ while the length of one side is proportional to $\sqrt{BR(K^\pm \rightarrow \pi^\pm \nu \bar{\nu})}$. Moreover, any disagreement between this kaon UT with that obtained by B meson decays, is a signature for physics beyond the Standard Model. This is particularly important since these very rare processes have the appealing feature of being theoretically clean. Unfortunately all of them suffer of major experimental disadvantages, as specified in the following.

At present, experimental evidence for such decays has been reported only for the channel $K^\pm \rightarrow \pi^\pm \nu \bar{\nu}$. The E787 Collaboration at BNL has observed two events ²⁷⁾, giving the branching ratio of $1.57_{-0.82}^{+1.75} \times 10^{-10}$. This has to be compared with the SM prediction of $(0.77 \pm 0.11) \times 10^{-10}$ ²⁸⁾. A preliminary result reporting the evidence for a third event has been announced recently by the E949 ²⁹⁾ experiment, the evolution of E787, which would move the BR to the value of $1.47_{-0.89}^{+1.30} \times 10^{-10}$. This result is about two times larger than the SM prediction, although still consistent with it. E949 was originally planned to collect data at the AGS with the goal of increasing the above statistics by a factor 3-4. Unfortunately, mostly because of lack of funding by the US DoE, this possibility has become very unlikely.

Letters of intent exist for experiments to increase the sensitivity of the measurement of the BR ($K^\pm \rightarrow \pi^\pm \nu \bar{\nu}$), respectively an extension of the NA48 experiment at CERN ³⁰⁾, and a new project at the Japanese proton facility J-PARC ³¹⁾ to start in 2008 (Sec. 3.3.1). Both projects have the goal to collect a statistics of 50 $K^\pm \rightarrow \pi^\pm \nu \bar{\nu}$ keeping the background level as low as 5-10

events.

$K_L^0 \rightarrow \pi^0 \nu \bar{\nu}$ is the most attractive channel to measure in the kaon system, since it is a direct CP-violating decay, $\text{BR}(K_L^0 \rightarrow \pi^0 \nu \bar{\nu}) \propto \eta^2$. It is also well under control on the theoretical side, its SM branching ratio being calculated to be $\text{BR}(K_L^0 \rightarrow \pi^0 \nu \bar{\nu})_{SM} = (0.26 \pm 0.05) \times 10^{-10}$ ²⁸⁾. Experimentally, however, it represents a tremendous challenge. The signature of the signal is faint, a π^0 originated by a kaon beam and nothing else. Physics backgrounds are enormous, especially from $K_L^0 \rightarrow 2\pi^0$ decays. At any hadron machine beam related backgrounds are also a problem. The present experimental limit is poor, $\text{BR}(K_L^0 \rightarrow \pi^0 \nu \bar{\nu})_{exp} \leq 5.9 \times 10^{-7}$ ³²⁾.

There are at least two competitive programs to perform the measurement in the not-too-far future. The first one is a two-step Japanese program, in which the signature of the decay should be obtained from a high energy pencil kaon beam, by the observation of a single high- p_T neutral pion. As a first step, the experiment E391a, which in 2005 is taking data at the KEK-PS ³³⁾, is expected to assess the feasibility of the method and to reach a single event sensitivity of $\sim 10^{-10}$. The final experiment ³⁴⁾ is then planned to operate at the J-PARC facility, presently under construction at Tokai, Japan, with the goal of observing 100 SM events by year 2012.

The second program consists of the KOPIO experiment at BNL ³⁵⁾. A low-momentum, ~ 700 MeV/c, micro-bunched kaon beam will be used to determine through time-of-flight measurements the K_L decay position, time and thus velocity. Therefore KOPIO should be able to kinematically suppress backgrounds by working in the K_L center-of-mass system. In three years of running, starting from 2010, KOPIO should be able to observe ~ 40 SM events upon a background of 20, yielding a 20% measurement of $\text{BR}(K_L^0 \rightarrow \pi^0 \nu \bar{\nu})$.

Other proposals ³⁶⁾ for experiments to improve the precision of the measurements of the charged kaons have been presented to the Board of the Japanese Hadron Facility J-PARC ³⁷⁾. They include the study of the semileptonic, leptonic, and non-leptonic decay channels, of interest for CP violation, to verify the unitarity of the first row of the CKM matrix and to assess the theoretical models to obtain predictions in the area of non-perturbative QCD.

As it has been mentioned in the case of the measurement of $\text{Re}(\epsilon'/\epsilon)$ flavor physics often deserve a difficult interpretation because is affected by hadronic uncertainties. The study of weak interaction phenomena and the extraction of quark mixing parameters remain limited by the capacity to deal with non-perturbative strong interactions. Techniques such as lattice QCD (LQCD) or Chiral Perturbation Theory (χ PT) have produced calculations of non-perturbative quantities with accuracies of 10-20%. The path to higher precisions require in some cases more accurate data to test and calibrate new theoretical techniques.

The scientific program of the charm factories, CESR-c at Cornell ^{38, 39, 40)} and BEPC at Beijing ⁴¹⁾ (Sec. 3.7.3), is focused on the study of charm data addressing topics like the charmonium spectroscopy, the charm decay constant f_D , the charm semileptonic decay factors and branching ratios to determine V_{cd} and V_{cs} , which benefit from the experimental constraints given by the energy near threshold for charm production. These measurements can provide validation of the LQCD calculations at few percent level ³⁸⁾.

During first quarter of 2004, CLEO-c has been running ⁴⁰⁾ at a peak luminosity of about $5 \times 10^{31} \text{ cm}^{-2} \text{ s}^{-1}$. Their plan from today to 2007 is to integrate 3 fb^{-1} at the $\psi(3700)$ (or $1.3 \times 10^9 J/\psi$), then switch to the $D_s D_s$ threshold and accumulate another 3 fb^{-1} (or 3×10^7 events), and finally to switch to the J/ψ aiming to collect 10^9 events, i.e., twenty times the BES statistics.

The experiments at the asymmetric B-factories, BABAR at SLAC ⁴²⁾ and BELLE at KEK ⁴³⁾, are performing comprehensive studies of CP violation in the B_d meson system, searches for B rare decays and precision measurements in the charm and τ sectors. B-factories are performing particularly well since the very beginning in year 1999, delivering to BABAR 244 fb^{-1} and to BELLE

286 fb⁻¹. Their outstanding results have been reported for example at the ICHEP Conference ⁴⁴⁾. Both experiments have measured the time dependent asymmetry in the decays in the pure CP state $B(\bar{B}) \rightarrow J/\Psi K_S$ ($b \rightarrow c\bar{c} s$ transition) on the basis of 8,000 (BABAR) and 4,500 (BELLE) tagged events, obtaining comparable, very precise results on the UT angle $\sin 2\beta = 0.726 \pm 0.037$, in agreement with the SM predictions constrained by previous measurements of ϵ_K , Δm_D , Δm_s and V_{ub}/V_{cb} . Time asymmetry has also been measured in various other CP eigenstates, involving transitions $b \rightarrow s\bar{s}s(s\bar{d}d)$, i.e. $f_0 K_S$, $K_S \pi^0$, ϕK_S , $\eta' K_S$ and $(KK)K_S$. In the SM is also possible to connect these asymmetries to the $\sin 2\beta$ even if they can not proceed at tree level. The experimental values are in agreement, $\sin 2\beta = 0.42 \pm 0.10$ and show a deviation of $\geq 2 \sigma$ from the result obtained with charmonium. Such a deviation provides a possible effect of new physics in this sector. Much more statistics (1500 fb⁻¹) is needed to confirm such an effect at 5 σ level, that is beyond the expected final integrated luminosity at the present B-factories, in the range of 500 fb⁻¹.

The physics potential of a Super-B-factory with $L \sim 10^{36} \text{ cm}^{-2} \text{ s}^{-1}$ is currently under discussion ⁴⁵⁾ by the SLAC and the KEK community as well. This mid-term project, in the 2010s, would be the logical continuation of the present B-factory program in the LHC era, complementing the measurements at the hadronic machines with the study of rare, fully reconstructed channels.

To complete the measurements of the UT, isospin analysis of the decays $B \rightarrow \pi\pi$, $\rho\rho$ and $\rho\pi$ and the $B \rightarrow DK$ decay amplitudes must be determined. BABAR and BELLE recently reported the first measurements of α , $\alpha = (100 \pm 10)^\circ$ and $\gamma_{BELLE} = (77 \pm 19 \pm 13 \pm 11)^\circ$, $\gamma_{BABAR} = (88 \pm 41 \pm 19 \pm 10)^\circ$.

At the LHC, LHCb, dedicated to B-physics, as well as the general purpose experiments ATLAS and CMS, will provide new results, including precise measurements of the B_s/B_c mesons, in the mid-term future. The high statistics recorded will allow the CKM parameters to be measured in different channels, giving additional tests of the SM and hopefully revealing aspects of the physics beyond SM.

The new experiment dedicated to B-physics, LHCb ⁴⁶⁾ has a forward detector geometry exploiting the fact that both b and \bar{b} hadrons, faster in the forward (backward) than in the central region, are predominantly produced in the same direction at high energies. LHCb will study B mesons produced at the LHC proton collider being built at CERN. The experiment will be ready for data taking at the beginning of the LHC operations, by the end of 2007.

The detector (Sec. 2.8.4) has been designed to select B decays out of the huge hadronic background by means of multi-level triggering, vertex detection, forward multiparticle magnetic spectrometer, RICH particle ID, electromagnetic calorimetry and muon detection.

The experiment claims to reach in one year of data taking a precision in the measurement of $\sin(2\beta)$ of 2%, in $\sin(2\alpha)$ of 5%, and in $\sin(2\chi)$ of 4%.

3.3 Hadronic and nuclear physics

The physics of hadrons and nuclei is the physics of strong force. The theory of the strong interaction, Quantum Chromodynamics (QCD), is remarkably successful in describing high-energy experiments involving quarks and gluons. The application of QCD to the lower energies (and longer distance scales such as the size of atomic nucleus) is a major challenge. The rapidly increasing strength of the interaction at low energies makes it impossible to apply perturbative techniques. However, the situation has improved considerably in recent years due to several theoretical developments (Sec. 3.1.4). As a result, various QCD-based predictions are now available in the non-perturbative domain, which can be tested experimentally in the coming decade. Steps can now be made towards the realisation of long-standing objective of hadronic nuclear physics, as understanding basic properties of nucleons, as their mass (related to the chiral symmetry breaking

mechanism) and spin, and their mutual interactions (and how both act inside nuclei) in terms of the underlying theory of the strong interaction.

Substantial progress can be expected over the next decade on some items, as the form factors, the hadron spectroscopy, the chiral symmetry breaking mechanism, the nucleon spin structure and the generalized parton distributions.

3.3.1 Hadron spectroscopy

The spectroscopy of hadrons has always been a key source of information to investigate the non-perturbative regime of QCD.

A complete mapping of mesonic and baryonic resonances in the mass region between 1 and 3 GeV will be particularly important to the understanding of the underlying dynamics of QCD and of quark confinement mechanism.

The standard quark model classifies hadrons as quark-antiquark $q\bar{q}$ states for mesons and three-quarks (qqq) states for baryons. Any state with different quark content is labeled as exotic, such as the multiquark mesons ($qq\bar{q}\bar{q}$) and baryons ($qqqq\bar{q}$), the dibaryons ($qqqqqq$), the hybrid states ($q\bar{q}g$ and $qqqg$) and the glueballs. In the meson sector, several candidates for ($qq\bar{q}\bar{q}$) states have been suggested, but no conclusive results have been drawn. In the baryon sector, recently evidence for the existence of the first pentaquark states (the $\Theta^+(1540)$) has been reported by several experiments, but this result is still under investigation and need to be verified with high statistic experiments.

Hadron spectroscopy will be an important part of the recently approved 12 GeV JLab physics programs. It includes the upgrade of the CLAS detector ⁴⁷⁾ in the Hall B and the construction of the GlueX ⁴⁸⁾ detector in the new Hall D, which will be dedicated to the search of gluonic excitations in real photon experiments.

In Europe, the GSI laboratory is on the way of constructing a new accelerator Facility for Antiproton and Ion Research (FAIR) ⁴⁹⁾ for the research with ion and antiproton beams, in cooperation with their users and the international community. The PANDA ⁵⁰⁾ experiment (which will be installed at the HESR ring at GSI) will be in a unique position to search for the existence of glue balls, hybrid and novel charm quark states. The use of an antiproton beam and the chosen energy enables the exploration of states of all possible quantum numbers in a mass domain populated by only very few known states. Moreover, the facility offers the possibility to provide high quality beams of antiprotons and ions for the experimental program.

The main points of the antiproton physics program are: search for gluonic degrees of freedom; spectroscopy of charmonium states; γ -spectroscopy of single and double-hypernuclei; in-medium modifications of charmed mesons.

In Japan, within the J-Parc project ³⁷⁾ an accelerator facility consisting of a 400 MeV LINAC, a 3 GeV proton synchrotron (RCS) and a second proton synchrotron (MR) of 50 GeV, has been planned. This complex will performe accelerator-driven trasmutation experiment (LINAC beam); materials and life science (3 GeV beam); nuclear and particle physics and neutrino experiments (50 GeV beam). The 50 GeV proton synchrotron will be used to address many problems of hadronic physics: strangeness nuclear physics; mesons in nuclear matter; hadron spectroscopy; investigation of S=-2 and S=-1 nuclear systems.

3.3.2 Chiral symmetry breaking by means of exotic-atom studies

One of the key-questions in the today physics is related to the process bringing to the mass generation. The chiral symmetry represents the symmetry of the QCD valid in the limit of vanishing

quark masses. If the masses of the three lightest quarks were different from zero but equal among themselves, the $SU(3)_f$ flavor symmetry would still be valid. In the real world, both the chiral and the $SU(3)_f$ symmetry are broken. Studying the way in which this happens can therefore give us important insights related to the mass generation mechanism. One of the ways to study the chiral symmetry breaking mechanism is related to the measurement of the X-ray transitions in the exotic hadronic atoms, as pionic hydrogen and deuterium and kaonic hydrogen and deuterium. The 1s level for these atoms suffers a shift and a broadening with respect to the purely electromagnetic-calculated values, generated by the presence of strong interactions. The measurements of the shifts and widths are further on used to determine the meson-nucleon scattering lengths, used in the calculation of the so-called meson-nucleon sigma terms. The meson-nucleon sigma terms ⁵¹⁾, which measure the nucleon mass shift away from the chiral limit, parametrize the explicit breaking of chiral symmetry in the QCD due to the non-zero quark masses, thus giving crucial information about the nature of chiral symmetry breaking, and to what extent it must be broken. A meson nucleon sigma-term is defined as the nucleon expectation value of the equal-time double commutator of the chiral symmetry breaking part of the strong interaction Hamiltonian. The sigma terms are related to the meson-nucleon scattering amplitudes via the corresponding low-energy theorem in the soft meson limit. The sigma terms are also important inputs for the determination of the strangeness content of the proton ⁵²⁾. The pionic hydrogen and deuterium were and are being measured at the Paul Scherrer Institut (PSI) ⁵³⁾ and the pion-nucleon sigma term has been determined ⁵⁴⁾, even if there are still open problems ⁵⁵⁾. The kaon-nucleon sigma terms have not determined yet and only estimates are available. This is due to the lack of complete experimental data: the kaonic hydrogen was recently measured at the DAΦNE accelerator in Frascati by the DEAR experiment to be continued by the SIDDHARTA experiment ^{56, 57, 58)} (Sec. 4.8), while the measurement of kaonic deuterium is to come in the framework of the SIDDHARTA experiment. The low-energy $\bar{K}N$ system, the kaonic hydrogen in particular, is of special interest for chiral $SU(3)$ symmetry in QCD and for the role of explicit symmetry breaking induced by the relatively large mass of the strange quark ⁵⁹⁾. The future of the chiral symmetry breaking mechanism study is necessarily related to the DAΦNE machine, due to the unique kaon beam quality, which should allow unprecedented quality measurements of kaonic atoms.

3.3.3 Spin structure of the nucleon: status and perspectives

In the naive quark model, the spin of the proton is carried by its three valence quarks. However, in recent years it has been understood that the gluons and possibly the orbital angular momentum of the quarks and gluons also contribute to the total spin content of the nucleon, through the equation $1/2 = 1/2\Delta\Sigma + \Delta G + L_z$. $\Delta\Sigma$ represents the summed contributions of the quarks spins, ΔG the contribution of the gluons, and L_z the orbital angular momentum of the partons. Experimental information on the summed quark contributions has been obtained in polarized inclusive deep-inelastic scattering experiments, through the measurement of the longitudinal spin (or helicity) distribution function $g_1(x)$. When integrated over, this yields a value for $\Delta\Sigma$. The results obtained at CERN with SMC ⁶⁰⁾, DESY with HERMES ⁶¹⁾ and SLAC with E142, E143, E154, E155 ⁶²⁾ are of high quality and fully consistent with each other, but future extension of them are needed at very low x ($x < 10^{-2}$) and at very high x (close to 1): they can be carried out at the foreseen e-RHIC facility ⁶³⁾ and the 12 GeV JLab upgrade ⁶⁴⁾, respectively. The high quality data at present provided the total quark spin contribution $\Delta\Sigma/2 = 0.1-0.3$ of the nucleon spin, indicating that additional carriers of angular momentum are needed in the nucleon.

To understand further the spin structure of the nucleon, the dependence of the spin distribution functions has been determined by the semi-inclusive deep-inelastic scattering experiments,

in which one of the final hadrons is detected. Data recently obtained by HERMES ⁶⁵⁾ for five different quark distributions suggest that all extracted sea quark polarizations are consistent with zero and the light quark sea helicity densities are flavor symmetric within experimental uncertainties. A more definite conclusion can be drawn only by obtaining more data at low and high x values: COMPASS ⁶⁶⁾ will extend the measurements of $x\Delta s$ well below $x=10^{-2}$, the 12 GeV JLab upgrade up to $x=0.8$. Also RHIC will provide data for various quark flavours.

As the polarizations of the valence and sea quarks taken together cannot account the full spin of the nucleon, efforts are now being made to measure the gluon polarization. QCD analyses of the polarized structure function $g_1(x)$ indicate that the gluon polarization could be large and positive. The proposals for determining ΔG are based on identifying photon-gluon fusion events in deep-inelastic scattering experiments, where the virtual photon annihilates with a gluon from the target to produce a quark and its antiquark. The asymmetry of the process is sensitive to the gluon polarization. HERMES has recently explored this process by detecting pairs of hadrons with high transverse momentum ⁶⁷⁾: a positive value for ΔG has been found, but with large statistical and systematic uncertainties. Measurements of $\Delta G/G$ at COMPASS are based on isolating the photon-gluon fusion process through open charm production or by identifying high- p_T pion pairs. At RHIC prompt photons originating from $qg \rightarrow \gamma q'$ process in photon-proton collision need to be identified in order to measure $\Delta G/G$.

While the structure functions $F_1(x)$ and $g_1(x)$ represent the momentum and spin distributions of the quarks, a third leading twist function $h_1(x)$ represents the transverse spin distribution of quarks, that is the probability of finding a quark with its spin-orientation parallel to that of the nucleon when the nucleon spin is perpendicular to the incident beam. Almost nothing is known at present about the transversity distribution $h_1(x)$, even though it is of great interest since data on it would enable to investigate two remarkable QCD-based predictions. Gluons are predicted not to contribute to the transverse spin distribution and so the structure functions $F_1(x)$ and $h_1(x)$ are expected to differ considerably. The tensor charge is predicted to be much larger than the integral over $g_1(x)$ which leads to $\Delta\Sigma$.

Inclusive deep-inelastic scattering cannot be used to measure $h_1(x)$ as it is a chiral-odd quantity. In semi-inclusive DIS, information on $h_1(x)$ can only be obtained if it appears in the cross section expression in combination with a chiral-odd fragmentation function. At present HERMES provided first data in this field ⁶⁸⁾ and actually it is still running with a transversely polarized hydrogen target. A considerable effort is foreseen at COMPASS, JLab and RHIC to further measure the transversity distribution $h_1(x)$ in the nearby future. At a somewhat longer timescale the proposed PAX ⁶⁹⁾ internal target experiment at HESR may provide a direct measurement of this quantity.

3.3.4 Understanding the nucleon structure by the Generalized Parton Distributions

The internal quark-gluon structure of hadrons is encoded in a well defined hierarchy of correlation functions, the simplest of which are the parton distributions. In recent years, much progress has been made in developing a broader framework of so-called Generalised Parton Distributions (GPDs), known also as skewed, off-forward or non-forward parton distributions ⁷⁰⁾. They are a generalization of the usual parton distributions describing the momentum or helicity distributions of the quarks in the nucleon. The GPDs are also sensitive to quark-antiquark configurations in the nucleon, hence they provide information on nucleon properties that otherwise are hard to access. The most prominent example is the total angular momentum carried by the quarks in the nucleon, which can be obtained from an integral over a certain combination of GPDs. It has been shown

theoretically that the amplitudes for various reactions factorise in a calculable hard scattering part and a combination of such GPDs if the momentum transfer involved is sufficiently high. This proof makes it possible to extract GPDs from experimental data, and the GPDs thus offer a new unified interface for comparing experiments and non-perturbative QCD calculations. From the theoretical point of view, the introduction of these new distributions builds a bridge between fundamental QCD, phenomenology and experimental observables. Moreover, such measurements are sensitive to the total angular momenta carried by quarks of given flavor in a polarized nucleon. Exclusively deeply virtual meson production (DVMP) and deeply virtual Compton scattering (DVCS) provide a handle on the experimental determination of these distributions.

The DVCS is the simplest reaction from the theoretical point of view, but also the most difficult experimentally because one has to select perfectly the final state (one lepton, one proton and one photon) among all reactions. DVCS is accessed by photon lepto-productions $lp \rightarrow l'p'\gamma$, where the final photon can be emitted either by the leptons (Bethe-Heitler process) or by the proton (genuine DVCS process). The hard production of photons within the target nucleon is indistinguishable from the Bethe-Heitler process in which the photons are emitted by the incident or scattered electrons. At high enough energies, the DVCS is expected to dominate in most of phase space, whereas at somewhat lower energies the interference between the two processes may be used to study DVCS at the amplitude level. A careful analysis of the dependence of the cross section on the azimuthal angle ϕ between the leptonic and hadronic planes and on Q^2 allows to disentangle higher twist effects and to select the real (proportional to $\cos\phi$) and imaginary (proportional to $\sin\phi$) parts of the DVCS amplitude. Beam spin asymmetries, measured both at HERMES ⁷¹⁾ and CLAS ⁷²⁾, display a characteristic $\sin\phi$ dependence, due to the above mentioned interference, while the first measurement of Beam Charge Asymmetry obtained at HERMES is indicative of the expected $\cos\phi$ dependence, and it is identifying the role of $q\bar{q}$ in the proton. The statistic and kinematic coverage of such measurements has to be dramatically improved before DVCS data can be used to extract information on the total angular momentum carried by quarks, or to use these data for mapping the spatial distribution of quarks in the nucleon. As reported in Sec. 4.3.1, dedicated DVCS experiments will be performed at JLab and HERMES starting from 2005 and 2006, respectively. Moreover, a large fraction of the JLab 12 GeV upgrade program will also be devoted to the study of the exclusive reactions at high luminosity. Also the planned measurements at COMPASS, will be promising for extracting the invariant momentum transfer t -dependence of the GPDs. Since the integral of the GPD's are related to the hadronic form factors, the t -dependence of hard electroproduction amplitudes and the elastic form factors are interconnected.

3.3.5 Elastic Form Factors

The elastic form factors of hadrons as measured in both space-like and time-like regions provide fundamental informations on their structure and internal dynamics. The interest for nucleon form factors has been recently raised by the measurement of electron-to-proton polarization transfer in electron-proton elastic scattering at Jefferson Laboratory ⁷³⁾, which showed that the ratio G_E/G_M is monotonically decreasing with increasing $Q^2 = -q^2$, in strong contradiction with the flat ratio close to 1 determined by the traditional Rosenbluth separation method ⁷⁴⁾. These results raise serious questions: first, how to best combine data from these two techniques; and second, if some correction that has been neglected in the cross section can be the source of the discrepancy. New data are expected to answer these questions, in particular from the new polarization experiment approved at JLab ⁷⁵⁾ that will extend measurements up to $Q^2 \approx 10 \text{ GeV}^2$.

Although the space-like form factors of a stable hadron are real, the time-like form factors are complex functions of the total energy squared $s = q^2$, due to the Final-State Interaction (FSI) of

the outgoing hadrons ⁷⁶⁾. The analytic structure and phases of the form factors in this regime is connected by dispersion relations to the space-like regime ^{77, 78, 79)}, and also reflects the presence of resonances in the unphysical region $0 < q^2 < 4M_p^2$ in the $J^{PC} = 1^{--}$ channel ⁷⁷⁾, including gluonium states and dibaryon structures. The moduli of nucleon form factors can be derived from cross section measurements in $e^+e^- \rightarrow N\bar{N}$ experiments, while the determination of their phases requires the measurement of polarization observables. At present, experimental data on time-like nucleon form factors have huge experimental uncertainties (proton data on $|G_E|$ and $|G_M|$ are based on the assumption $|G_E| = |G_M|$, valid only at threshold, the neutron form factors have been derived on the basis of 74 events only in the FENICE experiment ⁸⁰⁾ or are completely missing (as for the phases). A complete determination in terms of moduli and phase of the nucleon form factors in the time-like region can be achieved in the proposed high energy upgrade of DAΦNE, as reported in Sec. 4.9. The measurement of proton form factors is also part of the experimental program of the PAX Collaboration ⁶⁹⁾ at GSI, which is expected to start in 2012. They proposed to measure the reversed channel $\bar{p}^\dagger p \rightarrow e^+e^-$ using a transversely polarized proton target. The relative phase is measured from the single spin asymmetry data, while the modulus of $|G_M|$ and $|G_E|$ can be deduced from angular distributions in unpolarized measurement as it can be carried out independently at PANDA ⁵⁰⁾ as well as at PAX.

3.3.6 The search of the Quark Gluon Plasma

Understanding the properties of elementary particles at high temperature and density is one of the major goals of contemporary physics. Through the study of properties of elementary matter exposed to such extreme conditions it is possible to learn about the equation of state that controlled the evolution of the early Universe as well as the structure of compact stars.

A large experimental program is devoted to the study of hot and dense matter created in ultra-relativistic heavy ion collisions. Lattice studies of QCD thermodynamics have established a theoretical basis for these experiments by providing quantitative information on the QCD phase transition, the equations of state and many other aspects of QCD thermodynamics.

Already 20 years ago lattice calculations first demonstrated that a phase transition in purely gluonic matter exists and that the equation of state of gluonic matter rapidly approaches ideal gas behavior at high temperature. These observables have been of central interest in numerical studies of the thermodynamics of strongly interacting matter ever since. Heavy-ion collisions allow to study strong interactions under extreme conditions of the hadronic matter. Indeed, by increasing the atomic number of the colliding systems and by raising the energy of the collision, it is possible to access to a regime where a high energy density is created in the collision volume, and very high dense matter at high temperature and pressure is produced. This regime generally is denoted as the Quark Gluon Plasma (QGP). The search of the experimental signatures that can provide evidence for the thermal properties of the QGP is the goal of many experiments running at RHIC and of the ALICE experiment planned at LHC ⁸¹⁾.

3.4 Astroparticle physics

In the last decade, a growing interest in particle physics related to space has become a focus of great activity. Indeed, the study of particles from cosmic sources appears to provide most interesting clues for questions originating from particle physics proper as well as from astrophysics. The Astroparticle physics is a new interdisciplinary field and represents the intersection of astronomy, astrophysics, cosmology and particle physics: it combines the present knowledge about the smallest

fundamental particles and the largest structures in the Universe. Astroparticle physics explores the sources of ultrahigh energy cosmic rays and the mechanism of cosmic accelerators, and studies the Universe beyond classical multi-wavelength observations, using gamma rays, neutrinos and cosmic rays at all energies. In the following, it is briefly review some of the most important topics that are presently drawing major interests both from the experimental and theoretical point of view.

3.4.1 Ultra High Energy Cosmic Rays

The highest energy particles in Nature are cosmic rays. The most energetic one yet detected has an energy of 3×10^{20} eV. This energy is probably not set by Nature but by the relatively small area ($\approx 100 \text{ km}^2$) of the devices that have been used to search for them, the rate above 10^{20} eV being only about 1 per km^2 per century. A still open issue concerns these Ultra High Energy Cosmic rays (UHECR) beyond the so-called GZK cut-off ⁸²⁾, i.e. particles that seem to have escaped absorption by scattering on the cosmic microwave background (CMB). Even their existence remains to be demonstrated, since the present available experimental results (e.g. from Fly's Eye, AGASA, HiRes experimental arrays) cannot settle the issue. The AUGER programme ⁸³⁾ - with its first site of 3000 km^2 in Argentina - as a result of its two independent and concurrent techniques to detect an atmospheric shower (fluorescence detectors plus an array of ground detectors) should bring the answer and, if they exist, perhaps tell something on their nature. Another way to tackle the problem and to achieve a greater exposure is planned with the space experiment EUSO ⁸⁴⁾ to be placed on the 'International Space Station which will detect the trails of nitrogen fluorescence light made by giant extensive air showers as seen from space down to Earth. It is expected that EUSO will be able to detect some 10^3 events per year above 10^{20} eV and also open a new window into the high energy neutrino universe.

3.4.2 Gamma Rays

Gamma astronomy studies incoming photons, detected either above the atmosphere in balloons and satellites, or on the ground, by large mirrors focusing the Čerenkov light of their shower onto a fine-grained array of photodetectors. Its main objective at present is to fill the gap between low energies (a few GeV, the domain of satellites, EGRET in the past, AGILE ⁸⁵⁾ and GLAST ⁸⁶⁾ in the future) and high energies (a few hundred GeV, the threshold of ground detectors up to now). This region can in particular give information about the distribution of the CMB with which the photons interact. In fact, these detectors are able to provide information on several other subjects and search for relic dark matter candidates (WIMPs, Weakly Interacting Massive Particles). Preliminary results from HESS ⁸⁷⁾ a stereo-imaging Čerenkov telescope located in Namibia, and the recent start of the 17-meter diameter MAGIC ⁸⁸⁾ telescope in Las Palmas (Canarias) are shedding new light in this field of research. Despite fundamental progress over the past few years, many intriguing and deep questions about the origin of Gamma ray Bursts (GRBs) still remain open such as what is the relation of GRBs to galaxies, stellar populations and to the history of star formation in the Universe. By identifying accurate positions of bursts with respect to their host galaxies, and their redshift distribution, one can tackle the problem of whether bursts are indeed related to the death of compact stars such as neutron stars and/or black holes, or to unusual star formation paths, or yet again to unknown and unidentified objects. The burst redshift distribution will provide crucial information about the star formation in the Universe which is known to strongly evolve up to redshifts of 1.5–2.0. If, as predicted by at least some models, bursts are indeed related to some peculiar death mode of massive stars, binary or otherwise, their redshift distributions ought to match that of star formation in the Universe. Moreover, they are so

bright to allow us to measure the star formation history of massive stars to very high redshift, with $z > 5$ or even 10, if there are stars already formed at these early ages. Finally, GRBs will allow to determine the dust material in distant galaxies, deducing the extinction curve, and to determine the structure and ionisation of intergalactic medium at very high redshifts. To improve the present understanding in this field it is necessary to build a large database including high quality data taken on different timescales and at various frequencies that can be used to constrain current and future theories. It is clear that this requires new satellite missions like the above mentioned AGILE and GLAST, together with SWIFT ⁸⁹⁾ fully dedicated to the study of GRBs and their afterglows.

3.4.3 High Energy Neutrinos

Neutrino telescopes allow today the detection of Solar MeV neutrinos, thus enabling direct observations of nuclear reactions in the core of the Sun, which is opaque to photons, as well as studies of fundamental neutrino properties. High energy, more than 100 GeV, neutrino telescopes are currently operating in deep lake water (BAIKAL ⁹⁰⁾) and under Antarctic ice (AMANDA ⁹¹⁾). Two under-water detectors are currently under construction in the Mediterranean (ANTARES ⁹²⁾ and NESTOR ⁹³⁾), aiming at achieving effective volumes $\sim 0.1 \text{ km}^3$, comparable to that of AMANDA. Much larger, 1 km^3 telescopes are under construction in Antarctic ice (the IceCube ⁹⁴⁾ extension of AMANDA), and under development in the Mediterranean (NEMO ⁹⁵⁾). The driving motivation for the construction of km-scale neutrino telescopes is the observation of cosmic point sources. At present, several neutrino telescopes monitor solar MeV neutrinos, and may also detect MeV neutrinos from Supernova explosions, such as Supernova 1987A, in the local galactic neighborhood. The construction of high energy neutrino telescopes is aimed at extending the distances accessible to neutrino astronomy to cosmological scales. This new window onto the cosmos will provide a probe of the most powerful sources in the universe through observations of high-energy neutrinos.

3.4.4 Dark Matter

It is presently admitted that a substantial part of the Universe is “dark”, i.e. invisible and felt only through its gravitational effect. Moreover, most of it must be “cold”, i.e. non-relativistic at the time relevant for galaxy formation. The cold dark matter (CDM) contribution to the content of the Universe has been accurately determined by the satellite experiment WMAP ⁹⁶⁾ to be $(29 \pm 4\%)$. Concerning its baryonic part, $(4.4 \pm 0.4\%)$, of which only a tenth corresponds to visible stars), the possibility that it could be mostly due to dark objects like “failed stars” is now excluded. Gas and dust may be the answer. For non baryonic dark matter, the axion and the neutralino (the lightest supersymmetric particle) are still favoured candidates. In the direct search for neutralinos and more generally for WIMPS, fossile Weakly Interacting Massive Particles, one looks for the tiny recoil energy that a nucleus struck by the projectile leaves in a detector. This has to be well shielded from cosmic radiation. The Gran Sasso Laboratories of INFN provide a natural shield of 1400 m of rock and important Dark Matter experiments (DAMA ⁹⁷⁾, CRESST, HDMS) are conducted in its three galleries equipped as experimental halls. In particular, the DAMA experiment has shown a result which suggests a seasonal variation of its counting rate, for a very low threshold, as could be expected from a halo of fossil neutralinos of about 60 proton masses and the seasonal variation of the Earth’s velocity relative to the halo. Other experiments - CDMS ⁹⁸⁾ and EDELWEISS ⁹⁹⁾ - are presently searching for this effect and new results are expected for independent confirmation.

3.4.5 Matter-Antimatter asymmetry in the Universe

The apparent absence of antimatter (antihelium, anticarbon, etc.) in the universe is one of the great puzzles in particle physics. Theories that predict either the existence of antimatter in segregated domains or the total absence of antimatter have no firm foundation in experimental data. The existence (or absence) of antimatter nuclei in space is closely connected with the foundation of the theories of elementary particle physics, CP-violation, baryon number non-conservation, Grand Unified Theory (GUT), etc. Balloon-based cosmic ray searches for antinuclei at altitudes up to 40 km have been carried out for more than twenty years; all such searches have been negative. The absence of annihilation gamma ray peaks excludes the presence of large quantities of antimatter within a distance of the order of 10 Mpc from the Earth. Baryogenesis models are not yet supported by particle physics experimental data. To date baryon non-conservation and large levels of CP-violation have not been observed. Cosmological observations show that the matter of the universe is mostly dark matter. If dark matter, or a fraction of it, is non-baryonic and consists of almost non-interacting particles like neutralinos, it can be detected in cosmic rays through its annihilation into positrons or antiprotons, resulting in deviations (in the case of antiprotons) or structures (in the case of positrons) to be seen in the otherwise predictable cosmic ray spectra¹⁰⁰). The search for antimatter and dark matter is greatly facilitated if performed outside the Earth's atmosphere. The space experiments PAMELA¹⁰¹) (on Russian satellite to be launched in autumn 2005) and AMS-02¹⁰²) (on ISS, scheduled for early 2008) will extend the search for antimatter and dark matter signatures over a wide energy range and with unprecedented sensitivity, greatly increasing the low statistics presently available from balloon-borne experiments.

3.5 Neutrino physics

Since 1998, an impressive sequel of experimental results have provided evidence in favor of the neutrino oscillation hypothesis¹⁰³). The long-standing puzzle of the solar neutrino deficit seems well understood once the existence of oscillations among different flavors (enhanced by matter effects in the sun and the earth) is assumed. Such an hypothesis has been tested in a very straightforward manner both through the NC/CC ratio of the solar neutrino interactions and through the observation of a deficit of artificial ν 's from reactors consistent with the parameter set suggested by solar data. Similar results have been collected for atmospheric neutrinos; here, evidence is claimed by experiments that detect neutrinos produced by the interactions of primary cosmic rays in the atmosphere. These results were corroborated by the study of neutrinos produced at accelerators with path-length over energy ratios L/E comparable to the one of the atmospheric ν 's.

The present standard interpretation suggests the existence of only three massive neutrinos. The flavor eigenstates result from the mixing of the mass eigenstates and the leptonic mixing matrix can be parametrized in a CKM-like form by three real Euler angles and one CP violating complex phase (Dirac phase). No information is available on the Dirac or Majorana nature of neutrinos. In the latter case, two additional complex phases contribute to the leptonic mixing (Majorana phases), which are, however, irrelevant for the oscillation phenomenology. In this scenario, the frequency of the oscillations at the atmospheric scales depends on the (absolute value) of the mass squared difference between the third and second family ($|\Delta m_{32}^2| \equiv |m_3^2 - m_2^2|$) and its magnitude is mainly related to the θ_{23} angle. Similarly, the solar oscillations depend on Δm_{21}^2 and θ_{12} ; the occurrence of matter effect fixes the sign of Δm_{21}^2 ($\Delta m_{21}^2 > 0$). The full three family interference pattern has never been observed and direct mixing between the first and the third family is suppressed by the smallness of the θ_{13} angle ($\theta_{13} \lesssim 11^\circ$)¹⁰⁴). The evidence for ν_e appearance of the LSND

experiment is in contradiction with this standard scenario.

There is consensus on the fact that the precise determination of the mixing matrix will likely come from new generations of accelerator experiments. In fact, the next round of these experiments (MINOS, ICARUS, OPERA, MiniBOONE) is aimed at the precision test of the parameters leading the atmospheric oscillations (θ_{23} and Δm_{32}^2), the direct test of the oscillation paradigm through the observation of the appearance of new flavors ($\nu_\mu \rightarrow \nu_\tau$ oscillations) and the test of the LSND claim. This experimental program will cover the next 5-8 years; INFN (and LNF, in particular) is strongly involved in the CNGS (Cern Neutrinos to Gran Sasso) programme, which is currently in construction phase. Commissioning and data taking will start in 2006 and a five year duration is foreseen.

A second generation of experiments will start data taking in ~ 2009 with the aim of testing the smallness of the θ_{13} angle at the $\sim 3^\circ$ level and further improving the precision on θ_{23} and Δm_{32}^2 . The size of the 1-3 Euler angle is crucial for the determination of the future experimental strategy. In particular, $\theta_{13} \gtrsim 3^\circ$ could allow to establish CP violation in the leptonic sector using high intensity traditional neutrino beams and a new generation of massive detectors. CP violation would be tagged as an asymmetry between the $\nu_\mu \rightarrow \nu_e$ and $\bar{\nu}_\mu \rightarrow \bar{\nu}_e$ oscillation probability at the atmospheric scale. At this scale, in the standard scenario the oscillations are dominated by the $\nu_\mu \rightarrow \nu_\tau$ transition and $\nu_\mu \rightarrow \nu_e$ or its CP-conjugate arises as a three-family perturbation to the leading contribution. This sub-dominant transition comprises information on the size of θ_{13} , the Dirac phase δ and, if baselines are such that matter effects are not suppressed, the sign of Δm_{32}^2 . The extraction and disentangling of all these information is a formidable task, which will likely define a roadmap for the experimental neutrino physics along the next 10-20 years. For smaller values ($\theta_{13} \gtrsim 1^\circ$) new technologies for neutrino beam production could be envisaged although the complexity and cost of these innovative facilities make a preliminary determination of the size of θ_{13} mandatory. Unfortunately, no compelling theoretical prior on the mixing angle size is available, yet. It is therefore clear that neutrino oscillations are going to enter an era of precision measurements where most of the information will come from accelerator experiments. A new generation of reactor experiments could also explore θ_{13} values of the order of 5° while additional insights could come from new atmospheric experiments only if the 1-3 sector of the mixing matrix turns out to be sizable (just below present limits). Future solar experiments would contribute to the understanding of star evolution and test non standard neutrino interactions but, in the current scenario, they are not expected to contribute significantly to our understanding of leptonic mixing.

Differently from the case of oscillations, the absolute determination of the neutrino mass scale is still in a discovery phase¹⁰⁵⁾. If neutrino masses are hierarchical, the largest mass is expected to be of the order of $\sqrt{\Delta m_{23}^2} \simeq 50$ meV, well below the sensitivity of the future experiments based on tritium decay or cosmological bounds. This region could be marginally accessed by future neutrinoless double beta decay experiments assuming that neutrinos are Majorana particles. It is a remarkable fact that the next generation of double beta experiments will test in a nearly conclusive way (under the assumption of Majorana ν) the so called degenerate case, i.e. the possibility of almost degenerate neutrino masses giving rise to small Δm^2 differences and large absolute values $m_1 \simeq m_2 \simeq m_3$. On the other hand, current large uncertainties on nuclear matrix elements for $0\nu\beta\beta$ decays prevent us from imaging a precision physics scenario even in the occurrence of positive signal¹⁰⁶⁾.

3.6 Experimental detection of gravitational waves

Gravitational waves (GW) are an inescapable consequence of Einstein's general relativity and, indeed, of any gravitational theory which respects special relativity. They correspond to quadrupolar oscillations of the spacetime continuum itself, produced by a non-spherical acceleration of mass-energy distribution, propagating with the velocity of light, and having two independent transverse polarization states. For many years after the Einstein prediction, the same existence of these waves, and their detectability have been a matter of debate. To date, a strong indirect evidence for the existence of the GWs comes from the interpretation of the orbital evolution of the binary pulsar system PSR1913+16. The observed secular change in the orbital parameters of this system agrees with the general relativity prediction for the energy loss of a binary system via emission of gravitational radiation, to within less than 0.3 % error.

A GW shows up as a local tide, or a gradient in the local gravitational field. This means that the effect of a GW is to produce a time-dependent strain in space, and all detection schemes presently adopted lie on the measurement of this strain. The simplest detector one could envisage would consist of *two* free falling test masses a distance L apart, whose separation is monitored. A suitably polarized GW of amplitude h will produce a strain given by $\Delta L/L = h/2$ where ΔL is the length change induced by the GW. As a consequence of the weakness of gravitational interaction, sensible levels of radiation are produced only when very huge amounts of mass-energy are accelerated in very strong gravitational fields. These extreme conditions are reached only in astrophysical systems. The difficulty of direct detection of GWs derives from the fact that the amplitude h of the signal from realistic astrophysical sources is expected to be exceedingly small on the Earth, of the order of or smaller than 10^{-21} (i.e. two masses at 1000 km are needed to observe a variation in their separation of the order of 1 fm!).

In light of this order-of-magnitude estimate, it seems hard to motivate the efforts (and the sensible amount of money) presently spent worldwide in the operation and construction of GW detectors. The reason for the enterprise lies in the fact that gravitational radiation promises to open a unique window onto the most violent astrophysical phenomena. This expectation clearly emerges from an analysis of the differences between the GWs, and the electromagnetic waves (EW) on which the present knowledge of the Universe is founded¹⁰⁷. Just as an example: i) cosmic EWs are almost always radiated from individual emitters (electrons, atoms or molecules) while cosmic GWs are produced by coherent, bulk motions of mass-energy; ii) EWs are easily absorbed, scattered and dispersed by matter while GWs, as a consequence of their weak coupling with matter, travel nearly unaffected through all forms and amounts of intervening matter; iii) cosmic EWs cover the frequency region $\sim (10^7 \div 10^{27})$ Hz while the frequency of the cosmic GWs is expected to fall in the region $\sim (10^{-16} \div 10^4)$ Hz. These enormous differences make it likely that "GW astrophysics" may bring great surprises that, as in the case of the radio waves, X-rays or microwave radiation, could have a profound, indeed revolutionary, impact on astrophysics.

The GW sources are usually classified into three types, depending on the radiation temporal behaviour. These are:

- *Impulsive* sources, such as supernovae explosions. The expected supernovae event rate of $1/(30 \div 40 \text{ yr})$ per galaxy forces to look out of the Galaxy in order to bring the event rate up to several per year. Monitoring of the Virgo cluster of galaxies (about 2500 galaxies a distance 20 Mpc away from the Earth) would increase the supernova rate to a few events per year. By assuming a core mass equal to 1.4 solar masses in the Virgo cluster, collapsing to a size ten times its Schwarzschild radius ($r_s \equiv 2GM/c^2$), would lead to $h \sim 10^{-23}$. Since most of the energy released in the explosion originates from gravitational binding energy, the expected wave-frequency is of the order of kHz, the natural dynamical frequency of the source.

- *Quasi-periodic* and *Periodic* sources, such as coalescing binaries and spinning neutron stars. The coalescing compact binaries consist of neutron star and/or black holes. Assuming masses of the order of 1.4 solar masses at a distance of 10 Mpc in the 100 Hz frequency range, leads to $h \sim 10^{-21}$. It is worth noticing that the signal-to-noise ratio for such a signal can be improved by time integrating for a sufficiently long periods once the waveform is known. Even though the mechanism behind the coalescence of compact binaries is well understood, the event rate is not clear. Estimates range from $1/(10^5 \text{ yr})$ to $1/(10^6 \text{ yr})$ per galaxy. In order to have a rate of several event per year, one may have to monitor as far as 400 Mpc. Rotating neutron stars are the remnants of supernovae explosions, and they radiate GWs only if there is a deviation from the symmetry around its rotational axis. For a neutron star of radius $R = 10 r_s$, located a 10 kpc from the Earth, and with a 10 % asymmetry, the amplitude of waves emitted at 100 Hz is $h \sim 10^{-22}$.
- *Stochastic* sources, such as a large number of distant GW sources whose signals overlap or relics of the big bang. The latter component is the gravitational analogue of the cosmic microwave background. The main difference is that while the EWs decouple from the evolution of the universe about 4×10^5 years after the big bang, the GWs could come from times as early as the Planck epoch at $t_{\text{Pl}} \simeq 5 \times 10^{-44}$ s. This means that the relic GWs offer the tantalizing possibility of probing the universe very near to the moment of creation, and, correspondingly, give information on physics in a region of energies which cannot be accessed experimentally in any other way. Contrary to the other sources, an unambiguous detection of this background can be obtained only by cross-correlating the output signals of nearby detectors.

At basic level, a GW detector consists of a pair of masses which can move “freely” with respect to each other. They can be suspended as pendula, so that in the horizontal direction they can be treated as nearly free masses above the pendulum resonant frequency. To date, the efforts of the experimentalists have been mainly focused on the realization of two different types of detectors: resonants and interferometrics. In particular, LNF host the resonant detector NAUTILUS¹⁰⁸ whose operation is under the responsibility of the ROG group. This group is also responsible for the operation of the EXPLORER detector located at CERN and collaborates at the development of the spherical detector MiniGRAIL. The near term perspectives for NAUTILUS/EXPLORER are discussed in Sec. 4.14; the LNF involvement into interferometric detection of GW is summarized in Sec. 5.6. In general, the planned upgrades for the existing detectors (resonant and interferometric) are essentially based on sound engineering practices and do not require major scientific breakthroughs. At the same time the GW-detectors community is exploring the feasibility of third generation facilities involving advanced techniques that require detailed study and technical demonstration. These proposals are discussed in Sec. 5.6.1.

The interferometric detectors presently in operation are: GEO600 near Hannover, the two LIGO observatories in US, respectively located at Hanford (WA) and Livingston (LA), TAMA at Tokyo, and VIRGO in Cascina, near Pisa. The latter is described in detail in Sec.5.6. All these detectors employ a 10-20 W diode-pumped Nd:YAG solid state lasers as light sources, and are power-recycled¹ Michelson interferometers where, except for GEO600, the end mirrors are replaced by Fabry-Perot cavities.

TAMA is a 300 m arms interferometer in operation since 2002 with performances in agreement with the design ones. It should be thought as testing ground for a possible future 3 km detector

¹Because the Michelson interferometer antisymmetric port is held at a dark fringe, and because the Fabry-Perot cavities are low loss, most of the light returning from the two arms is transmitted by the beam-splitter back towards the laser. A “power recycling” mirror located between the laser and the beam-splitter re-injects that light, resonantly, into the interferometer.

(LIGO). LIGO consists of three interferometers. At Hanford there are two identically oriented interferometers which share a common vacuum envelope: one having 4 km long arms, and one having 2 km arms. At Livingston operates a single 4 km long detector. The two observatories are approximately 3000 km apart, corresponding to 10 ms of light travel time. The detectors are approximately co-aligned, so that a GW should appear with comparable signals at both sides. GEO600 is a 600 m long arms interferometer built by a German-British collaboration, where, contrary to the other interferometers, the light path in each arm is enhanced to 1.2 km by an optical delay line. After a series of engineering runs, the LIGO, GEO600, and TAMA detectors operated in coincident observation mode for the first time for two weeks in August and September 2002. The scientific runs performed up to now provided the opportunity for the experimentalists to improve detector understanding, test the data processing procedures and build confidence in their ability to establish the detection of GWs in future science runs. It should also be noted that during these runs the detectors were far from the design sensitivity reported in Fig. 3.3.

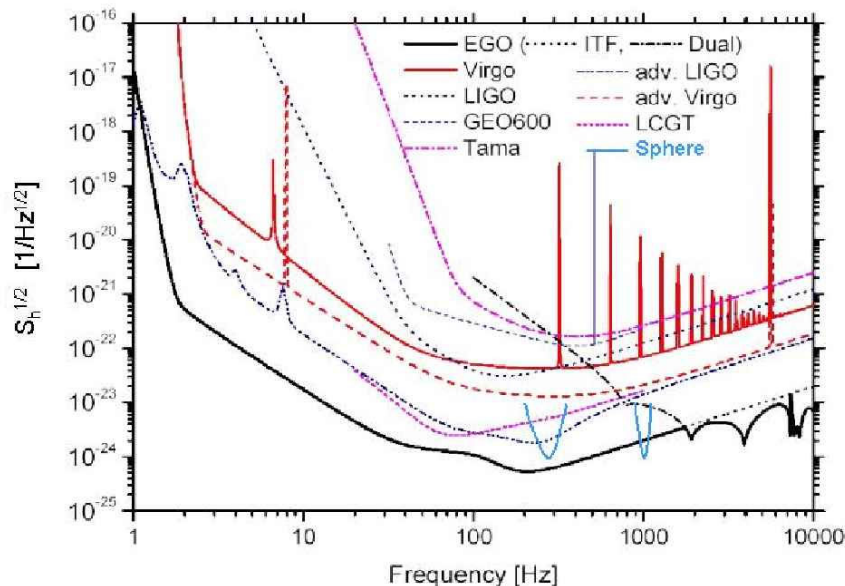


Figure 3.3: Sensitivities of the current and future interferometric detectors. For VIRGO the design sensitivity is reported. For comparison, the expected sensitivity for the 3rd generation observatory EGO is also shown.

World scenario on e^+e^- accelerators

3.7 Electron-positron storage rings

Electron-positron storage rings have been one of the most successful enterprises in the accelerators field for what concerns design, operation and reliability. In the last decade their luminosities have greatly risen, thanks to the experience in handling high beam currents and multibunch operation together with a deeper understanding of the beam-beam interaction limits and of the beam dynamics. Moreover the use of the lepton annihilation process for the production of elementary particles is ideal for the clean signature and the production of particle-antiparticle pairs. Experiments are asking for more precise measurements and the accelerator community is facing projects where an increase of luminosity by orders of magnitude is conceivable. A brief summary of the present world activities in this field is presented in the following and the luminosity for past and future colliders is shown in Fig. 3.4.

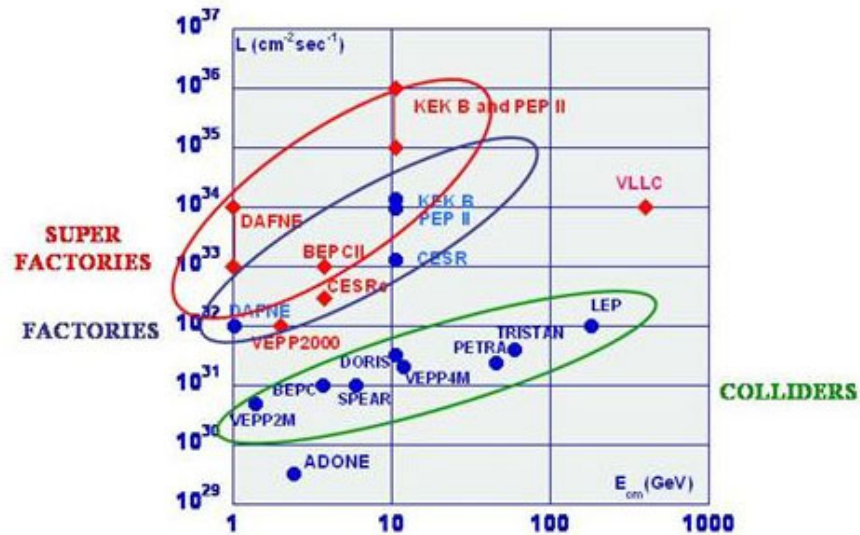


Figure 3.4: Achieved peak luminosity vs energy for colliders (green) and factories (blue), target peak luminosity for Super-factories (red).

3.7.1 ϕ -factories

A ϕ -factory is a unique tool to study Kaon physics, since it produces a large flux of K_L , K_S , K^+ and K^- pairs at low energy and almost monochromatic. When DAΦNE was proposed, in early '90s, similar project in Mainz and Novosibirsk were studied, but they were never built and DAΦNE remains the only facility to operate at this energy. The choice of the 2 rings/multibunch/high current design has proven to be successful and five years of operation at DAΦNE have been extremely useful to understand all the important parameters to reach high luminosity even at such a low energy and in such a small ring. DAΦNE has two Interaction Regions (IR) with horizontal crossing angle and two high solenoidal detector fields are embedded in the lattice. The large induced coupling is corrected down to values below 1%. World record current exceeding 2.3 A

has been stored in the electron ring, and more than 1.4 A in the positron one. The DAΦNE performances have been described in Sec. 2.2 and possible upgrades will be discussed in Sec. 4.2.

3.7.2 Light-quark factories

Physics at energies between the ϕ and τ have been covered in the past years by VEPP-2M (shut down in 2000) and BEPC. A new innovative project, VEPP 2000, is at present in construction at Novosibirsk (Russia). Its design is based on the concept of round colliding beams. This will be a very important step in understanding the beam-beam interactions. With the same number of particles the expected beam-beam tune shift should be twice as small as the corresponding one with flat beams. Moreover beam-beam simulations predict that larger tune shifts can be achieved. The goal luminosity in single bunch is $10^{32} \text{ cm}^{-2} \text{ s}^{-1}$. This collider could also operate with flat beams and at energies ranging from 0.5 GeV to 1 GeV/beam. Its compact design is based on very high field (2.4 T) normal conducting dipoles, with symmetric Interaction Regions for two experiments. Focusing at the IRs will be performed by super conducting (SC) solenoids which rotate by $\pi/2$ the x-y planes of betatron oscillation, thus creating emittance in both x and y modes. First beams are expected for Spring 2006. A proposed DAΦNE upgrade, as discussed in Sec. 4.2.2, would also allow studying this energy region at LNF.

3.7.3 τ -charm factories

CESR at Cornell, Ithaca (US), after almost twenty years of successful operation as a B-factory, with a long lasting record in peak luminosity ($1.3 \times 10^{33} \text{ cm}^{-2} \text{ s}^{-1}$ at the $\Upsilon(4S)$ energy), has been recently modified in order to run at lower center-of-mass energies (CESR-c). SC wigglers have been added to increase the radiation damping and improve luminosity. CESR-c will run until 2008 at the τ , $D\bar{D}$ and $D_s\bar{D}_s$ thresholds. The goal peak luminosity is $3 \times 10^{32} \text{ cm}^{-2} \text{ s}^{-1}$.

BEPC, at Beijing (China), which reached a peak luminosity of $1.1 \times 10^{31} \text{ cm}^{-2} \text{ s}^{-1}$, has been dismantled and is being upgraded to become BEPC-II, the first completely dedicated τ -charm factory, still maintaining synchrotron radiation production. Its design is based on a double ring scheme, with energies ranging between 1.5 and 2.5 GeV/beam, optimized at 1.89 GeV, with a design luminosity of $10^{33} \text{ cm}^{-2} \text{ s}^{-1}$. A new inner ring will be installed inside the old one, so that each beam will travel in half outer and half inner ring. SC cavities will also be installed. A by-pass will allow the electron ring to be used as a synchrotron light source as well. Commissioning of the new rings are planned for 2006.

3.7.4 B-factories

The requirement of observing the decay vertex of B mesons has led to choose asymmetric energies for the B-factories projects. This introduced new challenges beyond those of rings with ampere currents and micron beam sizes at the Interaction Point (IP). The Interaction Region became a new accelerator physics and engineering challenge. In particular: low beta optics and beam separation to avoid parasitic crossings for different energy beams, kilowatt synchrotron radiation striking nearby chambers, solenoid compensation for the two beams, small detector vertex chambers which must be protected from different backgrounds. At present two B-factories are in operation: PEP-II at SLAC (US) and KEK-B at Tsukuba (Japan). Their performances are comparable: they have rapidly reached their design luminosities, although these values were considered challenging at the time of their conception. Both these colliders rely on the 2 rings/multibunch/high currents philosophy, KEK-B having also a small horizontal crossing angle at the IP. The problems they face are the same, in particular the Electron Cloud Instability (ECI) that affects the positron

ring causing increase of the transverse beam dimensions and consequently reduction in attainable luminosity. The cure found up to now has been to wind solenoidal coils all over the field free regions, typically the long drifts in between the arcs, and for PEP-II to add “micro gaps” in the bunch pattern. PEP-II reached the design luminosity ($3 \times 10^{33} \text{ cm}^{-2} \text{ s}^{-1}$) in October 2000 and a peak luminosity of $9.2 \times 10^{33} \text{ cm}^{-2} \text{ s}^{-1}$ in May 2004, delivering more than 250 fb^{-1} to the BABAR experiment. The “twin” collider KEK-B has reached a peak luminosity close to $14 \times 10^{33} \text{ cm}^{-2} \text{ s}^{-1}$, the largest ever measured, delivering more than 280 fb^{-1} to the BELLE experiment. Continuous beam injection performed in both colliders has been also a key point to increase the integrated luminosity. These projects have proven that increasing design difficulties can be successfully overcome; however the particle physics items studied at these colliders still demand higher peak luminosities to collect, in a reasonable amount of time, a huge amount of good quality data.

3.7.5 Next generation factories

The next generation factories aim at increasing the luminosity by two orders of magnitude. In particular B-factories are planning upgrades to reach 10^{35} - $10^{36} \text{ cm}^{-2} \text{ s}^{-1}$, and DAΦNE to $10^{34} \text{ cm}^{-2} \text{ s}^{-1}$. The recipe to reach such an ambitious goal is of course to increase the number of colliding bunches and the currents and to decrease bunch length, β_y^* and damping times. This approach requires new solutions, for example compact superconducting quadrupoles must be used to control the beam sizes close to the IP, more powerful and SC RF systems to restore energy losses and shorten the bunches, new design of bellows, masks, pumps and vacuum chamber to control the high order modes induced by the currents and to handle higher synchrotron radiation fluxes. In the asymmetric B-factories also injecting positrons in the high energy ring, and electrons in the low energy one, since the ECI is less dangerous at higher energy, is being considered. A higher RF frequency is also considered in some of the upgrades. Optics modifications, such as high and/or negative momentum compaction, and modified arc lattices, as the KEK-B 2.5π cell that allows for wide tunability and large dynamic aperture, or the DAΦNE upgraded arc, which allows for shorter damping times, are also studied. In KEK-B, which observed a reduction in luminosity at very high tune shifts because of the crossing angle, crab cavities are also foreseen. The next steps of the lepton factories are straightforward and consist in optimizing all the techniques developed in the last ten years to improve the peak and integrated luminosity by a factor 10 at least. New ideas and important modifications in the layout are needed to gain a factor 100. However many topics can still be studied, both theoretically and by accelerator studies on the present colliders, which will be very important for the design of the future lepton colliders. Fig. 3.5 summarizes the possible future upgrades for the present factories in the next future.

3.8 Free Electron Laser

The new facilities and projects based on Free Electron Lasers (FEL) (see e.g. in ¹¹⁰) usually consist of a long undulator with typically a few hundred to a thousand magnet periods, driven by a high-quality electron beam with high charge density, low emittance and low energy spread. The interaction of the electron beam with the spontaneous radiation emitted by itself in the undulator leads to a longitudinal charge density modulation which makes the electrons radiate in phase. This effect is called self-amplified spontaneous emission (SASE). Here the output peak power is orders of magnitude higher than that of conventional undulator used in storage rings, where the electrons radiate independently, as it can be seen in Fig. 3.6. The FEL radiation is spatially coherent, the pulse duration is of the order of 100 fs, and an extremely wide spectral range from micrometer to Angstrom wavelengths can be covered by varying the electron beam energy and the magnetic period and field of the undulator. The dramatic quality improvement of these new X-ray sources

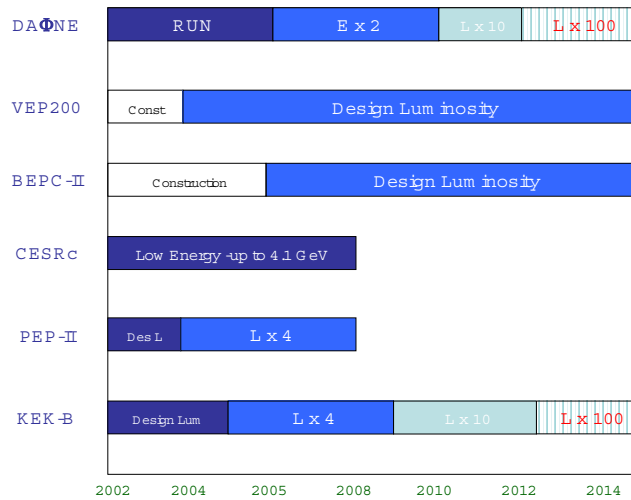


Figure 3.5: Projection of the upgrades of the meson factories.

can only be compared to that achieved by the invention of the optical laser forty years ago. However the high quality electron beams required for these FELs cannot be generated in electron storage rings, but rather require linear accelerators and special photocathode radiofrequency (RF) guns together with emittance compensation and bunch compression techniques.

Pioneering work on SASE has been done in the US, e.g. at Los Alamos at $12 \mu\text{m}$ wavelength and at Argonne National Laboratory in the visible and ultraviolet. At Brookhaven National Laboratory first experimental results were recently obtained on a high gain harmonic-generation (HGFG) FEL in the ultraviolet (DUV-FEL), using an 800 nm Ti:Sapphire laser as a seed and reaching saturation at 266 nm. The HGFG technique is a very promising possibility to avoid the inherently noisy SASE process and to produce fully coherent, stable FEL radiation throughout the XUV spectral range.

The current upgrade of the FEL at DESY will make radiation wavelengths from 60 to 6 nm available for European users; the first user experiments are planned for early 2005. The next facility will most likely be the Linac Coherent Light Source (LCLS) at SLAC (US) based on the existing S-band normal conducting 3-miles long linear accelerator, which is expected to start operation in 2008 with wavelengths down to 0.15 nm.

In February 2003, the German Federal Ministry of Education and Research decided that a XFEL, proposed by the International TESLA Collaboration, should be realized as a European project and located at DESY/Hamburg. Germany is prepared to cover half of the investment and personnel costs for the XFEL. The electron beam of the XFEL proposal is accelerated in a linear accelerator using superconducting RF technology to about 20 GeV and then distributed into several beam lines. This will allow using the electron beam for several FELs and spontaneous radiators and facilitates parallel operation of many experiments with wavelengths down to 0.08 nm. Another soft X-ray FEL facility currently under development is the Spring-8 Compact SASE Source (SCSS) in Japan.

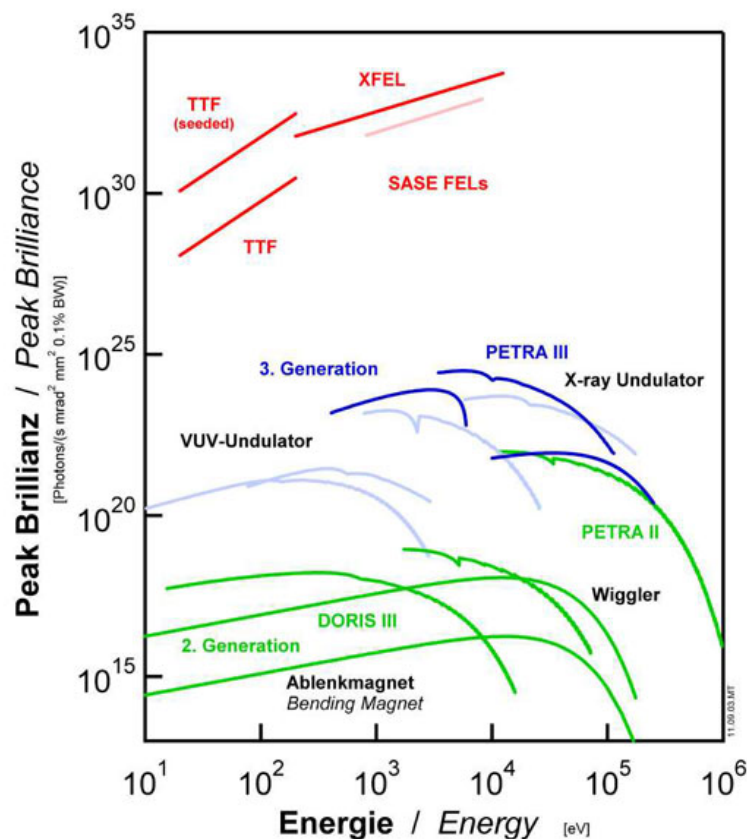


Figure 3.6: The comparison of the peak brilliance of synchrotron radiation sources (green lines) with free-electron lasers (red lines) shows the great leap in brilliance offered by the FELs.

The experimental and theoretical work done at SLAC, DESY and in many other laboratories in Europe, USA and Japan, shows clearly that further research and development on critical issues is required in order to prepare the design and construction of the new infrastructures. This is not only necessary for reducing the radiation wavelength further, but also to develop and test seeding techniques in order to improve the temporal coherence of the radiation and to avoid the statistical fluctuations caused by the start-up from noise in the SASE process and to develop high average current options. Therefore several test and prototype facilities have been built or are currently being prepared. The projects in Europe are summarized in the following.

The VUV-FEL at DESY, although primarily focusing on user applications, does include a significant R&D program during the first years, focusing in particular on online photon diagnostics, synchronization of all subsystems to better than 100 fs, and a self-seeding scheme to improve the temporal coherence of the radiation.

The objective of FERMI@ELETTRA is the construction of a user facility providing photons in the 100 to 10 nm range. It will utilize the existing 1.2 GeV linac upgraded with a high-brightness photo-injector, bunch compression system and advanced diagnostics. In parallel the first undulator chain covering the range 100-40 nm will be developed and exploited for experimental studies of HGHG schemes.

SPARX is an evolutionary project proposed by a collaboration among ENEA-INFN-CNR-

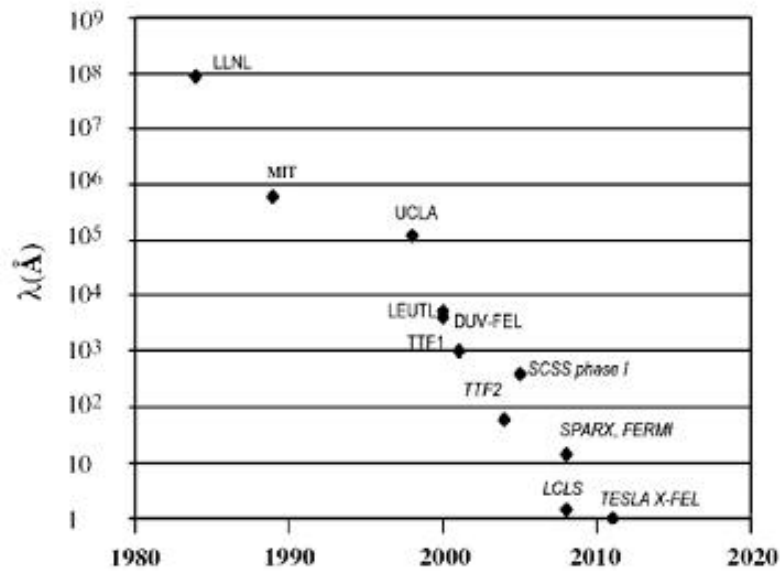


Figure 3.7: SASE FEL devices operating wavelength vs. foreseen year of start of operation.

Roma Tor Vergata University, aiming at the construction of a FEL-SASE X-ray source in the Tor Vergata Campus. The first phase of the SPARX project, funded by Government Agencies with 10 MEuro plus a preliminary contribution of 2.35 MEuro by INFN, will be focused on R&D activity on critical components and techniques for future X-ray facilities. A R&D program towards a high brightness photo-injector, the SPARC project (Sec. 2.3) is already under way at LNF-INFN and it will be commissioned within 2006. The R&D plans for the X-ray FEL source will be developed along two lines: (a) use of the SPARC high brightness photo-injector to develop experimental test on RF compression techniques and other beam physics issues (SPARC phase II, Sec. 4.1.1), (b) explore the production of soft and hard X-rays in a SASE-FEL with harmonic generation, in the so called SPARXINO test facility (Sec. 4.1.2), upgrading in energy and brightness the existing Frascati 800 MeV Linac at present working as injector for the DAΦNE ϕ -factory.

A recirculating 35 MeV energy-recovery linac prototype (ERLP) with a FEL that will generate THz to mid IR radiation is currently under construction at the Daresbury Laboratory. Work on this facility will complement and support the design study for the full 4GLS (4th Generation Light Sources) facility. ERLP will allow the testing of recirculation concepts, as well as instrumentation and diagnostics developments.

BESSY will set up a cryogenic Horizontal Bi-Cavity Test-facility (HoBiCaT). This facility is designed especially for the qualification of superconducting RF components for superconducting CW (continuous wave) linacs, which many of the proposed new infrastructures are based on. The HoBiCaT will provide unique possibilities to investigate TESLA-type cavity units (including all ancillary components) in CW operation. A summary of the SASE FEL operating wavelength vs. the foreseen operation start time is reported in Fig. 3.7.

In addition, several projects for low-intensity femtosecond X-ray sources have been started in order to stimulate experimental and scientific developments on the user side to be better prepared

when the new FEL infrastructures become operational. For example the sub-picosecond pulse source (SPPS) build on the SLAC linac is producing 100 fs X-ray pulses since 2003. The pulse energy is sufficient for time-resolved X-ray diffraction experiments.

Most likely all XUV sources will use laser seeding and harmonic generation from the beginning to provide fully coherent FEL radiation without the statistical fluctuations typical of SASE. At short wavelengths they all exceed the brilliance and peak power of present undulator sources on modern electron storage rings as well as laser plasma and high-harmonic generation sources by several orders of magnitude, as illustrated in Fig. 3.6.

3.9 Linear Collider

The particle physics community has endorsed a Global e^+e^- Linear Collider (LC) in the TeV energy scale as the next major step in the field. The physics case for its construction is well established. In the last decade different teams in Asia, USA and Europe have produced intense and successful R&D based on different technologies in order to reach the high gradients required, such as:

- Superconducting cavities at 1.3 GHz (L-band) developed by the TESLA Collaboration (Germany).
- Room temperature cavities at 11.4 GHz (X-band) developed by a joint effort of the NLC (USA) and JLC (Japan) collaborations.
- Two beams acceleration scheme, CLIC; with room temperature 30 GHz cavities, which aims at the multi TeV energy range (Europe).

The experience gained in designing and operating the SLC (Stanford Linear Collider) at SLAC will be crucial for the LC design. To demonstrate its feasibility, test facilities have been built in different parts of the world: Final Focus Test Beam at SLAC, Accelerator Test Facility at KEK, TTF at DESY and CTF at CERN.

In 2004 ICFA (International Committee for Future Accelerators) has endorsed the International Technology Recommendation Panel (ITRP), an international “wise men” committee in charge of choosing the technology for the 1 TeV LC so that the different teams can concentrate on a single project avoiding dispersion of resources.

This choice has been done in August 2004. From the ITRP Executive Summary: “*During the past decade, dedicated and successful work by several research groups has demonstrated that a linear collider can be built and reliably operated*”¹⁰⁹). The Committee stated that both technologies can achieve the design goals for the LC; however it recommended the Super Conducting (SC) RF technology because of its features, as the low RF frequency, that will facilitate the future design.

This choice will certainly produce acceleration in the international organization to produce, in about three years, a design and costing for a 0.5-1 TeV LC based on SC technology. The design will involve all the collaborations that have been working up to now separately on the “warm” and “cold” technology plus new laboratories and universities. The FP6 network EuroTeV aims at being the nucleus of this global team in Europe.

At the same time, the research on the two beams acceleration scheme will continue with CTF3 at CERN, to put the basis for the multi-TeV next generation collider.

In this scenario the LNF Accelerator Division is already collaborating with the international R&D efforts on the linear colliders: TESLA, TTF, EUROTEV, CARE and CTF3 (Sec. 5.1.1). Moreover, this activity has a strong synergy with the R&D activity on X-FEL carried on by the Accelerator Division (SPARC, SPARX and EUROFEL), since both aim at the production and acceleration of extremely high quality electron beams.

References

1. J. Ellis, Eur. Phys. Journ. C **34** (2004) 51.
2. S. P. Martin, hep-ph/9709356, and references therein.
3. See e.g. *Proceedings of the High Intensity Frontier Workshop*, La Biodola, Isola d'Elba (Italy), 5-8 June 2004, <http://www.pi.infn.it/pm/2004/>.
4. A. Masiero, S. K. Vempati and O. Vives, New Journ. Phys. **6** (2004) 202, and references therein.
5. Y. K. Semertzidis, Nucl. Phys. Proc. Suppl. **131** (2004) 244, and references therein.
6. G. Isidori, Int. Journ. Mod. Phys. A **17**(2002) 3078; Annales Henri Poincare 4 (2003) S97, and references therein.
7. J. Gasser and H. Leutwyler; Annals Phys. **158** (1984) 142; Nucl. Phys. B **250** (1985) 465.
8. M. Neubert, Phys. Rept. **245** (1994) 259, and references therein.
9. G. Colangelo, hep-ph/0501107, and references therein.
10. http://www.fnal.gov/directorate/program_planning/schedule/index.html
11. D0 Collaboration, hep-ex/0407005, CDF and D0 Collaborations and TeVatron EW Working Group, hep-ex/0404010.
12. <http://lepwwg.web.cern.ch/LEPWWG/>
13. P.J. Bell, hep-ex/0405015.
14. <http://cmsinfo.cern.ch/Welcome.html/CMSdocuments/CMSplots/CMSplots.html> hep-ex/0203019.
15. F. Gianotti *et al.*, Eur. Phys. Journ. C **39** (2005) 293; G. Azeulos *et al.*, Journ. Phys. G **28** (2002) 2453.
16. <http://www.interactions.org/linearcollider>
17. CLIC Physics Working Group, hep-ph/0412251.
18. H. Abramowicz *et al.*, physics/0410017 and references therein.
19. LHC/LC Study Group, hep-ph/0410364 and also <http://www.ippp.dur.ac.uk/~georg/lhclc/lhclcdoc.ps.gz>
20. http://tesla.desy.de/new_pages/TDR_CD/start.html
21. J-C. Brient and H. Videau, hep-ex/0202004 and also <http://polywww.in2p3.fr/flc/calice.html>
22. N. Akchurin *et al.*, Nucl. Instr. Meth. A **533** (2004) 305.
23. <http://vlhc.org/>
24. J.H. Christenson *et al.*, Phys. Rev. Lett. **13** (1964) 138.
25. NA48 Collaboration, Phys. Lett. B **465** (1999) 335; Eur. Phys. Journ. C **22** (2001) 231; Phys. Lett. B **544** (2002) 97.

26. KTeV Collaboration, Phys. Rev. Lett. **83** (1999) 22; Phys. Rev. D **67** (2003) 012005.
27. S. Adler *et al.*, Phys. Rev. Lett. **88** (2002) 041803.
28. G. Isidori, hep-ph/0307014.
29. <http://www.phy.bnl.gov/e949>
30. NA48-Future Working Group, CERN-SPSC-2004-10/SPSC-EOI-002 (2004) also on <http://www.cern.ch/NA48/NA48-3/Overview/LOI.pdf>
31. T.K. Komatsubara *et al.*, <http://www-ps.kek.jp/jhf-np/LOIlist/pdf/LO4.pdf>
32. A. Alavi-Harati *et al.*, Phys. Rev. D **61** (2000) 072006.
33. <http://psux1.kek.jp/~391/>
34. Y.B. Hsiung *et al.*, <http://www-ps.kek.jp/jhf-np/LOIlist/pdf/LO5.pdf>
35. <http://www.bnl.gov/rsvp/KOPIO.htm>
36. P. Depommier *et al.*, <http://www-ps.kek.jp/jhf-np/LOIlist/pdf/L16.pdf>; Y. Asano *et al.*, <http://www-ps.kek.jp/jhf-np/LOIlist/pdf/L19.pdf>; S. Shimizu *et al.*, <http://www-ps.kek.jp/jhf-np/LOIlist/pdf/L20.pdf>
37. JAERI and KEK Joint Project: Japan Proton Accelerator Research Complex, <http://j-parc.jp>
38. R. A. Briere *et al.*, “CLEO-c and CESR-c: a new frontier of weak and strong interactions,” CLNS-01-1742
39. D.G. Cassel, hep-ex/0307038.
40. B. Heltsley, CLEO-c program, Quarkonium Working Group, Beijing October 2004, <http://www.qwg.to.infn.it/WS-oct04/index.html>
41. Z.A. Liu, BES III project, Quarkonium Working Group, Beijing October 2004, <http://www.qwg.to.infn.it/WS-oct04/index.html>
42. <http://www.slac.stanford.edu/BFROOT>
43. <http://belle.kek.jp>
44. M. Giorgi, http://www.slac.stanford.edu/BFROOT/www/Public/ichep2004/8238_ichep04_giorgi_final.pdf
45. M. Neubert, hep-ex/0405105; The SuperKEKB Physics Working Group, hep-ex/0406071.
46. <http://lhcb.web.cern.ch/lhcb>
47. <http://www.jlab.org/Hall-B/clas12>
48. The GlueX Collaboration, Hall D CDR.
49. “An International Accelerator Facility for Beams of Ions and Antiprotons”, Conceptual Design Report, <http://www.gsi.de/GSI-Future/cdr/>
50. PANDA Collaboration, “Antiproton Physics at Darmstadt”, Letter of Intent GSI-ESAC/Pbar, Jan 21, 2004.
51. E. Reya, Rev. Mod. Phys. **46** (1974) 545; H. Pagels, Phys. Rept. **16** (1975) 219.

52. R.L. Jaffe and C.L. Korpa, Comments Nucl. Part. Phys. **17** (1987) 163.
53. H.C. Schroder *et al.*, Eur. Phys. Journ. C **21** (2001) 473; M. Hennbach *et al.*, Progr. Part. Nucl. Phys. **50** (2003) 363.
54. M.E. Sainio, PiN Newslett. **16** (2002) 138.
55. M.M. Pavan *et al.*, PiN Newslett. **16** (2002) 110.
56. DEAR Collaboration, Phys. Rev. Lett. (2005) , in print.
57. J. Zmeskal, SIDDHARTA Note-IR-2, 25 August, 2003; C. Curceanu (Petrascu), SIDDHARTA Note-IR-3, 25 August, 2003.
58. SIDDHARTA Collaboration, SIDDHARTA Note-IR-1, 25 August, 2003.
59. B. Borasoy, R. Nisler and W. Weise, hep-ph/0410305.
60. SMC Collaboration, Phys. Rev. D **56** (1997) 5330, Phys. Rev. D **58** (1998) 112001.
61. HERMES Collaboration, Phys. Lett. B **404** (1997) 383, Phys. Lett. B **442** (1998) 484, <http://www-hermes.desy.de>
62. E142 Collaboration, Phys. Rev. D **54** (1997) 6620; E143 Collaboration, Phys. Rev. D **58** (1998) 112003; E154 Collaboration, Phys. Rev. Lett. **79** (1997) 26, Phys. Lett. B **405** (1997) 180; E155 Collaboration, Phys. Lett. B **493** (2000) 19, <http://www.slac.stanford.edu/exp/e155/home.html>
63. <http://www.bnl.gov/rhic/>
64. http://www.jlab.org/div_dept/physics_division/pCDR_public/pCDR_final/pCDR_final.pdf
65. HERMES Collaboration, Phys. Rev. Lett. **92** (2004) 012005, Phys. Rev. D **71** (2005) 012003.
66. <http://wwwcompass.cern.ch>
67. HERMES Collaboration, Phys. Rev. Lett. **84** (2000) 2584.
68. HERMES Collaboration, Phys. Rev. Lett. **94** (2005) 012002.
69. PAX Collaboration, *Antiproton-Proton Scattering Experiments with Polarization*, Letter of Intent, Jan 15, 2003.
70. D. Muller *et al.*, Fortsch. Phys. **42** (1994) 101; X. Ji, Phys. Rev. Lett. **78** (1997) 610, Phys. Rev. D **55** (1997) 7114; A.V. Radyuskin, Phys. Lett. B **380** (1996) 417; A.V. Radyuskin, Phys. Rev. D **56** (1997) 5524.
71. HERMES Collaboration, Phys. Rev. Lett. **87** (2001) 182001.
72. CLAS Collaboration, Phys. Rev. Lett. **87** (2001) 182002.
73. M.K. Jones *et al.*, Phys. Rev. Lett. **84** (2000) 1398; O. Gayou *et al.*, Phys. Rev. Lett. **88** (2002) 092301.
74. J.D. Walecka, Nuovo Cim. **11** (1959) 821; R.G. Sachs, Phys. Rev. **126** (1962) 2256.
75. C.F. Perdrisat, V. Punjabi, M.K. Jones, E. Brash *et al.*, Jefferson Lab. experiment E01-109

76. A.Z. Dubnickova, S. Dubnicka, P.M. Rekaló, *Nuovo Cimento* **109** (1966) 241.
77. R. Baldini *et al.*, *Eur. Phys. Journ. C* **11** (1999) 709; R. Baldini *et al.*, in *Proc. of the $e^+ e^-$ Physics at the intermediate Energies Conference*, edited by D. Bettoni, eConf **C010430**, T20 (2001), hep-ph/0106006.
78. B.V. Geshkenbein, B.L. Ioffe, M.A. Shifman, *Yad. Fiz.* **20** (1974) 128.
79. R. Calabrese, in *Proc. of the $e^+ e^-$ Physics at the intermediate Energies Conference*, edited by D. Bettoni, eConf **C010430**, W07 (2001); H.W. Hammer, *ibid.*, No. W08; C.E. Carlson, *ibid.*, No. W09; M. Karliner, *ibid.*, No. W10.
80. A. Antonelli *et al.*, *Phys. Lett. B* **313** (1993) 283, *Nucl. Phys. B* **517** (1998) 3.
81. <http://aliceinfo.cern.ch>
82. Greisen, K., *Phys. Rev. Lett.* **16** (1966) 748; Zatsepin, G.T. and Kuzmin, V.A., *Zh. Eks. Teor. Fiz.*, *Pis'ma Red.* **4** (1966) 144.
83. L.A. Anchordoqui, "The Pierre Auger Observatory: Science Prospects and Performance at First Light", to appear in the Proceedings of PASCOS'04, astro-ph/0409470.
84. M. Teshima *et al.*, "EUSO (The Extreme Universe Space Observatory) - Scientific Objectives", *Proc. 28th ICRC, Tsukuba 2003 Vol.HE*, p.1069.
85. C. Pittori and M. Tavani, *Nucl. Phys. B (Proc. Suppl.)* **134** (2004) 72.
86. P.F. Michelson *et al.*, *Bull. Am. Astron. Soc.* vol.**36** n.5 (2004).
87. J.A. Hinton, *New Astron. Rev.* **48** (2004) 331.
88. C. Baixeras *et al.*, *Nucl. Instr. Meth. A* **518** (2004) 188.
89. N. Gehrels, *Ap. Journ.* **611** (2004) 1005.
90. C. Spiering, "The Baikal Neutrino Telescope: Results, Plans, Lessons", published in "Technical aspects of a Very Large Volume Neutrino Telescope in the Mediterranean Sea", p.26, Amsterdam 2003, astro-ph/0404096.
91. J. Ahrens *et al.*, *Phys. Rev. Lett.* **92** (2004) 071102.
92. B. Vallage, "Status report on the Antares project", to appear in *Proc. XIII Int. Symp. on Very High Energy Cosmic Ray Interactions*, Pylos, Greece 6-12 Sept 2004.
93. A. Ball and A. Tsirigotis: "Light in the darkness"; *CERN Courier*, Nov.2003 p.23
94. O. Botner, *Nucl. Phys. B (Proc. Suppl.)* **143** (2005) 367.
95. P. Piattelli, *Nucl. Phys. B (Proc. Suppl.)* **143** (2005) 359.
96. C.L. Bennett *et al.*, *Ap. Journ. Suppl.* **148** (2003) 1.
97. R. Bernabei *et al.*, *Nucl. Phys. A* **719** (2003) 257c
98. D.S. Akerib *et al.*, *Phys. Rev. Lett.* **93** (2004) 211301.
99. O. Martineau *et al.*, *Nucl. Instr. Meth. A* **530** (2004) 426.

100. L. Bergstrom, Rep. Prog. Phys. **63** (2000) 793 and references therein.
101. M. Boezio *et al.*, Nucl. Phys. B (Proc. Suppl.) **134** (2004) 39.
102. B. Demirköz “AMS: a particle physics experiment in space”, to appear in Proc. 3rd Int. Conf. Frontier Science 2004: “Physics and Astrophysics. in Space”, Frascati, Italy 14-19 June 2004
103. B.T. Cleveland *et al.*, Astrophys. Journ. **496** (1998) 505; SAGE Collaboration, Phys. Rev. C **60** (1999) 055801; GALLEX Collaboration, Phys. Lett. B **447** (1999) 127; SNO Collaboration, Phys. Rev. Lett. **87** (2001) 071301; KamLAND Collaboration, Phys. Rev. Lett. **90** (2003) 021802, hep-ex/0406035; Super-Kamiokande Collaboration, Phys. Rev. Lett. **81** (1998) 1562, Phys. Rev. Lett. **86** (2001) 5651, hep-ex/0404034; MACRO Collaboration, Phys. Lett. B **517** (2001) 59; Soudan 2 Collaboration, Phys. Rev. D **68** (2003) 113004; K2K Collaboration, Phys. Rev. Lett. **90** (2003) 041801.
104. CHOOZ Collaboration, Eur. Phys. Journ. C **27** (2003) 331; PALO VERDE Collaboration, Phys. Rev. D **64** (2001) 112001.
105. S. M. Bilenky *et al.*, Phys. Rept. **379** (2003) 69; S. M. Bilenky, A. Faessler and F. Simkovic, Phys. Rev. D **70** (2004) 033003; G. L. Fogli *et al.*, Phys. Rev. D **70** (2004) 113003.
106. V. Barger *et al.*, Phys. Lett. B **540** (2002) 247. J. N. Bahcall, H. Murayama and C. Pena-Garay, Phys. Rev. D **70** (2004) 033012.
107. K.S. Thorne, arXiv:gr-qc/9704042; S.A. Hughes, Annals Phys. **303** (2003) 142.
108. INFN-LNF 2004 Annual Report - LNF-05/05 (IR) - available on <http://www.lnf.infn.it/rapatt>
109. Executive Summary ITRP, 19 august 2004-09-01.
110. AAVV Proposal of European FEL Design Study EUROFEL, to be published.

Chapter 4

Future Activities at the LNF

The chapter includes both, mid-term initiatives currently funded, and the activities that have been discussed as possible extensions of the already fixed experimental programs. First section is devoted to the funded continuation of the present Free Electron Laser project at the LNF; the second part is a status report on the conceptual accelerator studies carried out so far for one facility replacing/upgrading DAΦNE; following sections refer to different parts of the research program related to the new facilities; the last part presents the perspectives of the experimental detection of gravitational waves in the LNF.

Accelerators Activities

4.1 R&D on Free Electron Laser

The path for experimentation on the Free Electron Laser field is largely set by the line guides of the EUROFEL project, which is the framework and the most relevant funding source of this kind of activities in the LNF.

4.1.1 SPARC Phase II

SPARC Phase II, expected to start in 2007 after completion of the Phase I, will be mainly devoted to beam dynamics studies related to bunch compression systems and tests of new FEL schemes, like for example the “seeding”, in connection with the EUROFEL programs. In view of the SPARXINO application (Sec. 4.1.2) two possible bunch compressor schemes will be compared, as shown in Fig. 4.1. A standard magnetic chicane will be installed in a parallel beam line, parallel to the SPARC undulator, while a new technique based on the so-called velocity bunching (VB) scheme will make use of the first linac sections to provide longitudinal focusing ¹⁾.

A parallel program is also under way in order to profit of the SPARC facility for other applications. For example the PLASMON proposal, a Thomson source for tunable (20-500 keV) monochromatic X-ray beams, is under study ²⁾. For this aim an additional beam line to transport the beam out of the photo-injector up to the final focus is required, as shown in Fig. 4.1, and an upgrade of the Ti:sapphire laser system driving the photo-cathode should be implemented. The main purpose of the experiment is to test the focusing of the high brightness electron beam down

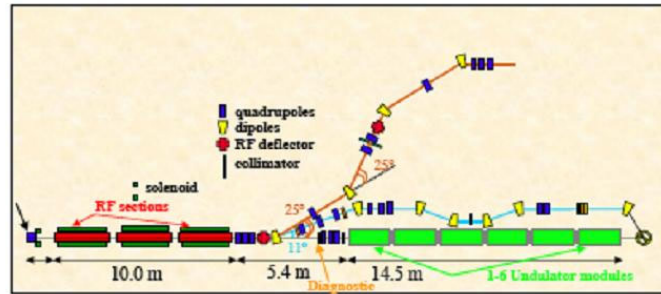


Figure 4.1: Layout of SPARC Phase II.

to $10\mu\text{m}$ spot sizes, at a variable energy in the 30 to 150 MeV range, and to collide with counter propagating laser pulses carrying up to 1 J per pulse. X-ray fluxes up to 5×10^8 photons per pulse can be generated with a small energy spread inside a highly collimated beam. Several applications ranging from advanced clinical diagnostics (in particular mammography, as in the MAMBO project ³⁾, and non-invasive angiography) to biological imaging could use this facility. Other applications of the SPARC high brightness beam are related to advanced acceleration techniques, like plasma accelerator and new radiation sources by crystal channeling.

4.1.2 SPARXINO

The Quick-start program of the European Initiative for Growth has recently identified next generation lasers as a “*key technology sector for the Union long-term competitiveness and strength of the European economy*”. Support for the development of a network of national facilities working on next generation laser technologies is explicitly mentioned in the final report “A European Initiative for Growth” of the European Commission to the European Council (November 2003). The new infrastructures are based on single-pass Free Electron Lasers (FELs) which are the most advanced short-wavelength radiation sources available. Their unique properties are extremely interesting for researchers from many different areas, including physics, chemistry, biology and materials science. They include extremely high peak intensity at a high repetition rate, pulse durations in the 100 fs regime or less (i.e. a thousand times shorter than synchrotron radiation pulses), continuous tunability covering the complete spectral range down to below 0.1 nm, and a high degree of coherence. For the first time, these new FEL sources will provide sufficient flux at short wavelengths for a broad spectrum of new scientific applications requiring sub-picosecond time resolution.

In this framework R&D plans for a X-ray FEL source at LNF will be developed along two lines: (a) use of the SPARC high brightness photo-injector ⁴⁾ (Sec. 2.3) to develop experimental test on RF compression techniques and other beam physics issues, like emittance degradation in magnetic compressors due to CSR, (b) explore production of soft and hard X-rays in a SASE-FEL with harmonic generation, in the so called SPARXINO test facility, possibly upgrading in energy and brightness the existing Frascati 800 MeV Linac. A number of interesting physics items have already been proposed (Sec. 4.10, Sec. 4.11, Sec. 4.12) that would use such a facility.

A parallel program will be aimed at the development of other critical component for X-rays FEL sources like high repetition rate S-band guns, high Quantum Efficiency cathodes, high gradient

X-band RF accelerating structures ⁵⁾ and harmonic generation in gas. In order to generate SASE-FEL radiation from 10 nm to 1 nm it is necessary to produce a high brightness beam to inject inside the undulators. The basic scheme is shown in Fig. 4.2 and consists of an advanced high brightness photo-injector followed by a first linac driving the beam up to 350 MeV with the correlated energy spread required to compress it in a subsequent magnetic chicane. The second linac drives the beam up to 1 GeV while damping the correlated energy spread taking profit of the effective contribution of the longitudinal wake fields provided by the S-band accelerating structures. Time dependent FEL simulations show saturation after 16 m of active undulator length. The same undulator of the SPARC project ⁶⁾ with two additional 2 m long modules required to saturate at 10 nm can be used.

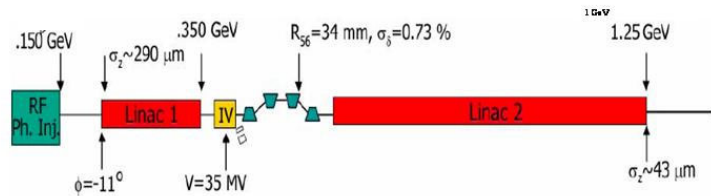


Figure 4.2: Scheme of the SPARXINO test facility.

The DAΦNE 60 m long LINAC, equipped with 15 S-band (2.865 GHz) SLAC-type accelerating structures, at present delivers $0.8 \mu\text{s}$ RF pulses at a repetition rate of 50 Hz as required for DAΦNE operation. It accelerates the positrons emerging from the positron converter up to the maximum energy of 550 MeV and the electrons up to 800 MeV. By upgrading the accelerating field of the existing units up to 26 MV/m and by adding 2 new SLAC-type sections, 1.1 GeV could be reached. The Linac waveguide network should also be modified in order to supply two accelerating units per RF station. This configuration requires also the addition of two new 45 MW klystrons. High beam brightness can be achieved by installing a copy of the 12 m long SPARC photo-injector upstream the DAΦNE linac with a minor modification of the existing building and a magnetic compressor at 350 MeV in the area of the Positron Converter, thus keeping the possibility to operate the linac as DAΦNE injector. About 15 m of drift space is required at the linac output for the installation of an undulator. A detailed analysis of the compatibility of the SPARXINO test facility with the proposed DAΦNE energy upgrade operation is under way ⁷⁾.

4.1.3 PVFEL

The presence of a soft x-ray FEL project such as SPARXINO (Sec.4.1.2) to be developed at LNF opens the unprecedented opportunity of using an intense, ultra-high brilliance source for particle physics applications. In particular, intense photon sources can probe various QED regimes and search for possible dark matter constituents ^{8, 9, 10)}. In this framework, since 1997 results have been obtained by the PVLAS experiment concerning the study of vacuum magnetic birefringence: an effect predicted by Quantum Electrodynamics but not yet experimentally confirmed ^{9, 10)}. According to QED, the quantum vacuum behaves as an optically active medium when perturbed

by an external magnetic field. A linearly polarised light beam can be used as a probe of this effect: after propagating through a vacuum region in the presence of a transverse magnetic field its polarization state will change to elliptical; the parameters of the polarization are directly related to the fine structure constant and the Compton wavelength of the electron. Anomalous contributions to the vacuum magnetic birefringence could also come from light scalar/pseudoscalar particles that couple to a photon pair¹¹). The various physical phenomena that can induce such a birefringence have a different dependence on the photon energy and the possibility of using soft x-ray to excite birefringence rather than, as in the present experiment, a IR or Green laser light, could significantly help in clarifying the origin of this effect.

4.2 Studies on new accelerators

Since 1999, DAΦNE has delivered luminosity to the experiments with increasing performance. KLOE has collected 450 pb⁻¹ in years 2001-2002, DEAR 100 pb⁻¹ in 2002, and FINUDA 250 pb⁻¹ in 2003-2004. A second round of data collection has started in May 2004 with the aim of delivering about 2 fb⁻¹ to KLOE within the end of 2005, and several hundreds of pb⁻¹ to FINUDA and SIDDHARTA (the continuation of DEAR with an upgraded detector and physics program) in the following 1-2 years. After these short-term achievements the mission of DAΦNE, as it is, can be considered concluded, although data analysis will continue to deserve efforts for few years after.

From the physics point of view, there are three possible options for an evolution of the machine in a longer term perspective:

- increase of the machine energy above the nucleon-antinucleon production threshold. This will allow the precision measurement of the nucleon form factors (FF) in the time-like region, quantities which suffer at present of huge experimental uncertainties (the neutron FF, especially, has been measured on the basis of the observation of only 74 events);
- increase of the luminosity of the machine, while remaining at the ϕ peak, to continue the present experimental program, especially in the field of rare K_S decays and kaon quantum interferometry;
- increase of the energy up to the $\psi(3770)$ or τ pair production threshold, to perform precision spectroscopy measurements in the energy range below and at the charmonium threshold, and, depending on the reachable luminosity, precision measurements of the τ lepton mass and decay branching ratios.

The feasibility of the accelerator upgrades and the motivations for the three options are summarized in the following. The planning of the activities related to the different projects, that are not necessarily mutually exclusive, are discussed in Chapter 7.

Particle factories are facing their future by looking at the possibility of upgrading the luminosity by orders of magnitude. The upgrade challenges are more stringent at lower energies. At present, DAΦNE is operating at a luminosity peak exceeding $1.4 \times 10^{32} \text{cm}^{-2} \text{s}^{-1}$, as reported in Sec. 2.2.

In this section possible future scenarios for DAΦNE are presented; the focus is on the expected ultimate performances of the machine as it is now and on the issues of a design for an energy and/or luminosity upgrade, listed by increasing cost, complexity and challenge. Different upgrade options of the collider fitting the existing infrastructures have been examined: an energy upgrade to reach the $N\bar{N}$ threshold with minimal changes, a higher luminosity ϕ -factory, a τ -charm factory.

4.2.1 DAΦNE luminosity optimization

Even though the DAΦNE progresses over the years have been continuous and substantial, a significant further improvement in terms of peak and integrated luminosities is still possible. These expectations mainly rely on:

- implementing a lattice providing negative momentum compaction factor to shorten the bunch and decrease the vertical β -function at the IP (β_y^*);
- moving progressively the betatron tunes toward the integer to reduce the beam-beam induced blow-up of the bunches;
- increasing the beam currents by improving the beam dynamics and the performances of the active feedback systems.

The decrease of β_y^* is beneficial to the luminosity because it results in a reduction of the vertical size of the bunch σ_y^* and of the linear tune shift parameter ξ_y which is an indicator of the strength of the beam-beam effect. However, the beta-function has a parabolic shape around the IP, therefore the length of the region where the beta-function remains small is comparable to the σ_y^* value itself; the latter cannot be reduced below the bunch length value σ_l , in order to avoid a geometrical reduction of the luminosity known as “hourglass effect”. A very effective way to shorten the bunch is to implement a lattice with negative momentum compaction factor α_c . The momentum compaction is the ratio between the relative closed orbit elongation normalized to the relative energy deviation of a particle in a storage ring. Negative momentum compaction lattices have been tested in DAΦNE during machine study shifts and bunch shortening by about 30-40% has been measured. The potential benefits of this kind of lattice are evident, but retuning the machine and all the feedback systems to optimize the luminosity in this configuration will require a significant amount of time.

The beam-beam effect, which is especially severe in the low-energy colliders, is also limiting the luminosity performances of DAΦNE. The primary effect induced by the beam-beam interaction is the blow-up of the transverse (in particular the vertical) size of the bunches of one beam as a function of the current in the bunches of the other one. Presently in DAΦNE an increase by about 50% in the vertical size of the two beams is observed when colliding 10 mA bunches. From beam-beam simulations as well as from experimental data from other colliders such as the B-factories KEK-B and PEP-II, it is known that a way to limit the beam-beam induced blow-up is to work with betatron tunes close to the integer or half integer. However, since any storage ring is unstable at these integer betatron tunes, working close to the integer is very critical and requires extremely fine machine tune-up, especially on the lattice non-linearities. The reduction of the DAΦNE betatron tunes towards lower values has already started as a slow, adiabatic process requiring a machine re-optimization at every step. An optimization of the operational parameters aimed to increase beam lifetimes should also be pursued, finely tuning machine nonlinearities and possibly increasing the injection rates.

4.2.2 DAΦNE energy upgrade

The interest in the $N\bar{N}$ threshold, reported in Sec. 4.9, has originated studies for increasing the DAΦNE energy at least by a factor of two, with a luminosity peak of the order of $10^{32} \text{ cm}^{-2}\text{s}^{-1}$ (12). Since the luminosity naturally increases with the energy, this peak luminosity can be obtained with currents of the order of 0.5 A per beam, much lower than the present stored currents. Almost all the systems of DAΦNE are already dimensioned for such currents and energy, with the exception of the dipoles and the injection system. In the hypothesis of minimum changes in the hardware, a

preliminary design of new normal conducting dipoles fitting the present vacuum chamber has been done ¹³⁾. This design leads to a maximum magnetic field just at the limit for neutron-antineutron production at threshold. Other solutions ¹⁴⁾, based on superconducting dipoles and new vacuum chambers, are being investigated for reaching the $p\bar{p}$ threshold, i.e. 1.2 GeV per beam.

No significant differences are expected for the operation at the ϕ energy since the hardware and the machine layout basically remain the same. Two main options can be foreseen for injection: to upgrade the DAΦNE linac for injecting at full energy (without damping ring) or to preserve the present injection system (including the damping ring) implementing an energy ramping scheme in the main rings. The energy ramping option requires a synchronized control of the magnet power supplies that is allowed by the existing hardware. However this option does not allow topping-up injection in the high energy operation. On the other side, a linac upgrade (Sec. 4.1.2) allowing for a faster and more flexible injection procedure, is more expensive and requires also upgrading kickers and septum magnets in the ring, as well as the transfer lines dipoles.

4.2.3 Higher Luminosity ϕ -Factory

Any upgrade design of DAΦNE as a ϕ -factory has to start from an increase of the machine radiation damping rate. In fact, the physics of the beam-beam effect, thoroughly investigated both theoretically and experimentally, shows that fast radiation damping rates are essential to limit the beam-beam induced vertical blow-up and increase the attainable values of the linear tune shift parameters, thus increasing the achievable luminosity, since the faster the damping rate, the shorter the time needed by a particle to loose the “memory” of any experienced perturbation including those coming from beam-beam interactions.

Another parameter for a luminosity increase is the minimization of the bunch length at the IP to overcome the hourglass effect in the regime of very low β^* . There are two possible approaches in the path to higher luminosities: the first one is the upgrade of the present DAΦNE collider in order to reach luminosities of $\sim 10^{33} \text{cm}^{-2} \text{s}^{-1}$, the other one is to redesign and rebuild the collider to obtain luminosities above that value.

The first approach foresees new superconducting wigglers to add radiation damping, to be installed in one of the two IR; new vacuum chambers with lower impedance and antechambers in the positron ring to increase the electron-cloud instability threshold; a new Interaction Region to lower the β^* and the parasitic crossing effects.

The second approach is the study of a new collider, fitting the existing buildings and pushing the design luminosity at the limit of the accelerator physics state of the art ¹⁵⁾. The ultra-high luminosity design is based on a mix of standard and new concepts, the most important ones being: strong radiation emission to increase radiation damping; negative momentum compaction lattice; strong RF focusing scheme to get bunch lengths in the mm scale.

The importance of enhancing the radiation emission and the advantages of the negative momentum compaction factor has already been illustrated in the previous paragraphs. In the preliminary design a basic “wiggling” cell, made of a sequence of inward and outward bending dipoles, provides both large radiation damping and large negative momentum compaction. Due to partial compensation of positive and negative dipoles, the total bending angle of one cell is small and a large number of cells (i.e. a large number of dipoles) are necessary.

To make a substantial step in luminosity it is necessary to decrease by about one order of magnitude the vertical beta-function at the IP β_y^* passing from the cm scale to the mm one. Then the bunch length has to be reduced to about the same value to avoid the hourglass effect. Recently, a novel technique called Strong RF Focusing (SRFF) has been proposed to meet this requirement ¹⁶⁾. By combining a very large RF gradient with a large momentum compaction factor, a bunch length modulation along the ring can be induced. The bunch length has its

maximum in the RF section, and the lattice can be tuned such that the bunch length reaches its minimum at the IP. This condition requires that the two portions of the ring delimited by the RF and the IP contribute equally to the total momentum compaction of the ring. However even with a large momentum compaction (of the order of 10^{-1}), the voltage needed to produce sizeable variations of the bunch length along the ring is of the order of 10 MV, a very large value for a 100 m long ring, which surely requires a very efficient superconducting RF system. The SRFF principle has never been observed and studied experimentally. Many aspects of beam physics (such as Touschek lifetime, dynamic aperture, beam-beam, coherent synchrotron radiation emission, etc.) need to be studied in more detail to establish whether or not a collider may efficiently work in this regime. In order to add solidity to a design based on this scheme, an SRFF experiment to be carried out at DAΦNE has been proposed¹⁷⁾. If funded the experiment could be completed in six months and could give the first SRFF experimental observation, together with other useful experimental results on the impact of this regime on the beam dynamics and on the bunch-by-bunch feedback systems. The experiment cost estimate is about 1 MEuro mainly for the construction of the new SC cavity and cryostat, and to the upgrade of the DAΦNE cryoplant to produce 2K liquid Helium.

4.2.4 τ -charm-Factory

Exploring all the possibilities for the future of the LNF in the panorama of the high energy physics during and after the LHC era includes also the τ -charm physics. The infrastructures of the LNF are in principle compatible with a τ -charm project, a collider with an energy in the center of mass of 3.8 GeV, and luminosity of 10^{34} cm⁻²s⁻¹, i.e. an order of magnitude above the BEPC-II design value. Such a machine could be based on a double symmetric ring collider, flat beams in multibunch operation, normal conducting magnets, one Interaction Region, and on-energy injection system.

Research Programs

4.3 Kaon physics

As reported in Sec. 3.2.3, there are near and mid-term plans in the world to achieve high statistics at the hadron machines for studying rare and very rare kaon decays. At the ϕ -factory, integrated luminosities >20 fb⁻¹ (delivered in one year by a machine with peak luminosity of 2×10^{33} cm⁻² s⁻¹) allow the study of tagged, selected samples of the order of 10^{10} kaons of any species. This is not enough to compete with hadronic machines for the search for $K_L \rightarrow \pi\nu\nu$ but sufficient to improve the results in other channels, as explained in the following. In this realm, a ϕ -factory can compete for precision measurements of leptonic, semileptonic and hadronic decays and in the improvement of the absolute branching ratios (BR) of the channels with BR $> 10^{-9}$. The new results can be provided thanks to the low background environment, to the possibility to tag the kaon beams, to the kinematic knowledge of the events and to the fact that the kaon system is produced in a coherent quantum state.

The discussion is centered on few topics taken as benchmarks of wider physics programs, including different tests of the discrete symmetries and precise measurements of interest for Chiral Perturbation Theory (χ PT), i.e. for studying low energy properties of the strong interactions in terms of effective theories.

4.3.1 K_S decays

The KLOE experience has demonstrated that a ϕ -factory has to be considered the best place for the study of K_S decays. K_S 's are produced at a rate of 10^6 particles per pb^{-1} . Assuming typical KLOE detection efficiencies, one can deal with statistical sample as rich as 10^5 events/ pb^{-1} . Therefore a data collection of $\geq 20 \text{ fb}^{-1}$ would translate in the first observation of a signal of the CP violating transition $K_S \rightarrow 3\pi^0$, whose branching ratio is expected to be $\sim 2 \times 10^{-9}$. At present, the best limit on this branching ratio is set by KLOE at 2×10^{-7} , on the basis the analysis of $\sim 400 \text{ pb}^{-1}$.

The $K_S \rightarrow \pi^+\pi^-\pi^0$ decay can proceed with or without CP violation. The CP-conserving (CPC) amplitude is suppressed by $\Delta I = 3/2$ rule and by angular momentum barrier, giving the predicted branching ratio of $\sim 3 \times 10^{-7}$. The CP-violating (CPV) amplitude is enhanced by the $\Delta I = 1/2$ rule and the predicted branching ratio is $\sim 1.2 \times 10^{-9}$. The interference between CPC and CPV amplitudes, vanishing in the total rate, gives rise to a 10% left-right asymmetry in the charged pions from which it is possible to derive η_{+-0} . The dominant CPC amplitude is interesting by itself since it is a pure $\Delta I = 3/2$ transition and it can be used to test for the first time the χ PT calculations that have an accuracy at 10% level.

Current experimental knowledge of $\text{BR}(K_S \rightarrow \pi^+\pi^-\pi^0)$ is relatively poor. Measurements of $\text{BR}(K_S \rightarrow \pi^+\pi^-\pi^0)$ have been performed using interference techniques at the CERN CPLEAR and Fermilab E621 experiments. The results are:

$$(2.5_{-1.0}^{+1.2+0.5}) \cdot 10^{-7} \quad \text{CPLEAR 18, 19)}$$

$$(4.8_{-1.6}^{+2.2} \pm 1.1) \cdot 10^{-7} \quad \text{E621 20)}$$

The world average value for $\text{BR}(K_S \rightarrow \pi^+\pi^-\pi^0)$, as calculated by the Particle Data Group is $(3.2_{-1.0}^{+1.2}) \cdot 10^{-7}$ 21).

With $\sigma_\phi \sim 3 \mu\text{b}$ and $\text{BR}(\phi \rightarrow K_S K_L) = 0.336$, this corresponds to about 0.3 $K_S \rightarrow \pi^+\pi^-\pi^0$ decays produced per pb^{-1} . Assuming the present KLOE selection efficiency, with an integrated luminosity of 50 fb^{-1} , one expects to collect a sample of 200 events, large enough to measure the pion left-right asymmetry with 30% accuracy and the total $\text{BR}(K_S \rightarrow \pi^+\pi^-\pi^0)$ with a precision of 7%.

The K_S semileptonic decays represent another process of interest for the ϕ -factory. The value of the branching ratio of this transition can be derived from the measured value of the same BR for the K_L and from the ratio of the two lifetimes by the simple relation:

$$BR_S = BR_L \times \tau_S / \tau_L \quad (4.1)$$

The above formula implies that $\Delta S = -\Delta Q$ transitions are not allowed. Any deviation from it, therefore, is a signature of violation of the $\Delta S = \Delta Q$ rule, which in the SM is expected at the 10^{-6} level. In general, the amount of this violation is parametrized by the quantity $Re(x_+)$:

$$Re(x_+) \equiv \frac{1}{2} \left[\frac{\langle e^+ \pi^- \nu | T | \bar{K}^0 \rangle}{\langle e^+ \pi^- \nu | T | K^0 \rangle} + \frac{\langle e^- \pi^+ \bar{\nu} | T | K^0 \rangle^*}{\langle e^- \pi^+ \bar{\nu} | T | \bar{K}^0 \rangle^*} \right], \quad (4.2)$$

which can be measured from the relative difference of K_S and K_L decay widths into $\pi e \nu$:

$$Re(x_+) = \frac{1}{2} \frac{\Gamma(K_S \rightarrow \pi e \nu) - \Gamma(K_L \rightarrow \pi e \nu)}{\Gamma(K_S \rightarrow \pi e \nu) + \Gamma(K_L \rightarrow \pi e \nu)}. \quad (4.3)$$

The most precise published value of $Re(x_+)$ is given by CPLEAR Collaboration ²²⁾, $Re(x_+) = (-1.8 \pm 4.1_{stat} \pm 4.5_{syst}) \times 10^{-3}$. The KLOE preliminary measurement is $Re(x_+) = (0.9 \pm 2.9_{stat} \pm 2.9_{syst}) \times 10^{-3}$, obtained with $\sim 400 \text{ pb}^{-1}$ of integrated luminosity.

CPT violation in the kaon system is parametrized by the complex quantity δ , which is proportional to the difference between the amplitudes describing the time evolution of the two mass eigenstates, K^0 and \bar{K}^0 . CPLEAR has found $Re(\delta)$ to be compatible with zero, with an error of $\sim 3 \times 10^{-4}$, using tagged K^0 and \bar{K}^0 semileptonic decays.

Alternatively, $Re(\delta)$ can be measured comparing the charge asymmetries A_S and A_L of the K_S^0 and K_L^0 mesons to $\pi^\pm e^\mp \nu$, through the relation: $A_S - A_L = 4 \times Re(\delta)$.

While A_L has been recently measured with a precision of $\sim 10^{-4}$ ²³⁾, the present KLOE preliminary measurement gives the first ever made measurement of $A_S = (-2 \pm 9_{stat} \pm 6_{syst}) \times 10^{-3}$.

By simply extrapolating the statistical error quoted above, one can argue that a data collection corresponding to $\sim 20 \text{ fb}^{-1}$ would provide a measurement of A_S with $\sim 30\%$ accuracy.

Another kind of very interesting decays are $K_S \rightarrow \pi^0 l^+ l^-$, and especially the theoretically cleanest decay into one pion and one $e^+ e^-$ pair. The knowledge of the relative branching ratio is important since it fixes the indirect CP-violating contribution to the same decay of the K_L , which could be measured in the near future by fixed-target experiments. The accuracy in the knowledge of this contribution directly translates in the precision of the SM prediction for the K_L decay, as shown in Fig. 4.3. The only experimental evidence for $K_S \rightarrow \pi^0 e^+ e^-$ has been given by NA48 ²⁴⁾ on the basis of 7 events, corresponding to $BR(K_S \rightarrow \pi^0 e^+ e^-) = (5.8_{-2.4}^{+2.9}) 10^{-9}$. Integrated luminosities at the Φ -factory of the order of 50 fb^{-1} are needed to collect samples of dozens of events, assuming conservative efficiencies of 10%.

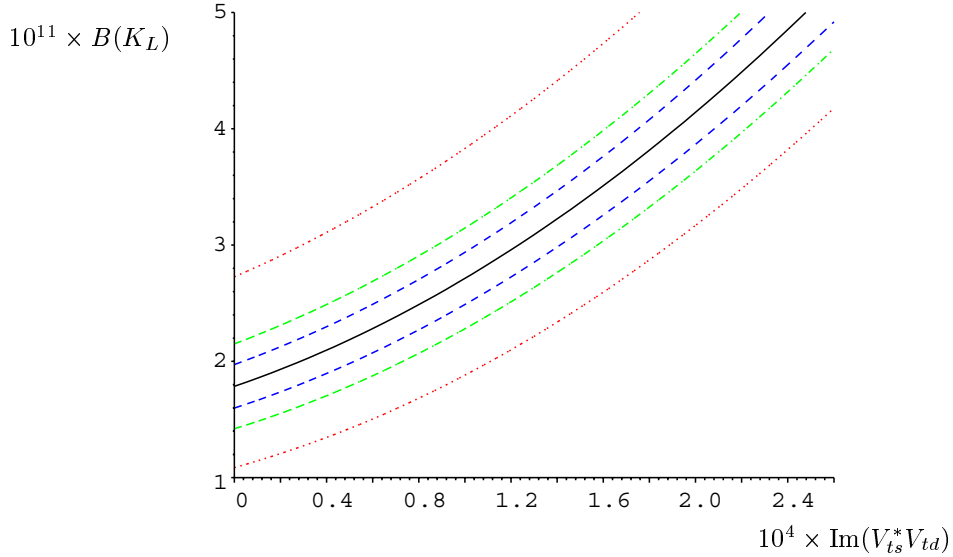


Figure 4.3: *SM Prediction for $B(K_L \rightarrow \pi^0 e^+ e^-)$ as a function of $\text{Im}(V_{ts}^* V_{td})$, neglecting CPC contributions and assuming a positive interference between direct- and indirect-CP-violating components. The four curves correspond to the central value of $B(K_S \rightarrow \pi^0 e^+ e^-)$ and no error (central full line); 10% error (dashed blue lines); 20% error (dashed green lines); present error (red dotted lines).*

Two important facts must be underlined here. First, a careful study on the impact of machine

background is crucial to reach the sensitivity needed to measure these rare processes. Second, since it is assumed everywhere present KLOE selection efficiencies, there is room for improvements by optimizations of the analysis cuts and/or by detector upgrades. On this respect, an increase in the event acceptance is conceivable by means, for example, of the construction of a new, light tracker near the interaction region and a careful tuning of the magnetic field value, presently optimized for the separation of $K_L \rightarrow \pi\pi$ from $K_L \rightarrow \pi\mu\nu$ decays.

4.3.2 Neutral Kaon Interferometry

Since at the ϕ -factory the neutral kaons are produced in a coherent state $J^{PC}=1^{--}$, the decay lengths of the two kaons are correlated and the interference patterns in different decay channels permit precision measurements of the kaon parameters, including the phases ϕ_{+-} , $\phi_{+-} - \phi_{00}$, and the CPT violation parameters $Im(\delta_k)$, $Re(\delta_k)$ ²⁵⁾.

The parameters related to the conservation of the discrete symmetries are sensitive to the behaviour of the decay length correlations at short decay distances so that attainable accuracies are dominated by the limited statistics of K_L decays occurring within $\sim 5-10 \tau_S$ or $0.01-0.02 \tau_L$.

With integrated luminosities of the order of 50 fb^{-1} the real parts of the CP/CPT violation parameters could be measured at the $\mathcal{O}(10^{-4})$ level of the statistical error.

Since all final state combinations can be measured with high statistics at the ϕ -factory, it is also possible to infer the CP/CPT violation parameters in the mixing and in the decay amplitudes separately. Moreover, final results can benefit of a global fit to all the distributions, certainly useful to limit systematic errors.

4.3.3 Charged Kaons

At the funded Japanese Proton Facility JPARC a physics program ²⁶⁾ centered on precision measurements of the major branching fractions of charged kaons has been submitted to the Scientific Committee. The goal of the program, starting in 2008, is to reach 5 per mil accuracy (systematics-dominated) in the K_{e3} mode and similar precisions in purely leptonic, semi-leptonic, hadronic decays with or without photons in the final state. The new measurement of $K^+ \rightarrow \pi^0 e^+ (\mu^+) \nu$ allows the extraction of the $|V_{us}|$ CKM matrix element with a precision of 10^{-3} . The study of the decay spectra addresses questions on the nature of weak interactions (scalar, vector and tensor type), lepton universality and models of hadron dynamics.

The ϕ -factory, at integrated luminosities of the order of 100 fb^{-1} , can well compete with this program achieving similar or better precisions in a completely new environment, dominated by different systematics. In particular, the program will include new measurements of the direct photon emission contributions to the hadronic modes, very poorly known today. Moreover, at the ϕ factory direct CP violation can be addressed by the measurement of the asymmetries in the Dalitz plot of $K^+/K^- \rightarrow 3\pi$ decays.

4.4 Light Quark Spectroscopy

The hadron physics program points to high-energy, in the B-meson sector and above, aiming to unveil the evidence of new physics at very short distances in loop-diagram dominated processes. There is however the opposite direction that is actively pursued by a wealth of experimental programs, which includes the confinement regime where one aims to study hadronic phenomena in the GeV region and to connect them to fundamental parameters of QCD.

The energy region below the charm quark threshold is of interest for the possibility of studying light scalar candidates, glueballs, hybrids, multi-quark states. Detailed study of the enigmatic f_0 , as well as other topics related to η, η' pseudoscalars, can be carried out in the ϕ energy region. But surprises do lurk in the 2 GeV vector meson region, which await to be clarified. One can only name two of them, the $X(1750)$ and the $\rho(1900)$.

- The $X(1750)$ was only recently conclusively shown to be different from the $\phi(1680)$, following high-statistics data in high-energy photoproduction ²⁷⁾ which shows a 10,000 event enhancement in the K^+K^- final state with a signal/background ratio ~ 1 . The same data shows no enhancement in K^*K , which is the dominant mode for the $\phi(1680)$, also recently confirmed by preliminary BABAR data. The interpretation of both remains uncertain.
- Evidence for the radial excitations of ρ vector meson have remained for long time cladded by mystery. For a brief but complete account see the mini-review in ²⁸⁾. Definite evidence for the $\rho(1700)$ has come from photoproduction experiment E687 ²⁹⁾ in the 6π final state. The $\rho(1700)$ is observed interfering destructively with a narrow resonance at 1.9 GeV previously observed in e^+e^- ^{30, 31)}, namely the $\rho(1900)$. The new narrow resonance is discussed in relation to the dip observed in the form factors around 1.9 GeV, the $N\bar{N}$ threshold, and a possible hybrid $q\bar{q}g$ origin has been proposed.

Finally, the light hadron sector, and especially light scalars, can be studied at a high-luminosity charm factory via Dalitz plot analysis of charm meson decays ^{32, 33)}. This is actually an interesting example of synergy and joint efforts between two communities: on one hand the charm meson decays represent a new source of information on light hadrons, on the other the charm meson interpretation requires the understanding of strong effects in the final states. Among examples of such an interplay it is possible to quote the Dalitz plot analysis of $D \rightarrow \pi\pi\pi$ for $f_0(980)$ and $\sigma(500)$, and $D \rightarrow K\pi\pi$ for f_0/a_0 mixing.

4.5 Charm physics

Studying charm decays at the threshold process $e^+e^- \rightarrow \psi(3770) \rightarrow D\bar{D}$ offers many advantages. Threshold production of charm hadrons leads to extremely clean events, with optimum signal/background ratios; the background due to not- $D\bar{D}$ processes can be directly measured running below the production threshold. It is possible to tag the events to obtain absolute branching fraction measurements; the $D\bar{D}$ pairs are produced in a coherent Quantum-Mechanic state providing information on D mixing and CP violation. In the SM, CP-violating amplitudes arise from penguin or box diagrams with b-quarks; however they are strongly suppressed by the small $V_{cb}V_{ub}^*$ combination of the CKM matrix elements. The observation of CP violation in charm decays would be an unambiguous signal of new physics. The $D\bar{D}$ pairs are produced in a C=-1 initial state so that final states containing two CP eigenstates of the same parity is a manifestation of CP violation. With integrated luminosities of the order of 100 pb^{-1} the discovery window in the analysis of these final states could be extended to the 10^{-4} level.

Moreover, it is possible to put stringent limits on the oscillations in the charm sector running above the $\psi(3770)$ and comparing the correlations in D decays produced in $e^+e^- \rightarrow D^0\bar{D}^0, e^+e^- \rightarrow D^0\bar{D}^0\gamma$ and $e^+e^- \rightarrow D^0\bar{D}^0\pi^0$ ³²⁾. Although $D^0\bar{D}^0$ oscillations are not the most suitable tool to look for New Physics, their study at the τ -charm factory (τ cF) is unique because of the absence of concurrent Doubly Cabibbo Suppressed decays in most of final states. At the τ cF is also possible the measurement of the strong phase shift comparing oscillations in hadronic and semileptonic final states. Other channels of interest are the FCNC decays, in particular the $D \rightarrow \pi l^+l^-$ and $D \rightarrow \rho$

l^+l^- which in the SM are expected to have a BR of the order of 10^{-6} : effects of new physics could show up in the region of low di-lepton masses ³⁴).

Integrated luminosities of the order of 100 fb^{-1} would provide statistics for many important studies of the SM, summarized in Table 4.1.

- Precision measurement of the $D^+ \rightarrow \mu^+\nu$ branching ratio, allowing the extraction of the charm decay constant f_D , can be carried out with unrivaled control over systematics. Extracting precise numbers for the decay constant f_D represents an important test for lattice QCD calculations, that are expected to become very precise in this sector in the near future ³⁵).
- Significant improvements in the measurements of $|V(cd)|$ and $|V(cs)|$ from $D \rightarrow \ell\nu\pi$ and $D \rightarrow \ell\nu K$ modes could be obtained, providing another sensitive test for the attainable precision with lattice QCD, that is expected to reach the percent level in this sector ³⁵). Accurate charm data are very useful to understand the reliability of the description of non-perturbative dynamics and thus indirectly to support the lattice calculations done in the beauty sector.
- Also the absolute branching ratios for non-leptonic decays like $D^0 \rightarrow K\pi$ and $D^+ \rightarrow K\pi\pi$ could be measured with uncertainties of the order of per mil.
- The completion of the charmonium spectroscopy would provide authoritative answers concerning charmonium hybrids and clarify the situation with respect to candidates for glueballs and hybrids in charmonium decays like $J/\psi \rightarrow \gamma X$.

It is worthwhile to mention that there is a deep synergy between precision measurements in the charm sector and the present/future physics programs in the beauty sector. Absolute charm branching ratios and decay chains represent important inputs for B decays, and the present uncertainties are becoming a bottleneck in the analysis of the beauty decays.

4.6 The τ lepton

An e^+e^- collider reaching $\mathcal{L} \sim 10^{34} \text{ cm}^{-2} \text{ s}^{-1}$ at \sqrt{s} just above 3.7 GeV could deliver 100 fb^{-1} per year ($1 \text{ y} = 10^7 \text{ s}$), allowing for the study, with ~ 3 years of data taking, of the lepton-number violating channel $\tau \rightarrow \mu\gamma$ on the basis of a sample of 10^9 events, i.e. in the region of interest for the SUSY theories ³⁶).

From the feasibility point of view, it is worthwhile to remind that the machine project to reach $\mathcal{L}_{peak} \sim 10^{34} \text{ cm}^{-2} \text{ s}^{-1}$ at $\sim 3.7 \text{ GeV}$ is less challenging than to reach such a luminosity at lower energies, also because of the shorter damping times due to the higher radiation emission.

The highest cross section for $\tau\bar{\tau}$ production occurs at the ψ' resonance (3.69 GeV) where visible cross section is approximately proportional to $1/\sigma(E)$ ($\sigma(E)$ is the machine beam energy spread) and it is $\sim 3 \text{ nb}$ for machines adopting standard optics.

The recent upper limit obtained by BABAR Collaboration for the $\tau \rightarrow \mu\gamma$ ³⁷) is $\text{BR}(\tau \rightarrow \mu\gamma) \leq 6.8 \times 10^{-8}$ at 90% C.L., based on the analysis of $\sim 2 \times 10^8$ produced τ pairs. The sensitivity is limited by the background, mainly from $\mu\mu(\gamma)$ and $\tau\tau(\gamma)$ events. Running near threshold the radiative $\tau\tau\gamma$ component is suppressed, and the kinematics of the 2-body τ decays is almost-monochromatic (Fig. 4.4), giving further elements besides statistics to definitively improve the results from the B-factories. Radiative τ decays such as $\tau \rightarrow \pi\nu\gamma$ and $\tau \rightarrow \mu\pi\nu\nu\gamma$ are for the same reason best studied immediately above τ threshold.

Charmed Meson	Produced	Detected
D^0	400×10^6	160×10^6
D^+	160×10^6	63×10^6
D_S^+	30×10^6	9×10^6
Mode	Decay Constant	$\Delta f_{D_q}/f_{D_q}$
$D^+ \rightarrow \mu^+ \nu$	f_D	0.5%
$D_S^+ \rightarrow \mu^+ \nu$	f_{D_S}	0.4%
$D_S^+ \rightarrow \tau^+ \nu$	f_{D_S}	0.3%
$\Delta(V_{cd})$	$\Delta(V_{cs})$	$\Delta R/R; R \equiv V_{cd} / V_{cs} $
0.3%	0.3%	0.2%
Abs. Hadronic BRs	Num. Double Tags	Stat. Error
D^0	1500	0.1%
D^+	1800	0.1%
D_S^+	180	0.3%

Table 4.1: Physics reach for outstanding SM studies at $\tau - c$ factory. Estimates are extrapolated from CLEO-c, the factory presently operating at the Cornell storage ring, and projected to 100 fb^{-1} luminosity.

Moreover, the τ physics program includes precise measurement of the τ mass, sensitive studies of weak couplings and lepton universality via purely leptonic and semileptonic decays, and the measurement of other rare processes as those involving kaons. Thanks to the kinematic constraints, the $\tau \rightarrow \pi\pi^0\nu$ channel can be well separated from the other decays giving the opportunity for a new test of the CVC rule via the comparison with the $e^+e^- \rightarrow \pi^+\pi^-$ data. This is particularly interesting to solve the discrepancy between τ and e^+e^- data in deriving the hadronic vacuum polarization corrections to the anomalous magnetic moment of the muon ³⁸⁾.

4.7 High-resolution spectroscopy of hypernuclei

The study of hypernuclear physics represents a way to address several fundamental questions of modern physics: hyperon-nucleon (YN) and hyperon-hyperon (YY) strong interaction; four baryon strangeness changing weak interaction through the analysis of the non-mesonic weak decays $\Lambda N \rightarrow NN$; change of hyperons and mesons properties in the nuclear medium; existence of dibarionic resonances; the role played by quark degrees of freedom, flavor symmetry and chiral models in the nuclear and hypernuclear sector. In the last years, the use of γ -ray detectors for hypernuclear physics studies has determined a significant breakthrough in this field. In fact, by exploiting the unique energy resolution achievable with germanium detectors (few keV at 1 MeV) it has been possible to shed new light both on low energy hyperon-nucleon interaction and on impurity nuclear physics. Hence high-resolution γ -spectroscopy represents the new frontier for hypernuclear physics. In this section, the possibility to carry on such an experimental program with a modified FINUDA setup (FINUDA2) exploiting the increased luminosity of DAΦNE is described.

Thanks to high resolution γ -ray spectroscopy with germanium (Ge) detectors, detailed level structures of hundreds of nuclei have been precisely measured with energy resolution of about few keV. However, this experimental technique has not been successfully used for Λ hypernuclei since 1998 due to the difficulty of operating Ge detectors in high-counting rate environments. Nevertheless, with the construction of the large-acceptance Ge detector array (Hyperball) at KEK ³⁹⁾

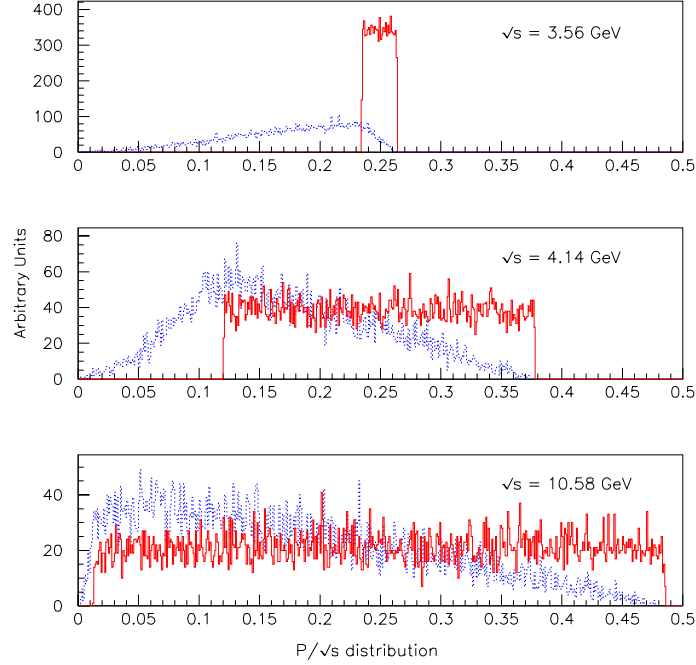


Figure 4.4: *Track momentum distributions normalized to \sqrt{s} at the τ pair production threshold (top), at 4.14 GeV (middle) and for comparison at the $Y(4s)$ resonance (bottom). Dotted, blue histograms are the distributions for the $\tau \rightarrow l\nu\nu$ channels and continuous, red histograms refer to the two-body decays $\tau \rightarrow \pi\nu$.*

it has been demonstrated that this powerful experimental technique is nowadays available also for hypernuclear physics. This bring down the energy resolution on the hypernuclear levels to few keV (FWHM) 39, 40, 41) allowing to explore new physics topics.

4.7.1 Hyperon-nucleon interaction

Hypernuclear γ spectroscopy gives information on the interaction between a Λ and a nucleon which is the first step toward the unified theory of baryon-baryon interaction. In light Λ hypernuclei, the level structure can be described as the weak coupling of a Λ to the nuclear core. When the structure of the considered hypernuclear system is relatively simple, like in the case of light Λ -hypernuclei, it can be described in the frame of the shell model. Therefore, the YN interaction can be expressed by the following equation:

$$V_{\Lambda N}(r) = V_0(r) + V_\sigma(r)\vec{s}_N \cdot \vec{s}_\Lambda + V_\Lambda(r)\vec{l}_{\Lambda N} \cdot \vec{s}_\Lambda + V_N(r)\vec{l}_{\Lambda N} \cdot \vec{s}_N + V_T(r)[3(\vec{\sigma}_N \cdot \vec{r})(\vec{\sigma}_\Lambda \cdot \vec{r} - \vec{\sigma}_N \cdot \vec{\sigma}_\Lambda)] \quad (4.4)$$

where $r = |r_N - r_\Lambda|$ and $l_{\Lambda N}$ is the relative orbital angular momentum. Each of the five terms of Eq. (4.4) 42) corresponds to a radial integral commonly denoted as \bar{V} , Δ , S_Λ , S_N and T. The average central interaction (\bar{V}) is determined by reproducing the measured Λ binding energies for several p -shell hypernuclei. The other four parameters express spin-dependent forces. For low-excitation levels, where the Λ occupies the $0s$ orbit, each level of the nuclear core having spin J ($\neq 0$) is split into two levels with $J + \frac{1}{2}$ and $J - \frac{1}{2}$. The spacing of these levels is of the order of 100 keV hence to measure such a fine structure it is necessary to use Ge detectors. The levels

structure and the energy of the γ transitions of some p -shell hypernuclei have been theoretically studied in relation to the spin-dependent contributions (42, 43, 44), but the measured energy level spectra cannot be completely reproduced by a simplified two-body effective interaction. In order to describe the experimental data a so called three-body force, due to intermediate Σ states, has to be considered. Since the mass difference between Σ and Λ particles is smaller than that of Δ and N , the three-body force is stronger than the analogous interaction involving intermediate Δ states in ordinary nuclei. Moreover, since the ΛNN interaction is mediated by two-pion exchange, while the one-pion exchange is forbidden by isospin conservation, the ΛNN force is expected to be larger than the ΛN one. Therefore, the study of the hyperfine hypernuclear levels has produced a first result in the understanding of baryon-baryon interaction.

4.7.2 Impurity nuclear physics

A hypernucleus can be regarded as a nuclear system with an explicit content of strangeness. The introduction of one (or two) hyperon(s) in a nucleus may give origin to various modifications of the nuclear structure, like changes of the size and of the shape, changes of the cluster structure, manifestation of new symmetries, changes of collective motions, etc... An interesting topic of modern nuclear physics is the study of nuclear matter with an extreme N/Z ratio, the so called neutron-rich nuclei. Hypernuclei in general and neutron rich hypernuclei in particular (i.e. ${}^7_{\Lambda}\text{H}$, ${}^6_{\Lambda}\text{H}$, ${}^{12}_{\Lambda}\text{Be}$) (45) may be even better candidates to study nuclear matter far from the stability line, because more extended mass distributions are expected than in ordinary nuclei thanks the “glue-like role” of the Λ particle. This effect has been experimentally determined through γ -ray spectroscopy of ${}^7_{\Lambda}\text{Li}$ (41). The method used to put in evidence such an effect, and that can be used to explicitly determine other nuclear modification, is again the study of the energy level spectrum of Λ -hypernuclei. By comparing the $B(E2)$ of ${}^7_{\Lambda}\text{Li}$ ($5/2^+ \rightarrow 1/2^+$) with that of the core transition ${}^6\text{Li}$ ($3^+ \rightarrow 1^+$) it has been found that the size of the ${}^7_{\Lambda}\text{Li}$ is $19 \pm 4\%$ smaller than that of ${}^6\text{Li}$. The measurement of $B(E2)$ has been carried out with the Doppler-shift attenuation method (DSAM). This method, developed at KEK, is based on the assumption that if γ ray emission is fast enough after the production of the hypernucleus, the width of the detected energy peak is broadened by the Doppler effect. The lifetime of the excited state is then obtained from the observed peak shape compared with that coming from a MonteCarlo simulation.

4.7.3 Medium effect

The last topic that may be addressed by means of hypernuclear γ spectroscopy is related to the origin of baryon’s masses. The properties of a baryon embedded in a nucleus may change due to the partial restoration of chiral symmetry in nuclear matter. This effect might be measured by comparing the g -factor of a Λ in the nucleus with that in free space. However, due to its short lifetime, it is difficult to measure hypernucleus g factor directly, one could derive it from the probability of the spin-flip transition $B(M1)$ between hypernuclear spin-doublets states (46).

4.7.4 High resolution hypernuclear γ spectroscopy with FINUDA

The FINUDA experiment has demonstrated that the low energy kaons available at the LNF Φ -factory (47) are extremely useful to perform hypernuclear physics. Therefore, as soon as FINUDA completes its scientific program, it would be possible to envisage a detector upgrade in order to perform γ ray spectroscopy. It implies the removal of a couple of drift chambers both from the

inner and the outer arrays: such a modification provides room to install a couple of VEGA γ -ray detectors ⁴⁸⁾ inside the FINUDA magnet coil directly looking at the nuclear targets with a reduction of the present solid angle covered by the spectrometer ($\sim 3\pi$ sr) of only $\sim 28\%$. This segmented clover Ge detector has been developed at GSI and represents the most advanced device presently available. At current DAΦNE luminosities ($\sim 10^{32}\text{cm}^{-2}\text{s}^{-1}$), the expected counting rates will range from ~ 1000 events/day down to a few events/day, depending on the selected γ -transition. Of course the scenario will be more attractive when it will be possible to exploit the new potentialities, in terms of luminosity, of DAΦNE ^{49, 50)}. It is worth recalling that the major drawback of Ge detectors is their low efficiency: the feasibility of the FINUDA2 experiments will crucially depend on the brilliance of the ϕ source.

By simply extrapolating the Monte Carlo calculations for the FINUDA apparatus in present configuration, at a luminosity of $10^{33}\text{cm}^{-2}\text{s}^{-1}$ one can expect to observe the formation of $\sim 1.6 \times 10^3$ ${}^{12}_\Lambda\text{C}$ hypernuclei per hour in their ground state. By taking into account a machine duty cycle of 75%, a reduced spectrometer acceptance of 72%, a Ge detector acceptance of $\sim 30\%$ and a Ge detector efficiency $\sim 30\%$ one finally gets $\sim 1.87 \times 10^3$ events/day. By integrating this number over a typical data-taking period of 50 days one can expect to collect $\sim 9.33 \times 10^4$ events; this number is very close to the one foreseen for a proposed experiment ⁵¹⁾ at the recently approved Japanese facility J-PARC ⁵²⁾: on the same target and in the same amount of time the authors predict to observe 11.2×10^4 events.

Besides these very encouraging perspectives, it is worthwhile to remind the great advantages offered by low-energy DAΦNE K^- : they can be stopped in a very thin target greatly reducing the hadronic background, which represents the major concern for the Ge detectors safety due to the hazard of radiation damages. As a matter of fact the huge hadronic background inherent to the high-energy secondary meson beams was the main problem that in the past prevented the use of γ -ray detectors in hypernuclear physics. Therefore even with a lower machine luminosity this scientific issue still remains very appealing.

4.8 Kaonic-atom physics

The interest in the kaonic atoms study is related to the possibility they offer in understanding aspects of the non-perturbative QCD which are not accessible otherwise. A kaonic atom is formed when a negatively charged kaon enters a target, loses its kinetic energy through ionization and excitation processes, and is eventually captured in an atomic orbit, replacing an electron. Usually the kaonic atom forms in a highly excited state ($n \simeq 25$ for kaonic hydrogen). After the formation, the kaonic atom decays through a series of processes; those of interest are the radiative X-ray decays. The measurement of the X rays generated in these decays offers an unique tool for low-energy antikaon-nucleon and antikaon-nuclei study.

DAΦNE represents a unique “kaonic-atom factory” - due to the high quality of the “kaon beam” obtained by the ϕ -decay: low-energy, low hadronic contamination and low energy spread.

Therefore, DAΦNE is the ideal place where a systematic study of exotic atoms can be accomplished and where fundamental information, completely missing from today experimental scenario, can be achieved.

4.8.1 Precision measurements of kaonic hydrogen and deuterium

The interest in the study kaonic hydrogen and deuterium, is connected to the fact that when the kaon, as a result of de-excitation processed, reaches a low- n state with small angular momentum the strong interaction with the nucleus starts playing an important role. This strong interaction causes

the shift in energy of the lowest-lying level from the purely electromagnetic value and the finite lifetime of the state - corresponding to an increase in the observed level width. For kaonic hydrogen and deuterium the K-series transitions are of experimental interest, since they are the only ones affected by the strong interaction. The shift ϵ and the width Γ of the 1s state of kaonic hydrogen are related, at first approximation, by the use of the so-called Deser-Trueman formula ⁵³⁾, to the real and imaginary part of the complex s-wave scattering length a_{K-p} : $\epsilon + i\Gamma/2 = 412 a_{K-p}$ eV·fm⁻¹. A similar relation holds for the kaonic deuterium and for its corresponding scattering length a_{K-d} .

Recent results by using the non-relativistic Lagrangian approach to bound states have shown that the isospin-breaking corrections to the lowest order Deser relations might be large ⁵⁴⁾. Further investigations using effective field theories of lattice calculations are needed.

Moreover, the measured scattering lengths are used for the determination of the K⁻N isospin-dependent scattering lengths, a_0 and a_1 , where the use of three-body Faddeev equations is required in order to extract a_{K-n} from a_{K-d} . An accurate determination of the K⁻N isospin dependent scattering lengths will place strong constraints on the low-energy K⁻N dynamics, which in turn constrains the SU(3) description of chiral symmetry breaking, as specified in Sec. 3.3.2.

From the experimental point of view, the most precise measurement of kaonic hydrogen was performed in 2002 by the DEAR (DAΦNE Exotic Research Experiment) experiment at DAΦNE ⁵⁵⁾, and are reported in Fig. 4.5 (left panel), while no measurement exists for kaonic deuterium. The obtained results are: $\epsilon = -193 \pm 37$ (stat) ± 6 (sys) eV and $\Gamma = 249 \pm 111$ (stat) ± 30 (sys) eV. In the near future the eV precision measurement of kaonic hydrogen and the first measurement of kaonic deuterium are planned to be performed at DAΦNE by the new SIDDHARTA ⁵⁶⁾ experiment, which represents a continuation of DEAR, planned to be in data taking during 2007. SIDDHARTA is an international collaboration among 8 institutions out of 6 countries. No competitors exist for these measurements, due to the uniqueness of the quality of the kaon beam at DAΦNE.

SIDDHARTA is going a step forward with respect to DEAR, thanks to the use of large area Silicon Drift Detectors (SDD) as triggerable X-ray detectors, which are replacing the non-triggerable CCD (Charge Coupled Device) detectors used in DEAR. Preliminary tests of SDD prototypes performed at the Beam Test Facility (BTF) of Frascati ⁵⁷⁾ as well as in the laboratory showed that a trigger could be applied in SIDDHARTA, with a trigger window of 1 μs, which, as calculated by Monte Carlo simulations will cut the background with respect to DEAR by few orders of magnitude. Further details concerning the SDD large area detector are reported in Sec. 6.3.1.

A cryogenic and pressurized target of hydrogen (deuterium) will be used, with a density optimized such as to have the maximum number of measured X rays.

With an integrated luminosity of about 100 pb⁻¹ a measurement at the level of eV for the kaonic hydrogen will become feasible. For the kaonic deuterium case the required luminosity is about 200-300 pb⁻¹.

4.8.2 Kaonic-helium measurement

At present, the only three kaonic helium X-ray transition measurements refer to the transitions from the 3d to the 2p level ⁵⁸⁾. The measurements are more than 30 years old and the results are much larger than the theoretical prediction from optical models.

The average values of the measured shift and width of the 2p level are: $\epsilon = -43 \pm 8$ eV and $\Gamma = 55 \pm 34$ eV while the optical-model ⁵⁹⁾ calculation predicts a shift of the order of 0.1 eV and a width of about 2 eV.

It is thought that the optical-model is inadequate due to the fact that the effect of the $\Lambda(1405)$

resonance is not taken into account. Because the protons in the helium nucleus are tightly bound, the effective energy of the K^-p interaction in helium is much closer to the energy of the resonance than in other nuclei.

Moreover, recent KEK results on deeply bound kaonic states in helium show that the $\Lambda(1405)$ might have a non-trivial dynamics ⁶⁰⁾ which should reflect itself in the kaonic atom as well.

In principle, since the overlap of the kaon and nucleus wave functions is small for the atomic 2p level, one expects the shift to be small. If the strong interaction shift of the 2p level is confirmed to be large, then the shallow and absorptive $\bar{K}N$ potential is excluded ⁶¹⁾. The large shift (bigger than 10 eV) can only occur if the kaonic “nuclear” 2p pole comes close to the atomic one and this happens only in a very narrow window of the $\bar{K}N$ interaction. A better determination of the strong interaction parameters for kaonic helium is consequently needed.

Therefore, it is planned to measure again the kaonic helium X-ray transitions to the 2p level in the framework of SIDDHARTA (in 2007) and to check the discrepancy reported by the previous experiments with a much smaller errors. This measurement, due to the fact that the yield of the kaonic helium $3d \rightarrow 2p$ transition is about 10% for liquid helium, and bigger for gaseous one, should be feasible with an integrated luminosity of few tens of pb^{-1} . Due to a large energy efficient range of the SDD detectors used in SIDDHARTA, which extends to 30–40 keV, the X-ray transitions to 1s level might be as well accessible, if yield is big enough. The study of the 1s level shift and width might prove to be very interesting.

4.8.3 Measurement of other kaonic atoms

Other light and less light kaonic atoms can be systematically studied by SIDDHARTA. These measurements help to establish a potential and compare it to the kaon-nucleon interaction, deepening our understanding of the role of nuclear matter on kaon-nucleon interactions. In particular, these studies are related to the deeply bound atomic as well as nuclear levels - as those recently measured at KEK ⁶²⁾. These measurements have astrophysics implications as well, related to the kaon-condensate in the neutron stars.

4.8.4 Sigmonic-atom physics

The study of sigmonic atoms gives complementary information to the kaonic ones and are important for the understanding of QCD non-perturbative aspects, in particular of the chiral symmetry breaking mechanism in systems containing the strange quark. In the case of DAΦNE the Σ^- hadron is obtained as a product of the interaction of the negative kaon with nuclear matter, in particular with the proton. The Σ^- such obtained with a certain probability might then form an exotic sigmonic atom. The efficiency of this process is limited by the lifetime of the Σ^- and the study of such atoms and the corresponding X-ray transitions might ask for a higher luminosity machine than DAΦNE. A feasibility study is in progress.

4.8.5 Precision measurement of the charged kaon mass

The 2004 Review of Particle Physics assigns a precision to the charged kaon mass which is an order of magnitude worse than the one of the charged pion mass $M_K = 493.677 \pm 0.013$ MeV, the errors representing an uncertainty of about 26 p.p.m.; the pion mass is determined to about 2.5 p.p.m. The value reported above is obtained by making a weighted average of six measurements ⁶³⁾ and has a huge scale factor ($S=2.4$) to account for a serious disagreement between the most recent and precise results, which differ by 60 keV.

The uncertainty on the kaon mass has severe implications on the extraction of the K^-p and K^-d scattering lengths out of the kaonic hydrogen and kaonic deuterium measurements. The shift is related to the scattering length by a relation in which the reduced mass of the system enters. Then, it is clear that the precision of the kaon mass limits the knowledge of the scattering length.

A new method based on the measurement of kaonic nitrogen X-ray transitions was already checked in the framework of the DEAR experiment ⁶⁴). Three previously unseen transitions, at 14.0, 7.6 and 4.6 keV, were measured and the yield determined ⁶⁵). The spectrum of kaonic nitrogen transitions is shown in Fig. 4.5 (right panel). The energy of these transitions is related, through the Klein-Gordon formula, to the kaon mass, allowing its extraction with a precision limited by statistics and systematic errors.

Based on this feasibility study a new setup, with crystals and CCD detectors, was proposed to perform the charged kaon mass measurement at DAΦNE in the near future. The kaon mass could be extracted with a precision better than 10 keV with an overall integrated luminosity of few hundreds of pb^{-1} ⁶⁴). As an alternative, a feasibility study is undergoing in the framework of the SIDDHARTA experiment as well.

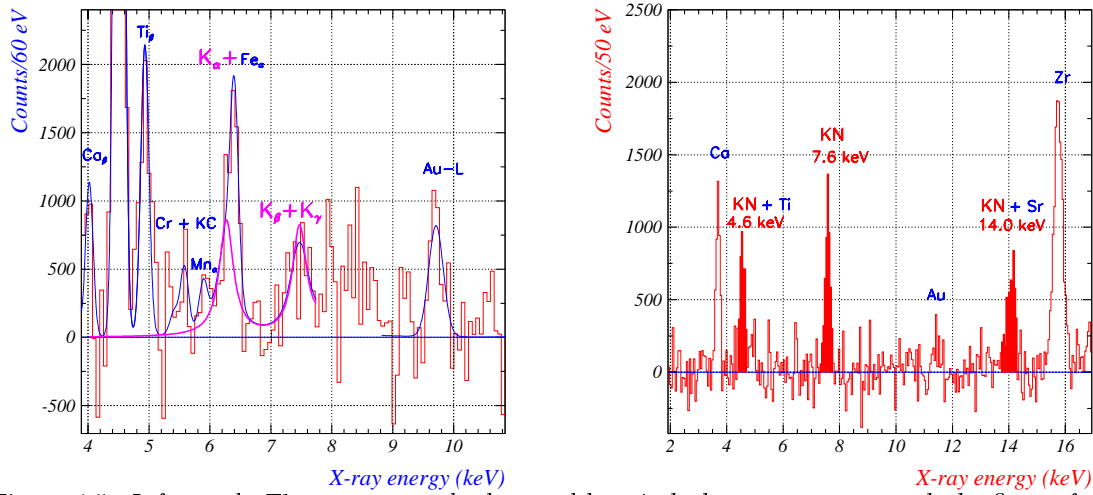


Figure 4.5: *Left panel: The continuous background kaonic hydrogen spectrum with the fitting function. Right panel: The kaonic nitrogen background subtracted spectrum measured by DEAR at DAΦNE ⁶⁴*

4.9 Time-like nucleon form factors

As mentioned in Sec. 3.3.5, time-like nucleon form factors are complex functions of the total energy squared $s = q^2$, thus their determination requires the measurement of both moduli and phases. The center-of-mass differential cross section for $e^+e^- \rightarrow B\bar{B}$ with a spin-1/2 baryon B as a function of the square of the total energy s is given by ⁶⁶)

$$\frac{d\sigma}{d\Omega} = \frac{\alpha^2\beta}{4s} D \quad (4.5)$$

where

$$D = |G_M|^2 (1 + \cos^2\theta) + \frac{1}{\tau} |G_E|^2 \sin^2\theta \quad ; \quad \beta = \sqrt{1 - 4m_B^2/s}, \quad \tau = \frac{s}{4m_B^2} \quad (4.6)$$

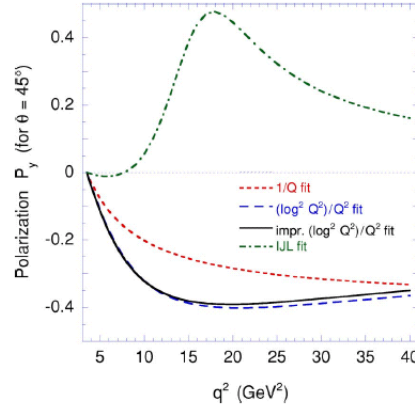


Figure 4.6: *Theoretical predictions for proton polarization P_y as a function of total energy s at $\theta = 45^\circ$. See ⁷¹⁾ for details on different models.*

and provide the analog of the Rosenbluth formula for measuring the time-like form factors. At high energy the cross section is dominated by the magnetic term, due to the presence of the factor $1/\tau$ in front of the electric form factor. At the physical threshold $|G_E| = |G_M|$ by definition, thus the angular distribution should be isotropic.

Present data on proton and neutron come from total cross section measurements assuming for the proton $|G_E| = |G_M|$ and for the neutron $|G_E| = 0$ in all the explored energy region, thus the magnetic form factor can be obtained (even if not in a model independent way). Based on this approximation, the absolute value of the proton magnetic form factor has been measured by several experiments ^{67, 68)} from the threshold up to 15 GeV², while for the neutron it has been measured only by one experiments ⁶⁹⁾. On the other hand, the electric form factor remains completely unmeasured.

Polarization observables can be used to completely pin down the relative phase of time-like form factors ^{66, 70, 71)}. In fact, the complex phases of the form factors make it possible for the outgoing baryon to be polarized normally to the scattering plane without polarization in the initial state. This polarization is given by ^{66, 71)}

$$P_y = \frac{\sin 2\theta}{D\tau} \Im(G_E^* G_M) = \frac{\sin 2\theta}{D\tau} |G_E| |G_M| \sin \delta_{ME} \quad (4.7)$$

It is directly proportional to the phase difference between the two form factors and, due to the presence of the factor $\sin 2\theta$, takes its maximum value at 45° and 135° and vanishes at 90° .

Different models have been developed to calculate the outgoing proton polarization, based on different extrapolation in the time-like region of space-like fits (for a review see ⁷¹⁾). The predicted polarization is substantial and has a distinct s -dependence which strongly discriminates between the models, as shown in Fig. 4.6. No experimental measurement of polarization observables have been done so far, thus leaving the form factor phases completely unknown.

As the minimum beam energy required is ≈ 1 GeV, the complete determination (moduli and relative phase) of the nucleon form factors can be obtained in the high energy upgrade of DAΦNE (Sec.4.2.2). Total $e^+e^- \rightarrow N\bar{N}$ cross section as well as the normal polarization of the outgoing baryon have to be measured. A high intensity beam is necessary in order to measure cross sections of the order of 1 nb. The extraction of $|G_M|$ and $|G_E|$ requires a large acceptance

detector in order to carefully measure angular distributions. Both $p\bar{p}$ and $n\bar{n}$ final states must be detected with suitable efficiency and resolution, and the installation of a proton polarimeter for the measurement of δ_{ME} must be possible. Beam polarization is not mandatory, nevertheless, if available, it will help in the extraction of the form factors with smaller systematic uncertainty by measuring the longitudinal (P_z) and sideways (P_x) components of the nucleon polarization, which are proportional to the initial electron polarization.

How to perform this program using the FINUDA detector ⁷²⁾ at the upgraded DAΦNE collider, is discussed in the following. This detector has the advantages to be conceived so to minimize the amount of material crossed by particles, thus reducing the proton detection threshold. For the measurement of $e^+e^- \rightarrow n\bar{n}$ cross section, a suitable cylindrical antineutron converter has to be inserted. It could be placed immediately beyond the OSIM array, 9 cm from the beam: in this way the annihilation charged products emitted towards the outer part of the apparatus can be traced. A good converter material must have high antineutron annihilation cross section, low charged pion absorption, high conversion efficiency for π^0 . The choice of 1.5 cm of carbon seems optimal, because the same material can be used as proton polarimeter as well.

The counting rates described below are computed assuming a beam luminosity of $10^{32} \text{ cm}^{-2} \text{ s}^{-1}$ corresponding to an integrated luminosity of 9 pb^{-1} per day, which is reasonably achievable with electron beams of energy of the order of 1 GeV or more.

4.9.1 Moduli of Form Factors: cross section measurement

The $n\bar{n}$ final state is detected through the identification of the antineutron annihilation star on the converter. Taking into account the detector response, one can estimate ⁷³⁾ a detection efficiency for the annihilation star ranging from 30% at threshold decreasing up to 6% for neutron kinetic energy of 40 MeV and higher.

Assuming an integrated luminosity of 9 pb^{-1} per day and with 60 days of data taking at each fixed beam energy starting from 1 GeV beam energy and using reasonable values of $|G_M|$ taken from the available data ⁶⁷⁾, the projected experimental yield is shown in the two upper plots of the left panel in Fig. 4.7. Full (open) points refer to the assumption $|G_E| = 0$ ($|G_E| = |G_M|$). In this calculation, an angular bin of 15° has been chosen, obtaining a statistical error on each point of the order of 20% or less. By fitting these angular distributions over the FINUDA angular coverage $\theta = 45 - 135^\circ$ with the function

$$f(\theta) = A(1 + \cos^2\theta) + B\sin^2\theta \quad (4.8)$$

it will be possible to extract both neutron form factors with reasonable precision, as shown in the lower left plot of Fig. 4.7 for the case $|G_E| = |G_M|$.

In the case of $p\bar{p}$ final state, one has to identify the emitted proton, having a much higher efficiency as compared to detection of the antiproton annihilation star. Taking into account the amount of material crossed by the outgoing protons (the 1.5 cm of carbon converter included), one can estimate a detection kinetic energy threshold $T \approx 40 \text{ MeV}$, which corresponds to 1 GeV beam energy. At fixed polar angle, one can assume a detection efficiency close to 1 and geometrical azimuthal acceptance of $\epsilon_p \approx 0.85$. The projected data are computed again assuming an integrated luminosity of 9 pb^{-1} per day and with 60 days of data taking at each fixed beam energy, taking the proton magnetic form factor from experimental data and assuming $|G_E| = |G_M|$, as generally done to extract the $|G_M|$ experimental data, or assuming the ratio $|G_E|/|G_M|$ decreases with the total energy s with the same slope as in the space-like region ⁷⁴⁾. By fitting the angular distribution with the Eq. 4.8, one can extract the form factors shown in the upper plot of the right panel in Fig. 4.7. In the whole energy range up to $s = 9 \text{ GeV}^2$, the statistical error on $|G_M|$ is

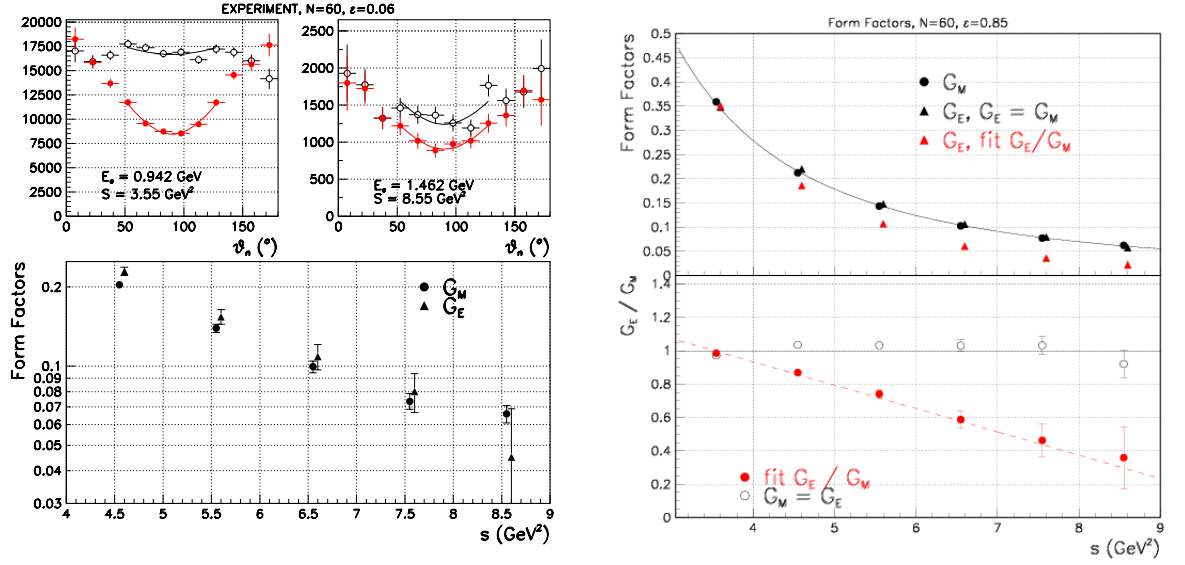


Figure 4.7: Projected data for neutron (left) and proton (right) form factor extraction in 60 days of data taking for each beam energy.

few percent and below 10% on $|G_E|$. In the lower plot of the right panel in Fig. 4.7 the ratio of the electric to magnetic form factor is shown: the data will allow a clear distinction among the different behaviours.

4.9.2 Phase of proton Form Factors: polarization measurement

The proton polarization can be measured through secondary scattering of the emitted proton in a strong interaction process, where the spin-orbit coupling causes an azimuthal asymmetry in the scattering. The scattering cross section is given by

$$\frac{d\sigma}{d\Omega} = \sigma_0(\theta_s, T)[1 + A(\theta_s, T) P_y \cos\phi_s] \quad (4.9)$$

where θ_s and ϕ_s are the angles of the scattered proton with respect to the initial direction and P_y is the polarization on the polarimeter plane. The function $A(\theta_s, T)$ is the analysing power of the material. A commonly used material for polarimeter is carbon, for which the analysing power is well known at least up to 20° for proton kinetic energy from few tenth of MeV up to 1 GeV.

Experimentally, the polarization P_y is obtained by measuring the left-right asymmetry

$$R = \frac{N_R - N_L}{N_R + N_L} = \frac{2}{\pi} \langle A \rangle P_y \quad (4.10)$$

where N_L (N_R) is the number of protons scattered on the left (right) with respect to the y axis on the polarimeter plane. An angular cut at small angles has to be set in order to suppress the background of multiple scattering events, leading to a polarimeter efficiency of the order of few percent ⁷⁵⁾.

In the counting rate estimations, a polarimeter efficiency $\epsilon_{pol} \approx 3\%$ is assumed. Due to this low efficiency, a longer data taking run must be dedicated to the polarization measurement,

however in principle this measurement can be done together with the cross section on proton and neutron measurements. Assuming an integration on all proton production angles between 45° and 135° and averaging the analysing power over scattering angles between 5° and 20° , one can estimate that in one year of data taking at the beam energy of 1.2 GeV the proton polarization can be measured at the level of 30%. For lower or higher photon energies, the relative error will rise by a factor of two, due to either the lower polarization (according to theoretical calculations) or the decrease of the $e^+e^- \rightarrow N\bar{N}$ cross section. It must be stressed that these counting rate estimates have been conservatively performed assuming a luminosity of $1 \times 10^{32} \text{ cm}^{-2}\text{s}^{-1}$.

4.10 Use of the LINAC/SPARXINO beam as a neutron source

The usefulness of low-energy, high average intensity electron beam for production of secondary neutron beams is well known since many years, although in the past it has always suffered from the lack of power-effective accelerating structures. The presence at Frascati of the LINAC of DAΦNE and of the SPARXINO facilities (Sec. 4.1.2), with an intensive R&D program, might open the way to obtain and use a pulsed neutron beam at LNF.

The construction of a simple low-cost neutron source to be built around the existing accelerator (the DAΦNE linac) appears as a rather interesting opportunity in the near future. In a longer timescale, it could be followed by the development of a high intensity neutron facility to be implemented on SPARXINO.

The main applications of a fairly intense, pulsed neutron source are to establish a nuclear data system, to develop instrumentation for future spallation neutron sources, to test and prove models in experimental neutron astrophysics. It allows material science and medical applications and provide some insights in fundamental items (e.g. neutron electric dipole moment and charge-independence of nuclear force).

The neutron yield per kW of beam power has been estimated ⁷⁶⁾ for electron energies above 40 MeV to be $1.21 \times 10^{11} \times Z^{0.66}$ for high-Z material targets. The yield of photoneutron is proportional to the convolution of the (γ, n) cross section and the bremsstrahlung spectrum, which decrease rapidly with photon energies. The resulting curve increases rapidly for constant current up to ~ 25 MeV and more slowly afterwards ⁷⁷⁾. For constant beam power, the neutron yield changes very little with electron energy above 35 MeV. A low-energy, high-current Super Conducting LINAC, as ELBE machine, seems best suited to a neutron production, allowing to obtain a high duty-cycle too. High fluxes have been obtained also at normal conducting, conventional electron LINAC, like Pohang, Oak Ridge, Geel, Dubna.

The first phases of a long term project, which has already started by performing Monte Carlo simulations ⁷⁷⁾, are:

- the design of the neutron radiator, implying the optimization of neutron production material, target geometry and mechanical structure; the choice of an adequate moderator, the evaluation of effects on the neutron-beam and the accurate simulations (EGS, FLUKA, MCNP) of neutron flux, energy and time spectra;
- the design of the neutron beam line: realization of a prototype, testing and implementation of detectors, measurement of standard capture and fission cross sections to determine neutron fluences and energy resolution and the evaluation of different background components.

4.11 Testing T invariance in electromagnetic interactions

Experiments to study the symmetry properties of physical system can set limits on the degree of which the discrete symmetries such as P , CP and CPT are conserved. These limits constitute direct informations about the basic character of the fundamental interactions. Since the discovery of the violation of CP invariance in the decay of the long-lived neutral K meson ⁷⁸⁾, interest has been frequently revived in the search for violation of time-reversal (T) invariance which must occur if CPT holds. The extremely good limits on parity conservation for strong interactions also provide evidence that electromagnetic interactions are invariant under parity (P_{st}), since the limits are much smaller than electromagnetic corrections to the strong interactions. There is also strong evidence that the electromagnetic interaction is invariant under the product $C_{st} \cdot P_{st} \cdot T_{st}$, where the subscript st denote the particular choices of these discrete symmetry operators that are determined by the strong interaction alone. For strong interacting particles no complete theory of electromagnetic interactions exists, and it turns out that there exist no evidence that electromagnetic interactions is, or is not, invariant under C_{st} or T_{st} and this should provide sufficient incentive for further experimental efforts in this direction.

A direct test of T invariance in the electromagnetic interactions by hadrons can be done by measuring the inclusive asymmetry in the scattering of electron/positron beam on polarized proton target in the region of the nucleon resonances. It will be possible to consider any final state or all the final state combined, if they are not identical to the initial state. In fact, this latter case corresponds to the elastic scattering, where the asymmetry is null by current conservation and hermiticity in the single photon exchange approximation.

For example, T -invariance can be tested looking at the reaction $e^\pm + N^\uparrow \rightarrow e^\pm + \Gamma$, where N^\uparrow is the transversely polarized target and Γ is different from N and it can consist of all possible final states (continuum and resonances) of the same total energy and momentum, or of certain resonance states.

No sizable violation of T have been found in previous experiments performed at Cambridge ⁷⁹⁾ and at SLAC ⁸⁰⁾ in the first few resonances region, over a range of Q^2 between 0.4 and 1.0 GeV². A more precise study can be done using a positron and electron beam and looking at the asymmetry:

$$A_{T^{viol}} \equiv \frac{(\sigma_{e-\uparrow} - \sigma_{e-\downarrow}) + (\sigma_{e+\uparrow} - \sigma_{e+\downarrow})}{(\sigma_{e-\uparrow} + \sigma_{e-\downarrow}) + (\sigma_{e+\uparrow} + \sigma_{e+\downarrow})} \quad (4.11)$$

where the \uparrow and \downarrow are two different state of polarization of the target. Eq. (4.11) is free from Final State Interactions (FSI) by definition, because only the scattered lepton is detected. Moreover it's not sensitive to higher-order effects, such as the interference between one photon exchange and two photon exchange amplitudes. This contribution should be small, because it involves an additional power of α (it is proportional to α^3). Furthermore it depends on the sign of the lepton charge and, therefore, it cancels when beams of opposite charge are used ⁸¹⁾.

Using the e^+ source already available for DAΦNE, it is possible to have both beams of the same quality and of the same energy. The desired energy for the proposed measurement will be 3 GeV, in order to cover the first 3 resonances. This energy would need a further upgrade of the DAΦNE linac beyond the proposed SPARXINO one (Sec. 4.1.2).

Taking into account a current of $I=100-200$ nA, that is already available at the DAΦNE injector, the only solution for a transversely polarized target is a solid one. The best target material for polarized protons in terms of polarization, resistance to radiation damage and fraction of polarizable nucleons is the ammonia NH₃ ⁸²⁾. Using a standard electron spectrometer with a

solid angle of several msr, it is possible to increase the precision of the previous measurements by two orders of magnitude after 1 month of data taking for each beam.

In fact, a possible test of T invariance could also be made looking at slightly different reactions, although experimentally less clean:

a) $e^\pm + N^\dagger \rightarrow e^\pm + N + \pi$, where a pion is detected in the final state. The problem of eliminating spurious effects arising from FSI, that may simulate a T violation, has been studied in ⁸³⁾. However, with this channel it's possible to investigate all Generalized Parton Distributions, which give important informations on the internal structure of the nucleon.

b) $e^\pm + N \rightarrow e^\pm + N^*$, with an unpolarized target and one of the outgoing particle transversely polarized; the spin of the final state can be analysed by measuring the spin of the final nucleon in its subsequent decay $N^* \rightarrow N + \pi$.

c) Reactions with e^+e^- annihilation in the final state, like $\pi^- + p \rightarrow n + e^+ + e^-$.

d) $\nu + N \rightarrow \pi + N + l$, for testing T invariance in weak interactions.

4.12 Measurement of 2γ contributions in elastic scattering

As already mentioned in Sec. 4.9, there is strong discrepancy in the measurements of G_E/G_M , the ratio of proton electric and magnetic form factors, obtained from Rosenbluth separation and from polarization transfer techniques at large value of Q^2 ⁸⁴⁾. It has been suggested ⁸⁵⁾ that this discrepancy could be described taking into account two-photon exchange (TPE) contributions ^{85, 86)}. Dedicated experiment is planned at JLab by using the e^- beam ⁸⁷⁾. However, the most straightforward way to measure these effects is through the comparison of the cross sections obtained in the positron-proton and in the electron-proton elastic scattering. In this case, TPE corrections have opposite sign, resulting in a magnification of the effect. The elastic cross sections of electron and positron-proton scattering can be written as $\sigma(e^\pm) = \sigma_{Born}(1 \mp e_e Z \delta_{2\gamma})$, where $\delta_{2\gamma}$ is the TPE correction. The charge asymmetry is defined as:

$$R = \frac{\sigma(e^+)}{\sigma(e^-)} - 1 = -2e_e Z \delta_{2\gamma} \quad (4.12)$$

and it represents a direct and model-independent measurement of the TPE contribution.

Only old measurements from '70s have been done to date ⁸⁸⁾. All of them suffer of low accuracy due to the low intensity of the secondary positron beams obtained impinging the electron beam on a converter.

As for the case mentioned in Sec. 4.11, using the e^+ source already available for DAΦNE, it will be possible to obtain a primary positron beam. The desired energy is again 3 GeV: in fact, in this case, the value $Q^2=6 \text{ GeV}^2$ can be reached, that is the region where the discrepancy of the measurements of G_E/G_M is bigger. Current intensity of 1–3 μA are expected. Using a standard electron spectrometer and a standard unpolarized target, 1 month of data taking for each beam will explore in a satisfactory way the region of interest.

4.13 Experiments with Synchrotron Radiation

DAΦNE is an extremely intense and high performing synchrotron radiation (SR) source from the infrared to the soft X-ray energy range. The high current circulating in the ring, the possibility of collecting a significant emission from the bending magnet by inserting optical elements close

to the accelerator, the presence of several wigglers to push the energy range of the light up to few keV, the low heat load on mirrors and optics elements due to the low critical energy of the machine, are significant features that make DAΦNE a very interesting SR source in a wide and very peculiar energy range. For example, running up to 2 A, a total flux in the vertical plane of about 2×10^{13} ph/s/mrad/0.1%bw, at critical energy, can be easily obtained from bending magnets. By collecting a reasonable amount of horizontal divergence very high fluxes on the sample can be achieved; in many cases they are comparable to those obtained using undulators on third generation sources. Nowadays the potentialities of DAΦNE have been partially explored and, the use of this machine as a competitive SR light source open to a wide national and international multidisciplinary community requires a strong commitment of INFN with an investment both in equipment and human resources.

The SR use requires a long-term schedule and a “stable” and “repetitive” operation conditions with a clear assignment of dedicated time (to be negotiated with other users of DAΦNE) to allow a plan of beam time for the different SR experiments. In SR dedicated shifts it will become also possible to run DAΦNE in low emittance mode, thus increasing the brilliance up to values comparable with those available at low energy third generation synchrotron radiation facilities. In this way both the national and the international SR user community will really experience this facility as an attractive and competitive synchrotron radiation laboratory.

Moreover, any further developments, which need several years to be completed, requires the knowledge of the “fate” of DAΦNE at least in the next 5-10 years. In fact, all planned upgrades are strongly linked to the existing machine parameters and the new planned beam lines needs a clear characterization of the light source.

The possible presence of a X-FEL source at LNF in the coming years implies a scenario where the laboratory may become crucial to develop the necessary know-how and support for the use of next 4th generation FEL sources.

4.13.1 Infrared

Nowadays infrared synchrotron radiation (IRSR) studies are growing at a fast rate and the increasing demand of new beam lines emerges in the most industrialized countries. In the infrared region, a low energy electron beam (e.g., for $E > 0.5$ GeV) does not affect the synchrotron radiation spectral distribution, while intensity is proportional to the current circulating in a storage ring, as a consequence an ideal infrared source to be used for spectroscopy and micro-spectroscopy is a low emittance, stable low energy storage ring with high current (> 1 A) possibly working in topping up mode. Moreover, a low energy storage ring, because of the bigger source size better match an infrared Focal Plane Arrays (FPA) detector, a device that strongly enhances capabilities for infrared spectro-microscopy.

In the last ten years there has been considerable progress in the application of infrared micro spectroscopy to the analysis of human tissues in the context of disease diagnosis. It has been convincingly demonstrated in many studies that infrared spectroscopy can be used to classify tissues as normal or pathological. The central tool used in such studies is the infrared microscope, used for single point spectroscopy, for two-dimensional scanning and, more recently, for imaging with focal plane array detectors.

Impressive results of diagnostic relevance have been achieved using the existing instrumentation but it is necessary not only to coordinate the research effort but also increase the number of the existing synchrotron infrared facilities to promote access to European experts from all countries to identify the technological developments of both instrumentation and detectors to extend diagnostic achievements towards clinical diagnostic methods. The special contribution that synchrotron infrared microscopy can make to this field lies in the up to 1000x higher brilliance (photon flux

per unit source area and unit emission angle) of synchrotron light sources.

Regardless of the light source, lateral resolution in infrared micro spectroscopy is defined by the aperture used in the microscope, down to the diffraction limit of $0.61 \lambda/\text{NA}$ (in the case of a focal plane detector array, the pixel size is the aperture). Fourier transform-infrared micro-spectroscopy using synchrotron radiation may collect data with high resolution on the scale of 10-100 seconds up to area of a few microns opening a new scenario: infrared spectroscopy of entire cells and tissue.

In practice, synchrotron light sources provide good spectral data at a lateral resolution less than the size of a single human cell, whereas with a conventional source an assembly of up to 1000 cells would need to be measured in order to achieve the same data quality. The latter approach would require that the assembly of cells is homogeneous and pure, which is not a realistic requirement for biological materials. Moreover, in this field, IR spectroscopy has important advantages compared to other techniques: the use of non-ionising radiation and the almost negligible damage of the samples under analysis. While in light microscopy image contrast is achieved with stains or a fluorescent material, the use of chemical reagents or stains is not necessary with IR. Image contrast is simply produced from intrinsic IR absorption bands.

Starting from these considerations, a new project for a spectro-microscopy optimised IRSR beam line is strongly suggested at DAΦNE because with its high-brilliance, polarized and broad-band radiation one will be able to perform experiments competitive with those performed at other IRSR facilities from the near-IR up to the far-IR range.

4.13.2 Soft X-Ray

X-ray Absorption Spectroscopy applied to biophysics is a key technique to establish the local electronic structure of metal atoms inside proteins; in this context crystallography is ineffectual. About 30% of proteins coded by genomes are metalloproteins, and $\sim 40\%$ of all enzymes carries a metallic catalytic site. Biologically interesting metals include *Mg*, *Ca* and many members of the first transition series plus *Se*, *Mo*, etc. Such application has emerged slowly and its potential is far from being fully exploited. Nowadays, it is partly limited by experimental difficulties, provided that access to state-of-the-art soft X-ray beam lines is possible. The latter condition is barely satisfied at the SR European sites. X-ray imaging is a well-sound multidisciplinary technique that profits of the brilliance and continuous spectral distribution of SR.

Today, most of the soft X-ray studies for biomedical microscopy/imaging work in the so-called water window: between the K shell edges of *O* and *C*, the absorption of the organic matrix is minimal. The photoelectric cross-section of higher Z atoms, e.g. *Ca* or metals, or contaminants present as traces in the biological systems, provides the natural X-ray image contrast. In the soft X-ray range, contrast absorption microscopy exploits the element specific absorption by a dual imaging of the sample below and above the K (or L) edges of the atomic species under investigation and the image difference enhances its spatial distribution.

New labelling techniques for localizing specific proteins within cellular structures are nowadays functional: natural and/or biotechnological antibodies can bind high Z elements, e.g. silver and gold particles, to the protein of interest in order to locate the sharp absorption increases and identify the regions of protein concentration.

The development of SR sources typically 10 orders of magnitude more brilliant than conventional X-ray tubes has boosted the interest in X-ray optics for microbeam forming: tapered polycapillaries (Kumakhov lenses) are particularly interesting for soft X-ray optics due to their inherently hollow structure (no low energy cut-off), and reduced chromatic aberration (white beam focusing). Polycapillaries are among the most promising systems for increasing 100-1000 times the flux density while concentrating the beam spots below $0.1 \mu\text{m}$.

One of the most interesting development in SR research is related to the combination of micro focusing with spectroscopy: X-ray spectromicroscopy allows performing micro X-Ray Fluorescence (μ -XRF) and micro X-Ray Absorption Spectroscopy (μ -XAS) on non homogeneous or spatially structured materials. μ -XRF exploits the excitation of secondary X-ray fluorescence by scanning the micro-beam over the sample area and provides the 2-D distribution of the atomic elements constituting the material, or the trace elements map. Micro X-ray absorption near edge spectroscopy, μ -XANES, provides complementary information on the electronic state, local structure (and chemical speciation) of the atomic scatterers (in selected sites) by tuning the beam energy across their absorption edges. These techniques are gaining popularity in biomedical research, technological applications (e.g. microelectronics), and materials science. For instance, in geosciences *Mg*, *Al*, *Si* and *S* are among the major constituents of the Earth's crust. Any fine sample analysis by μ -XAS needs to be coupled with an imaging technique, like μ -XRF, capable to firstly identify the regions of interest by mapping the elemental distributions. An interesting development of performing time resolved X-ray spectroscopy is given by quick Extended X-ray Absorption Fine Structure (quick EXAFS): here the energy scan time is reduced moving continuously the monochromator and recording the data on the fly. In this case, the use of an intense photon flux from a spectrally continuous X-ray source is mandatory: in this sense, the SR from insertion devices on high circulating current machines, like the wiggler source and beam line at DAΦNE, is appropriate in the soft X-ray range. The use of fluorescence, or secondary electron detection is suitable for studying reactions at a minute scale range also in dilute samples: in particular, organic systems can be analysed by quick EXAFS during their redox reactions, furthermore reducing their irradiation damaging. X-ray Magnetic Circular (Linear) Dicroism, XMCD (XMLD), coupled to XAS is the workhorse technique for studying the physics of magnetic systems. It is the only element-specific spectroscopy that can distinguish between the spin and orbital part of the magnetic moment. Important edges covered by electric dipole transitions into empty magnetic states are present in the soft X-ray region, namely the transition metal $L_{2,3}$ edges, the rare earth $M_{4,5}$ edges and actinide $N_{4,5}$ edges. Recently, XMCD and XMLD extend also into other areas, such as magneto-electronics, organo-metallic chemistry, earth and environmental sciences and biophysics (e.g. metalloproteins).

4.13.3 VUV Beam Lines

DAΦNE is an extremely intense and high performing SR source in the energy range between 5 eV up to 1000 eV. Such characteristics will be exploited at best by performing a number of specific spectroscopy experiments which require high flux but not an extreme high energy resolution and brilliance. Along with such "machine specific" experiment a wide variety of other techniques, which will benefit from, but do not necessarily require, very high fluxes, can be performed. Since no single beam line can be efficiently used in the energy range of interest, two beam lines are proposed; the first one (BL1) is suitable for the lower energy range, from 5 eV up to 150 eV, while the second one (BL2) will cover the region from 60 eV to 1000 eV. BL1 will be mainly dedicated to the study of band dispersion in solids, to angle-resolved resonant photoemission and to shallow core levels photoemission. It will operate between 5 and 150 eV using both a normal incidence monochromator and a plane grating monochromator. BL2 will be used for X-ray absorption spectroscopy (XANES and SEXAFS), micro-spectroscopy, photoelectron diffraction and resonant photoemission, using a plane grating monochromator in the photon energy range 60-1000 eV. A technical and detailed proposal is available for evaluation. The scientific motivations can be summarized as follows:

- SR spectroscopy has a large impact on the study of the properties of advanced materials such as semiconductor interfaces and heterostructures, magnetic thin films, biological samples, superconductors and clusters. This type of applications is of considerable importance and interest; funding of this laboratory will catalyse at LNF high-level research in materials

science of interest for physics, chemistry, biology and technology.

- The branch-lines are designed for spectroscopy (photoemission, core absorption and emission); this field corresponds to the interests of numerous potential users in Universities and research centres in Italy and abroad. The branch-line energy range (5 to 1000 eV) is ideally matched to the emission of DAΦNE bending magnets (whose critical energy is 208 eV).
- The access to a spectro-microscopy, which needs a high flux photon source, will allow to use the aforementioned techniques with sub-micron spatial resolution, opening unprecedented capabilities to study nano-structures, nano-technology as well as biology on its close to natural scale.
- Interdisciplinary research, R&D, and technologically oriented studies of interest to INFN, shows a growing attention to experiments where the use of a well equipped ultraviolet synchrotron radiation center will be beneficial. Soft X-ray optics to be used in astrophysics experiments, low photon energy detectors also used in high energy physics (like RICH), high flux and emittance electron sources, etc. need to be calibrated just in the energy range that will be available in this laboratory. Proposals that involve the construction of large VUV detectors to be used in space missions could also benefit from the availability of such a facility because VUV beam line offers several advantages over traditional sources. In fact VUV beam line have a continuum emission covering a very broad energy range with a flux that may be precisely calculated, and a well defined time structure in the ps or even in the ns scales. Several INFN sections are interested in such activity. Moreover, accelerator vacuum science needs input from material science in order to correctly predict dynamical vacuum behaviour relevant for the operation of machines like the LHC or the Free Electron Lasers.
- The plans of building an X-ray FEL near Frascati will require the use of SR to face some of the most complex technological challenges and an effort to develop and characterize optics and fast detectors to be adapted to the unprecedented characteristic of a FEL. A test facility could represent a key issue to a successful scientific exploitation of such new light source. In fact the SPARX/SPARXINO (Sec. 4.1.2 projects require the R&D of detectors and optics that can be carried out using the high photon flux in the 5-1000 eV range available at DAΦNE. For the X-FEL projects, the presence of an active SR laboratory at the LNF would represent a very effective way to develop and implement the necessary know-how to get full advantage of the 4th generation FEL sources.

4.14 Resonant detectors for gravitational waves

A resonant detector for gravitational waves (GW) consists of a large cylindrical mass, suspended around its middle circumference and hanging in a vacuum chamber. By considering only the dominant lower-order resonant mode, a bar of mass M can be schematized as two point bodies of mass $M/2$ each, joined by a spring. Such mechanical resonator will be driven by a GW as long as it has spectral components at the resonant frequency of the mass-spring system. If the detector is a high- Q resonator it will continue to vibrate long after the GW has passed and the oscillations are monitored by a suitable transducer attached to one of the end faces of the bar. Since a multi-spring mass resonator can detect not only the amplitude but also the propagation direction of the waves, recently the idea to construct spherical antennas has been seriously considered. By their nature this kind of detectors are narrow-band devices, with good sensitivity in a bandwidth of a few Hz around their fundamental resonant frequency (typically of the order of 1 kHz). The fundamental limitation to their sensitivity comes from the thermal motion of the atoms in the bar: it produces an average

noise level against which one search the GW signal. For this reason, in the modern resonant detectors the bar and the transducer operate at a temperature of 4 K or less. Four resonant bar detectors distributed worldwide are presently in operation: ALLEGRO at Louisiana State University, AURIGA at INFN Legnaro Laboratories, EXPLORER at CERN, and NAUTILUS at LNF. All these instruments consist of a bar made of Al 5056, 3 m long (so that the resonance frequency is around 900 Hz), and involve the use of cryogenic and superconducting technique for noise reduction. Their main features and performances are summarized in Table 4.2 (for details see ⁸⁹⁾ and references therein). LNF is strongly involved in the running and development of EXPLORER and NAUTILUS. These detectors are operated by the same collaboration (the ROG group) and are the only detectors equipped with a cosmic-ray veto system.

Detector	T (°K)	f (Hz)	Δf (Hz)	$\sqrt{S_h}$ (Hz ^{-1/2})
ALLEGRO	4.0	915	50	1.2×10^{-21}
AURIGA	4.5	870,930	120	1.5×10^{-21}
EXPLORER	2.6	905,921	35	1.5×10^{-21}
NAUTILUS	3.5	935	30	3×10^{-21}

Table 4.2: *Main characteristics of the resonant-mass detectors presently in operation. S_h is the minimum noise power spectral density. The bandwidth Δf is defined as the frequency range where $\sqrt{S_h} \leq 10^{-20}$ Hz^{-1/2}. Notice that AURIGA performances refer to a non stationary operation condition.*

At present, small (about 60 cm diameter) spherical detectors are also under development: at Leiden University in Holland (MiniGRAIL) and at São José dos Campos INPE in Brazil ⁸⁹⁾. These detectors are expected to cover a frequency window of about 200 Hz centered around 3 kHz with a sensitivity level to GW bursts better than 10^{-20} . Beside the data taking, resonant-mass detector community is devoting a relevant effort in enhancing the performances of their devices. The improvements are mainly focused on: i) increasing the duty cycle and lowering the background noise by upgrading the cryogenics and acting on the vibration attenuation system, and ii) increasing the sensitivity and the useful bandwidth by improving the coupling bar-transducer and the noise performances of the SQUID amplifier. The near future goal is to get a duty cycle higher than 90 %, to increase the sensitivity by about a factor 10, and to enlarge the useful bandwidth above 100 Hz.

The analysis of the data collected by NAUTILUS and EXPLORER during the 2001 run produced a very interesting result ⁹⁰⁾: the sidereal time distribution of the coincidence events shows a small excess around the sidereal hour 4, when the detectors are favourably oriented with respect to the galactic disc. The analysis of the 2003 run data is still in progress, but, independently by its result (confirmation or disproof of the coincidence excess), it appears very important to maintain in operation these detectors in the near future. In fact, as demonstrated in ⁹¹⁾, a search for GW burts based on the coincidence between LIGO and VIRGO (Sec. 5.6) has a very poor sky coverage. This means that NAUTILUS and EXPLORER (and, of course, AURIGA), even if in a restricted band around 1 kHz, could be the only detectors enabling to perform sensible coincidence studies with initial VIRGO. These studies will also be important for improving the present upper limit in the amplitude of the stochastic background.

References

1. L. Serafini, M. Ferrario, "Velocity Bunching in PhotoInjectors", AIP CP 581, 2001, pg.87
2. D. Alesini *et al.*, "Design Study For Advanced Acceleration Experiments And Monochromatic X-Ray Production at SPARC", Proceedings of the 9th EPAC, July 2004, Lucerne.
3. U. Bottigli *et al.*, "Monochromatic, quasi-monochromatic and polychromatic sources in mam-mography and new perspectives", to be published.
4. SPARC Project Team, Sparc Injector TDR, <http://www.lnf.infn.it/acceleratori/sparc/>
5. A. Bacci, M. Migliorati, L. Palumbo, B. Spataro, "An X-Band structure for a longitudinal emit-tance correction at Sparc", LNF-03/008(R); D. Alesini, A. Bacci, M. Migliorati, A. Mostacci, L. Palumbo, B. Spataro, "Studies on a Bi-Periodic X-Band Structure for SPARC", LNF-03/013(R).
6. A. Renieri *et al.*, "Status Report on SPARC Project", Proceedings of FEL-04, Trieste, Sept. 2004
7. R. Boni, "Feasibility of the DAΦNE-Linac energy doubling", Proceedings of the "ICFA Mini-workshop - Working Group on High Luminosity e^+e^- Colliders", Sept. 2003, Alghero (SS), Italy.
8. R. Cameron *et al.*, Phys. Rev. D **47** (1993) 3707.
9. D. Bakalov *et al.*, Quantum Semiclass. Opt. **10** (1998) 239.
10. D. Bakalov *et al.*, Hyperfine Interact. **114** (1998) 103.
11. L. Maiani, R. Petronzio and E. Zavattini, Phys. Lett. B **175** (1986) 359.
12. G. Benedetti *et al.*, *Proceeding of the PAC03*, May 2003, Portland (US).
13. C. Ligi, R. Ricci, Preliminary Feasibility Study for Energy Ramping Dipoles for DAFNE2, Pro-ceedings of the "ICFA Mini-workshop - Working Group on High Luminosity e^+e^- Colliders", 10-13 Sept. 2003, Alghero (SS), Italy
14. D. Alesini *et al.*, DAFNE Technical Note G-63/5. 17 July 2005, Lucerne.
15. C. Biscari *et al.*, *Proceeding of the 9th EPAC*, 5-9 Jul. 2004, Lucerne.
16. A. Gallo *et al.*, physics/0404020.
17. A. Gallo *et al.*, LNF Internal Note LNF-05/4(R).
18. R. Adler *et al.*, Phys. Lett. B **407** (1997) 193.
19. A. Angelopoulos *et al.*, Eur. Phys. Journ. C **5** (1998) 389.
20. Y. Zou *et al.*, Phys. Lett. B **369** (1996) 362.
21. S. Eidelman *et al.*, "Review of Particle Physics", Phys. Lett. B **592** (2004) 626.
22. A. Angelopoulos *et al.*, Phys. Lett. B **444** (1998) 38.
23. A. Alavi-Harati *et al.*, Phys. Rev. Lett. **88** (2002) 181601.

24. NA48 Collaboration, Phys. Lett. B **576** (2003) 43.
25. C. Buchanan *et al.*, Phys. Rev. D **45** (1992) 4088.
26. P. Depommier *et al.*, <http://www-ps.kek.jp/jhf-np/LOIlist/pdf/L16.pdf>; Y. Asano *et al.*, <http://www-ps.kek.jp/jhf-np/LOIlist/pdf/L19.pdf>; S. Shimizu *et al.*, <http://www-ps.kek.jp/jhf-np/LOIlist/pdf/L20.pdf>
27. FOCUS Collaboration, Phys. Lett. B **545** (2002) 50.
28. S. Eidelman *et al.*, “Review of Particle Physics”, Phys. Lett. B **592** (2004) 576.
29. P.L. Frabetti *et al.*, Phys. Lett. B **578** (2004) 290.
30. DM2 Collaboration, “The Pi, K, Proton Electromagnetic Form-Factors And New Related Dm2 Results” **LAL-88-58**, presented at the Workshop on Nucleon Structure, Frascati, Italy, Oct. 1988.
31. FENICE Collaboration, Phys. Lett. B **365** (1996) 427.
32. S. Bianco *et al.*, Riv. Nuovo Cim. **26N7** (2003) 1, hep-ex/0309021.
33. S. Malvezzi, AIP Conf. Proc. **549** (2002) 569.
34. G. Burdman *et al.*, Phys. Rev. D **66** (2002) 014009.
35. C.T.H. Daviet *et al.*, Phys. Rev. Lett. **92** (2004) 022001.
36. X.G. He, G. Valencia and Y. Wang, Phys. Rev. D **70** (2004) 113011.
37. BABAR Collaboration, hep-ex/0502032
38. A.Hocker, hep-ph/0410081 and references therein.
39. H. Tamura *et al.*, Nucl. Phys. A **639** (1998) 83c.
40. H. Tamura, *et al.*, Nucl. Phys. A **691** (2001) 86c.
41. K. Tanida *et al.*, Phys. Rev. Lett. **86** (2001) 1982.
42. R. H. Dalitz and A. Gal, Ann. Phys. (N.Y.) **116** (1978) 167; R. H. Dalitz and A. Gal, J. Phys. G **4** (1978) 889.
43. T. Motoba *et al.*, Prog. Theor. Phys. **70** (1983) 189.
44. D. J. Millener *et al.*, Phys. Rev. C **31** (1995) 499.
45. L. Majling, Nucl. Phys. A **585** (1995) 211c.
46. Y. Miura *et al.*, Acta Phys. Pol. B **35** (2004) 1019.
47. P.Gianotti, proceeding of the conference “DAΦNE 2004: Physics at meson factories”, to be published on Frascati Physics Series.
48. J. Gerl *et al.*, “VEGA: a proposal for Versatile and efficient Gamma-detectors”, GSI Report (1998) 1.
49. C. Biscari, proceeding of the “ICFA Mini-workshop - Working Group on High Luminosity e^+e^- Colliders”, Sept. 2003, Alghero (SS), Italy

50. A. Gallo, proceeding of the conference “DAΦNE 2004: Physics at meson factories”, to be published on Frascati Physics Series.
51. J-PARC Strangeness Nuclear Physics Group, Letter of Intent for “New Generation Spectroscopy of Hadron Many-Body Systems with Strangeness $S = -2$ and -1 ” (2002) 1.
52. The Joint Project team of JAERI and KEK, Proposal for High-Intensity Proton Accelerator, KEK Report 99-4 (1999) 1.
53. S. Deser *et al.*, Phys. Rev. **96** (1954) 774; T.L. Truemann, Nucl. Phys. **26** (1961) 57; A. Deloff, Phys. Rev. C **13** (1976) 730.
54. U.-G. Meissner, U. Raha and A. Rusetsky, Eur. Phys. Journ. C **35** (2004) 349.
55. DEAR Collaboration, Phys. Rev. Lett. (2005) in print.
56. J. Zmeskal, SIDDHARTA Note-IR-2, 25 August, 2003; C. Curceanu (Petrascu), SIDDHARTA Note-IR-3, 25 August, 2003.
57. SIDDHARTA Collaboration, SIDDHARTA Note-IR-1, 25 August, 2003.
58. G. Bakenstoss *et al.*, Nucl. Phys. A **232** (1974) 519; C.J. Batty *et al.*, Nucl. Phys. A **326** (1979) 455.
59. R. Seki, Phys. Rev. C **5** (1972) 1196.
60. Y. Akaishi, Proceedings of the *DAΦNE 2004: Physics at meson factories* Conference, Frascati, 7-11 June 2004, to appear.
61. M. Iwasaki, seminar at LNGS 16 December 2004, C.J. Batty, Nucl. Phys. A **508** (1990) .
62. T. Suzuki *et al.* Phys. Lett. B **597** (2004) 263.
63. S. Eidelman *et al.*, “Review of Particle Physics”, Phys. Lett. B **592** (2004) 605.
64. DEAR Collaboration, Phys. Lett. B **535** (2002) 52.
65. DEAR Collaboration, Phys. Lett. B **593** (2004) 48.
66. A.Z. Dubnickova, S. Dubnicka, P.M. Rekalov, Nuovo Cimento **109** (1966) 241.
67. M. Ambrogiani *et al.*, Phys. Rev. D **60** (1999) 032002 and references therein.
68. M. Andreotti *et al.*, Phys. Lett. B **559** (2003) 20.
69. A. Antonelli *et al.*, Phys. Lett. B **313** (1993) 283, Nucl. Phys. B **517** (1998) 3.
70. S. Rock, *Proc. of the $e^+ e^-$ Physics at the intermediate Energies Conference*, edited by D. Bettoni, eConf **C010430**, W14 (2001), hep-ph/0108106.
71. S.J. Brodsky *et al.*, Phys. Rev. D **69** (2004) 054022; H.W. Hammer and U.G. Meissner, hep-ph/0312081.
72. FINUDA Collaboration, *Finuda, a detector for Nuclear Physics at DAΦNE*, LNF Preprint LNF-93/021(IR), 1993.
73. A. Filippi, *Proc. of Workshop on e^+e^- in the 1-2 GeV range: Physics and Accelerator Prospects*, 10-13 Sept. 2003, Alghero, Italy.

74. M.K. Jones *et al.*, Phys. Rev. Lett. **84** (2000) 1398; O. Gayou *et al.*, Phys. Rev. Lett. **88** (2002) 092301.
75. T. Pospischil *et al.*, Nucl. Instr. Meth. A **483** (2002) 713.
76. W.P. Swanson, SLAC-PUB-2042, 1987.
77. S. Bartalucci, LNF-02/011(IR), 2002.
78. J.H. Christenson, J.W. Cronin, V.L. Fitch, and R. Turlay, Phys. Rev. Lett. **13** (1964) 138.
79. J.R. Chen *et al.*, Phys. Rev. Lett. **21** (1968) 1279; J.A. Appel *et al.*, Phys. Rev. D **1** (1970) 1285.
80. S. Rock *et al.*, Phys. Rev. Lett. **24** (1970) 748.
81. R.N. Cahn and Y.S. Tsai, Phys. Rev. D **2** (1970) 870.
82. C.D. Keith *et al.*, Nucl. Instr. Meth. A **501** (2003) 327.
83. F. Cannata, R. Leonardi and F. Strocchi, Phys. Rev. D **1** (1970) 191.
84. J. Arrington, Phys. Rev. C **68** (2003) 034325.
85. P.A.M. Guignon and M. Vanderhagen, Phys. Rev. Lett. **91** (2003) 142303.
86. P. Blunden, W. Melnitchouk and J. Tion, Phys. Rev. Lett. **91** (2003) 142304; Y.C. Chen *et al.*, hep-ph/0403058.
87. R. Gilman, L. Pentchev, C. Pendrisat, R. Suleiman *et al.*, Jefferson Lab. experiment E04-019.
88. J. Mar *et al.*, Phys. Rev. Lett. **21** (1968) 482; R.L. Anderson *et al.*, Phys. Rev. Lett. **17** (1966) 407 and Phys. Rev. **166** (1968) 1336; B. Bouquet *et al.*, Phys. Lett. B **26** (1968) 178; W. Bartel *et al.*, Phys. Lett. B **25** (1967) 242; A. Browman *et al.*, Phys. Rev. **139** (1965) B1079; D. Yount and J. Pine, Phys. Rev. **128** (1962) 1842.
89. V. Fafone, Class. Quantum Grav. **21** (2004) S377.
90. P. Astone *et al.*, Class. Quantum Grav. **19** (2002) 5449.
91. N. Arnoud *et al.*, Phys. Rev. D **65** (2002) 042004.

Chapter 5

Participation to Offsite Activities

The LNF is involved (see Chap. 3) in the major scientific programs of the international laboratories (CERN, DESY, Fermilab, JLab, LNGS and SLAC), contributing to the design and the operation of the state-of-art devices needed to the research in different fields of fundamental physics. In the following, the most natural extension of the LNF projects in the near and mid-term future is presented. Each section is devoted to a particular field of interest, i.e. Accelerators (Sec. 5.1), HEP (Sec. 5.2), Nuclear Physics (Sec. 5.3), Astroparticle (Sec. 5.4), Neutrino Physics (Sec. 5.5), Detection of the Gravitational Waves (Sec. 5.6) and Synchrotron Radiation experiments (Sec. 5.7).

5.1 Accelerators

The future activities of LNF Accelerator Division (AD) will be mainly related to the Linear Collider accelerator physics, with the CLIC and TESLA collaborations and the European projects ELAN, PHIN and EUROTeV, with an involvement in the X-FEL project (EUROFEL). These projects have in principle programs which extend in the next decade at least. Their feasibility will depend on the decision of the governments and international communities such as high energy particle physics and synchrotron light users. In any case the AD has both the expertise and a very good involvement in the international collaborations to participate to these enterprises. Of course the amount of involvement will depend on the weight of the on site activities and on the resources available at LNF. In the following is a brief description of the LNF AD involvement.

5.1.1 Linear Collider

CARE (Coordinate Accelerator Research in Europe) is a project financed by the 6th EU Framework Programme (FP6); it will last 5 years starting from January 2004. Its objective is structuring and coordinating European research on accelerators for particle physics and it is focused on three main items: neutrino beams, e^+e^- colliders and high intensity proton beams. Most European particle physics laboratories and many universities from 12 different countries are participating with about 50 scientists. CARE includes 3 “Network Activities” (NA) and 4 “Joint Research Activities” (JRA). The NA will provide a unique European Forum to develop a coordinated program for accelerator R&D and experimental studies in existing machines relevant for the selected theme, assemble a community capable of sustaining these realizations, foster the participation of new

groups in the European countries and enhance the present synergy to avoid duplication of work. In particular:

- BENE (Beams for European Neutrino Experiments) has as objective to establish a roadmap to upgrade the current CNGS (neutrino beam to Gran Sasso) facility and to propose the next major neutrino facilities. Three possibilities are presently considered: an intense muon-neutrino beam (Superbeam), a Neutrino Factory, a Beta-Beam.
- HEHIHB will focus on High Energy High Intensity Hadron Beams.
- ELAN (Electron Linear Accelerator Network) has the following objectives:
 - to coordinate European R&D on electron linear accelerators and colliders;
 - to optimize present technologies (TTF, TESLA);
 - to define a roadmap for multi-TeV colliders (CTF, CLIC).

The JRA will provide powerful means for carrying specific accelerator R&D activities to develop new components or systems required for improving the existing HEP infrastructures or necessary for new infrastructures. JRA are divided into 4 subgroups:

- SCRF (R&D on Superconducting Radio Frequency) will further develop superconducting technologies toward higher gradient and optimized RF systems to be used on TTF and new linear accelerators and on X-FEL.
- PHIN (Charge production with electron Photo-Injectors) will develop new electron photo-injectors for high charge and high brightness beams for linear colliders and related state-of-the-art technologies to be used on CTF and multi-TeV linear accelerators, with some application at X-FEL.
- HIPPI (High Intensity Proton Pulsed Injector) will study system components for realizing high-intensity proton pulsed injectors, to improve the proton flux for different facilities at CERN (fixed target experiments, neutrino beams for CNGS experiment, ISOLDE, LHC), CCLRC-RAL (ISIS, potential for neutrino beams), GSI (heavy ion synchrotron SIS).
- NED (Next European Dipole) will promote, in collaboration with the European industry, the development of enhanced performance magnets, allowing to upgrade the LHC toward higher luminosity and possibly higher energy on the long term.

LNF has the responsibility of the coordination of PHIN JRA, dedicated to the production of long trains of high charge bunches, development of photo-cathodes, laser systems, RF guns, and alternative e- source. The AD is also involved in the work package on beam diagnostics of SCRF and in all the three Network Activities.

EUROTeV is the Design Study for a 1 TeV Global Linear Collider. Submitted to the EU on March 2004 it has been approved by the reviewers in July. It has started in January 2005 and will last three years. This collaboration aims at being the nucleus of the European section of a Global Design Team. It is dedicated to those subjects requiring R&D to improve the performance or reduce the costs for the realization of a linear collider. It is subdivided into eight work packages: Beam Delivery System, Damping Ring, Polarized Positron Source, Diagnostics, Integrated Luminosity Performance Studies, Metrology and Stabilization, Global Accelerator Network (GAN) Multipurpose Virtual Laboratory. There are 23 participating laboratories from 6 countries. The LNF AD has the responsibility of coordinating the effort on the Damping Ring work-package, dedicated to study items crucial to achieve the extremely small emittances required. LNF AD is also involved in the Global Accelerator Network.

5.1.2 EUROFEL

EUROFEL is a Design Study to prepare the construction of several new infrastructures in Europe which will provide intense, short pulse continuously tunable laser radiation in the VUV and X-ray regimes, exceeding both modern synchrotron radiation and laser plasma sources by several orders of magnitude in peak and average brilliance. Submitted to the EU in March, it has been approved by the reviewers in July 2004.

The objectives of the Design Study sub-groups in which INFN-LNF is involved are described hereafter:

- *Photo-Guns & Injectors*: for the improvement and optimization of high brightness electron sources for the new European infrastructures. The project is focused on the design, construction and testing of new components, subsystems, materials or techniques for the production, manipulation, diagnostics and control of low emittance and high current beams, up to the early stage of acceleration. The new components, devices and techniques will be tested at the test facilities PITZ (Zeuthen) and SPARC (Frascati), and in the existing major European laboratories. This sub-group is coordinated by the SPARC group leader.
- *Beam Dynamics*: for the study of the critical beam dynamics effects that impact on the transport of high quality electron beams for FELs, specifically the case of small emittance (~ 1 mm-mrad) combined with short bunch length (< 1 ps) and high charge (~ 1 nC).
- *Synchronization*: for synchronisation issues of the FEL machines, where many devices need to operate synchronous on sub-picosecond timescales, maintaining synchronization for many hours of operation.
- *Seeding and harmonic generation*: to find answers and test techniques essential for the design of the seeding and high-gain harmonic-generation (HG) mechanisms of the new VUV-X-ray FELs in Europe, aimed to increasing the stability, coherence and wavelength region of these FELs. Both theoretical investigations and tests with prototypes of new hardware will be performed. Special attention will be made to make use of available infrastructure, like SPARC, in these tests.
- *Superconducting CW and near-CW linacs*: for the proposed CW linac-based light sources, a number of critical aspects of the superconducting linac must be resolved for these infrastructures to be technically realizable and to reduce the required investment and operating cost. They include the development of superconducting RF photoguns/injectors that are able to (a) operate CW and (b) produce low-emittance beams at high bunch charge and average current needed for FEL light generation in the VUV and X-ray range.

Experimental Activities

5.2 High Energy Physics

The participation to short and medium-term activities of the experiments at CERN, Fermilab and SLAC can be mostly seen as the logical continuation of the programs already launched that have been presented in Sec. 2.8. In the following few considerations on the ongoing project are reported.

5.2.1 Physics at Tevatron

Tevatron, at Fermilab, will continue to investigate the high-energy frontier till the end of 2008 when the LHC at CERN is expected to be operational. In the meantime at Fermilab there are plans to complete the upgrade of the accelerator complex by the end of year 2007 in order to increase machine luminosity, and to acquire new computational resources to support analysis of the larger volume of data. The physics issues to be addressed by CDF-II include searches for the Higgs boson, supersymmetry, B-meson studies, and precision measurements of the top quark and the W boson properties. During the previous Tevatron run (RUN-I), of the order of 100 top quarks was studied. The new run (RUN-II) will produce an order of magnitude more top quarks allowing precise measurements of its mass and couplings.

The involvement of the LNF in CDF-II would be kept for the few remaining years of Tevatron running with a renewed participation on data analysis. During RUN-I, the LNF group contributed mainly on the measurement of the top cross-section ¹⁾ and in the study of anomalies/excess observed in the “lepton + 2,3 Jets” events ²⁾.

Relevant contributions to the analysis of the new data would be favorably considered also because CDF-II could represent a sort of training for the LHC era for the people involved in both the experiments, CDF and ATLAS, and for the students that could acquire a fruitful experience in the usage of the new software technologies and in the analyses of the data at proton colliders.

5.2.2 B physics at PEP-II

The huge amount of unique data delivered to BABAR (over 100 fb^{-1} in 2004), will allow the completion of the vast physics program of the experiment ³⁾. Data collected so far are consistent with the CP violation description provided by the SM, although there are possible indications of new phenomena (Sec. 3.2.3).

The U.S. HEP program assigns high priority to the operations, upgrades and infrastructures for the B-factory at SLAC. Support for B-factory is expected through 2008 and includes “...the completion of the upgrade to the accelerator complex and the BABAR detector to provide more data; additional computational resources to support analysis of the larger volume of data; and, increased infrastructure spending to improve reliability. Funding for SLAC operations includes support from the Basic Energy Sciences (BES) program for the Linac Coherent Light Source (LCLS) project, marking the beginning of the transition from HEP to BES as B-factory operations are terminated by FY2008 at the latest ” (from FY2006 Congressional Budget - Science/High Energy Physics, p.274).

BABAR data taking will continue through 2008 and the PEP-II luminosity will increase from the present $\sim 0.9 \times 10^{34} \text{ cm}^{-2} \text{ s}^{-1}$ to $2\text{-}3 \times 10^{34} \text{ cm}^{-2} \text{ s}^{-1}$ in year 2007.

The LNF participation to BABAR (Sec. 2.8.2), and especially to the data analysis activities would be compelling in the next five years, giving the opportunity to reach remarkable results in flavor physics, including improved measurements of the α and γ angles of the unitarity triangle, of the $|V_{ub}|$ parameter, new searches for physics beyond SM and for exotic states like pentaquarks or new (double) charm states.

5.2.3 The LHC program

Major efforts to construct, test, commission the LHC detectors began in 2002 and a significant ramp-up of these activities will continue through 2006 in anticipation of the accelerator turn-on in 2007.

The LHC Software and Computing program will deserve special work in order to develop a computing system to process, store and distribute for the analyses the huge amount of anticipated data.

The physics goals of the LHC have been reported in Sec. 3.2.1, 3.2.2, 3.2.3 and include searches for the Higgs boson, supersymmetric particles, the exploration of the top quark structure, among other topics. Novel sensitivity in the study of B-mesons to improve and complement the knowledge provided by the experiments at the asymmetric B-factories is expected since the beginning of the LHC operation.

The ATLAS-LNF group, once the installation and commissioning of the muon detector will be completed in 2007, will focus the efforts on data reconstruction and analysis. The acquisition of the new software technologies, like in the case of CDF-II, is crucial. This topic could represent the opportunity to initiate in the LNF a new kind of collaboration among people belonging to different experiments interested to contribute to the computing program. In this context, the participation to the Atlas GRID with the realization of a TIER-2 node in close collaboration with the LNF Computing center, constitutes a working example for the next generation of experiments of the whole LNF high-energy physics community.

Another field of interest of the ATLAS group is the handling of the data-flow and the event filtering. This issue will become particularly relevant in ATLAS when, in 2010-2011, the LHC will reach its design luminosity, crossing at a frequency of 40 MHz and producing an average of 23 inelastic $p-p$ interactions per crossing. The Trigger-DAQ system⁴⁾ at that point must be capable of a total bandwidth of 160 Mb/s: such a tremendous throughput must be reduced by means of further two trigger levels to the final expected rate of 100 Hz on disk. The last, High-Level-Trigger is composed by a level-2 trigger followed by an Event Filter where a reconstruction as similar as possible to the offline one will be applied. The involvement on this multi-sided activity, leading to the growing of yet well experienced skills in a field of interest for the experiment, could be compelling for the group in the mid-term future.

Road map in the next years is well marked also for the other experiment at CERN, LHCb. The group has strong construction, installation and commissioning responsibilities on the muon detector system covering the time scale until 2008. After this phase, the efforts would be turned on the side of the software development for Monte Carlo simulations and data analysis. The common computing strategy of the experiments at the LHC is coordinated by the LHC Computing Grid (LCG). LHCb intends to utilize many aspects of LCG and will have in addition experiment-specific components. Before the processing of real physics data can begin, simulations campaigns, or Data Challenges, have been planned to test the adopted computing model, to verify the related software and to generate Monte Carlo events for detector and High-Level-Trigger studies and physics analyses. In year 2004 the Data Challenge result has been the production of $\mathcal{O}(10^8)$ events, half of which generated with LCG resources, mostly at CERN, UK and Italy (CNAF). On this respect the opportunity to realize in the mid-term future an LCG center at the LNF would deserve some discussion in relation with the INFN commitment on LCG.

Besides the ongoing projects summarized above there are new experiments deserving more attention and discussion in a medium and long-term perspective.

5.2.4 Kaon physics at hadron machines

The LNF research activities have been focused on Kaon physics by the experiments at DAΦNE. The remarkable expertise and the strong interest in this field could suggest in a natural way

the participation to the new experiments at the hadron machines (Sec. 3.2.3) devoted to the measurement of the $K \rightarrow \pi \nu \nu$ decays, especially if the proposal for performing the measurement with K^+ beams at the CERN SPS in 2011 ⁵⁾ will be approved.

The goal of the project is the collection of about 100 $K^+ \rightarrow \pi^+ \nu \nu$ events with a signal:background ratio of 10:1 in two years of data taking.

Challenging aspects of the NA48-3 experiment include particle tracking at 1 GHz total rate, high-purity kaon identification, hermetic photon vetoes for π^0 rejection in excess of 10^7 , muon rejection in excess of 10^5 , minimization of accidental backgrounds. State-of-art detectors are needed to fulfil the experimental requirements.

The potentially overlapping schedules of new projects at DAΦNE would be discussed considering also the advantage of a more strict collaboration between the CERN and the LNF community involved in the study of the kaon sector. The level of the involvement in the project would be determined after the decision on the future activities will be taken in 2006.

5.2.5 Plans for the International Linear Collider

The High Energy Physics Advisory Panel (HEPAP) identified an e^+e^- accelerator at a c.o.m. energy of 500 GeV or higher as the highest priority next research facility for high energy physics. The world-wide participation in Linear Collider R&D is increasing to reach the long-term goal of the construction start of an international facility in the next decade. Active international participation to the study of the accelerator systems, physics studies and detector development is underway since the past decade (Sec. 3.2.2).

The R&D work carried out in the Lab on the detectors at the International Linear Collider ILC still maintains the aspect of a facultative, single-man/small-group activity. This has been the way to approach the ILC project in Italy. Other nations have a more developed strategy and nation-/world-wide collaborations are growing to discuss and study the best experimental setup for physics at the ILC (Sec. 3.2.2).

The International Linear Collider Steering Committee (ILCSC) and the International Committee for Future Accelerators plan a Global Design Initiative (GDI) to start in 2005 ⁶⁾ hosted by a laboratory (to be chosen) for logistic support. The GDI milestones include a preliminary costing document for at least one complete experimental setup (2005), a Technical Design Report (TDR) for the Accelerator (2007), the LC site selection (2008), submission of the Letters of Intent to the Global Lab that will select the experiments and will asks for two TDRs (2009-2010).

At present, small Italian groups from LNF, Como/Milan, Padua, RomaIII, Turin and Trieste have been involved in the R&D work for the Electromagnetic Calorimeter (LCcal), the Tail catcher (Capire) and the Vertex Detector (Mimosa, SUCIMA).

The project would deserve more efforts, starting with the organization of an Italian group of dedicated people. For the near-term future the LNF involvement could represent an opportunity to develop new expertise in physics and in the field of the detector technologies.

5.3 Hadronic and Nuclear Physics

The activity described in the following represents a continuation of the program described in Sec. 2.10. The short and medium-term activities of the experiments at DESY and JLab will have a logical evolution in the proposed PAX experiment ⁷⁾ at GSI and in the approved 12 GeV upgrade at JLab ⁸⁾. The hypernuclear study of the FINUDA experiment will be continued by the approved PANDA experiment ⁹⁾ at GSI that will perform precision γ -ray spectroscopy of single and double hypernuclei.

5.3.1 Experimental measurements for accessing Generalised Parton Distributions

As mentioned in Sec. 3.3.4 the Generalized Parton Distributions (GPD) ¹⁰⁾ are able to offer a unified theoretical description of hard exclusive and inclusive processes, giving a clear connection between fundamental QCD, phenomenology and experimental observables. For a review see ¹¹⁾. Experimentally, the GPDs can be accessed in Deeply Exclusive Scattering (DES), such as Deeply Virtual Meson Production (DVMP) and Deeply Virtual Compton Scattering (DVCS). In case of DVMP (like π^0 , ρ^0 , ω , ϕ , etc.), a QCD factorization proof was given recently ¹²⁾. It is mandatory to impose that the virtual photon should be longitudinal, in order to select the perturbative gluon exchange. This process permits to have in a separate way the polarised and unpolarised GPDs, by the selection of specific channels. In fact, the vector meson channels ($\rho_L^{0,\pm}$, ω_L , ϕ_L) are sensitive only to the unpolarised GPDs, while the pseudoscalar channels ($\pi^{0,\pm}$, η , ..) only to the polarised one.

Dedicated DVCS experiments, using upgrades of the existing detectors, will be performed at HERMES and JLab in the very near future. These will provide much better statistics and an improved separation of the exclusive process by detecting all final state particles. Specifically a Recoil Detector will be installed in HERMES at the end of 2005: it will cover a large fraction of the solid angle around the HERMES target and it will improve the identification of exclusive events in DVCS and in DVMP. The expected running period will be 2006-2007. In addition, in the Hall B at JLab, dedicated data taking for DVCS are scheduled for this year ¹³⁾. A small forward $PbWO_4$ calorimeter has been recently installed close to the target point of the CLAS detector to allow the detection of photons emitted at small angles.

It appears worth noting that the complete extractions of the GPDs requires an extensive program, involving the measurement of a variety of channels and observables. Such kind of measurements are among the primary goals of the 12 GeV upgrade approved at JLab ⁸⁾.

5.3.2 Transversity measurements

The complete description of the parton distributions of the nucleon in leading twist (leading order in Λ_{QCD}/Q) requires three sets of distributions: the unpolarised distributions contained in $F_1(x)$, the helicity distributions contained in $g_1(x)$ and the still unmeasured transversity structure function $h_1(x)$, as already discussed in Sec. 3.3.3. Transversity has been explored in theory, nevertheless it escaped experimental attention due to the fact that it is chiral-odd, and therefore it is not accessible via inclusive lepton scattering measurements, where chirality is conserved. Semi-inclusive DIS in which a chiral-odd observable may be involved provides a valuable tool to probe the transversity distribution. The chiral odd and T-odd Collins fragmentation function H_1^\perp correlates the transverse polarization of the struck quark with the transverse momentum of the produced hadron ¹⁴⁾, leading to characteristic single spin asymmetries in the ϕ distribution of the outgoing hadron. Recently it has been shown that also the final state interactions via soft gluon can result in leading twist single spin asymmetries, involving the T-odd distribution function F_{1T}^\perp , called also Sivers distribution function ¹⁵⁾. The Collins and the Sivers effects are virtually indistinguishable when scattering off a longitudinally polarised target, then a transverse polarised target is necessary, as discussed in Ref. ¹⁶⁾

At present HERMES provided first data ¹⁷⁾ on transverse asymmetries, using a transversely polarised hydrogen target. 2M events are expected for the end of 2005 by this experiment, allowing not only a more precise determination of the Collins and Sivers asymmetries but also enabling to look at various other channels to access transversity, i.e. double spin asymmetries in pion

leptoproduction or two hadron (interference) fragmentation. After completion of this transversity measurement, a first experimental determination of the u and possibly the d quark transversity distribution is envisaged.

Also the CLAS collaboration proposed the measurement of transverse polarized effects in hard scattering by using a transverse polarized target ¹⁸⁾. The foreseen transverse target single spin asymmetries in combination with the data available from longitudinally polarised target would allow extraction and separation of different GPDs and transverse momentum dependent distributions, eventually giving access to the orbital angular momentum of partons.

A full investigation in different laboratories and in different kinematical domain will allow to verify the predictions of QCD for the transverse spin structure of the nucleon.

5.3.3 Exotic hadrons of multiquark states

In the past, the search of pentaquark states, i.e. baryons with a minimal $qqqq\bar{q}$ structure, where the antiquark has a different flavor than the other quarks, has been pursued for many years in πN and KN experiments (see for example ¹⁹⁾). However, the quality of the data available at that time and the lack of precise theoretical predictions did not allow any conclusive result.

Few years ago, precise predictions about masses and widths of an antidecuplet of pentaquark baryons have been made ²⁰⁾. In this antidecuplet, three states have exotic quantum numbers: the Θ^+ with strangeness $S = 1$, predicted to be the lightest particle and very narrow ($\approx 10-15$ MeV), and the Ξ^{--} and Ξ^+ with $S = -2$. Only last year, evidence of the existence of the Θ^+ has been suggested by several experiments ²¹⁾, by studying different reactions with different experimental methods and observing peaks in the invariant mass of the KN system. The discovery of the Pentaquark has been considered by the USA Department of Energy (DOE) office of science as one of the ‘‘Top 10 achievements in 2003 in all areas of science’’ ²²⁾. However, due to the low statistic, none of these experiment alone is able to make systematic studies and set in an unambiguous way all the properties of the Θ^+ . Moreover, several other experiments ²³⁾, exploring different kinematic regions and with different reactions, doesn’t have any evidence for the Θ^+ . All these experimental findings have triggered a rapid increase in the theoretical activities: in the last year, hundreds of papers have been published on this subject, but the predictions on pentaquark properties, its production mechanism and excitation spectrum is still debated. Clearly, more accurate studies are needed before the observed peaks in the NK system can be identified with the baryon pentaquark state Θ^+ .

Further evidence for the Θ^+ should be searched for in a variety of reactions, and spin, isospin and parity of this state should be established in future experiments. A lot of proposal have been submitted and approved in 2004 at JLab. New data on p ²⁴⁾ and d ²⁵⁾ targets have been taken in 2004 with photon energy up to around 4 GeV and by using an upgrade of the Start Counter detector and dedicated triggers for the detection of multiparticle final states, in order to measure both decay modes of the Θ^+ into K^0p and K^+n . The primary goal of these experiments is to confirm with higher (by factor of 10) statistics the published results, establishing the KN mass spectrum with precise measurement of mass, width and errors of any observed peak. Total and differential production cross section as well as the decay angular distributions will be measured, for the determination of the quantum numbers still unknown. Thanks to the high acceptance and resolution of the CLAS detector, all reaction channels, exclusive and inclusive, will be investigated.

Two more experiments ^{26, 27)} are planned at higher energy, by using tagged photons from a 6 GeV electron beam on proton and deuterium. Both experiments, together with the Θ^+ , will search for the higher mass pentaquark states (as the Ξ^{--} for which evidence has been reported by the NA49 experiments at CERN ²⁸⁾) and also non exotic pentaquarks, such as the Ξ^- and Ξ^0 ,

the three Σ and the two N^0 and N^+ states. These latter states are not expected to be narrow, and may require a significant amount of data to be identified.

As can be seen, a large part of the 2004 and 2005 JLab activity has been dedicated to the study of the pentaquark baryons. If their existence will be confirmed, the hadron spectroscopy of exotic multi-quark states will become a key subject of the JLab future physics program.

5.3.4 Antiproton Physics at GSI with PANDA Spectrometer

A new international accelerator facility for research with ions and antiprotons (FAIR) is under construction at GSI and the experimental program will start in 2012²⁹⁾. The project foresees a scientific program that covers a broad range of aspects of modern hadronic physics like nuclear structure physics, nuclear matter physics, plasma physics, atomic physics and antiproton physics. Experiments with antiprotons have demonstrated to be a rich source of high quality information for hadronic physics; therefore with the new High Energy Storage Ring (HESR) for antiprotons at GSI the physics of strange and charm quarks will be deeply explored. With a high performance full solid angle magnetic spectrometer (the PANDA detector) some crucial points of this scientific field will be analyzed and hopefully clarified⁹⁾.

Experimentally, studies of hadron structure can be performed with different probes such as electron, pion, kaon, proton or antiproton beams, each of which have its specific advantages. In antiproton-proton annihilation, particles with gluonic degrees of freedom as well as particle-antiparticle pairs are copiously produced, allowing spectroscopic studies with unprecedented statistics and precision. Antiprotons of 1–15 GeV/c will therefore be an excellent tool to address the open problems mentioned above. The following experiments are foreseen:

- Charmonium ($c\bar{c}$) spectroscopy: precision measurements of mass, width, decay branches of all charmonium states, especially for extracting information on the quark-confining potential. The unequaled resolution in the $p\bar{p}$ formation process and small systematic uncertainties give the unique opportunity to improve dramatically our knowledge which can not be achieved elsewhere.
- Firm establishment of the QCD-predicted gluonic excitations (charmed hybrids, glueballs) in the charmonium mass range (3–5 GeV/c) using high statistics in combination with sophisticated spin-parity analysis in fully exclusive measurements.
- Search for modifications of meson properties in the nuclear medium, and their possible relationship to the partial restoration of chiral symmetry for light quarks. Particular emphasis is placed on mesons with open and hidden-charm, which extends ongoing studies in the light quark sector to heavy quarks, and adds information on contributions of the gluon dynamics to hadron masses.
- Precision γ -ray spectroscopy of single and double hypernuclei for extracting information on their structure and on the hyperon-nucleon and hyperon-hyperon interaction.

Furthermore, as soon as the HESR facility will reach the full design luminosity other physics opportunities will open up like:

- extraction of generalized parton distributions from $p\bar{p}$ annihilation,
- D meson decay spectroscopy (rare leptonic and hadronic decays), and
- search for CP violation in the charm and strangeness sector (D meson decays, $\Lambda\bar{\Lambda}$ system).

For the envisaged experimental program a nearly full coverage of the solid angle together with good particle identification and high energy and angular resolutions for charged particles and photons are mandatory. The proposed detector is subdivided into the target spectrometer (TS) consisting of a solenoid around the interaction region and a forward spectrometer (FS) based on a dipole to momentum-analyze the forward-going particles. The combination of two spectrometers allows a full angular coverage, it takes into account the wide range of energies and it still has sufficient flexibility, so that individual components can be exchanged or added for specific experiments, e.g. for the experiments with hypernuclei or for the special needs of CP violation studies.

The workload required for the design and the construction of all components of the PANDA detector is shared among the institutions involved. At present these are 44 from 12 countries. Italy in general, and INFN in particular, is deeply involved in the project with many groups. At present each group has just expressed its interest in some technical issue. The commitments concerning the effective contribution of each group to the PANDA project will be defined during 2005 in a Memorandum of Understanding. In the preliminary distribution of tasks LNF is involved in the tracking of the TS. More details on the detector development activity related to this project are given in the chapter devoted to the future detector developments.

5.3.5 Spin Physics at GSI: PAX project

The proposed polarized antiproton beam at HESR will give a wealth of single and double spin observables opening a window to new fundamental physics, which can be studied neither at other facilities nor at HESR without transverse polarization of protons and/or antiprotons like the transversity distribution. The most direct way to obtain information on transversity is the measurement of double transverse spin asymmetry A_{TT} in Drell-Yan production of lepton pairs by using both transversely polarized beam and target. The measurement of A_{TT} is also planned at RHIC, in Drell-Yan processes with transversely polarized protons, through the measurement of two transversity distributions, one for a quark and one for an antiquark (both in a proton). The double spin asymmetry A_{TT} expected is very small, of the order of the per cent or less³⁰).

The situation with the PAX measurement of the A_{TT} in Drell-Yan processes with polarized antiprotons and protons, $\bar{p}^\uparrow p^\uparrow \rightarrow l^+ l^- X$, is a much more favorable one. The expected PAX values of square energy of center mass $s=30-50 \text{ GeV}^2$ and the square of the invariant mass of the lepton pair $M^2=10 \text{ GeV}^2$ are well suited for the definitive observation of A_{TT} ⁷). There are some unique features which strongly suggest to pursue the study of h_1^q in the $\bar{p}p$ channel with PAX:

- a) In $\bar{p}p$ processes both the quark (from the proton) and the antiquark (from the antiproton) contributions are large. The measurement of a large A_{TT} and the determination of the valence quark dominated h_1^q at PAX is distinct from the possible measurement of a very small asymmetry at RHIC which would probe the very different sea quark region. Furthermore, the Drell-Yan events at HESR will get their main contribution from the $x_1 \simeq x_2$ region so that from the PAX data alone one can essentially access and deduce the x-dependence of $h_1^u(x, M^2)$, which is important for any further applications of the so determined $h_1^u(x, M^2)$ to the interpretation of the single spin asymmetry measurements.
- b) There is the possibility of using the Drell-Yan continuum expression at $M < 4 \text{ GeV}$ in the J/Ψ , Ψ' resonance region because the unknown quantities cancel in the ratio giving A_{TT} ; this, in conjunction with the resonance data, enhances substantially the sensitivity of the PAX experiment to A_{TT} and to obtaining direct information on $h_1^u(x_1, M^2) h_1^u(x_2, M^2)$.

5.3.6 The Quark Gluon Plasma at LHC: the ALICE experiment

The real challenge in Quark Gluon Plasma (QGP) physics is to find, study and combine many different observables that carry information on a state of the matter which is short lived and not at all observable. These observables can be classified into two large groups:

- global observables, which help in determining the geometry of the collision, the initial conditions, and some general feature of the produced system such as its shape and spatial evolution, and
- the signatures of the QGP, i.e. these observables which have a different behavior whether the plasma is formed or not. All these observable must be globally analyzed to understand the properties of this matter.

The Relativistic Heavy Ion Collider (RHIC) at BNL is the first collider specifically designed to study heavy ion collisions and characteristics of the QGP. Four experiments are presently running at RHIC, and their results have demonstrated a universal in-medium suppression of high transverse momentum hadron production as compared to elementary collisions at similar \sqrt{s} . The RICH results can be interpreted in terms of modification of parton fragmentation functions due to the parton energy loss in “hot” nuclear matter, in analogy to the recent HERMES results for the “cold” nuclear matter. While RHIC is expected to study accurately the phase transition from normal matter to deconfined matter, since it may produced energy density which are close to the critical one, the ALICE experiment ³¹⁾ at LHC will study the QGP phase well above the critical point. The ALICE experiment (A Large Ion Collider Experiment) has been designed with the goal to achieve the measurements of the largest possible set of observables (hadrons, leptons and photons) over a large portion of phase space. The proposed electromagnetic calorimeter ³²⁾ (combined with a TPC tracking system) will allow for the first time the measurements of the electromagnetic component of the jet which permit a detailed study of jet fragmentations functions. In addition with a such device it will be possible to study for the first time the quenching of hadrons up to transverse momentum of few hundred GeV where scattering (Cronin) effects are expected to be negligible.

5.4 Astroparticle physics

Astronomical and astrophysical signals are allowing us to test existing theory in entirely new ways, and new theoretical developments connecting the origin and evolution of the Universe to the laws of quantum physics, particle theory and general relativity are driving further observational tests. The major developments over the next decade can be summarized as follows. First of all, the mapping the relic radiation left over from the Big Bang to determine the nature of the primordial perturbations that gave rise to galaxies and stars. It is crucial the understanding of the nature of the Dark Matter, the confirmation that the Universe is dominated by vacuum energy (a cosmological constant) and that the expansion of the Universe is accelerating. As noted previously, a major breakthrough would be the understanding the origin of CP violation which was responsible for the production of the matter-antimatter asymmetry in the Universe. Studies of the neutrinos from astrophysical sources are needed to understand the nature of the source objects - the sun, supernovae, active galactic nuclei, gamma ray bursts. Finally, future programs plan detailed mapping of the sources of the ultra-high energy cosmic rays to solve the long-standing mystery of their origin. In the recent years, the progress in the field of fundamental physics has induced a growing number of INFN researchers to propose and carry out - in their own laboratories - scientific experiments to be conducted in space, by Russian and American carriers on board satellites, the Space Shuttle, the MIR Space Station and the International Space Station. These activities, also consisting in building space qualified instrumentation, are often conducted in the laboratories and divisions of INFN with a significant investment by INFN itself and with the contribution of other

Agencies like ASI (Italian Space Agency). INFN researchers have been and are - in part or fully - involved in the realization of instruments and apparatus which have already been launched in space (AMS-01, NINA 1 and 2, SilEye 1-2, SIRAD) or that will be put into orbit in the next years (ALTEINO, AGILE, PAMELA, LISA-Pathfinder, AMS-02, GLAST, LARES, EUSO). Most of these missions are to start taking data in orbit between 2005 and 2008; after this period (except for EUSO and LISA, due for 2010 and 2013 respectively) no further space experiments involving INFN researchers have been programmed, yet. Nevertheless, in the wave of the experience gained in planning and carrying out the present missions, discussions have started about perspectives of next generation space missions and of possible strategies to be followed in order to establish a kind of "road map" driven by the major scientific objectives and by the technical capabilities and skills so far acquired. It is also worth mentioning that this possible "second phase" of Astroparticle Physics experiments conducted in space would greatly profit from the development of a specific R&D carried out not only on single detectors or instruments, but also by initiating, within INFN facilities, activities specifically devoted to space qualification and integration of payloads and micro-satellites (Sec.6.2.2.1).

5.5 Neutrino physics

As noted in Sec.3.5, the short-medium term perspectives in neutrino oscillation physics are rather well defined (Fig.5.1). LNF strongly contributes to the CERN to Gran Sasso Neutrino (CNGS) physics programme and in particular to the construction of OPERA. Frascati is presently involved in the design, construction and commissioning of the magnetic spectrometer, the brick assembling machine and wall support structure ³³). CNGS commissioning and data taking is scheduled in summer 2006. The OPERA data taking is highly non-trivial since it involves nearly on-line emulsion scanning. In the short-medium term, and in particular after the detector commissioning, LNF plan to contribute to the scanning task both locally with a dedicated microscope and at LNGS. The local scanning station is under construction. Emulsion scanning is a rich technology, requiring mastering of precision mechanics and optics, image grabbing and sophisticated 3D reconstruction techniques. A large range of applications, well beyond particle physics, are envisaged with emphasis on biotechnologies and space physics. The full exploitation of these possibilities is a fascinating experimental task for the medium term and it represents an interesting complementary activity deeply connected to the CNGS commitments of LNF.

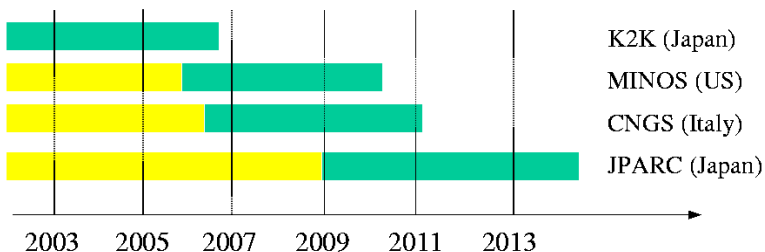


Figure 5.1: Medium term roadmap for the study of neutrino oscillations with long-baseline accelerator experiments.

It has often been remarked that the long term roadmap for neutrino oscillations is very unclear and highly debated. As pointed out in Sec.3.5, the main reason is the complete lack of

hints concerning the size of the θ_{13} angle. Relatively very large θ_{13} could be accessible already at CNGS/MINOS ($\theta_{13} \gtrsim 7^\circ$) or at new reactor experiments to be carried out before ~ 2010 (e.g. DoubleCHOOZ). A major improvement in the knowledge of this parameter is expected after the completion of the Japanese T2K experiment ³⁴). Large values of θ_{13} are needed to exploit the physics capabilities of massive long-baseline experiments with traditional high intensity proton beams (“Superbeams”). In spite of the various setups that can be envisaged, multi-kiloton detectors for $\nu_\mu \rightarrow \nu_e$ (low Z materials for ν_e appearance identification) combined with ~ 1 MW proton drivers operating at $\mathcal{O}(10 \text{ GeV})$ are able to explore region of $\sin^2 2\theta_{13}$ of the order of 10^{-2} (“Phase I superbeams”). To access the 10^{-3} region or address CP violation if $\sin^2 2\theta_{13} \sim 10^{-2}$, a new generation of massive detectors and multi-megawatt proton sources must be built (“Phase II superbeams”). This extension represents the ultimate evolution of traditional beams since the ν_e search is now limited by the intrinsic ν_e beam contamination and background systematics. Further progresses along this line could be obtained only with very unconventional proton drivers ³⁵). The overall costs of a Phase II superbeam overtake 1G\$ and synergies with other physics items must be found to justify such an investment. An upgrade of the Phase I Japanese superbeam from JAERI to SuperKamiokande (T2K) partially fulfills this requirements since the JAERI facility is a general purpose laboratory for particle physics, material science and biophysics while the construction of a new gigantic (~ 1 Mton mass) water Čerenkov detector (HyperKamiokande) could also allow a significant progress in the proton decay search and in the detection of solar, atmospheric and supernova neutrinos. However, it is very unlikely that any upgrade will be supported in case of null result at T2K. US physicists are currently considering a phase I setup based on the existing NuMI beam operated in the off-axis configuration ³⁶). It implies however the construction (on surface) of a 50 kton low-Z detector in a very short timescale to be competitive with T2K. A larger baseline (810 km versus 290 km) offers some sensitivity to matter effects (sign of Δm_{23}^2) but the latter can be exploited only for very high values of θ_{13} . Further increase of the sensitivity in the 10^{-3} region could be envisaged after the completion of a multi-megawatt proton driver operating at 8 GeV. Europe has currently neither a powerful proton driver nor a massive detector for ν_e appearance. Accessing the T2K sensitivity in a timescale comparable with the Japanese facility would be unlikely even with a very aggressive funding profile. In a longer timescale, an interesting way out is offered by the beam technologies that allow the detectors to operate in ν_μ appearance mode (i.e. search for $\nu_e \rightarrow \nu_\mu$ transitions and their CP conjugate) as the Beta Beams ³⁷) or the Neutrino Factories ³⁸). In particular, the Beta Beam concept offers a strong synergy with nuclear physics (high intensity radioactive beams) and low background contamination in the $\nu_e \rightarrow \nu_\mu$ channel. The small energy of the parent ions requires, anyway, the construction of the megaton water Čerenkov. The latter has been proposed as the principal detector for a new underground laboratory at Frejus, which could start data taking a few years earlier than HyperKamiokande ³⁹). Physics performances would be very similar since the improved background rejection is compensated by the lower neutrino energy ($\sim 300 \text{ MeV}$). An increase of the beta beam energy ⁴⁰) could be envisaged by a fast cycling refurbished SPS at CERN. This machine is currently considered as an option for the luminosity upgrade and (in a longer timescale) the energy upgrade of the LHC. In this case, the detector mass could be significantly reduced ⁴¹) and the baseline would match the CERN-LNGS distance. In this configuration, denser detectors operating in ν_μ appearance mode can be exploited and therefore smaller experimental halls than Frejus (e.g. LNGS) are needed. Finally, a refurbished SPS would simplify ion injection into the LHC and provide very high gamma betabeams ⁴²). High gamma beta beams are currently under investigation in the US, as well ⁴³).

Unless the value of θ_{13} is particularly high, full exploration of the leptonic mixing matrix will be carried out only with dedicated Neutrino Factories. Significant technical progresses have been achieved but several basic issues have to be fully addressed, yet. The Neutrino Factory is presently

considered as the ultimate facility for oscillation but a long and intense R&D (probably ~ 10 y) will likely be necessary to assess feasibility for this ambitious option.

As noted before, in the last decade a large effort to identify viable non-conventional neutrino sources has been made and several R&D are in progress in Japan, Europe and US. For what concerns the detector technologies, the large masses and costs involved drive most of newly proposed designs toward straightforward extensions of well-established techniques. By far the most successful technology in the $\mathcal{O}(1)$ GeV energy range is water Čerenkov, which could be scaled up to the 10^6 ton size even with state-of-the-art photodetectors. Besides conservativeness, the main advantage of this approach is the additional physics case that a gigantic water Čerenkov can provide (improved sensitivity to proton decay, additional supernova, atmospheric and solar neutrino studies etc.). On the other hand, the excavation of the cavern, the related engineering problems and the production of photodetectors raise up enormously costs and environmental impact with respect to present detectors. Moreover, pattern recognition in water Čerenkov is mainly limited to “single ring” events (sub GeV neutrinos) so that, depending to the outcome of the machine R&D, this detector could be poorly tuned for a high energy neutrino factory or a Beta beam. Clearly, the superior imaging capability of Liquid Argon TPCs à la ICARUS ⁴⁴⁾ represents an ideal solution to this limitation since it allows event identification in the multi-GeV range and preserves most of additional non-accelerator physics case of Čerenkov detectors. However, scaling of the ICARUS technology and cost in the range competitive for the precision determination of leptonic mixing (~ 100 kton) is highly non trivial, although recent progresses in LAr technology ⁴⁵⁾ are very encouraging. Finally, several possibilities are open for single-purpose detectors. By now, magnetized iron detectors are the most straightforward setup for physics programmes based on Neutrino Factories or high energy Beta Beams. Similarly, low-Z detectors optimized for the appearance of ν_e represents the obvious solution for Superbeams operating in the multi-GeV range.

LNF has been extensively involved into the design and construction of large scale neutrino detectors, especially at LNGS (LVD, MACRO, OPERA, ICARUS). It is clear that oscillation physics will continue to make use of these technologies although the role of LNGS after CNGS is currently undefined. We do not expect a clear roadmap to emerge before the completion of CNGS or even T2K (discovery of $\theta_{13} \neq 0$).

On the other hand, special attention should be paid to non-oscillation physics. In particular, next generation experiments for neutrinoless double beta decay are going to approach non trivial region of the parameter space and most of the new proposals show potential synergies with dark matter searches or high precision solar neutrino spectroscopy ⁴⁶⁾. In spite of the limited know-how at LNF, the next revolution in neutrino physics could come from the determination of the Dirac/Majorana nature of neutrinos themselves and technological progresses in this sector should be carefully monitored.

5.6 Interferometric detectors of gravitational waves

In its simplest scheme a laser interferometric detector is a Michelson interferometer whose mirrors and beam-splitter are suspended. Waves impinging upon the detector induces a differential motion in the mirrors at the ends of the two arms. This implies a difference between the phase of the light beams circulating in the two arms, and, thus, a change in the intensity of the recombined output light. The scale of such a detector is set, not by the velocity of sound (as in the case of a bar detector), but the velocity of the light. This implies that for the same GW the length of each arm of the interferometer has to be larger than the length of a bar by a factor $\chi = c/v_s$, and, correspondingly, is much larger the absolute displacement. However, since typical values of χ are of the order of 10^5 , each arm should have a length ~ 100 km. Due to the curvature of the Earth,

arms of this size are impossible to build on the surface of the Earth: practical values for the arm length cannot exceed a few km. This problem is solved in the interferometric detectors enhancing the effective optical length of the arms by folding the light in the arms with the use of optical delay lines or Fabry-Perot cavities. As a consequence of their nonresonant feature, the sensitivity of such detectors is inherently wideband. In fact, the noise always limits the bandwidth of laser interferometers. Their sensitivity is limited by seismic and thermal noise in the low frequency region (typically ≤ 100 Hz) and photon shot noise in the high frequency region (\geq few kHz).

VIRGO is a 3 km long arms interferometer built by an Italian-French collaboration, and is currently under final commissioning (the first scientific run is foreseen for the end of this year). A reduced version (without the Fabry-Perot cavities) of this interferometer has been under test with good results during the 2000-2002 period. As clearly evident from Fig. 3.3 of Sec. 3.6, VIRGO is the only instrument able to explore the low frequency region (just where more astrophysical GW sources are expected). This feature is due to the very efficient seismic attenuation system (the Super-Attenuator) to which all the main optical elements of this interferometer are suspended.

During the construction of current interferometric detectors (TAMA, LIGO, GEO600, VIRGO), the R&D and preparatory work for their upgraded versions have been going on. The design for the second generation upgrade of the LIGO detectors (Advanced LIGO) is based on the technology already employed in GEO600. The efforts are, essentially, focused on i) increasing the laser power, ii) implementing the signal recycling, and, iii) reducing the internal thermal noise by using monolithic suspensions for the main optical elements. These upgrades are expected to be implemented in 2007 and should consistently enlarge the useful bandwidth towards the low frequency region and improve the sensitivity by more than a factor 10 in amplitude, as shown in Fig. 3.3. In its present setup, the VIRGO interferometer already incorporates some advanced elements. For these reason the upgrade to an Advanced VIRGO is expected to be much less demanding and expensive. As for the future of GEO600, the plan is its conversion in a high-frequency detector. This strategy is motivated by the fact that, because its shorter arms, it will be more difficult to achieve a good low-frequency response against thermal noise at room temperature.

5.6.1 Long-term future of the GW experiments

As for Europe, a design study for a GW observatory (EGO) has been submitted to EU at the beginning of this year ⁴⁷). This observatory aims to reach a very high sensitivity in the frequency range $1 \text{ Hz} \div 10 \text{ kHz}$. To achieve this goal a multi-detector design is under study: an interferometer to cover the frequency band $1 \text{ Hz} \div 10 \text{ kHz}$, and a combination of a non-classical light interferometer and resonant detectors for frequencies greater than 1 kHz.

The interferometers are a third generation detectors that will require: i) an advanced version of the VIRGO Super-Attenuator; ii) the cooling of the last stage of the mirror suspension to a temperature of a few kelvin; iii) suspended optics of large masses or a quantum-non-demolition locking scheme for the interferometer mirrors (to limit the radiation pressure noise); iv) optical components with extremely low losses to tolerate the high light power (\sim MW) stored in the interferometer. Finally, the need to overcome the Standard Quantum Limit (due to the uncertainty principle) for traditional GW detectors will require the use of squeezed light. For the high frequency band will be used two resonant detectors of new conception:

- **Dual** is made by two nested cylindrical or spherical massive bodies whose quadrupolar modes resonate at different frequencies. The signal is read in the gap between the bodies as their differential deformations. During the oscillations of the bodies their coincident centres of mass remain at rest, thus providing for the rest frame of the measurement. The useful sensitivity band of this kind of detector extends between the first quadrupole modes of the two masses and is expected to be of a few kHz in the kHz range.

- **Sphere** is a large cryogenic hollow sphere optimized for detection around 300 Hz and 1 kHz. This detector present unique properties with respect to all the others: it is able to determine the source direction, the polarization and the spin of the GW. The latter feature appears very appealing in light of the possible existence of scalar GWs.

According to the time schedule outlined in the EGO proposal ⁴⁷⁾, after the design study and the construction phases (4-years long each), the observatory should be enter in operation at the beginning of 2013. In 2012 is also expected to be operative the space interferometer LISA. This is a joint NASA-ESA space mission that will place into a special solar orbit three laser transponding spacecraft to create a nested set of interferometers in a triangular configuration. The space environment allows the path length to be increased to 5 million kilometers. This detector has an excellent sensitivity ($\sqrt{S_h} \sim 10^{-22} \text{ Hz}^{-1/2}$) over the frequency band ($1 \div 100 \text{ mHz}$), beyond the reach of any ground-based detector. Sources in this detection band include both binary star systems in our Galaxy, and cosmological sources associate with massive (from 10 to 10^6 times the Sun mass) black hole interactions.

As for the long-term future, the ROG group is also actively involved in the design study of the EGO observatory. Taking into account the experience acquired during the operation of NAUTILUS and EXPLORER, it appears natural for the ROG people to be involved in the construction of the resonant high frequency detectors. Between Dual and Sphere, the latter appears more interesting because it is sensitive also in the medium frequency range covered by the interferometers and for its sensitivity to scalar GWs. Given the high sensitivity levels expected for this detector it could be necessary to reduce the effects of the cosmic ray background. For this reason an ideal location of Sphere could be the LNGS.

5.7 Synchrotron Radiation experiments at ESRF

The future of GILDA is strongly linked to the future of ESRF and the Italian participation to this European project. Two possible scenarios are taken into consideration: an increase of the current and a change of the magnetic elements to produce light. The first possibility requires only a light up grading of the optical elements to treat the higher flux coming from the bending magnet due to the increase of the circulating current. On the other hand, the change of the source from a bending magnet to an insertion device will require a very deep modification of the beam line due to the different nature of the source. Taking into account only the first possibility, improvements are foreseen to let the beam line be still very competitive in the near future. Big effort will be given to the development of the ancillary equipment for sample conditioning like high pressure and very high temperatures. A new experimental set up will give the opportunity to perform *in-situ* studies of the structural changes of catalysts in reaction environment. It will be possible to warm up the sample up to 1000°C and input different gasses monitoring the output gasses produced. This kind of studies will surely require improvements of the monochromator to perform on the beam line very fast X-ray absorption scans (Quick- EXAFS). A system for studies on *in-situ* grown clusters, by magnetron sputtering and rare gas aggregation, is being developed in Frascati. This apparatus will be designed to be easily inserted on the GILDA beamline. Concerning the detection of the X-fluorescence a new improvement is foreseen. Silicon drift detectors (SDD), originally developed for high energy physics experiments, have been recently successfully applied to X-ray spectroscopy. They are very promising because with Peltier cooling they reach an energy resolution ($\text{FWHM} < 168 \text{ eV}$ at 5.9 keV) comparable to that of liquid nitrogen cooled Ge detector. The plan is to first test SDD detectors on the beam line in different conditions and then, on the basis of the results and of the experience acquired, to develop a SDD crystal ball to cover a large solid angle. In order to extend the actual detectable reciprocal space in XRD measurements necessary to achieve very

fast and precise long-range order structural information the study of the use of a curved imaging plate is being taken into consideration. All the improvements reported and related to the future operation of the GILDA beam line will require a big effort from the Frascati group from a technical and a scientific point of view.

References

1. CDF Collaboration, Phys. Rev. D **64** (2001) 032002.
2. CDF Collaboration, Phys. Rev. D **65** (2002) 052007.
3. BABAR Collaboration, SLAC-504 (1998).
4. T. Schorner-Sadenius, hep-ex/0307078,
see also <http://atlas.web.cern.ch/Atlas/GROUPS/DAQTRIG/daqtrig.html>
5. NA48-Future Working Group, CERN-SPSC-2004-10/SPSC-EOI-002 (2004) and also
<http://www.cern.ch/NA48/NA48-3/Overview/LOI.pdf>
6. <http://www.interactions.org/linearcollider>
7. PAX Collaboration, *Antiproton-Proton Scattering Experiments with Polarization*, Letter of Intent, Jan 15, 2003.
8. http://www.jlab.org/div_dept/physics_division/pCDR_public/pCDR_final/pCDR_final.pdf
9. PANDA Collaboration, "Antiproton Physics at Darmstadt", Letter of Intent GSI-ESAC/Pbar, Jan 21, 2004.
10. D. Muller *et al.*, Fortsch. Phys. **42**, 101 (1994); X. Ji, Phys. Rev. Lett. **78** (1997) 610; X. Ji, Phys. Rev. D **55** (1997) 7114; A.V. Radyuskin, Phys. Lett. B **380** (1996) 417; A.V. Radyuskin, Phys. Rev. D **56** (1997) 5524.
11. K. Goeke, M.V. Polyakov, M. Vanderhaeghen, Prog. Part. Nucl. Phys. **47** (2001) 401; M. Diehl, Phys. Rept. **388** (2003) 41.
12. J.C. Collins, L. Frankfurt and M. Strikman, Phys. Rev. D **56** (1997) 2982.
13. CLAS Collaboration, E01-113 proposal.
14. J. Collins, Nucl. Phys. B **396** (1993) 161.
15. D. Sivers, Phys. Rev. D **43** (1991) 261.
16. P.J. Mulders, R.D. Tangerman, Nucl. Phys. B **461** (1966) 197; D. Boer, P.J. Mulders, Phys. Rev. D **57** (1998) 5780.
17. HERMES Collaboration, Phys. Rev. D **94** (2005) 012002.
18. CLAS Collaboration, "Letter of Intent 03-003: Transverse Polarization Effects in Hard Scattering at CLAS".
19. A. Berton *et al.*, Nucl. Phys. B **63** (1973) 54.
20. D. Diakonov, V. Petrov and M.V. Polyakov, Z. Phys. A **359** (1997) 305.

21. LEPS Collaboration, Phys. Rev. Lett. **91** (2003) 012002; DIANA Collaboration, Phys. Atom. Nucl. **66** (2003) 1715; A.E. Asratyan, A.G. Dolgolenko and M.A. Kubantsev, Phys. Atom. Nucl. **67** (2004) 682; CLAS Collaboration, Phys. Rev. Lett. **91** (2003) 252001; CLAS Collaboration, Phys. Rev. Lett. **92** (2004) 032001, Phys. Rev. Lett. **92** (2004) 049902(E); SAPHIR Collaboration, Phys. Lett. B **572** (2003) 127; HERMES Collaboration, Phys. Lett. B **585** (2004) 213.
22. http://www.science.doe.gov/Sub/Accomplishments/accomplishments/top_10_2003.htm
23. J.Z. Bai *et al.*, hep-ex/0402012; K.T. Knoepfle *et al.*, hep-ex/0403020; M.I. Adamovich *et al.*, hep-ex/0405042; C. Pinkeburg, hep-ex/0404001; BABAR Collaboration, hep-ex/0408064; Yu.M. Antipov *et al.*, hep-ex/0407026; S. Schaeet *et al.*, Phys. Lett. B **599** (2004) 1; CDF, E690, LEP, Focus, HyperCP Collaborations, Proceedings of QNP2004 conference.
24. CLAS Collaboration, JLAB Proposal PR04-021 "Spectroscopy of Exotic Baryons with CLAS: Search for Ground and First Excited States".
25. CLAS Collaboration, JLAB Proposal PR03-113 "Investigation of Exotic Baryon States in Photoproduction Reactions with CLAS".
26. CLAS Collaboration, JLAB Proposal PR04-010 "Proposal to search for exotic cascades with CLAS using an untagged virtual photon beam".
27. CLAS Collaboration, JLAB Proposal PR04-017 "Study of Exotic Baryons in Photoproduction off Protons".
28. NA49 Collaboration, hep-ex/0310014.
29. "An International Accelerator Facility for Beams of Ions and Antiprotons", Conceptual Design Report, <http://www.gsi.de/GSI-Future/cdr/>
30. <http://www.bnl.gov/rhic/>
31. <http://aliceinfo.cern.ch/>
32. T.M. Cormier, Eur. Phys. Journ. C **34** (2004) s333.
33. INFN-LNF 2004 Annual Report - LNF-05/05 (IR) - available on <http://www.lnf.infn.it/rapatt>
34. Y. Itow *et al.*, KEK-REPORT-2001-4, hep-ex/0106019.
35. S.V. Bulanov *et al.*, LNF-04/07, Nucl. Instr. Meth. A **540** (2005) 25.
36. NOvA Collaboration, "NOvA: Proposal to Build an Off-Axis Detector to Study muon-neutrino \rightarrow electron-neutrino Oscillations in the NuMI Beamline," FERMILAB-PROPOSAL-0929.
37. P. Zucchelli, Phys. Lett. B **532** (2002) 166.
38. S. Geer, Phys. Rev. D **57** (1998) 6989, Erratum Phys. Rev. D **59** (1999) 039903; M. Apollonio *et al.*, hep-ph/0210192 and references therein.
39. M. Mezzetto, J. Phys. G **29** (2003) 1771; M. Mezzetto, J. Phys. G **29** (2003) 1781; J. Bouchez, M. Lindroos and M. Mezzetto, hep-ex/0310059.
40. J. Burguet-Castell *et al.*, Nucl. Phys. B **695** (2004) 217.

41. F. Terranova, "Higher γ 's and smaller detectors for the Beta Beam", Talk at Nufact04, Osaka 24 Jul - 1 Aug 2004, to appear in Nucl. Phys. B (Proc Suppl).
42. F. Terranova *et al.*, Eur. Phys. Journ. C **38** (2004) 69.
43. S. Geer, "APS Study on Physics with Beta Beams and neutrino factory", Talk at Nufact04, Osaka 24 Jul - 1 Aug 2004, to appear in Nucl. Phys. B (Proc Suppl).
44. C. Rubbia, CERN-EP 77-08, 1977. The ICARUS Collaboration, "A second-generation proton decay experiment and neutrino observatory at the Gran Sasso Laboratory", LNGS - 94/99, Vol.I (1993) and Vol.II (1994).
45. S. Amerio *et al.*, Nucl. Instr. Meth. A **527** (2004) 329.
46. S.R. Elliott and J. Engel, J. Phys. G **30** (2004) R183.
47. <http://virgo-bwulf.pg.infn.it/punturo/FP6>

Chapter 6

Plans in High-Technology Areas

The progress on radiation detectors has been always correlated with the advancements on the various experimental physics fields. New physics challenges generally call for new advanced detectors; novel detector technology allows to achieve new physics frontiers.

At LNF the first example of new generation electronic detectors ¹⁾ was realized in the framework of the experiments at the ADONE electron-positron collider. In previous experiments, detectors like streamer chambers or flash tubes with photo-camera readout were generally used.

In the next years, extensive R&D on detectors was performed at LNF on different kinds of radiation devices, mainly gas detectors and scintillation detectors. These detectors were used in various applications: tracking and identification of charged particles, large electromagnetic and hadronic calorimeters and large area muon detectors, as reported in Table 6.1.

All these developments have been possible thanks to the high professional contribution of the various technical services (Sec. 2.7) that, during all these years, have grown up inside the Laboratory increasing significantly the role of the LNF groups in the framework of the international scientific collaborations.

In the following, taking into account the foreseen experimental physics scenarios in which LNF experimental physics community will be involved in the near and far future, possible R&D on new detectors for the different fields of application will be described, ranging from the high energy physics at accelerators to astroparticle, neutrino and cosmic ray physics, nuclear physics, matter studies and medical applications.

6.1 Detectors for High Energy Physics

The LNF high energy physics groups are heavily involved in the most important international experiments at the European and American hadronic machines. In particular a big effort on detector R&D and construction has been recently performed for ATLAS and it will continue in the near future (3-5 years) for LHCb. In the framework of the BTeV collaboration, R&D on straw tubes and their integration in the apparatus has also been performed.

There is also a great interest on possible upgrades of the KLOE apparatus in view of the possibility of a second generation high luminosity DAΦNE machine (Sec. 4.2.3).

Regarding long term projects (10-15 years) for the next Linear Collider there is a participation to the Muon and Calorimetry working groups.

Streamer Tubes	ALEPH, SLD, NUSEX, MACRO
Drift Chambers	KLOE
Drift Tubes	ATLAS
Straw Tubes	BTEV, FINUDA, PANDA
RPC	BABAR, OPERA, GLASS, CAPIRE
MWPC	LHCb
GEM	LHCb, ALFAP
Cerenkov(N ₂)	DIRAC
CCCD	DEAR
SDD	SIDDHARTA
Germanium	FINUDA2
BGO	GRAAL
HAD Calorimeters (Fe-stream.tubes)	ALEPH, SLD
EM Calorimeters (Pb-scintill.)	AIACE
RICH	HERMES
EM Calorimeters (Lead glass)	HERMES
HAD Calorimeters (Fe-plast.Scint.)	CDF
EM Calorimeters (Pb-Scint.Fibers)	KLOE, LCCAL

Table 6.1: Detectors know how at LNF

6.1.1 Gas Detectors: wire chambers

Large wire chamber systems have been designed for both ATLAS and LHCb detectors at LHC. At LNF high precision drift tubes and small gap Multi Wire Proportional Chambers (MWPC) have been developed.

6.1.1.1 MDT for ATLAS

The LNF-ATLAS group is responsible for the construction of all the muon precision tracking chambers ²⁾ of the middle stations in between coils of the air toroidal magnet, that is 94 chambers of dimensions ranging from 1.2 to 1.7×3.6 m. The chambers are composed by high pressure drift tubes (3 cm diameter), called MDT (Monitored Drift Tube), operated at 3 bars. The LNF group has significantly contributed to the R&D to fulfill the very tight requirements on both the mechanical precision of the assembly (absolute wire position accuracy down to 20 μm) and the single tube intrinsic performances (single wire position resolution of $\sim 80 \mu\text{m}$).

6.1.1.2 MWPC for LHCb

The LNF-LHCb group works on the muon apparatus with responsibilities for detectors, electronics and detector support mechanics.

The muon trigger of the experiment is given by a coincidence of five muon stations within a very short time window of 25 ns (the LHC bunch spacing time). In order to achieve a good trigger efficiency, the chambers must provide a very high detection efficiency, 99% in 25 ns time window, corresponding to a time resolution of better than 3 ns (r.m.s.).

The biggest part of the muon apparatus will be equipped with MWPCs ³⁾, while for the innermost part (R1) of the first muon station (M1), where particle rates up to 1 MHz/cm² are

expected, a new detector based on Gas Electron Multiplier (GEM) technology has been proposed (Sec. 6.1.2). To fulfill such very stringent requirements small gap (2.5 mm), small wire pitch (2.0 mm) quadri-gap MWPCs operated with fast CF₄ based gas mixture have been developed.

The LNF group has significantly contributed to the optimization and engineering of the detector needed for the mass production of about 300 MWPCs. The commissioning of the MWPCs is foreseen by the end of 2006.

6.1.1.3 Straw tubes for BTeV

The Frascati group is involved on the R&D ⁴⁾ on straw tubes technology, their mechanical integration with μ -strip Si detector and the position monitoring system of detectors with optical strain gauges with micrometric resolution. The R&D work is planned to continue during 2005, despite the cancellation of the experiment because of the US research budget cuts.

The straw tube detector design is similar to that one used by the ATLAS experiment, while a completely innovative design of the assembling and mechanical support of the straw tube, which acts, at the same time as support for the μ -strip Si detector, has been developed. The design is based on a straw-grooved rohacell sandwich, surrounded by a Carbon-Fiber reinforced plastic (CFRP) shell, on which the Si-detector will be assembled. Straw tubes are kept in place by the grooved rohacell without mechanical tension ⁵⁾. In order to verify the straws circularity after glueing, high-precision x-ray tomographic techniques are being developed ⁶⁾.

The position monitoring of pixel, microstrip and straw-tube detectors will be performed by position detectors using Fiber Bragg Grating (FBG) sensors that exhibit a sensitivity at μm level ⁷⁾. The R&D on FBG sensors foresees long term tests and radiation hardness characterization. Also, a repositioning device with micron precision for the accurate location of the pixel detector after each accelerator store is being developed ⁸⁾.

6.1.2 Gas Detectors: Micro-pattern

For the region R1 ($\sim 3\text{m}^2$ area) of the first muon station of the LHCb detector the LNF group, in collaboration with INFN-Cagliari, proposed ⁹⁾ a detector based on GEM, a relatively new micro-pattern detector technology developed at CERN by Sauli.

The GEM ¹⁰⁾ consists of a thin (50 μm) kapton foil, copper clad on each side, chemically perforated by a high density of holes having bi-conical structure, with external (internal) diameter of 70 μm (50 μm) and a pitch of 140 μm . By applying a suitable voltage (400-500 V) between the two metal sides, an electric field with an intensity as high as 100 kV/cm is produced inside the holes, which act as electron multiplication channels for the electrons released by ionizing radiation in gas. In safe condition, gains up to $10^4 \div 10^5$ are reachable using multiple structures, realized by assembling more than one GEM at close distance one to each other.

The GEM detector, recently approved required a extensive R&D in terms of gas mixture optimization in order to achieve good time resolution and aging properties under strong irradiation. The LNF group has the responsibility of the mechanical design of the final detector and will be involved in the construction of 50% of the chambers. The commissioning of GEM detectors for LHCb is foreseen by the end of 2006.

GEM technology, or more generally micro-pattern detector technology (like Micromegas), could have in the near future very interesting developments. As an example GEMs used as readout system in TPC (Time Projection Chamber) seem to offer many advantages with respect to the usual wire solution (Sec. 6.1.3). In addition GEMs, due to their intrinsic robustness, can be also

used in space physics for applications in which gas detectors are mandatory, such as in Transition Radiation Detection (TRD).

A further natural application of GEM detectors is the X-ray medical imaging, especially for soft X-ray detection ($< 10\text{-}15$ keV, in radiology), for which the use of Xenon based gas mixture ensure very high detection efficiency; while further R&D and new ideas are needed to exploit this technology in nuclear medicine where hard X-ray detection is required for high Z material as efficient converter.

6.1.3 KLOE upgrades

The KLOE detector, optimized for the study of CP violation in K^0 decays and more generally for Kaon physics, consists of a very large (3.5 m long, 4 m diameter) Drift Chamber (DC) surrounded by a lead-scintillating fibres EM calorimeter, immersed in a ~ 0.52 T solenoidal magnetic field.

A possible upgrade of the present apparatus could be the insertion of a light vertex detector. This upgrade is strongly suggested by various physics items, such as charged Kaon physics (to increase statistics ($>$ factor 4) and improve the identification of Kaon interactions in the material located at a small radius) and K_L - K_S interferometry at small ΔT (and ΔR). A vertex detector would also increase the tagging efficiency and push to the ultimate limit the systematic errors on tracking pattern recognition and event selection in the measurement of ϵ'/ϵ . Based on the experience of present physics analysis, KLOE would also greatly profit from the measurement of the longitudinal coordinate by an inner vertex detector. All of the above has a fundamental importance in case of a significant upgrade ($>$ factor 10) of the DAΦNE luminosity.

The vertex detector would be inserted between the beam pipe and the cylindrical inner wall of the DC ($10\text{ cm} < r < 25\text{ cm}$); the available space in Z ($-30\text{ cm} < Z < 30\text{ cm}$), probably including Front End Electronic (FEE), is limited by the QCAL EM calorimeters surrounding the two low- β quadrupoles. It is important to note that an upgraded accelerator implies a new beam pipe and Interaction Region (IR) quadrupoles, and therefore a brand new QCAL. Since the new IR quadrupoles and QCAL would be significantly smaller than the present ones, some more space in z could be available for the vertex detector.

The main requirements for a vertex detector at KLOE are:

- a transverse spatial resolution in X-Y of $\sim 100\text{-}200\ \mu\text{m}$, while $\sim 500\ \mu\text{m}$ in the Z direction should be sufficient;
- the detector must be very light, $< 1\%$ X_0 in the angular range of interest $20^\circ < \theta < 160^\circ$;
- it should operate at a background rate of the order of 100 kHz/cm^2 .

Two possible vertex detector technologies have been considered and will be described in the following: the first one, based on standard double-sided μ -strip Silicon technology, will provide few points along the track with very high spatial resolution on both X-Y and Z directions. The second option, based on the more innovative and light technique of the Time Projection GEM (TPG) allows for a more dense track reconstruction with lower but still sufficient spatial resolution.

6.1.3.1 μ -Strip Silicon Vertex detector

The double-sided μ -Strip Silicon technology represents the standard choice for a compact vertex detector. Considering the limitation on material budget imposed by physics, a maximum number of three layers with a single wafer thickness of $\sim 300\ \mu\text{m}$ (0.3% X_0) can be proposed. This thickness would ensure the lowest cost and highest reliability. However it should be noted that developments in the near future might allow the use of $100\text{-}200\ \mu\text{m}$ thick wafers (which are already commercially

available) with a similar cost and reliability. In this case five or more layers, instead of three, could be installed.

The wafer length could be 4-6 inches, the strip pitches 100 μm and 150 μm respectively in $r-\phi$ and Z direction. Considering a mechanical support made of 0.5-1 mm thick composite material (0.1-0.2% X_0 in case of carbon fiber), such a silicon detector will fulfill the stringent requirement on material budget.

Concerning the detector performances, spatial resolutions of $\sigma_{r-\phi} \sim 60 \mu\text{m}$ and $\sigma_Z \sim 100 \mu\text{m}$ can be easily achieved with alternate $r-\phi$ and Z strips readout. Following such a readout scheme the number of electronic channels would be $\sim 30,000$ and $\sim 70,000$ respectively for $r-\phi$ and Z directions.

A careful evaluation of the FEE positioning (near or far the detector) should be done considering both performance and material budget requirements.

The main advantage of this solution is that both the detector and the FEE are practically commercially available and then easy to be implemented. In particular, buying entire “ladders” (modular units equipped with silicon, support substrate and integrated electronics) is possible and it might be more convenient, financially and technologically, than going through the effort of acquiring the required sophisticated silicon detector assembly tools (alignment machine, bonding device, etc...) and the needed know-how.

One of the strong advantages of a Si detector is that it represents a well-proven and reliable technology both from the point of view of operational experience and physics reach, successfully adopted in all possible accelerator environments (electron-positron colliders, like LEP and PEP-II; CERN and FNAL fixed target beam lines; hadron colliders, like Tevatron and LHC).

6.1.3.2 Time Projection GEM Vertex detector

The Time Projection GEM, or TPG, is an innovative high performance version of the standard TPC. The idea is to use a multi-step GEM instead of the usual MWPC system for the end-cap readout of the TPC.

The advantages of a TPG with respect to a TPC are manifold:

- absence of direct non-gateable ionization in the end-cap;
- intrinsic ion feedback suppression, close to 1%, and possibly as low as 10^{-3} . No gating is required, then the detector is self-triggering;
- high (>95%) ionization electron collection efficiency;
- fast electronic signals due to the total absence of ion tail and to the reduced induction gap thickness;
- narrow pick-up pad response function, $\Delta s \sim 1 \text{ mm}$;
- improved intrinsic two-track resolution, due to the absence of ion tail and the small induction gap: $\Delta V \sim 1 \text{ mm}^{-3}$, compared to 1 cm^{-3} of a classic TPC;
- no Lorentz distortions: the electric field is essentially parallel to the magnetic field throughout all the GEM, small local distortion being possible only inside the GEM holes.

To the above list possible advantages due to the high modularity, robustness, simplicity of assembly procedures and low cost of the GEM technology should be added.

The GEM solution seems to be the natural choice for the readout of the TPC: the GEM detector is intrinsically a “TPC” with a small drift region.

Presently there are several groups around the world working on TPG R&D for different applications. At LNF the required know-how to start a profitable R&D for the proposed new KLOE vertex detector is present.

A possible design of the KLOE TPG vertex detector, a barrel with dimensions of the order of $12 \text{ cm} < r < 22 \text{ cm}$ and $-30 \text{ cm} < Z < 30 \text{ cm}$, is based on the use of composite materials for both the internal (not structural) and external cylinder and also for the end-plate structural mechanical support. This solution easily allows to keep the material budget of the barrel structure to less than $1\% X_0$. While on end-plates, due to the contribution of the foreseen three GEM foils (globally $0,3\% X_0$) and the readout pad PCB ($<0,6\% X_0$), the material budget would be $\sim 1\% X_0$, excluding the FEE.

Considering 10 pad rows in $r-\phi$, with $\Delta r \sim 1 \text{ cm}$ and $\Delta\phi \sim 1-2 \text{ mm}$, the expected spatial resolutions are: $\sigma_{r-\phi} \sim 200 \mu\text{m}$ and $\sigma_Z < 500 \mu\text{m}$, for a total number of electronic readout channels of 50,000 or 100,000 depending on $\Delta\phi$ pad pitch. The lower performances of the TPG solution with respect to the μ -strip silicon detector is possibly balanced by the larger number of reconstructed track points available (10 for TPG instead of 3 of Silicon).

Also for the TPG solution a careful evaluation of the FEE positioning (near or far from the detector) should be done considering both performances and material budget requirements, even though in this case the possibility to put the FEE far from the end-plates of the detector seems more realistic.

6.1.4 Detector studies for next Linear Collider

There is global consensus in the high energy physics community that, after LHC, the next particle physics frontier machine will be an electron-positron linear collider (LC) with an energy up to about 1 TeV.

Physics and detector studies are in progress in Asia, Europe and North America. Linear colliders will allow precision studies of top quark and electroweak gauge bosons, Higgs boson properties and decays, Higgs mechanism tests and, beyond the Standard Model, supersymmetries searches in a complementary way to the LHC expected discoveries.

From the point of view of detector studies, although huge efforts have been performed in detector development for the LHC program, the LC environment requires significant additional and different detector R&D challenges. The main challenges at LHC were related to the high event rate and the prohibitive radiation levels associated with the $p-p$ energies and luminosity required.

At LC these problematics are sensibly reduced, but, with respect to LHC, detectors are required to exhibit unprecedented improved performances:

- improved position resolution ($\delta(\text{IP}) < 5 \mu\text{m}$ in $r-\phi, z$) and two-track resolution for vertex detectors that should be very light, to reduce multiple scattering and γ conversion, allowing flavor tagging;
- very light central tracker with better momentum resolution and reduced photon conversions, $\Delta(1/p) \sim 2 \div 5 \cdot 10^{-5} (\text{GeV}/c)^{-1}$;
- higher 3-D granularity electromagnetic and hadronic calorimeters to enable fine jet reconstruction and particle flow measurement ($\delta E/E \sim 30\%/\sqrt{E}(\text{GeV})$);
- improved hermeticity over the whole apparatus, implying excellent forward coverage at very small angle (down to $<5-10 \text{ mrad}$).

The most general detector design at LC foresees a vertex detector, a main and intermediate/forward tracker system, an electromagnetic and hadronic calorimeter inside a coil, the coil, an instrumented flux return yoke acting as muon detector and forward calorimeters.

Presently there are two LNF groups active in the R&D for the study of the muon and electromagnetic calorimeter detectors. Some interest could also arise in the near future for R&D on the central tracker, for the low mass high resolution TPG option (Sec. 6.1.3.2).

In the following, a brief description of such contributions is given.

6.1.4.1 Muon detector at the next Linear Collider

The muon detectors at LC, beside the identification of muons by their penetration through the iron, due to the limited calorimeter depth (from 5 to 7.5 interaction lengths) will serve also as backup calorimetry, allowing for the detection of significant deposits of leaking hadronic energy. Two candidate technologies, Resistive Plate Counters (RPC) or strips made of plastic scintillation counter are being studied.

The proposed detector is realized with screen-printed resistive coated float glass (high volume resistivity, $\rho \sim 5 \times 10^{-12} \Omega\text{cm}$, glass), exhibiting a moderate rate capability in streamer mode, $\sim 90\%$ efficiency at 10 Hz/cm^2 . Improvement of the rate capability is expected either operating the detector in avalanche mode (reducing dead zone), or using glass with lower volume resistivity. While the first option is relatively easy to implement, the second one might require some efforts for the engineering of the production procedures of the so called quasi-semiconductive glass, the only solution to substantially reduce resistivity in glass material ¹¹⁾.

6.1.4.2 EM Calorimetry at Linear Collider

The Electromagnetic at LC (LCCAL) is required to measure electromagnetic showers, deposited by single shower particles, with good energy resolution, of the order $\delta E/E \sim 10\%/\sqrt{E(\text{GeV})}$, and to be finely longitudinally and transversally segmented for the separation of the various jet components, in order to achieve the required jet energy resolution of $\delta E/E \sim 30\%/\sqrt{E(\text{GeV})}$. Different technologies are being considered:

- Silicon-Tungsten (Si-W) sandwich calorimeter, which provides the highest granularity ($\sim 1 \text{ cm}^2$);
- Tile-Fibre Calorimeter, which exhibits less granularity (from $3 \times 3 \text{ cm}^2$ to $5 \times 5 \text{ cm}^2$) but has significantly lower costs;
- a mixed option consisting in Tungsten-scintillator tiles, for energy reconstruction, plus some Si-pad layers suitable placed at different depths.

The LNF group involved on the R&D of this last option, in collaboration ¹⁴⁾ with other INFN institutions and ITE of Warsaw, has recently obtained interesting and promising results with a prototype of LCCAL tested in different experimental environments (CERN-SPS H6 beam line and LNF-BTF electron beam facility). The prototype, composed by 45 layers (50 in the final design) of 3 mm thick lead foil (Tungsten in the final version), interleaved with $5 \times 5 \text{ cm}^2$ plastic scintillator tiles (with WLS) with PM readout, and with three Silicon layers (at 2, 6, 12 X_0) with $0.9 \times 0.9 \text{ cm}^2$ pads, has shown an energy resolution of $\delta E/E \sim 11.1\%/\sqrt{E(\text{GeV})}$ in the energy range 5-30 GeV, a position resolution of $\sigma_{pos} \sim 2 \text{ mm}$ at 30 GeV and an e/π rejection $< 10^{-3}$.

6.2 Detectors for neutrino experiments and space physics

6.2.1 Detectors for neutrino physics

The design and construction of OPERA ¹⁵⁾ at Laboratori Nazionali Gran Sasso (LNGS) has been a remarkable opportunity to develop specific know-how at LNF. Frascati contributed enormously ¹⁶⁾ to the mechanical design of the experiment thanks to the skills of the technical services (SPAS and SSRC particularly), which turned out to be rather unique both within INFN and compared to the other international Labs that have joined the OPERA Collaboration.

For what concern the detector development, LNF has been mainly involved in the prototyping and construction of Bakelite RPCs ^{17, 18)}. The difficulty of this task is partially relieved by the very low counting rate in the underground site as compared to detectors operating at accelerators (e.g. the BABAR RPCs). On the other hand, the RPCs developed for OPERA have to be extremely reliable over time since they cannot be substituted after the installation of the magnet. Their area ($2.91 \times 1.14 \text{ m}^2$) is the largest built for a particle physics experiment and the border is irregularly shaped to allow the passage of the magnet bolts and limit the size of dead zones. Clearly, reliability has been the main concern. Several validation tests were performed before installation: test of gas tightness at the production site, mechanical and electrical tests and efficiency measurements with cosmic muons. In particular, the mechanical tests have been fully automatized in the surface laboratory hall of LNGS. In parallel, long term operation tests and studies of specific mixtures have been carried out. After more than three months of operation at cosmic ray fluxes, equivalent to five years of operation underground, the detectors show stable currents (lower than $1 \mu\text{A}$) and counting rates (around 300 Hz/m^2), with no efficiency losses. Commissioning of the magnet and data taking with cosmic rays will be carried out in 2005 and 2006 while beam data taking is foreseen for summer 2006.

The next technological challenge for OPERA at LNF is the emulsion scanning during data taking. Modern emulsion scanning techniques are a mixture of state-of-the-art technologies: CCD/CMOS high speed image grabbing, real time filtering, low aberration optics and precision mechanics for emulsion positioning and handling. Current microscopes developed outside LNF have reached the nominal speed of $20 \text{ cm}^2/\text{h}$ optimized for vertex detection. Similar devices will be installed at LNF but will be dedicated to more specialistic searches after a preliminary candidate selection. These searches are mainly related to electron identification or π/μ separation at the end-point of their range. Their physics applications range from the identification of the $\tau^- \rightarrow \nu_\tau \bar{\nu}_e e^-$ channel, to pure ν_e appearance without decay kinks (an indication of $\nu_\mu \rightarrow \nu_e$ oscillations), to charm rejections in τ appearance searches.

6.2.2 Detectors for space physics

6.2.2.1 μ -satellites

The space qualification, the cost of launches for satellite weights above a few hundred Kg and their time duration represents an obstacle, which is out of the control of HEP funding agencies, like DOE and INFN, which in many cases pay and build half (or more) of the experiments. This difficulty has recently led to the consideration of an additional and complementary approach, based on the deployment by commercial launchers of small and light (1-100 Kg) satellites (μ -satellites), where the acceptance is recovered by networking them. This option was discussed at an internal

INFN meeting about the on-going and future INFN initiatives in astro-particle physics in space held at LNGS in May 2004 ¹⁹⁾.

This “modular” approach is scientifically sound provided that the physics case can be pursued by segmenting the experimental acceptance (GF) into a network. It also allows a lower cost feasibility test, like test-beam experiments in HEP. The approach seems also financially affordable for INFN, given that typical costs are few MEuro for the first μ -satellite, decreasing with multiplicity. As an example, at the Surrey Space Center ²⁰⁾, was launched and operated about 1 μ -satellite/yr since the mid '80s. This modular approach, if viable, would be strategically convenient, since one should not rely completely on national space agencies: μ -satellites can be launched commercially within months. When possible and strategically convenient, selected INFN sites could acquire partial certification for Space Qualification (SQ).

6.2.2.2 Satellite laser-ranging experiments

This category of satellites carries on board many Corner Cube Reflectors (CCRs), which are used to track (“ranging”) their positions along their orbits. CCRs are special mirrors which always reflect an incoming light beam back in the direction it came from. The satellite ranging is achieved by shining from Earth multiple laser beams (each coupled to a telescope for aiming at the satellite) managed by the International Laser Ranging Network (ILRS). The reflected laser beam is also observed with the telescope, providing a measurement of the round-trip distance between Earth and the satellite.

The general relativity predicts that a rotating central body like Earth will drag the local space-time around it (*frame dragging*). This effect, predicted by Lense and Thirring (LT) in 1918, will cause the precession of the node of an artificial satellite of Earth (the node, or nodal line, is the intersection of the Earth equatorial plane with the satellite orbit). LARES/Weber-Sat, is being designed by a Collaboration of Italian and US Universities, the ILRS, INFN-LNF and INFN-Lecce. LARES will measure LT at 1% or better, taking advantage of the recent high-accuracy EGMs (Earth Gravity Models) and exploiting a thorough geometrical, mechanical and thermal characterization and, possibly, a new satellite design to reduce and control the thermal thrusts. The LNF group has been funded by INFN to perform R&D activity to find a suited satellite structure to strongly suppress the thermal thrusts (TTs) due to radiation pressure from the sun and the earth. An additional physics goal of LARES is the improvement of the limits on the violation of the Einstein Equivalence Principle.

A strong suppressions of the TTs, which are nowadays the limiting non-gravitational perturbations, opens the way to study new physics effects on the orbital elements of artificial satellites like LARES. In particular, perigee shifts are among the most sensitive observables to new physics. For example, a recent string-inspired brane model ²¹⁾ might imply perigee shifts observable after five years of ranging data for LARES on an orbit similar to the LAGEOS ones; this possibility is currently under study. Measuring such an effect for the Moon with Lunar ranging data is greatly complicated by the difficulty of knowing the Moon center of mass; while this knowledge is extremely simplified for an artificial satellite. Of course, models like ²¹⁾ are on a less firm theoretical ground than GR, but are still appealing, also because superstrings are thought to offer a way to the quantization of gravity. New ideas coming from the intersection of experimental particle physics and relativistic astrophysics can rinvigorate the use and scope of the International Space Station in the next ten years. See also the discussion by the ESA astronaut R. Vittori in ²²⁾.

6.3 Detectors for nuclear experiments

6.3.1 A Large Area Silicon Drift Detectors for SIDDHARTA

The Silicon Drift Detectors (SDD) were developed as position sensing detectors which operate in a manner analogous to gas drift detectors²³). Recently, SDD started to be also used as X-ray detectors in X-ray Fluorescence spectroscopy, electron miniprobe analysis systems and synchrotron radiation applications. SDDs with sensitive areas of up to 10 mm² are commercially available for several years already. The typical energy resolution is better than 140 eV (FWHM) at 5.9 keV and -20°C. The outstanding property of a SDD is its extremely small anode capacitance, which is independent of the active area. Thus, the electronics noise is very low, and much shorter shaping times than for PIN diodes or Si(Li) detectors can be used. Hence it can be expected that SDDs with an area much larger than 10 mm² still have a good energy resolution. Taking into account the small shaping time, a triggered application of the large area SDD as an X-ray detector, with a time window limited by its active area (drift time), can be envisaged. One of the ideal applications of such a triggered large area SDD detector is the measurement of exotic atoms X-ray transitions at DAΦNE (SIDDHARTA). The X-ray energies, ranging from few to tens keV, are well in the range of maximum efficiency of SDDs, while a trigger based on a time-window of the order of μs was demonstrated by Monte Carlo simulation to dramatically reduce background rates and to allow for a precision measurement of exotic atom transitions. The trigger in this case is given by the specific process which generated the K^- at DAΦNE, namely a back-to-back reaction of the type $\phi \rightarrow K^+ K^-$.

A program to develop such a kind of large area triggerable (1 cm²) SDD detectors, with integrated electronics (JFET) on it, has started at LNF, in collaboration with MPI (Max-Planck Institut), PNSensors and Politecnico di Milano.

The experimental requests put forward for these detectors are:

- energy range of interest: 0.5 - 20/40 keV, with a selectable gain;
- capability to operate mainly under high energy events (backgrounds), with an event rate of the order of KHz/channel;
- energy resolution better than 140 eV (FWHM) at 6 keV of energy;
- stability and linearity better than 10⁻⁴ for a precision measurement;
- trigger at the level of 1μs.

The total number of channels to be processed is 200 for a total area of 200 cm².

6.3.2 The central tracker for PANDA

The PANDA experiment²⁴) at GSI aims to study fundamental questions on hadron and nuclear physics in interactions of antiprotons with nucleons and nuclei. The LNF group has responsibilities in the central tracker (CT), for which two alternative options are presently under study: a Straw Tube (ST) tracker and a Time Projection Chamber (TPC) with GEM readout. The tracking region of the PANDA spectrometer will occupy a region inside the superconducting solenoid starting at a radial distance of 15 cm from the beam line, up to 42 cm. Along z this region extends 40 cm upstream and 110 cm downstream of the interaction point. In this region the magnetic field will have a strength of 2 T with a homogeneity of about 10%. The CT should provide measurements of tracks coordinates, in both x and y directions, with a resolution of about 100 μm, and along z

of about 1 mm. The expected rate of events will be 10^7 per second, with a multiplicity of $4 \div 6$ tracks per event, therefore drift-chamber devices with small cells could be used.

6.3.2.1 Straw tube tracker

The PANDA ST tracker will consist of a set of double-layers of 150 cm long straw tubes filling the tracking volume. The first and the last double-layer will be parallel to the beam axis, while the remaining will be arranged at a tilted angle ranging from 2 to 3°, allowing z coordinate reconstruction. In the region closer to the beam axis the straws occupancy will be higher, due to curling low-energy tracks, therefore the straw diameters will be different: smaller for the inner layers, bigger for the outer ones. According to the experience of other experiments, and on the basis of software simulations, a detector with straw tube wall thickness of about 100 μm made of carbonated Kapton, and anode wire diameters of 30 μm is being studied. The gas mixture under test are all based on Argon. Another crucial point of this kind of detector will be how the straw tubes are mechanically sustained. A solution avoiding a heavy mechanical frame is envisaged, therefore tests to glue the tubes altogether building planar self-sustaining modules have been performed. Studies to produce cylindrical modules of glued straws are also under way at LNF.

6.3.3 Time Projection Chambers

A TPC with its low material budget constitutes an ideal device for tracking charged particles in 3D space, fulfilling all the requirements on PANDA tracking. Such a device consists of a large gas-filled cylindrical volume inside a solenoidal magnetic field, surrounding the interaction point and covering the full 4π solid angle. Up to now, all TPCs have been operated in a pulsed mode, where an electrostatic gate to the readout region is opened only when an interaction in the target has occurred, and is closed immediately thereafter, preventing avalanche ions from penetrating the drift volume. Due to the beam properties at the GSI storage ring, the TPC in PANDA has to operate continuously, i.e. the technique of gating cannot be applied. This determines obvious problems of ions feeding back into the drift volume, and about an order of magnitude higher granularity in all three spatial coordinates to be able to sustain a continuous readout. These limitations may be overcome using the GEM as charge amplifier. Therefore, a TPC readout by GEMs is an interesting alternative to the ST tracker for PANDA. The development of such a detector constitutes a challenge both scientifically and technologically, but would present a number of advantages, as very low material budget, particle identification at low momenta, and very good tracking performances. At LNF GEM devices are being studied (Sec. 6.1.2), therefore in case the PANDA tracking choice will be a TPC with GEM, the LNF PANDA group will contribute to the development of this detector too.

6.4 Synchrotron radiation

Silicon Drift Detectors (SDD, Sec. 6.3.1), originally developed for high energy physics experiments, have been recently successfully applied to X-ray spectroscopy. They look very promising because with Peltier cooling they can reach an energy resolution ($\text{FWHM} < 168 \text{ eV}$ at 5.9 keV) comparable to liquid nitrogen cooled Ge detector one. Therefore, SDD can be used for the detection of the X-fluorescence in synchrotron light sources. The plan is to first test SDD on a beamline in different conditions and then, on the basis of the results and of the experience acquired, to develop a SDD crystal ball to cover a large solid angle.

6.5 Capillary Optics

Presently X-ray optics (and, for that matter, neutron optics) is an independent area of physics undergoing a new stage in its development²⁵⁾. This fact can be explained by the close links to modern technology: the apparent decline of interest in studies of this kind, which can be explained by technological difficulties, has been successfully overcome. Lately a new area of X-ray optics, capillary optics (polycapillary optics) emerged. Capillary optics has for the first time allowed to really control X-ray radiation within a broad frequency range. The new optics, which differs favorably from other methods of X-ray radiation focusing, mainly due to the large angular acceptance (up to a few tens of degrees) at rather small spatial sizes, makes it possible to monochromatize a radiation beam, to effectively turn it by large angles, to transform a divergent beam into a parallel beam and vice versa, and finally to focus the radiation with intensity increasing by a factor of 100 to 1000 (or even more). All this has made the list of applied problems in which X-ray optics may produce a real breakthrough only longer.

The use of capillary structures has contributed greatly to experiments in diffractometry, in 3D elemental analysis, in controlling beams of synchrotron radiation, in the production of high-power sources of X-ray radiation, and in many other areas. Promising results have been obtained in the use of capillary optics in X-ray lithography, as well as in X-ray imaging techniques. So far these results have been obtained in laboratories, but pilot models on their basis are already in use. The widest area of research involves applications of the new optics in medicine, in particular in mammography and angiography, and in boron-neutron capture therapy (capillary optics is a powerful instrument for controlling beams of thermal neutrons). There is hope that research in these areas will produce in the near future new medical devices that will help in the early detection of cancer and cardiologic disorders, and devices for radiotherapy also.

In addition to what said above, capillary systems are really new interference elements. The manifestation of the wave properties in such macrostructures is of great interest, since the characteristics of interference can really be controlled. It is also interesting how capillaries and capillary systems can be used as X-ray waveguides.

One of the main research subjects of experiments on propagation of X-rays in capillary structures is a problem of its use for the increase of radiation density. In experimental tests performed at BESSY²⁶⁾ to study the focusing features of a capillary lens for various energies of synchrotron radiation in the range of $5 \div 20$ keV, the intensity of radiation was increased about 150 times for the optimum interval of $7 \div 8$ keV. As expected, for higher energies of radiation falling down in the gain has been detected as well as for lower energies. The latter is in a good agreement with the point that each capillary lens works effectively only for optimal energy range. Next step will be performed at the DAΦNE ring X-ray beamline, by focusing synchrotron radiation in order to increase the density of radiation on a sample. Special alignment procedures by means of conventional X-ray tube source and new compact and effective XRF spectrometers are being developed at the DAΦNE Synchrotron Radiation laboratory.

A milestone of capillary optics applications in medicine will be to decrease the irradiation dose by factor of 10 to 100 and to increase the contrast resolution, due to the strong suppression of radiation scattering, that will be very important for X-ray diagnostics at early stages of the disease (tumor size of 50 mm, present status ~ 150 -200 mm), for X-ray therapy of skin cancer (depth of treating ~ 1 -2 cm) and for therapy of small tumors. Capillary optics becomes a powerful instrument in boron-neutron capture therapy of cancer as well as in developing a new type of neutron microscope. Studies in these fields are presently performed within a mutual agreement between LNF and UNISANTIS SA (Switzerland).

Capillary optics can be used in many areas where it is necessary to increase the density of X-rays and thermal neutrons, in general, to monitor the level of radiation. Examples of possible

applications are: the creation of a new class of medical apparatus for early detection of cancer and cardiologic disorders; the creation of new types of microscopes and tomographs with a resolution of about 0.1 mm for biology and related areas of research; the creation of devices for elemental microanalysis (with a recording limit of about 10^{-13} g), transferring images, studying crystals, and perfecting diffractometers; the development of X-ray lithography for the fabrication of integrated circuits with a resolution of about $0.1 \pm 0.2 \mu\text{m}$; the design of new X-ray sources with a power of about 10 W and with an effective focal spot smaller than $20 \mu\text{m}$ (radiation pulses of about 10^{13} ph/s, which corresponds to an integrated intensity of about $10^7 \pm 10^8$ ph/s); the creation of new types of telescopes in the X-ray range; the exploitation of its bending efficiency, with special angle-tuning benders.

References

1. B. Bartoli *et al.*, Phys. Rev. D **6** (1972) 2374.
2. ATLAS Technical Design Report 10, CERN/LHCC/97-22.
3. G. Lanfranchi, Nucl. Instr. Meth. A **535** (2004) 221.
4. S. Bianco (on behalf of the BTeV Coll.) "Status of BTeV experiment at the Fermilab Tevatron", presented at the Conference on Physics at LHC, July 2004, Vienna (Austria), LNF-04/1(P).
5. E. Basile *et al.* "A New Configuration for a Strawtubes - Microstrips Detector", LNF-04-19(P).
6. G. Saviano, BTeV Note 3837-v3 (2004).
7. S. Bianco, BTeV Note 2922-v2 (2004).
8. M.A. Caponero, BTeV Note 3414-v1 (2004).
9. G. Bencivenni *et al.*, Nucl. Instr. Meth. A **488** (2002) 493.
10. F. Sauli, Nucl. Instr. Meth. **A386** (1997) 531.
11. G. Bencivenni *et al.*, Nucl. Instr. Meth. A **332** (1993) 368.
12. Tesla TDR Part IV "A Detector for TESLA", DESY 2001-11 ECFA 2001-209.
13. M. Anelli *et al.*, Nucl. Instr. Meth. A **300** (1991) 572.
14. M. Alemi *et al.*, Instrumentation and Measurement Technology Conference, IMTC 2004, Vol.2 pag.1263-1267.
15. M. Guler *et al.*, OPERA proposal, CERN/SPSC 2000-028, SPSC/P318, LNGS P25/2000.
16. INFN-LNF 2004 Annual Report - LNF-05/05 (IR) - available on <http://www.lnf.infn.it/rapatt>
17. M. Ambrosio *et al.*, IEEE Trans. Nucl. Sci. **51** (2004) 975.
18. G. Barichello *et al.*, Nucl. Instr. Meth. A **533** (2004) 42; M. Ambrosio *et al.*, Nucl. Instr. Meth. A **533** (2004) 173; A. Bergnoli *et al.*, Nucl. Instr. Meth. A **533** (2004) 203; R. Brugnera *et al.*, Nucl. Instr. Meth. A **533** (2004) 221.
19. <http://serms.unipg.it/conferenze/>

20. <http://www.ee.surrey.ac.uk/SSC>; <http://centaur.sstl.co.uk/SSHP>
21. G. Dvali, A. Gruzinov, and M. Zaldarriaga, Phys. Rev. D **68** (2003) 024012.
22. D. Babusci *et al.*, LNF-04/26 (IR).
23. E. Gatti and P. Rehak, Nucl. Instr. Meth. A **225** (1984) 608, Nucl. Instr. Meth. A **235** (1985) 224.
24. http://www.gsi.de/fair/experiments/hesr-panda/index_e.html
25. S.B. Dabagov, Physics-Uspekhi **46** (10) (2003) 1053.
26. <http://www.bessy.de>

Chapter 7

Conclusions

Next three years will be crucial for many of the activities in the Laboratory. Some of them require concern for a successful start-up (Sec. 2.3, 2.8.4, 2.9.1, 2.9.2, 2.10.1, 2.11) and others are well advanced or in the completion phase (Sec. 2.8.1, 2.8.2, 2.8.3, 2.10.2, 2.10.3, 2.10.4) and demand strong efforts to produce maximum scientific output from data analyses.

KLOE data taking, with the collection of 2 fb^{-1} , will be completed by the end of 2005. The following years (2006-2007) will be devoted to the Hypernuclear Physics program of the FINUDA experiment (Sec. 2.10.2) and to the study of kaonic atoms with SIDDHARTA (Sec. 2.10.1).

The accelerator experiment to exploit the Strong Radio Frequency Focusing concept (Sec. 4.2.3), although not funded yet, is expected to enrich the know-how on the high-luminosity frontier of the meson factories in the same period.

The two Synchrotron Radiation Lines are expected to face with increasing operativity. The approval of the proposal for a new line providing X-rays from 60 to 1000 eV could allow further activities on this interdisciplinary field of interest for material science, chemistry, biology and high-technologies.

The Sparc program, after the realization of the advanced photo-injector will progress in testing new accelerator concepts that hopefully will bring the technology to the stage where it can be considered for the use in a vast number of applications.

The Beam Test Facility will continue to provide e^+/e^- beams from few MeV to 750 MeV at tunable intensities to a wide user community interested to study the performance of new particle detectors.

It is important to push now for a call of interest for new experiments preparing the decision to be taken during 2006 for the future facilities in the Laboratory.

The major alternatives presented in Chap.4 have the potentiality to change the character of the LNF and differ for scientific programs, user communities and costs, among other factors.

The DAΦNE luminosity optimization, allowing peak luminosities of $2\text{-}3 \times 10^{32} \text{ cm}^{-2} \text{ s}^{-1}$ (Sec. 4.2.2), fulfills the requirements of the SIDDHARTA-2 experiment on kaonic atoms (Sec. 4.8), and of the Hypernuclear spectroscopy on medium-high atomic-number nuclei with FINUDA.

Since these programs require total integrated luminosities of the order of a few fb^{-1} , such an option presents the best compatibility with the development of a Synchrotron Radiation (SR) user facility, with the SPARXINO experiment, and the operation of the Beam Test Facility sharing the LINAC.

The DAΦNE energy upgrade from 0.51 to 1.2 GeV per beam allows the study of the threshold region for $N\bar{N}$ production and the measurement of the nucleon form factors presented in Sec. 4.9. A

preliminary version of the Letter of Intent ¹⁾ has been circulated at the Workshop on Nucleon Form Factors, held at the LNF in October 2005 ²⁾, where it was discussed and positively acknowledged. With minor modifications of existing detectors, the measurements of both, the moduli, and the phases of the proton and the neutron form factors in the time-like domain, should be accomplished. The LoI contains also requirements for the performance of the DAΦNE ring upgraded in energy.

The realization of a new ϕ -factory, capable to deliver integrated luminosities of at least 30 fb^{-1} in smooth, steady running conditions, open the possibility to achieve new results in the field of kaon physics. In particular, the study of rare K_S decays and K_L - K_S interferometry represent the highlights of the particle-physics program of this option (Sec. 4.3). Since the primary focus shifts from K_L decays to rare K_S decays and K_L - K_S interferometry, substantial upgrades of the KLOE detector are desirable. In particular, it is very natural to conceive the possibility of a vertex detector to improve the resolution close to the interaction region (Sec. 6.1.3). The physics program should also have a natural connection with existing and planned experiments on rare K^+ and K_L decays at fixed-target hadron machines. For instance, the measurements of the rare decays $K_S \rightarrow \pi^0 \ell^+ \ell^-$ at the ϕ -factory are closely linked to the measurements of the corresponding K_L modes at fixed-target experiments (Sec. 4.3).

The project could also be well suited for the Hypernuclear program with the Ge detectors (Sec. 4.7) and for the experiment on the kaonic atoms (Sec. 4.8.1).

In principle, by an increase of the cost under evaluation, the new ϕ -factory could also be designed for running at the $N\bar{N}$ threshold (Sec.4.9) without compromising the peak luminosity at the ϕ resonance.

The time-sharing of the facility is an issue for the accomplishment of different physics programs; in particular, the operation with different detectors require the study of an efficient solution for the installation/disinstallation procedure.

The discussion on the interest and the feasibility of these programs has been issued in a dedicated workshop at Alghero in September 2003 ³⁾ and in several international conferences ^{4, 5, 6, 7)}. More topical workshops and dedicated discussions have been done in 2005, namely at KAON05 ⁸⁾, at the LNF Spring School 2005 ⁹⁾, and at the International Workshop on Hypernuclei ¹⁰⁾.

Accelerator Design Studies for the energy upgrade and for the new ϕ -factory reported in Sec. 4.2 are advancing and should be finalized in the drafting of a Conceptual Design Report (CDR) by the end of 2005. Also the CDRs of the upgrades of the KLOE and FINUDA detectors should be circulated in the same period.

The project of a high-luminosity τ /charm factory (Sec. 4.2.4, 4.6, 4.5), which will be discussed in a Workshop ¹¹⁾ at the LNF in March, 2006, seems to be slightly over-dimensioned for the present LNF infrastructures and require the involvement of an international community much wider than for the realization of the other initiatives.

All the ongoing activities will be subjected to a multistage review by the LNF Scientific Committee and other advisory bodies appointed also by the National Scientific Committees of the INFN. It is worth stressing that a decision should be taken in 2006 not only to focus the local activities but also to settle the level of involvement in other international programs which will be determined after the selection of the new project.

References

1. M. Mirazita, "Measurement of the nucleon form factors in the time-like region at DAΦNE", Letter of Intent, http://www.lnf.infn.it/conference/nucleon05/loi_06.pdf
2. Workshop on Nuclear Form Factors N05, Laboratori Nazionali di Frascati (October 2005), <http://www.lnf.infn.it/conference/nucleon05/>
3. e^+e^- in the 1-2 GeV range: Physics and Accelerator Prospects, Alghero (2003), <http://www.lnf.infn.it/conference/d2/prog.htm>
4. International Conference on Exotic Atoms, Vienna (February 2005), <http://www.oeaw.ac.at/smi/exa05/>
5. Le Reccontres de la Vallee d'Aoste, La Thuile (March 2005), http://www.pi.infn.it/lathuile/lathuile_2005.html
6. CKM 2005 - Workshop on the Unitary triangle, San Diego (March 2005), <http://ckm2005.ucsd.edu/index.html>
7. Incontri di Fisica delle Alte Energie, Catania (March-April 2005), <http://cms.ct.infn.it/ifae>
8. Kaon 2005 - International Workshop, Northwestern University, Evanston (June 2005), <http://diablo.phys.northwestern.edu/andy/conference.html>
9. LNF Spring School "Bruno Touschek" in Nuclear, Subnuclear and Astroparticle Physics, Laboratori Nazionali di Frascati (May 2005), <http://www.lnf.infn.it/conference/lnfss>
10. International Workshop on Hypernuclei with Heavy Ion Beams HypHI05, GSI-Darmstadt (June 2005), http://www.gsi.de/forschung/kp/kp2/experiments/HYPERNuclei/Hyphi05_e.htm
11. International Workshop on Discoveries in Flavour Physics at e^+e^- Colliders - DIF06, LNF-Frascati (2006), <http://www.lnf.infn.it/conference/dif06>

Chapter 8

Acknowledgments

It is almost impossible to thank all of the people who have contributed to this work with many interesting discussions. We gratefully acknowledge S. Bertolucci who promoted the working group and fostered the debate on the future programs and M. Calvetti for the interest and the efforts devoted to pushing the decision process. We are most thankful for the strong support, help and advice received from M. Curatolo and L. Votano, and indebted to A. Calcaterra for the improvements in the sections on B-physics. We would also like to thank B. Dulach and M. Pistoni who have contributed to the sections on the technical services.